Using optogenetics to influence the circadian clock of *Drosophila melanogaster*

Die Verwendung der Optogenetik zur Beeinflussung der circadianen Uhr von *Drosophila melanogaster*

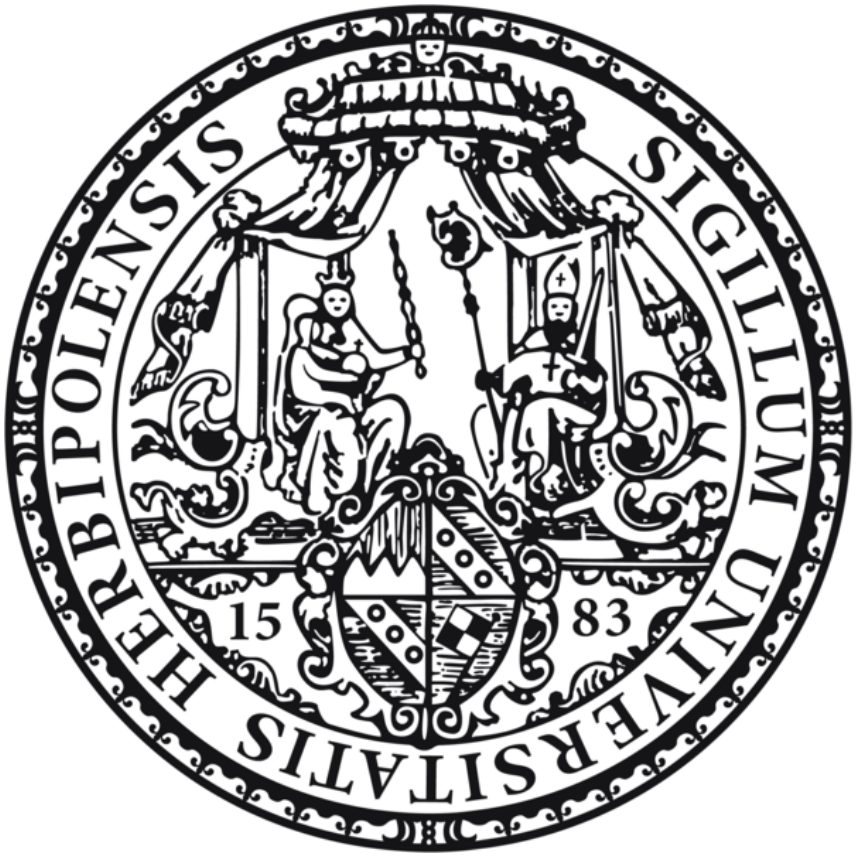

Doctoral thesis for a doctoral degree
at the Julius-Maximilians-University Würzburg

submitted by
Sebastian Beck
from Weilbach

Würzburg, 2019

Eingereicht am: _____

Mitglieder der Promotionskommission:

Vorsitzender: _____

1. Gutachter: Prof. Dr. Georg Nagel

2. Gutachter: Prof. Dr. Robert Kittel

Tag des Promotionskolloquiums: _____

Doktorurkunde ausgehändigt am: _____

Table of Contents

Summary

Almost all life forms on earth have adapted to the most impactful and most predictable recurring change in environmental condition, the cycle of day and night, caused by the axial rotation of the planet. As a result many animals have evolved intricate endogenous clocks, which adapt and synchronize the organisms' physiology, metabolism and behaviour to the daily change in environmental conditions. The scientific field that is dedicated to researching these endogenous clocks and to unravelling its mechanisms down to a molecular level, is called chronobiology and has steadily grown in size, scope and relevance since the works of the earliest pioneers in the 1960s, culminating in 2017, when the three most accomplished modern chronobiologists were awarded the Nobel Prize in Physiology or Medicine.

The number one model organism for the research of circadian clocks is the fruit fly, *Drosophila melanogaster*, whose clock serves as the entry point to understanding the basic inner workings of such an intricately constructed endogenous timekeeping system. Despite tremendous progress in recent decades, there is still a lot to be discovered about the workings of the circadian clock of *Drosophila melanogaster*. In this thesis it was attempted to combine the research on the circadian clock with the techniques of optogenetics, a fairly new scientific field, launched by the discovery of Channelrhodopsin 2 just over 15 years ago. Channelrhodopsin 2 is a light-gated ion channel found in the green alga *Chlamydomonas reinhardtii*, where it is used for phototaxis. In optogenetics, researches make use of these light-gated ion channels like Channelrhodopsin 2 by heterologously expressing them in cells and tissues of other organisms, which can then be stimulated by the application of light. This is most useful when studying neurons and neuronal networks, as these channels provide an almost non-invasive tool to depolarize the neuronal plasma membranes at will with high temporal precision. The goal of this thesis was to find, develop and refine an optogenetic tool, which would be able to influence and phase shift the circadian clock of *Drosophila melanogaster* upon illumination. A phase shift is the adaptive response of the circadian clock to an outside stimulus that signals a change in the environmental light cycle. Under natural conditions this process is used to synchronize the circadian clock to the gradual changes in day length over the seasons, caused by the earth's position relative to the sun and its axial tilt. An optogenetic tool, able to influence and phase shift the circadian clock predictably and reliably, would open up many new ways

and methods of researching the neuronal network of the clock and which neurons communicate to what extent, ultimately synchronizing the network.

The first optogenetic tool to be tested in the circadian clock of *Drosophila melanogaster* was ChR2-XXL, a channelrhodopsin variant with dramatically increased expression levels and photocurrents combined with a prolonged open state. The specific expression of ChR2-XXL and of later constructs was facilitated by deploying the three different clock-specific GAL4-driver lines, *clk856-gal4*, *pdf-gal4* and *mai179-gal4*. Although ChR2-XXL was shown to be highly effective at depolarizing neurons, these stimulations proved to be unable to significantly phase shift the circadian clock of *Drosophila.* The second series of experiments was conducted with the conceptually novel optogenetic tools Olf-bPAC and SthK-bPAC, which respectively combine a cyclic nucleotide-gated ion channel (Olf and SthK) with the light-activated adenylyl-cyclase bPAC. These tools proved to be quite useful when expressed in the motor neurons of instar-3 larvae of *Drosophila*, paralyzing the larvae upon illumination, as well as affecting body length. This way, these new tools could be precisely characterized, spawning a successfully published research paper, centered around their electrophysiological characterization and their applicability in model organisms like *Drosophila.* In the circadian clock however, these tools caused substantial damage, producing severe arrhythmicity and anomalies in neuronal development. Using a temperature-sensitive GAL80-line to delay the expression until after the flies had eclosed, yielded no positive results either. The last series of experiments saw the use of another new series of optogenetic tools, modelled after the Olf-bPAC, with bPAC swapped out for CyclOp, a membrane-bound guanylyl-cyclase, coupled with less potent versions of the Olf. This final attempt however also ended up being unsuccessful. While these tools could efficiently depolarize neuronal membranes upon illumination, they were ultimately unable to stimulate the circadian clock in way that would cause it to phase shift.

Taken together, these mostly negative results indicate that an optogenetic manipulation of the circadian clock of *Drosophila melanogaster* is an extremely challenging subject. As light already constitutes the most impactful environmental factor on the circadian clock, the combination of chronobiology with optogenetics demands the parameters of the conducted experiments to be tuned with an extremely high degree of precision, if one hopes to receive positive results from these types of experiments at all.

Zusammenfassung

Nahezu alle Lebewesen der Erde haben sich an den Tag-Nacht-Zyklus angepasst, die einflussreichste und verlässlichste wiederkehrende Veränderung der Umwelt-bedingungen, verursacht durch die axiale Rotation des Planeten. Daraus resultierend haben viele Tiere komplizierte innere Uhren entwickelt, welche ihre Physiologie, ihren Stoffwechsel und ihr Verhalten an die tägliche Veränderung der natürlichen Bedingungen anpassen. Das Wissenschaftsfeld, das sich der Erforschung dieser inneren Uhren und deren Mechanismen bis zur molekularen Ebene widmet, wird Chronobiologie genannt und hat seit der Arbeit der ersten Pioniere ab 1960 stetig an Größe und Relevanz gewonnen, bis schließlich 2017 die drei bedeutendsten Chronobiologen der Moderne mit dem Nobelpreis für Medizin ausgezeichnet wurden. Der prominenteste Modellorganismus für die Erforschung der circadianen Uhr ist die Fruchtfliege, *Drosophila melanogaster*, deren Uhr als Ansatzpunkt dient, die grundlegenden Vorgänge eines derart komplexen, endogenen Taktsystems zu verstehen. Trotz enormer Fortschritte in den vergangenen Jahrzehnten gibt es noch vieles zu enthüllen bezüglich der Funktionsweise der inneren Uhr von *Drosophila melanogaster*. In dieser Thesis wurde versucht die Forschung an der circadianen Uhr mit den Techniken der Optogenetik zu kombinieren, eines vergleichsweise jungen Forschungsfeldes, welches durch die Entdeckung von Channelrhodpsin 2 vor über 15 Jahren eröffnet wurde. Channelrhodopsin 2 ist ein Licht-gesteuerter Ionenkanal, der in der Grünalge *Chlamydomonas reinhardtii* entdeckt wurde, wo er der Phototaxis dient. In der Optogenetik machen sich Forscher diese Licht-gesteuerten Ionenkanäle zu Nutze, indem sie sie heterolog in den Zellen und dem Gewebe anderer Organismen exprimieren, welche dann durch Licht stimuliert werden können. Dies ist besonders nützlich bei der Untersuchung von Neuronen und neuronalen Netzwerken, da diese Kanäle ein nahezu nicht-invasives Werkzeug zur beliebigen Depolarisation neuronaler Membranen mit hoher zeitlicher Präzision bieten. Das Ziel dieser Thesis war es, ein optogenetisches Werkzeug zu finden, zu entwickeln und zu verfeinern, welches in der Lage ist, die circadiane Uhr von *Drosophila melanogaster* durch Licht zu manipulieren und deren Phase zu verschieben. Eine Phasenverschiebung ist die adaptive Antwort der circadianen Uhr auf einen äußeren Reiz, welcher eine Veränderung des natürlichen Lichtzyklus signalisiert. Unter natürlichen Bedingungen dient dieser Prozess dazu, die innere Uhr an die sich graduell verändernde Tageslänge

anzupassen, die durch die Achsenneigung der Erde in Kombination mit ihrer Ausrichtung zur Sonne erzeugt wird. Ein optogenetisches Werkzeug, das in der Lage ist, die Phase der inneren Uhr verlässlich und vorhersagbar zu verschieben, würde viele neue Möglichkeiten zur Erforschung des neuronalen Uhrnetzwerks eröffnen und wie genau welche Neuronen mit welchen anderen Neuronen kommunizieren um das Netzwerk letztendlich zu synchronisieren.

Das erste optogenetische Werkzeug das in der circadianen Uhr von *Drosophila melanogaster* getestet wurde war „ChR2-XXL“, eine Channelrhodopsin-Variante mit enorm erhöhter Expression und Photoströmen, gepaart mit einem verlängerten geöffneten Zustand. Die spezifische Expression von ChR2-XXL und auch die späterer Konstrukte wurde durch die Verwendung der drei Uhr-spezifischen GAL4-Treiberlinien *clk856-gal4*, *pdf-gal4* und *mai179-gal4* bewerkstelligt. Obwohl bereits gezeigt wurde, dass ChR2-XXL höchst effektiv die Depolarisierung von Neuronen bewirkt, waren diese Stimulationen jedoch nicht in der Lage die Phase der circadianen Uhr von *Drosophila* signifikant zu verschieben. Die zweite Serie an Versuchen wurde mit den konzeptionell neuartigen optogenetischen Werkzeugen Olf-bPAC und SthK-bPAC durchgeführt, welche jeweils einen durch zyklische Nukleotide gesteuerten Ionenkanal (Olf und SthK) mit der Licht-gesteuerten Adenylatcyclase bPAC kombinieren. Diese Werkzeuge erwiesen sich als äußert nützlich, solange sie in den Motoneuronen von *Drosophila*-Larven im dritten Larvenstadium exprimiert wurden, wo sie bei Beleuchtung die Larven sowohl paralysierten, als auch deren Körperlänge beeinflussten. Auf diese Weise konnten diese neuen Werkzeuge präzise charakterisiert werden, was in der erfolgreichen Veröffentlichung eines Forschungsartikels mündete, welcher hauptsächlich von der elektrophysiologischen Charakterisierung der Werkzeuge handelte und von deren Anwendungsmöglichkeiten in Modellorganismen wie *Drosophila*. In der circadianen Uhr verursachten diese Werkzeuge jedoch substantielle Schäden und produzierten schwere Arrhythmie und Anomalien in der neuronalen Entwicklung. Die Verwendung einer temperatur-sensitiven GAL80-Linie um die Expression zu verzögern, bis nachdem die Tiere geschlüpft waren, erzeugte ebenfalls keinerlei positive Ergebnisse. Für die letzte Serie an Experimenten wurde eine weitere Reihe neuer optogenetischer Werkzeuge verwendet, orientiert an Olf-bPAC und SthK-bPAC, wobei bPAC durch die membrangebundene Guanylatcyclase „CyclOp“ ausgetauscht wurde, welche wiederrum mit weniger wirkstarken Olf-Varianten kombiniert wurde. Dieser letzte

Ansatz scheiterte jedoch ebenfalls. Obwohl diese neuen Werkzeuge in der Lage waren die Neuronenmembran bei Beleuchtung effektiv zu depolarisieren, vermochten sie es letztendlich nicht die circadiane Uhr auf eine Art und Weise zu stimulieren, so dass eine Phasenverschiebung erfolgte.

Zusammengenommen zeigen diese überwiegend negativen Ergebnisse, dass die optogenetische Manipulation der circadianen Uhr von *Drosophila melanogaster* ein extrem anspruchsvolles Thema ist. Da Licht bereits ohnehin den einflussreichsten Umweltfaktor für die circadiane Uhr darstellt, verlangt die Kombination von Chronobiologie und Optogenetik eine extrem präzise Feinabstimmung der Versuchsparameter, um überhaupt darauf hoffen zu dürfen, positive Ergebnisse mit derlei Versuchen zu erzeugen.

1. Introduction

1.1. The science of chronobiology

“Sad soul, take comfort, nor forget
That sunrise never failed us yet!”

The certainty and predictability of earth’s day and night cycle has inspired countless quotes and proverbs, such as this one by the American novelist Celia Thaxter. But apart from its influence on human culture, earth’s day and night cycle, which is caused by its axial rotation, might be the most impactful as well as the most reliably changing environmental condition on the planet. Almost all life on earth that is subjected to the daily rising and setting of the sun, has adapted to the periodic changes in temperature and light intensity to some degree. Even prokaryotes, such as cyanobacteria [1, 2] or single cell algae like *Chlamydomonas reinhardtii* [3] have been reported to demonstrate a rhythmic and adaptive behaviour or metabolism towards the cycle of day and night. As life gets more complex, so do the adaptive mechanisms, with organisms on the highest levels of biological organisation having evolved intricate endogenous clocks that synchronize their physiological processes as well as the entire range of their complex behaviours to the daily environmental changes.

According to Johnson et al., a simplified model for these endogenous clocks can be summed up to be consisting of three parts, the input, the core clock and the output [4]. The input to the core clock is made up of the so-called “Zeitgebers” (german: “time-giver”) that entrain the endogenous molecular clock mechanism to the external cycle of environmental conditions. These Zeitgebers consist of environmental influences and cues of varying strength, with light being by far the strongest Zeitgeber [5, 6], followed by temperature [6, 7]. But also other factors have been reported to have an effect on the endogenous clock, such as social behaviour and social experiences [8]. The core clock then processes all the external influences to create a rhythmic and oscillating mechanism on a cellular and molecular level, which in turn generates the output. Outputs are considered to be for example, the display of different behaviours (locomotion, feeding, sleep), or changes in physiology (metabolism, body temperature, blood pressure), among other processes controlled by the core clock.

For any process or rhythm to be truly considered as being controlled by a circadian and endogenous clock it has to fulfil three criteria:

1) The process or rhythm has to “free-run” under constant conditions, i.e. even in the absence of external stimuli (Zeitgebers) the rhythm has to continue and repeat its output on a period close to 24 hours [9].
2) The rhythm has to be entrainable, i.e. it has to be able to adjust itself to external conditions, like light or temperature [10].
3) The rhythm has to be temperature compensated, i.e. it has to persist and continue to run stably and periodically even at higher or lower temperatures [11].

The field of chronobiology, like many other scientific fields, immensely profited from the use of *Drosophila melanogaster* as its primary model organism. The journey to uncover the molecular mechanisms of the circadian clock of *Drosophila melanogaster* began with the discovery of the first clock gene *period (per)* in 1971 by Konopka et al. [12]. By performing chemical mutagenesis on *Drosophila* flies, Konopka et al. produced three distinct mutations of the *period* gene, the first displaying no rhythmicity at all, called per^{01}, the second displaying a shortened period with of 19 hours, called per^{S}, and the third one displaying a lengthened period of 28 hours, called per^{L} [12]. Starting from this first revelation, chronobiologists have come a long way until today in slowly unravelling the makeup and components of the circadian clock of *Drosophila melanogaster* piece by piece. The scientific field of chronobiology continues to be a field of great relevance and scientific merit, epitomized by the awarding of the Nobel Prize for Physiology or Medicine to the three most accomplished chronobiologists of today, Jeffrey C. Hall, Michael W. Young and Michael M. Rosbash in 2017.

1.1.1. The molecular mechanism of the circadian clock of *D. melanogaster*

The core molecular mechanism of the circadian clock of *Drosophila melanogaster* is made up of two negatively coupled transcriptional and translational feedback loops (TTFL) that oscillate with a period of roughly 24 hours, enabling the fly to track the time of day reliably, even in constant darkness. At the center of these two TTFLs are the clock proteins Clock (CLK), Cycle (CYC), Period (PER) and Timeless (TIM). During the day the transcription factors CLK and CYC bind as a heterodimer to the E-box sequences that regulate the transcription of the clock genes *period (per)* and *timeless (tim)*, which subsequently leads to the accumulation of *per* and *tim* mRNA in the cytoplasm [13, 14]. Due to the Cryptochrome (CRY)-mediated light sensitivity of TIM,

the concentration of the PER/TIM heterodimer in the cytoplasm does not rise until nightfall, as light-activated CRY can bind to TIM and trigger its degradation [15]. Without the stabilizing effect of TIM, PER is phosphorylated by the protein kinase Doubletime (DBT) and subsequently degraded as well [16]. As a heterodimer the PER/TIM complex can enter the nucleus, mediated through the phosphorylation by the Glycogen Synthase Kinase (GSK-3) ortholog Shaggy (SGG), among other phosphorylation signals [17]. Inside the nucleus the PER/TIM complex then binds to the heterodimer of CLK and CYC via an interaction of PER and CLK, in turn ultimately preventing the CLK/CYC complex from binding to the E-box sequences regulating the transcription of *per* and *tim* [18, 19]. This negative feedback loop of TIM and PER, regulating their own expression, constitutes the backbone of the molecular circadian clock of *Drosophila melanogaster*, by ensuring continually cycling concentration levels of the two core clock components TIM and PER. Interlocked with this negative TTFL is a second negative feedback loop, centered around the rhythmic transcription of the *clk* gene. The heterodimer of CLK and CYC also binds to the E-box sequences that regulate the transcription of the *vrille (vri)* and *PAR-domain protein 1ε (pdp1ε)* genes, which encode for two basic leucine zipper transcription factors [20, 21]. The transcription factors VRI and PDP1Ɛ both interact with the V/P-box in the promoter sequence of the *clk* gene, with VRI inhibiting the transcription of *clk* and PDP1Ɛ activating it [20]. The accumulation and peak concentration of both *pdp1ε* mRNA and the PDP1Ɛ protein lags about three to six hours behind the peak concentration of *vri* mRNA and the VRI protein, creating a cycling concentration of *clk* mRNA, that is in antiphase to the concentrations of the mRNAs of *tim* and *per* [20].

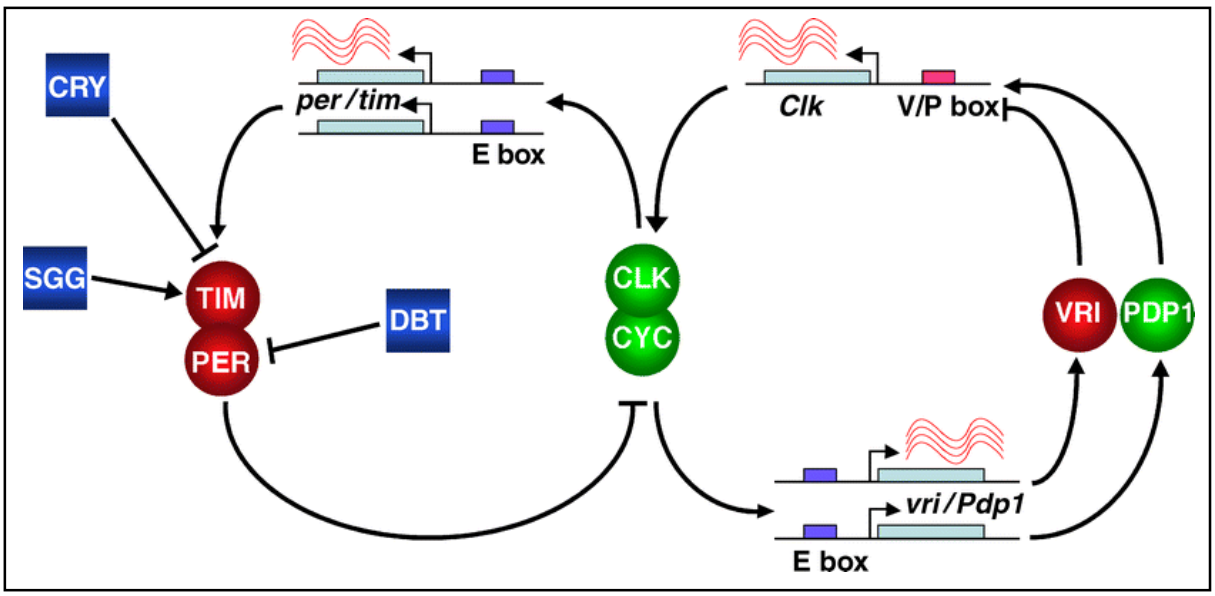

Figure 1.1: Schematic of the core molecular clock of *Drosophila melanogaster;* The heterodimer of the two transcription factors CLK and CYC activate the transcription of the two clock genes *per* and *tim* by binding to specific E-box sequences; As per and tim mRNA levels rise in the cytosol, so do the PER and TIM levels after darkness, as TIM is the target of light-induced degradation via CRY and TIM also protecting PER from degradation via phosphorylation by DBT; PER/TIM enters the nucleus and binds to CYC/CLK to prevent the transcription of *per* and *tim;* CLK/CYC also regulates the expression of *clk* by regulating the expression of VRI and PDP1, who in turn compete for the transcriptional regulation of *clk* with VRI inhibiting and PDP1 promoting it; image taken from Collins et al. [22]

1.1.2. The neuronal clock network of *D. melanogaster*

The neuronal clock network of *Drosophila melanogaster* is made up of roughly 150 neurons, which are all located in the central brain. The clock neurons are mostly organized in clusters and are named after their location in the brain. They are grossly divided into two main groups, the lateral neurons (LNs) and the dorsal neurons (DNs). The DNs are further divided into three sub-groups the DN1s, the DN2s and the DN3s. The cluster of DN1s can be further subdivided into the anterior ($DN1_a$s) and posterior ($DN1_p$s), with the latter $DN1_p$s reportedly playing a central role in incorporating and coordinating input form the Pigment Dispersing Factor positive (PDF) neurons, the s-LN_vs and light input [23]. The DN2s, of which there are only two neurons per brain hemisphere, have been shown to play a vital role in the temperature entrainment of the circadian clock [24]. The role of the largest group of dorsal neurons, the DN3s, has remained unclear to this day. The various subgroups of LNs on the other hand have been extensively researched over the years, with the ventral LNs (LN_vs) having been shown to be essential for robust circadian rhythmicity and having been considered to be the main pacemaker cells of the circadian clock for quite some time [25, 26].

The LN_vs are divided into two distinct groups, the small LN_vs (s-LN_vs) and the large LN_vs (l-LN_vs). The l-LN_vs project into the accessory medulla (aMe) and arborize quite densely on the surface of the medulla, while also projecting into the opposite brain hemisphere via the posterior optic tract/commissure (POT/POC) [27]. The aMe is a ventrally located neuropil that is believed to be an essential “communication center” of the clock neurons, bearing some homologies to the main circadian pacemaker structure of the same name in the cockroach *Leucophaea maderae* [27, 28]. The arborisation pattern of the l-LN_vs coupled with the fact that they have been shown to express Cryptochrome (CRY), a blue light receptor [5, 29], has led to the conclusion that the l-LN_vs most likely deliver light input signals to the circadian clock from the compound eye and the Hofbauer-Buchner eyelet (H-B eyelet), by having their neuronal firing rate be regulated by CRY [30, 31]. The H-B eyelet is located between the retina and the medulla and is believed to be another circadian photoreceptor, as it has been found to be involved in the coordinated expression of Period (PER) and Timeless (TIM) in different subsets of clock neurons [32]. The s-LN_vs are located in close proximity to the aMe and arborize into the dorsal protocerebrum where their fasciculations can be found in close proximity to the DN2s and the DN_p1s, which the PDF-positive s-LN_vs have been shown to signal downstream onto, via the interaction of PDF and the PDF receptor (PDFR) [23, 27, 33]. The s-LN_vs, unlike the l-LN_vs, have also been found to only project and arborize within their respective brain hemisphere and do not project into the opposite hemisphere via the POT/POC [27]. Four out of the five s-LN_vs and also all of the l-LN_vs express PDF, which is widely regarded as a central, internal synchronizer of the circadian clock in *Drosophila melanogaster*, with its demonstrated role in coordinating the oscillations of the clock neurons [34–36] (reviewed in [37, 38]). In several studies, the four PDF-positive s-LN_vs have been shown to be crucial for ensuring rhythmic behaviour under constant conditions [25, 26, 39, 40]. The role of the singular fifth PDF-negative s-LN_v is mostly unclear as of today, although it has been shown to cycle in phase with the LN_ds under constant conditions, with a very high amplitude in TIM and PER concentration and thus is likely an important circadian pacemaker neuron as well [41].

The LN_ds, of which there are six per hemisphere, project into the dorsal protocerebrum where they largely overlap with the fibres from the DNs, making it difficult to pinpoint their exact projection pattern in that area [27, 42]. It could be shown however that some LN_ds also project thin fibres ventrally, towards the aMe, while the main projection

crosses the dorsal fusion commissure, likely innervating the contralateral protocerebrum [27]. The function of the LN_ds is assumed to be quite diverse, suggested by their heterogeneous expression patterns of CRY (three out of six LN_ds are CRY-positive), and other neuropeptides, such as NPF (neuropeptide F – three out of six LN_ds are positive for NPF), sNPF (short NPF – two out of six) and ITP (ion transport peptide – one out of six) [43, 44]. The function and projection pattern of the LPNs (lateral posterior neurons) is mostly unclear so far.

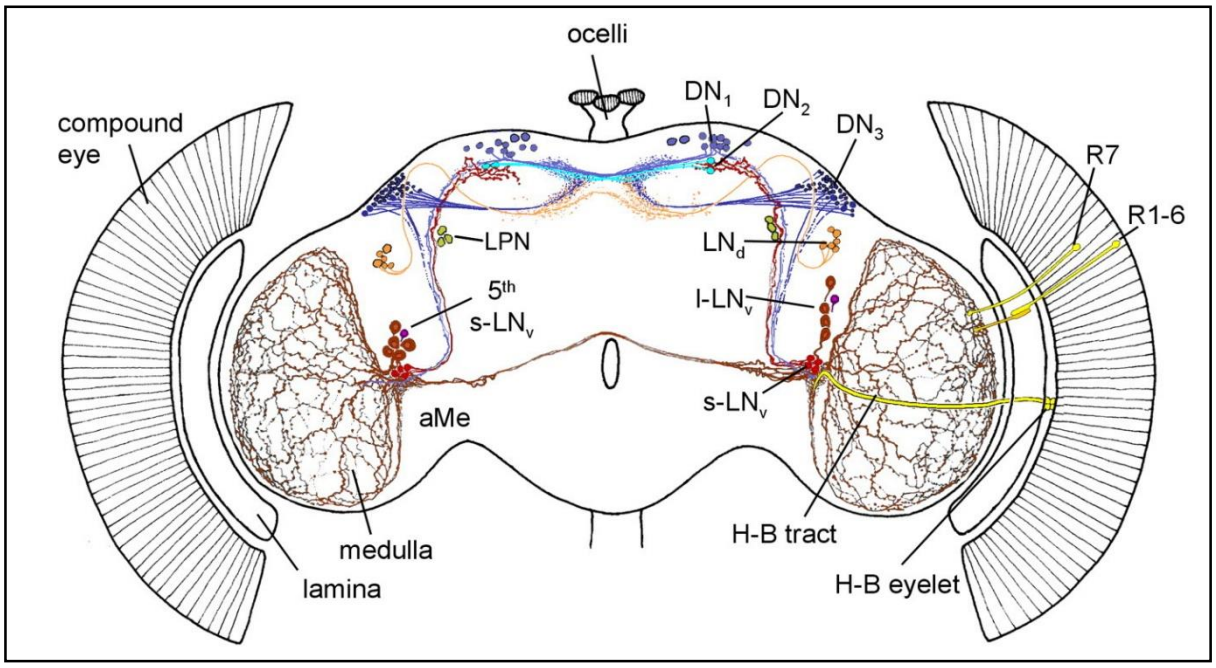

Figure 1.2: All circadian clock neurons in the brain of *Drosophila melanogaster*, along with their presumed neuronal projections; red: PDF-positive neurons (l-LN_vs and s-LN_vs), orange: LN_ds, green: LPNs, violet: 5th PDF-negative s-LN_v, blue: DN1s, light blue: DN2s, dark blue: DN3s, yellow: light input pathways from the compound eye and the Hofbauer-Buchner eyelet via the H-B tract; also marked are the photoreceptor cells R1-6 and R7, and the accessory medulla (aMe); image taken from Helfrich-Förster et al. 2007 [27]

Based on a hypothesis postulated by Pittendrigh et al. in 1976 for nocturnal rodents, a lot of research on the circadian clock of *Drosophila melanogaster* has been focused on establishing the dual oscillator model, which assumes the existence of two distinct oscillators, the E and M oscillator, each governing the respective output of the circadian clock in the morning and in the evening, to adjust the circadian clock to the seasonal changes in regards to the changes in length of day and light intensity [45]. It could be shown that in *Drosophila melanogaster* these two oscillators do in fact exist as proposed and have since been attributed to different clusters of clock neurons. The M oscillator has been assigned to the PDF-positive s-LN_vs, while the E oscillator has been assigned to a more heterologous cluster of cells, including some DN1s, the three CRY-positive LN_ds and possibly the fifth PDF-negative s-LN_v [41, 46, 47]. Recently

however, this rigid hierarchy has been drawn into question again, as the M and E oscillator function could be shown to be more flexible and be able to shift under different environmental conditions and to be not strictly coupled to a defined group of clock neurons [48–50].

1.1.3. The role of Cryptochrome in the circadian clock of *D. melanogaster*

Cryptochromes are flavoproteins and blue light photoreceptors that contain the N-terminal Photolyase-Homologous Region (PHR) domain which binds the chromophore Flavin-Adenine-Dinucleotide (FAD), with action spectra ranging from roughly 350 nm to 500 nm [51]. In *Drosophila melanogaster*, CRY is expressed in the compound eyes and in a number of circadian clock neurons, the l-LN_vs and the s-LN_vs, as well as three LN_ds and some DN1s [29, 52]. The role of cryptochrome in the circadian clock of *Drosophila* is multi-facetted. Among others, CRY has been demonstrated to regulate the neuronal firing rate of the l-LN_vs and has even been shown to enhance the light-sensitivity of the entire circadian clock in a light-independent manner by interacting with actin in the compound eye [31, 53]. But its most important function is unquestionably its light-induced interaction with TIM that leads to a reset of the circadian cycle [15]. Light-activated CRY recognizes and binds TIM, with the resulting complex then being in turn recognized and ubiquitinated by the Jetlag protein (JET) and subsequently degraded in the proteasome [54, 55]. This process restarts the oscillation cycle of TIM and PER levels and in consequence resets the entire circadian clock. The impact of this CRY-mediated light response has been documented by Kistenpfennig et al, who showed that it takes *cry*^{01} mutant flies, which express no functional CRY, about seven days to re-entrain to a new LD light regime, while wild types achieved the same result in one or two days [56]. It has also been shown that CRY-dependent light input to CRY-positive cells is able to induce CRY-independent TIM degradation in CRY-negative cells, therefore revealing the existence of neuronal communication pathway redirecting the light response to other neurons [57]. A bright light-pulse of ten minutes during the night has been shown to be enough to reduce TIM levels to an undetectable concentration in all clock neurons of wild type flies [58]. Also, wild type flies kept under constant light become arrhythmic due to the lack of TIM, further underlining the importance of CRY in the circadian clock [59].

1.1.4. Phase shifting the circadian clock and the Phase Response Curve

The circadian clock of any organism is constantly being entrained by the Zeitgebers that govern it. Very rarely does the endogenous clock of any given organism run with an intrinsic period of exactly 24 hours. Without constant entrainment, even a small divergence of the endogenous period from the Zeitgeber's period would ultimately sum up significantly and end up causing, for example, nocturnal animals to leave their den during the day, where they would likely fall victim to predation. Light plays the most important role in the daily entrainment of the circadian rhythm to the environment [6]. The effect of light pulses during different times of the day has been studied extensively for many years now [60]. The Phase Response Curve (PRC) has been established as a useful tool to gain insight into the circadian clock and its ways of entrainment and its sensitivity to exogenous stimuli. In a PRC, the response of a circadian clock-controlled variable (usually locomotion) to the same stimulus, administered at different circadian times (CT), is recorded and plotted. It is important to distinguish between the circadian time (CT), which refers to the phase and period of the endogenous time of the circadian oscillator and the Zeitgeber time (ZT), which refers to the phase and period of the exogenous Zeitgeber. While aligned under entrainment conditions, the values of CT and ZT are likely to diverge under free running conditions (see Fig. 1.3.). A bright light-pulse of a few minutes during the subjective night is enough to shift the circadian clock of *Drosophila melanogaster*, reset the molecular oscillator and shift the locomotor behaviour into the subjective night, either delaying or advancing the clock depending on the CT the light pulse was applied at [57, 58] (see Fig. 1.4.).

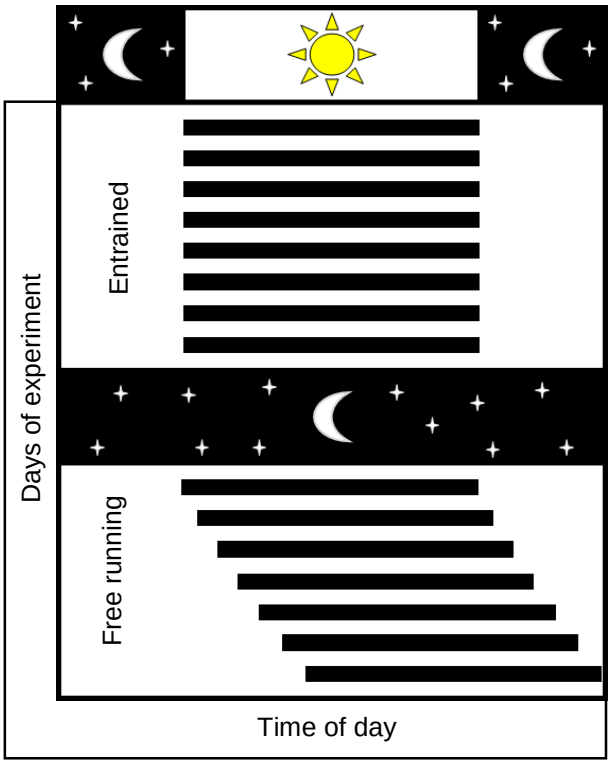

Figure 1.3. Entrainment of a circadian rhythm to a light regime; The initial entrainment to a 24 h light-dark cycle keeps the endogenous rhythm in phase to the exogenous rhythm of the Zeitgeber (light); during constant darkness the endogenous rhythm is free running, slowly diverging from the previous phase set by the Zeitgeber; image adapted from Golombek et al. [61]

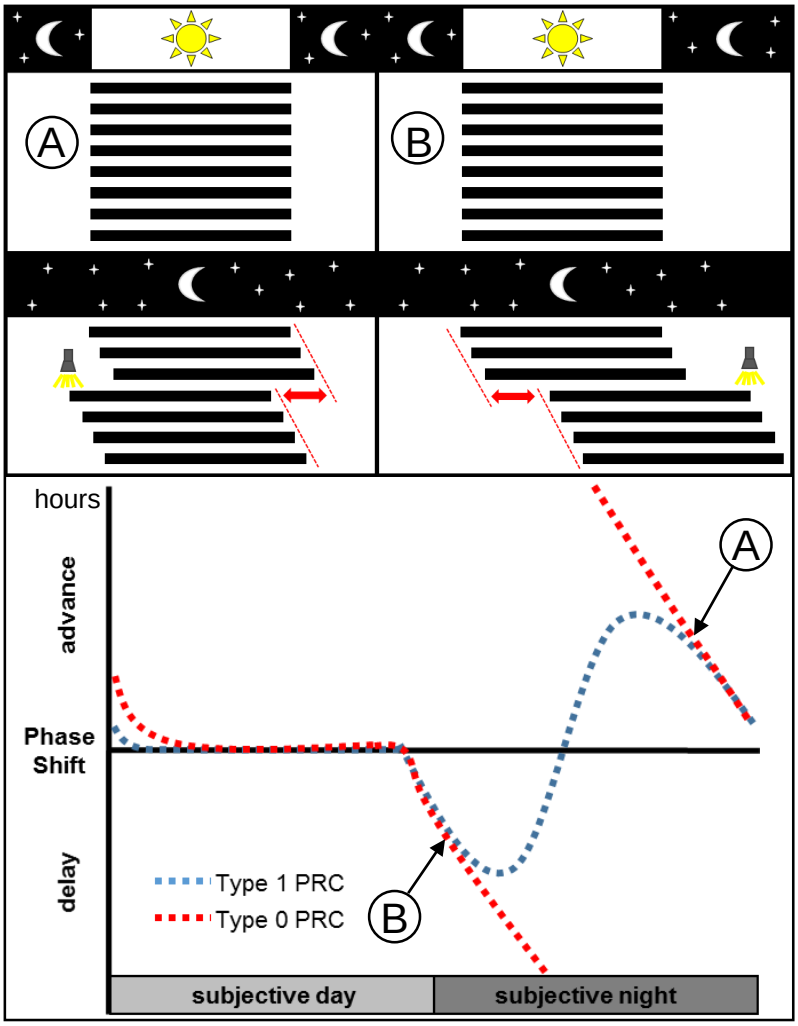

Figure 1.4. top: Two examples of phase shifts of a circadian rhythm, displayed by locomotor activity and evoked by the application of a light pulse during the subjective night (displayed by the flashlight in the actogram) – a phase advance following a light pulse during the late subjective night (A) – a phase delay following a light pulse during the early subjective night (B);
bottom: Two exemplary curves of the two types of PRC; type 0 PRC (strong, dotted line) with large phase shifts and an abrupt transition between phase advances and phase delays, type 1 PRC (weak, solid line) with smaller phase shifts and a gradual transition between phase advances and phase delays; Indicated in the PRC are CTs at which the light pulses from the two exemplary phase shifts might have been applied; image adapted from Golombek et al. [61]

A PRC is obtained, when all phase shifts are plotted against the CT (see Fig. 1.4.). Chronobiology grossly distinguishes between two basic types of PRCs. Type 1 PRCs (weak) display phase shifts of up to several hours and transition gradually between phase delays and phase advances, while type 0 PRCs (strong) show phase shifts of up to 12 hours and transition rather abruptly between phase delays and phase advances [61, 62]. *Drosophila melanogaster* as a species displays a type 1 PRC, but has also been shown to display a type 0 PRC at lower temperatures [63]. During the subjective day in the PRC exists a time span in which stimuli have no phase shifting effect, colloquially called the “dead zone” [60]. Looking at the molecular mechanism of the core clock of *Drosophila melanogaster* (see Fig 1.1.), the reason becomes apparent, as the levels of the TIM/PER heterodimer are already quite low during the subjective day. A light-pulse during the early subjective night will trigger a phase delay, as the pulse is applied during a time at which TIM/PER concentration is still low and *tim* and *per* mRNA levels are very high and can be translated shortly, so TIM and PER concentrations rapidly start rising again, after having been degraded

via CRY during the light pulse. This untimely degradation of PER and TIM however delays the translocation of the complex to the nucleus, causing a phase delay. A light-pulse during the late subjective night will advance the circadian clock, as TIM and PER concentrations are very high and *tim* and *per* mRNA levels very low, due to their transcription having been inhibited by the high levels of TIM/PER for several hours. The light-pulse degrades the TIM and PER prematurely, allowing the CLC/CYC heterodimer to promote the transcription of *per* and *tim* mRNA much earlier than usual, causing a phase advance.

1.2. The science of optogenetics

In chronobiology one of the most fundamental aspects is the research of how the endogenous clock perceives light and incorporates the light information into its oscillating mechanism. The research of the mechanisms of light perception is also at the very center of the comparatively young field of science, called optogenetics. In optogenetics, genetically modified living cells or tissues are controlled via the use of light-application. The cells are modified in a way so that they express certain light-sensitive ion channels in their membranes, giving researchers a spatiotemporally precise method to interact with certain cell types. Optogenetics is most commonly used in the field of neurosciences, where researchers use these light-sensitive ion channels to depolarize or hyperpolarize neurons, either activating or silencing them, in order to monitor the activities of individual neurons in real time and gain insight into the functionality of neuronal networks. Most optogenetic tools that are used are microbial rhodopsins, a class of transmembral proteins discovered in the early 1970s. In 1971 Oesterheld et al. described a transmembral protein called Bacteriorhodopsin from the purple membrane of the *Halobacterium salinarum* that acted as a light-activated outward proton pump, which serves in creating a proton gradient across the bacterial membrane that is used for ATP synthesis [64]. Bacteriorhodopsin was the first microbial rhodopsin to be characterized, but would eventually be followed by many more. In 1977 Matsuno-Yagi et al. discovered the protein Halorhodopsin, a light-driven chloride pump, also in the membrane of *Halobacterium salinarum* [65]. Two more rhodopsins from *Halobacterium salinarum* would later be discovered, Sensory Rhodopsin I (SRI) and Sensory Rhodopsin II (SRII), which respectively function as

positive and negative phototaxis sensors [66–68]. But although the class of microbial rhodopsins, which would eventually become the primary source of tools in the field of optogenetics, had been discovered as early as 1971, it took more than thirty years until neuroscientists started to discover the potential of using microbial rhodopsins in their research. In 2002 and 2003 Nagel et al. discovered Channelrhodopsin 1 (ChR1) and Channelrhodopsin 2 (ChR2), two light-gated cation-channels from the unicellular green alga *Chlamydomonas reinhardtii* [69, 70]. In contrast to Halorhodopsin and Bacteriorhodopsin, which actively pump chloride ions and protons respectively across membranes, ChR1 and ChR2 were found out to be ion-channels, passively transporting cations across the membrane along a electrochemical or concentration gradient. A few years later, studies were published in which ChR2 was demonstrated to be functional in rat hippocampal neurons and HEK cells [71], transgenic *Caenorhabditis elegans* [72] and the retina of mice [73]. These studies marked the beginning of the emerging field of optogenetics and in 2010 finally, optogenetics was named “Method of the Year” by the science methodology journal Nature Methods [74]. In the last eight years the scientific field of optogenetics has continuously grown and expanded in scope until this day, when optogenetic approaches are being used in research about depression and fear memory [75], research about the development of cochlear implants [76] and basic research about associative motor learning [77].

1.2.1. Channelrhodopsin 2 and Channelrhodopsin 2 XXL

Channelrhodopsin 2 is a transmembral protein with seven transmembral helices with an extracellular N-terminus and intracellular C-terminus [70]. All-trans-retinal (ATR) which functions as the channel’s chromophore is covalently bonded to the Lysine 296 as a Schiff Base [70]. Upon illumination with blue light, the ATR isomerizes into a 13-cis-conformation, followed by a deprotonation of the Schiff base, which gets reprotonated later in the photocycle by the Aspartate 156 [78]. The channel undergoes several conformational changes during its photocycle, which are accompanied by varying spectral intermediates, including a refractory phase, during which the channel is closed but unable to be excited by another photon, as it reisomerizes back into its ground state with a time constant of $\tau = 5s$ [79]. It was also shown that along with its function as a cation-channel, ChR2 also actively translocates protons across the

membrane from the cytosol to the extracellular medium, similar to Bacteriorhodopsin, suggesting that its function as a cation-channel was acquired at some point in an evolutionary process [80]. The crystal structure along with data about the pore and the retinal-binding-pocket was provided by the X-ray structural analysis of a chimera protein, called “C1C2” which fused the N-terminal part of ChR1 with the C-terminal part of ChR2, which also confirmed the hypothesis that ChR2 is integrated into the plasma membrane as a heterodimer (see Fig. 1.5.) [81].

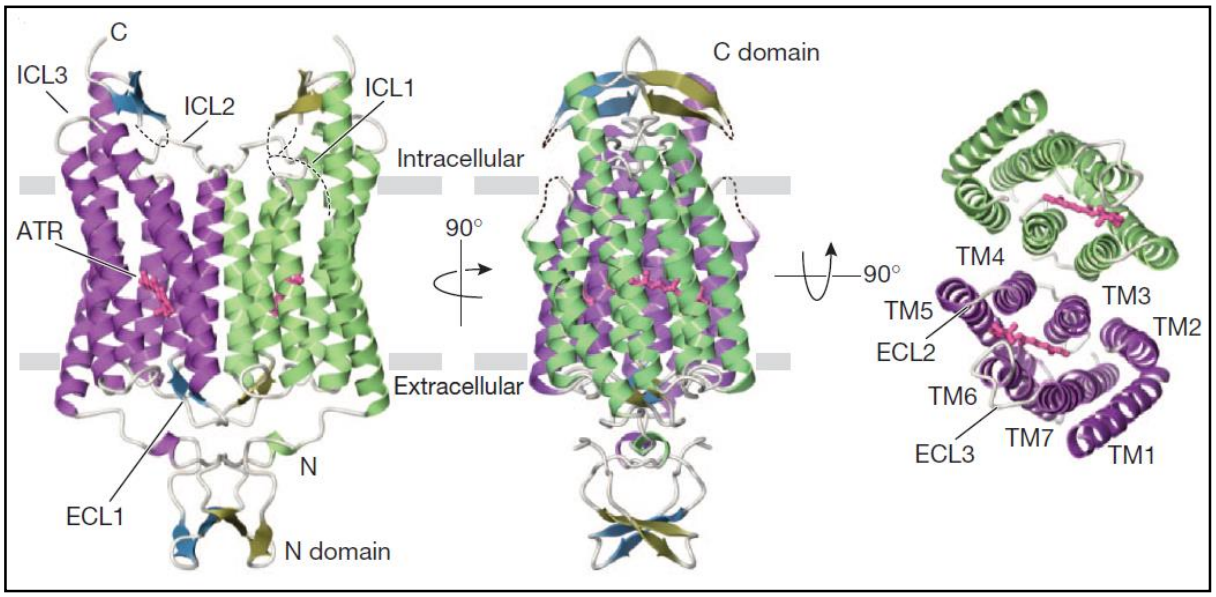

Figure 1.5. Model of the crystal structure of the C1C2 heterodimer viewed from different angles; labelled are the C-terminal and N-terminal domains, the transmembrane helices 1-7 (TM1-7), the intra- and extracellular sides of the membrane, the intracellular loops 1-3 (ICL1-3), the extracellular loops 1-3 (ECL1-3) and the chromophore all-trans-retinal colored in pink (ATR); image taken form Kato et al. [81]

As the number of optogenetic experimental approaches in the neurosciences grew, so did the need for more and more specific and powerful optogenetic tools. Electrophysiologists continued screening the genomes of potential candidates for novel channelrhodopsin variants to be used. Klapeotke et al. for example, described two more extremely useful channelrhodopsin variants, one ultra-fast variant, displaying the fastest closing kinetics measured to this date in the green alga *Stigeoclonium helveticum,* which they named “Chronos” and another variant displaying an extremely red-shifted absorption spectrum, from the green alga *Chlamydomonas noctigama* which they called “Crimson” [82]. Another approach to provide better and more powerful optogenetic tools revolves around introducing point-mutations into the sequence of already established ion-channels like ChR2, usually replacing highly conserved amino-acids in key positions in order to change the kinetic properties of the channel. Among many others, ChR2-variants were found with faster closing kinetics

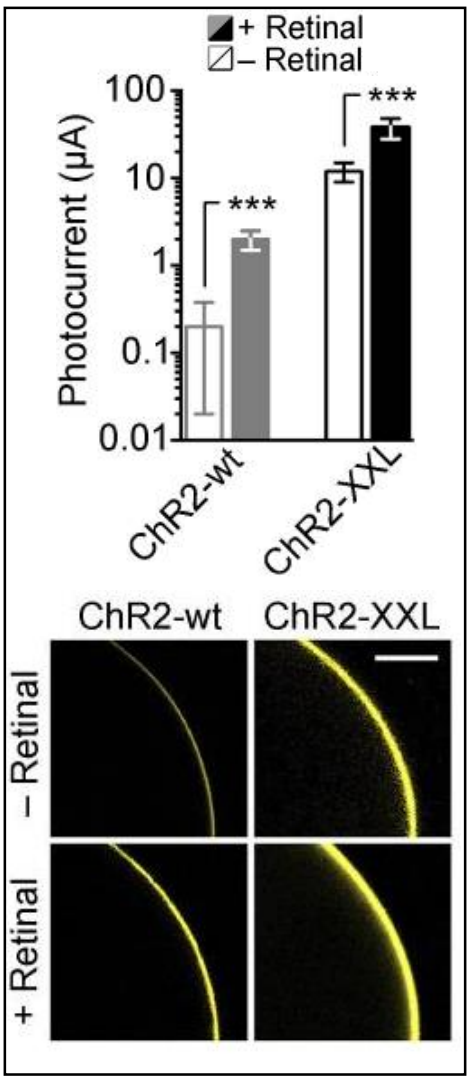

Figure 1.6. top: DEVC-recordings of *Xenopus leavis* oocytes expressing Ch2R-XXL and ChR2-wt upon stimulation with blue light, greatly increased photocurrents of ChR2-XXL comparative to ChR2-wt;
bottom: Representative confocal laser scanning images of *Xenopus leavis* oocytes expressing Ch2R-XXL and ChR2-wt, C-terminally tagged with YFP; images taken from Dawydow et al. [86]

[83], with a higher single-channel conductance for calcium ions [84] or with a higher light-sensitivity [85]. One of these variants obtained by point-mutating a conserved amino acid is the variant named “Channelrhodopsin XXL” described in 2014 by Dawydow et al [86]. Dawydow et al. replaced the Aspartate at position 156, which has been shown to be responsible for reprotonating the Schiff base, with a cystein [78, 86]. This tremendously increased the light-sensitivity of the channel, significantly slowed down its closing kinetics and increased the expression rate of the channel in the plasma membrane of oocytes of *Xenopus laevis* (see Fig. 1.6.) [86]. These photokinetics and the ability to induce relatively high photocurrents with a comparatively low light intensity make Channelrhodopsin 2 XXL especially suited for the use in *Drosophila melanogaster*, as was already demonstrated by Dawydow et al. When expressed in presynaptic motor neurons, ChR2-XXL fully paralyzed flies upon light exposure and driving expression of ChR2-XXL in gustatory sensory cells in the labellum and distal leg segments, enabled the authors to trigger the proboscis extension reflex through light-application [86]. The authors could also successfully use ChR2-XXL to activate large neuronal circuits in order to trigger complex behaviour. By using the fru-GAL4 driver [87], to drive the expression of ChR2 in a sex-specific neuronal network, made up of roughly 2000 cells, Dawydow et al. were able to elicit male courtship behaviour, a series of complex behaviours performed by the *Drosophila* male to court the female, including abdominal bending, proboscis extension and unilateral wing extension to produce a vibrating sound [86, 88].

1.2.2. Olf, CNGA3 and SthK

Despite the numerous successful attempts by electrophysiologists to expand and improve the optogenetic toolbox by altering the existing channelrhodopsin variants or scanning for new ones, some limitations of the channelrhodopsins that are available still exist. To this day, the conductance of the available channelrhodopsins for certain divalent cations, like Ca^{2+} is still quite low. The L132C mutation ("CatCh"), while increasing the conductance of ChR2 for Ca^{2+}, is still significantly more conductive for monovalent cations like Na^{+} or protons [84]. Two attempts to solve this specific issue are the recently described OptoSTIM1 [89] and OptoCRAC [90] which revolve around the interaction of a plant photoreceptor and Ca^{2+} release-activated Ca^{2+}-channels (CRAC), have other restrictions and limitations of their own.

Another desirable tool for optogenetic applications would be a light-gated channel that silences neurons upon activation. In this regard, the recently published anion channelrhodopsins (ACRs), which are highly conductive for Cl^{-} have been published by Govorunova et al. [91], which are also not a uniquely applicable solution, as their functionality depends on the intracellular Cl^{-} concentration and accordingly can't be put to use in any cell type [92]. Another approach at optogenetic targeted neuron silencing is a light-controlled K^{+} channel, published in 2004, for which conduction can be initiated with long-wavelength light and inhibited with short-wavelength light, by using a functional group for selective conjugation to the engineered K^{+} channel, a pore blocker and a photoisomerizable azobenzene [93]. A second light-gated K^{+} channel was published in 2015, named BLINK1 and was engineered by fusing the plant LOV2-Jα photosensory module to the small viral K^{+} channel Kcv [94]. In this thesis, we showcase the application of a novel approach both at a light-activated Ca^{2+} channel and a light-activated K^{+} channel in *Drosophila melanogaster.* Our new approach, which is also described in our scientific publication [95], consists of fusing cyclic nucleotide-gated ion channels (CNGCs) to a light-activated adenylyl cyclase and a light-activated guanylyl cyclase respectively (see Fig.1.7.). For neuronal inhibition we used the recently described cyclic nucleotide-gated K^{+} channel "SthK", named after the organism it was initially identified from *Spirochaeta thermophila* [96, 97]*.* The results published by Brams et al. suggest for SthK to be a highly selective K^{+} channel that can be activated by cyclic adenosine monophosphate (cAMP), but not by cyclic guanosine

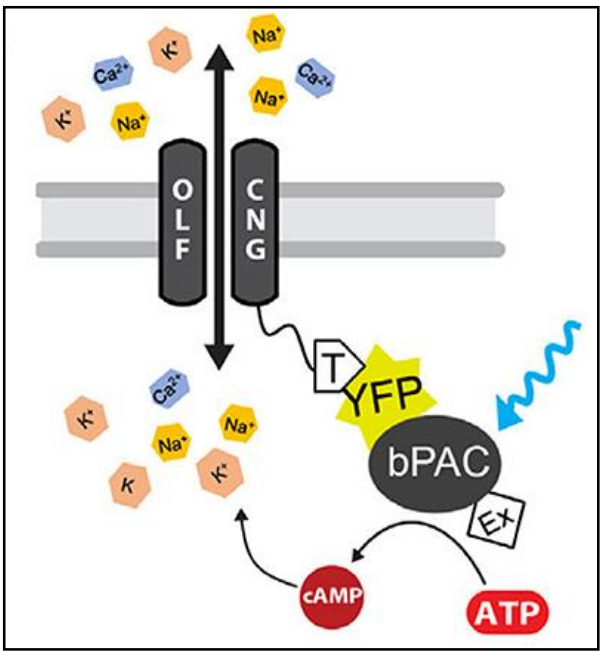

Figure 1.7. Schematic model of the designed fusion construct of a CNGC (OLF) and a light activated adenylyl cyclase (bPAC); additionally indicated is the cyclase function of the bPAC, using ATP to produce cAMP, a yellow fluorescent protein (YFP), fused between OLF and bPAC, the plasma membrane trafficking signal (T) and the endoplasmic reticulum export signal (Ex); image taken from Beck et al. [95]

monophosphate (cGMP), which marks the first time an antagonistic effect of a cyclic nucleotide monophosphate (cNMP) on a CNGC has been demonstrated [96]. The single channel conductance for SthK was reported to be at ~71 pS, with a current of 7,1 pA at +100 mV [96]. For light-gated control of Ca^{2+} conduction we used the CNGC mutant T537S from the bovine olfactory organ, named “Olf” [98]. This channel has been proven to be highly conductive for calcium, with its current having been shown to be entirely carried by Ca^{2+} at an extracellular Ca^{2+} concentration of ~3 mM [99]. Olf has been demonstrated to be sensitive to cAMP as well as cGMP, with an increased sensitivity towards cGMP [98].

Another channel used in this thesis for Ca^{2+} conduction was CNGA3, a CNG channel from canine cone cells, of which genetic mutations have been identified to be responsible for achromatopsia (color blindness) [100]. This particular channel was chosen for being almost non-sensitive towards cAMP, while still being sensitive towards cGMP, in the hope of this resulting in less undesired off-target effects [100]. Like most CNGCs, OLF, SthK and CNGA3 form homotetramers as a functional unit [97, 100, 101].

1.2.3. bPAC and CyclOp

As already outlined in 1.2.3. (see Fig. 1.7.) we used a fusion construct of a CNGC fused to either an adenylyl cyclase or a guanylyl cyclase, for either light-activated Ca^{2+} conduction or light-activated neuronal inhibition via a K^+ channel. Photoactivated adenylyl cyclases (PACs) were first discovered in 2002 by Iseki et al. in the unicellular flagellate *Euglena gracilis* were they were demonstrated to be involved in the protist's photophobic response [102]. A few years later PACs from *Euglena gracilis* were used in oocytes of *Xenopus laevis*, HEK cells and transgenic flies of *Drosophila melanogaster* for the first time for a light-induced manipulation of cAMP levels [103]. For our purposes we used the bacterial PAC (bPAC) described in 2010 from the sulfide-oxidizing soil bacterium *Beggiatoa* [104, 105]. Compared to the considerably large molecular masses of the PACs from *Euglena gracilis*, euPACα and euPACβ, with around 100 kDa, bPAC from *Beggiatoa* consists of only 350 amino acids and was therefore, among other reasons, shown to be a lot more efficient at manipulating cellular cAMP levels [105]. bPAC consists of a blue light-sensing FAD-binding domain called BLUF (sensor of blue-light using FAD) [106], C-terminally linked to a Type III adenylyl cyclase [105, 107]. bPAC has been shown to form a homodimer as its functional unit and has further been demonstrated to be incredibly efficient at increasing cAMP levels [105]. In *Xenopus* oocyctes that were expressing bPAC, the cAMP concentration could be increased from ~3,5 µM to ~140 mM after a 1 minute blue light-pulse [105].

While light-activated adenylyl cyclases have been known for over 15 years now, light-activated guanylyl cyclases on the other hand are a fairly recent discovery, also in the regards of them being available as an optogenetic tool. To enable light-controlled manipulations of cGMP levels in tissues, the already existing adenylyl cyclase bPAC from *Beggiatoa* was mutated at three specific amino acids to change the nucleotide binding specificity [104] and has already been put to use in an optogenetic experimental approach in male rats, aiming to develop a treatment for erectile dysfunction [108]. However there are problems plaguing the mutated "bPGC", like its comparatively low nucleotide specificity, which has the mutant enzyme still producing cAMP alongside cGMP with a ratio of roughly 1:7 [104]. In 2014, a membrane bound rhodopsin type guanylyl cyclase was discovered in the aquatic fungus *Blastocladiella emersonii,* named "BeGC1", where it was shown to be localized at the external surface

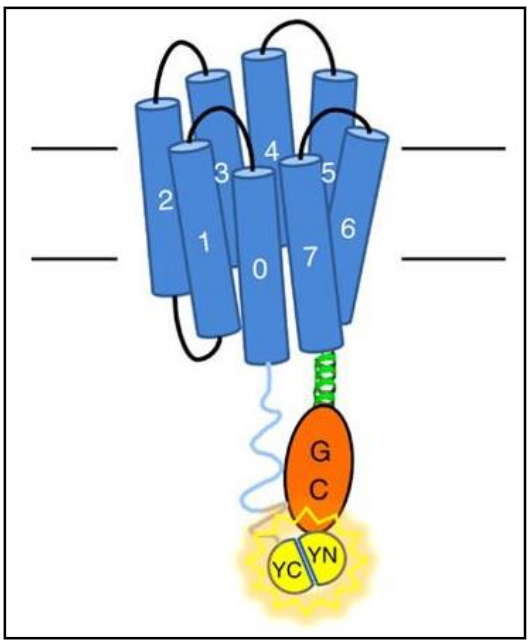

Figure 1.8. Schematic model of the designed BeCyclOp-YFP-BIFC fusion protein; indicated are the eight transmembrane helices (0-7), the guanylyl cyclase domain (GC), the first 155 amino acids of YFP fused to the C-terminal of BeCyclOp (YC) and the last 84 amino acids of YFP fused to the N-terminal of BeCyclOp (YN), image taken from Gao et al. [111]

of the zoospore eyespot, positioned close to the base of the swimming flagellum and was thus hypothesized to be very likely involved in the regulation of the fungus' phototaxis [109]. When transiently expressed in *Xenopus* oocytes, HEK cells, sensory neurons of *Caenorhabditis elegans*, hippocampal neurons and hamster ovary cells, it proved to be a reliable optogenetic tool for fast control of cGMP signalling [110, 111]. Using bimolecular fluorescence complementation (BIFC), fusing the C-terminal 85 amino acids of YFP to the N-terminus of the cyclase and the N-terminal 155 amino acids of YFP to its C terminus, Gao et al. were able to prove the structure of the renamed "BeCyclOp" or "CyclOp" (cyclase opsin) to consist of eight transmembrane helices, with both the N-terminus and the C-terminus located in the cytosol (see Fig. 1.8.) [111]. After adding the enzyme's chromophore all-trans-retinal (ATR) to the cultivation medium of *C. elegans*, which were expressing BeCyclOp in their muscle cells and illuminating the specimen with green light for 15 minutes, Gao et al. recorded roughly a 12-fold increase of the cGMP concentration [111]. Like most other type-III-cyclases, BeCyclOp very likely also forms a homodimer as its functional unit [107, 111]. Because of its evident advantages over the synthetic bPGC, BeCyclOp was ultimately chosen for cGMP mediated activation of the CNGCs used in this thesis.

1.3. Aim of this PhD thesis

The exact and detailed functionality of the neuronal clock network of *Drosophila melanogaster* is not clear to this day. While the roles of certain neurons like the s-LN_vs [25, 26] and the way they signal downstream onto the DNs via PDF [23, 27, 33] are well studied, a lot about the ways in which circadian clock neurons communicate or coordinate the state of molecular clock between each other is still unknown. It appears as if the electrical neuronal activity of the clock neurons is tied to the state of the molecular clock in an intricate way [112]. Artificially introduced electrophysiological activation or silencing of clock neurons has shown to impact the molecular clock of *Drosophila melanogaster* in major ways, like desynchronizing downstream oscillators [113], advancing downstream oscillators [114], or entirely uncoupling the molecular clock from the circadian output [115]. One study that was published while work was in progress on this thesis, used the red-shifted channelrhodopsin Crimson [82] to successfully study the effects of long-period optogenetical activation of circadian neurons on the sleep cycles of *Drosophila melanogaster* [116]. The aim of this thesis was to develop a molecular optogenetic tool, able to precisely and reliably shift the phase of the circadian clock of *Drosophila melanogaster* when expressed in selected clock neurons, while being as minimally invasive as possible in regards to other input pathways of the circadian clock. A thermogenetic approach in this regard by Eck et al. in the same laboratory group had already been successful [117]. Eck et al. used the temperature-sensitive dTRPA1 ion channel [118], to advance or delay the phase of the circadian clock of *Drosophila melanogaster* by applying a temperature-pulse during the subjective night, activating the thermo-sensitive channel [117]. While successful at phase shifting the locomotor output of the circadian clock as well as phase shifting the molecular clock, the handling of the dTRPA1 channel posed some problems and challenges of its own, which could possibly be overcome by an optogenetic approach. Applying a temperature-pulse proved to be of poor temporal resolution. The temperature had to be ramped up to deliver the pulse and ramped down again afterwards and also had to be continuously kept up during the pulse to ensure the activation of dTRPA1 [117]. An optogenetic approach using a brief and precisely timed light-pulse to activate a light-gated ion channel with slow closing kinetics like ChR2-XXL [86] would be much more controllable and of much higher temporal resolution. An optogenetic tool, able to phase-shift circadian neurons by applying a light-pulse would

open up many possibilities of researching the ways circadian neurons communicate with each other. It would, among others, enable researchers to use the tool in live imaging experiments of cultured *Drosophila* brains, monitoring the state of the molecular clock in specific neurons [119, 120]. A group of clock neurons expressing the light-gated ion channel could be selectively phase shifted via light-pulse, while the state of the molecular clock of other clock neurons could be monitored, to see if any might mirror or adapt the phase shift of the exited cells, revealing a direct transmission of the clock state from one neuron to another. The thermogenetic dTRPA channel proved to be unsuitable for such an approach, as the application of the temperature pulse proved to be difficult, while also causing the living brain tissue to expand due to the higher temperatures, disrupting the live-imaging and producing unreadable data [Dr. Dirk Rieger, personal communication]. When work on this thesis begun, some first attempts at influencing the circadian clock of *Drosophila melanogaster* using timed depolarization via ChR2-XXL had already been done by Dennis Segebarth and documented in his Bachelor's Thesis [121]. Segebarth was unsuccessful at evoking significant phase shifts using ChR2-XXL, mainly due to the fact that the respective UAS- and GAL4-control flies also exhibited major phase shifts, following the green light pulses [121]. While work was in progress on this thesis, new optogenetic tools had to be designed in order to further pursue the aim of the thesis. It then also became a secondary aim of this thesis to characterize and publish the newly developed optogenetic tools, establishing them as useful additions to the optogenetic toolbox and effective ways of activating or silencing neurons in live animals. This secondary goal was met and resulted in the publication of the paper "Synthetic Light-Activated Ion Channels for Optogenetic Activation and Inhibition" in the scientific journal "Frontiers in neuroscience" [95].

2. Material and Methods

2.1. The GAL4-UAS system

The most widespread system in *Drosophila* for achieving tissue specific gene expression is the GAL4–upstream activating sequences (UAS) system [122]. In this system, expression of the GAL4 yeast transcriptional activator is brought under the regulation of endogenous tissue-specific enhancers, while the target transgene is cloned alongside an upstream UAS sequence, ensuring the same tissue-specific expression pattern of the GAL4 activator also for the transgene [123]. This system has a number of advantages, the biggest indubitably being its high degree of flexibility. As the UAS-transgene and the GAL4-transgene are kept on separate parental fly lines, any GAL4-line can then be combined with any UAS-line. Once generated, a GAL4-line can be maintained and used as a resource for driving any target UAS-transgene in a tissue-specific manner. Conversely, a UAS-line can have its target gene expressed anywhere by combining it with the respective GAL4-line. One disadvantage of the GAL4-UAS system is its lacking ability of inducing the expression of the transgene. Most GAL4-lines drive the expression very early during larval development, which can cause problems with transgenes that encode toxic gene products [124]. This flaw was starting to be addressed by the introduction of another yeast transcriptional factor, GAL80. In yeast GAL80 antagonizes GAL4 by blocking it from interacting with its target sequences [125]. At first, this setup allowed for even more spatially refined expression patterns. Ultimately, when Zeidler et al. identified temperature-sensitive splicing variants of the yeast ATPase subunit intein and transferred them into GAL80, they created an efficient tool for temporal regulation of the GAL4-UAS system in a temperature-dependant manner [126].

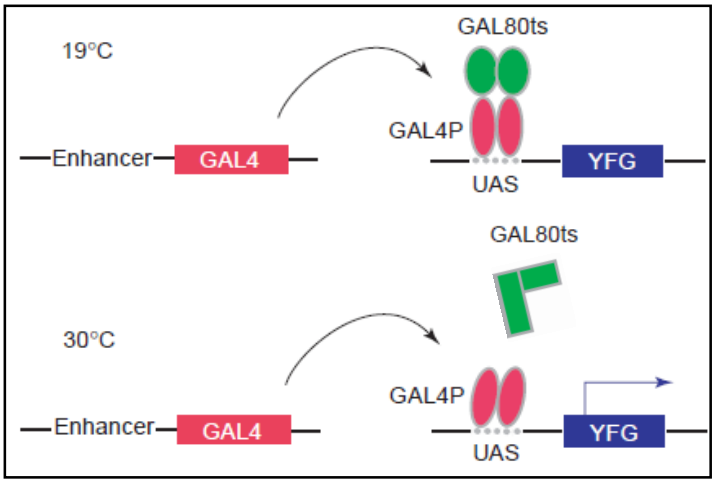

Figure 2.1. Schematic model of the GAL4-UAS system with temperature sensitive GAL80; at 19°C transcription is blocked by GAL80ts; at 30°C GAL80ts is inactive, allowing GAL4 to activate transcription of the target gene; image adapted from McGuire et al. [121]

2.2. Fly lines

All fly lines were reared on standard cornmeal/agar medium (0.8% agar, 2.2% sugar-beet syrup, 8.0% malt extract, 1.8% yeast, 1.0% soy flour, 8.0% corn flour, 0.3% hydroxybenzoic acid, H_2O) at 25°C (18°C for all GAL80-lines) and 60% relative humidity. The flies were subjected to a 12:12 light/dark cycle from 8am - 8pm. The following lines were used in this thesis.

Genotype	Source/Reference
wild types, balancer	
• *w^{1118}*	stock collection - C. Helfrich-Förster; wild type
• *w; CyO/Sco; TM6B/MKRS*	stock collection - C. Helfrich-Förster; balancer
GAL4-lines	
• *w; clk856GAL4; +*	stock collection - C. Helfrich-Förster Gummadova et al. [127]
• *y w; pdfGAL4; +*	stock collection - C. Helfrich-Förster Renn et al. [25]
• *w; mai179GAL4/CyO; +*	stock collection - C. Helfrich-Förster Grima et al. [47]
• *w; clk856GAL4; cry^{01}/TM6B*	stock collection - C. Helfrich-Förster Gummadova et al. [127] Dolezelova et al. [128]
• *y w; pdfGAL4; cry^{01}/TM6B*	stock collection - C. Helfrich-Förster Renn et al. [25] Dolezelova et al. [128]
• *w; mai179GAL4/CyO; cry^{01}/TM6B*	stock collection - C. Helfrich-Förster Grima et al. [47] Dolezelova et al. [128]
• *w; ok6GAL4; +*	stock collection - C. Helfrich-Förster Sanyal S. [129]
GAL80-lines	
• *w; Sco/CyO; tubP-GAL80ts*	stock collection - C. Wegener Bloomington #7018
• *w; clk856GAL4; tubGAL80ts/TM6B*	newly crossed from stock collections - C. Helfrich-Förster, C. Wegener
• *y w; pdfGAL4; tubGAL80ts/TM6B*	newly crossed from stock collections - C. Helfrich-Förster, C. Wegener

Table 2.1a: Parental fly lines used in this thesis; stock collection sources refer to the source from which the thesis' author initially received the fly lines; references refer to the initial publication of the respective line, two or more references refer to the different transgenes within one fly line

Genotype	Source/Reference
UAS-lines	
• *w; UAS-chop2^{D156C}/CyO; +*	stock collection - R. Kittel Dawydow et al. [86]
• *w; UAS-chop2^{D156C}/CyO; cry^{01}/TM6B*	stock collection - C. Helfrich-Förster
• *y^{1} w^{1118}; UAS-OLF-T-YFP::bPac-Ex/CyO;+*	stock collection - R. Kittel (RJK342) Beck et al. [95]
• *y^{1} w^{1118}; 20xUAS-SthK::YFP::bPAC/CyO; +*	stock collection - T. Langenhan (LAT388) Beck et al. [95]
• *w; UAS-bPAC/CyO*	stock collection - M. Schwärzel Stierl et al. [105]
• *y^{1} w^{1118}; Olf-CNG(T537S)::T::YFP::E/CyO; +*	stock collection - R. Kittel (RJK564) Beck et al. [95]
• *y^{1} w^{1118}; UAS-bPAC(R278A)::YFP/CyO; +*	stock collection - R. Kittel (RJK558)
• *y^{1} w^{1118}; UAS-CD8::YFP::bPAC/CyO; +*	stock collection - R. Kittel (RJK560) Beck et al. [95]
• *y^{1} w^{1118}; UAS-Glyco::YFP::bPAC(S27A)/CyO; +*	stock collection - R. Kittel (RJK562)
• *y^{1} w^{1118}; UAS-GOlf-m(R536K)::T::YFP::CyclOp/CyO; +*	stock collection - R. Kittel (RJK566)
• *y^{1} w^{1118}; UAS-GOlf-m(R536H)::T::YFP::CyclOp/CyO; +*	stock collection - R. Kittel (RJK568)
• *y^{1} w^{1118}; UAS-CNGA3::T::YFP::CyclOp/CyO ; +*	stock collection - R. Kittel (RJK570)

Table 2.1b: Parental fly lines used in this thesis; stock collection sources refer to the source from which the thesis' author initially received the fly lines; references refer to the initial publication of the respective line, two or more references refer to the different transgenes within one fly line

2.3. Generating transgenic flies

The new transgenic fly strains created in the context of this thesis carrying UAS-OLF-T-YFP::bPac-Ex, 20xUAS-SthK::YFP::bPAC, UAS-Olf-CNG(T537S)::T::YFP::E, UAS-bPAC(R278A)::YFP, UAS-Glyco::YFP::bPAC(S27A), UAS-CD8::YFP::bPAC UAS-GOlf-m(R536K)::T::YFP::CyclOp, UAS-GOlf-m(R536H)::T::YFP::CyclOp and UAS-CNGA3::T::YFP::CyclOp were generated, as already partially described in Beck et al. [95], by targeted PhiC31 recombinase-mediated insertion into the genomic P[acman] landing site attP-9A[VK18], located on the second chromosome [130]. The transgenic fly strains were generated externally by BestGene Inc. The three transgene sequences UAS-GOlf-m(R536K)::T::YFP::CyclOp, UAS-GOlf-m(R536H)::T::YFP::CyclOp and UAS-CNGA3::T::YFP::CyclOp contain the viral T2a "skip motif". This 18-residue long

motif originally found within the foot-and-mouth disease virus (FMDV) 2A region, produces an apparent cleavage of polyproteins, by not synthesizing an amide bond between the glycine and proline within the sequence [131, 132]. This was done in order to ensure the co-expression of the two transmembral proteins (Olf/ CNGA3 and CyclOp) from one singular transgene. Since the CNGCs from the TRP channel superfamily form a homotetramer as a functional unit [101] and CyclOp forms a homodimer [111], expression of both transmembral proteins as a covalently bonded fusion protein would have very likely been unsuccessful. The two transgene sequences UAS-Glyco::YFP::bPAC(S27A) and UAS-CD8::YFP::bPAC encode for two membrane bound protein domains Glycophorin and CD8. This was done in order to create controls that can be more reliably compared to the 20xUAS-SthK::YFP::bPAC and UAS-Olf-CNG(T537S)::T::YFP::E, as the covalently bonded bPAC would then be anchored to the membrane, as it is when co-expressed with Olf and SthK, instead of being expressed as a soluble protein. Glycophorin is the major glycoprotein of human erythrocytes which spans the membrane as a dimeric complex with the C-terminal ends extending into the cytoplasm of the red cell [133, 134]. CD8 is the mouse lymphocyte marker CD8 [135] that had already been used in *Drosophila* for membrane targeted expression of GFP [125].

2.4. Fly crossings

Crossings between the UAS and GAL4 lines were set up by crossing virgins of one line to the males of the other line. The choice which parental line would be supplying the female virgins and which one the males for one single crossing varied between experiments and was usually based on the availability of female virgins, as those tend to be the limiting factor for most crossings. In the context of this thesis all experimental crossings will be displayed using the following standard, demonstrated on the UAS-Olf-bPAC tubGAL80ts line.

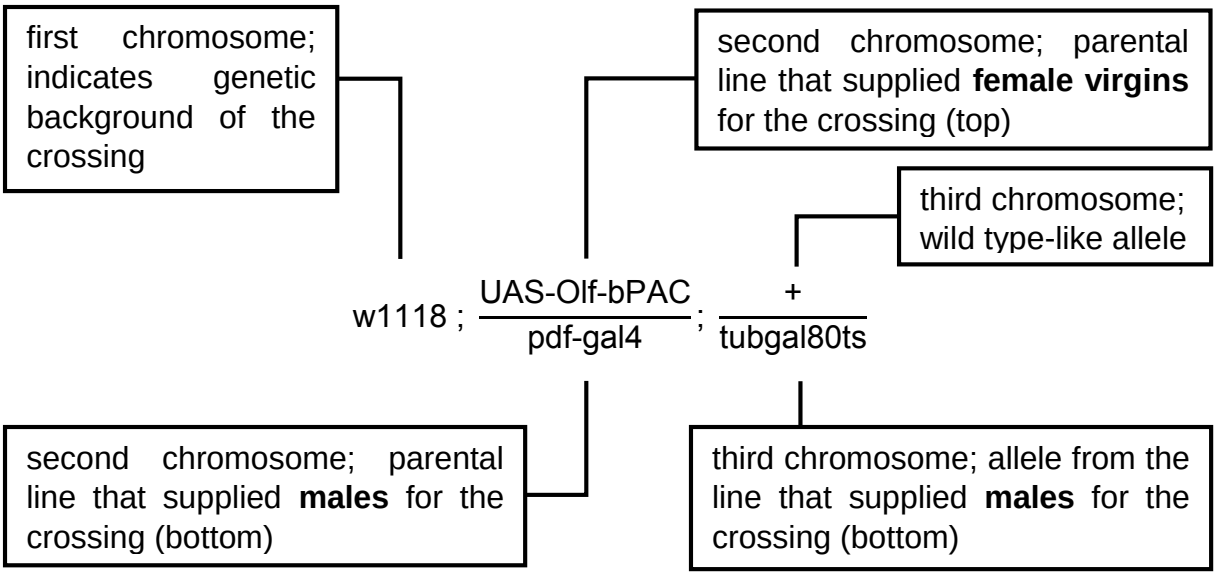

On occasion when displaying data, the strain labels will be shortened for the sake of clearness, omitting certain information like the genetic background on the first chromosome or the entire third chromosome when it bears no relevancy.

Generating the two lines combining GAL4 on the second chromosome and GAL80ts on the third chromosome (*w; clk856GAL4; tubGAL80/TM6B* and y *w; pdfGAL4; tubGAL80/TM6B*; see Table 2.1.) was achieved by first crossing female virgins from *w; clk856GAL4*; + and *y w; pdfGAL4* to males from the double balancer *w; CyO/Sco; TM6B/MKRS* and selecting the males of the F1 generation for the CyO balancer combined with the TM6B balancer. These males were then again crossed to female virgins from *w; clk856GAL4*; + and *y w; pdfGAL4* respectively, this time selecting for the TM6B balancer combined with the MKRS balancer. Flies from this F2 generation then homozygously carried the respective *gal4* transgene on the second chromosome and the TM6B and MKRS balancers on the third chromosome. Males from this F2 generation were then crossed to female virgins from w^+*; ScO/CyO; tubP-GAL80(ts)-7,* selecting for the CyO balancer and the TM6B balancer, generating the two finalized lines *w; clk856GAL4; tubGAL80/TM6B* and y *w; pdfGAL4; tubGAL80/TM6B*.

2.5. Immunofluorescence staining

All imaged *Drosophila* brains displayed in this thesis were prepared and immunostained according to the following protocol.

- Whole flies were collected in the morning (usually at ZT 2, equivalent to 10 a.m.) and fixated on a rotating and inverting tumbler for 3 hours, in a fixating buffer consisting of the following:

  Fixating buffer

  - 4% PFA (Paraformaldehyde) (Sigma-Aldrich)
  - 0,5% Triton X-100 (Carl Roth)
  - 95,5% PBS (Phosphate buffered saline) (Sigma-Aldrich)

- The flies were then washed in 3 steps of 15 minutes each, again on a rotating and inverting tumbler, changing the wash buffer on each step. The wash buffer I consisted of the following:

  Wash buffer I

  - 0,5% Triton X-100 (Carl Roth)
  - 99,5% PBS (Phosphate buffered saline) (Sigma-Aldrich)

- The washed whole flies were then transferred to a small operation tray, filled with wash buffer and placed under a binocular lab microscope. Using two pairs of sharpened tweezers, the flies‘ heads were separated from the torso, after which the skull cuticula was carefully removed, until the brain could be plucked from inside without damaging it and then transferred to a separate dish filled with wash buffer.
- In order to reduce unspecific binding of the antibody, the prepared *Drosophila* brains were then incubated over night at 4°C in a blocking buffer consisting of the following:

Blocking buffer

- 5% NGS (Normal Goat Serum) (Sigma-Aldrich)
- 0,5% Triton X-100 (Carl Roth)
- 94,5% PBS (Phosphate buffered saline) (Sigma-Aldrich)

- After blocking, the *Drosophila* brains were incubated at 4°C for 48 hours with the primary antibody. The incubation buffer for the primary antibody consisted of the following:

Incubation buffer primary antibody

- 5% NGS (Normal Goat Serum) (Sigma-Aldrich)
- 0,5% Triton X-100 (Carl Roth)
- 0,2% NaN^3 (Sodium azide) (Sigma-Aldrich)
- 0,1% primary antibody in 50% Glycerol (Sigma-Aldrich)
- 94,2% PBS (Phosphate buffered saline) (Sigma-Aldrich)

- The brains were then washed in 5 steps of 10 minutes each, being incubated at 25°C with the wash buffer II, which consisted of the following:

Wash buffer II

- 5% NGS (Normal Goat Serum) (Sigma-Aldrich)
- 0,5% Triton X-100 (Carl Roth)
- 94,5% PBS (Phosphate buffered saline) (Sigma-Aldrich)

- For the final step of the staining process, the brains were incubated with the secondary antibody, in the context of this thesis for the most part using the anti-mouse Alexa Fluor antibody line, depending on what the staining needed to illustrate in the respective experiment. If there was also an intrinsic fluorescent tag, like a fusion YFP or GFP (yellow/green fluorescent protein) to be observed, a fluorescent dye was selected whose emission maximum was farthest away from the maximum of the intrinsic fluorescent tag, in order to avoid the two fluorescent signals

overlapping in their respective detection channels. The brains were incubated over night for 24 hours at 4°C. The incubation buffer consisted of the following:

Secondary antibody incubation buffer

- 5% NGS (Normal Goat Serum) (Sigma-Aldrich)
- 0,5% Triton X-100 (Carl Roth)
- 1% Secondary antibody in 50% Glycerol (Sigma-Aldrich)
- 93,5% PBS (Phosphate Buffered Saline) (Sigma-Aldrich)

- Finally the brains were then washed at 25°C an additional time in 6 steps, 10 minutes each with wash buffer II, with the exception of the last step where a 0,1% Triton X solution was used instead of 0,5%.
- The brains were then mounted on a glass slide and embedded in Vecta Shield, a Glycerol-based solution [136] to protect the fluorescent dye and sealed airtight under a glass cover-slip using regular glue. Two glass cover-slips were also placed on the glass slide, framing the mounted brains, to act as a sort of spacer, to prevent the brains from being squeezed by the glass cover-slip above.
- The glass slides with the mounted brains were stored away at 4°C in darkness in order to protect the fluorescent dye, until they were imaged using a confocal laser scanning microscope (CLSM) (Leica SPE).

The following antibodies were used in this thesis:

	Immunogen	Donor Animal	Source/Reference
Primary antibody			
• anti-PDFc7	amidated PDF peptide	mouse	DSHB; Cyran et al. [137]
Secondary antibody			
• Alexa Fluor 488	anti-mouse	goat	Invitrogen
• Alexa Fluor 555	anti-mouse	goat	Invitrogen
• Alexa Fluor 635	anti-mouse	goat	Invitrogen
• Alexa Fluor 647	anti-mouse	goat	Invitrogen

Table 2.2: Antibodies used in this thesis; DSHB as source refers to the Developmental Studies Hybridoma Bank at the University of Iowa, USA

2.6. *Drosophila* locomotor activity recording

All activity recordings of *Drosophila melanogaster* in this thesis were facilitated using the Drosophila activity monitoring system (DAMS) (TriKinetics Inc, USA) [138]. The system utilizes standard built activity monitors that can simultaneously monitor 32 flies that are placed in the monitor inside small glass tubes. The tubes are approximately one third filled with a sugar-agar medium (2% agar 4% sucrose), which serves as food for the fly and are sealed from the other end with a poly-urethane foam plug. The 3-5 days old flies were anesthetized with CO^2 on a pad covered with a paper cloth and placed inside the glass tubes using a small brush and a pair of tweezers. The flies inside the monitors were then subjected to different light conditions and entrainment regimes and/or temperature cycles in a closed off climate chamber. The movement of the flies is tracked by the monitor with an infrared beam going through the middle of the tube. Every time the fly crosses the beam, the system's software marks the crossing on a plot, creating a so called actogram, a graphical display of the fly's activity throughout the day. The experiments were recorded in a cooling incubator (MIR-553; Sanyo Electric Co. Japan) or in a custom built large climate chamber. Entrainment light in the incubator was supplied by fluorescent lamps (Pollin Electronics GmbH, Germany), which were wrapped in 50% or 90% neutral density gel-filters (Rosco Laboratories, Inc. USA) or a red gel-filter (#27 MED RED, 5% transmission at 620 nm) (Rosco), depending on the experiment. Some DAMS recordings were performed after the flies had been fed ATR 24h hours prior to the experiment. In that case, 200 µl of 1 mM ATR in 99,9% EtOH were pipetted directly onto the cornmeal/agar medium inside the glass tubes. After the EtOH had dried, the flies were put on the medium for 24h.

2.7. Phase shift experiments

The fundamental goal of this thesis was to use optogenetic tools to evoke phase shifts of the circadian clock of *Drosophila melanogaster* by activating and stimulating the neurons of the circadian clock network with the help of the optogenetic tools expressed within their membranes. To apply the light-pulses needed to activate the optogenetic tools expressed in the neurons, two different technical approaches were employed. One of these approaches made use of the already established entrainment boxes,

used within the laboratory group. The boxes are ventilated and shielded from outside light sources and are able to fit up to three DAMS monitors. Light for the flies' entrainment is provided by seven sets of LEDs of different wavelengths built inside the boxes' ceiling, behind a matte glass plate for equal and diffuse light dispersion (375 nm, 405 nm, 420 nm, 470 nm, 530 nm, 574 nm, 660 nm).

Entrainment Box Advantages

- Variable light-pulse wavelength
- Variable total light intensity

Entrainment Box Disadvantages

- Overall low light intensity (maximum of ~1,5 µW/mm² at 530 nm)
- Light source from above does not guarantee for each individual fly to receive the same amount of light intensity (flies seated at the top of the monitor receive higher light intensity; flies might hide underneath the monitor's cross section to receive almost no light)

The other method employed light application devices, especially constructed for the purpose of this thesis that used glass fibres to apply laser light directly into the front of the glass tubes the flies were placed in, from the side that is usually sealed with a foam plug in other experiments. In this thesis, two sets of those devices were used, one powered by a 532 nm laser and one by a 470 nm LED.

Glass fibre Device Advantages

- Higher overall light-intensity (up to ~2 mW/mm² at 532 nm and ~100 µW/mm² at 470 nm
- Able to apply light-pulse to the flies always from the same angle and distance

Glass fibre Device Disadvantages

- Light intensity was not distributed evenly across all fibres
- only two wavelengths available (470 nm and 532 nm)

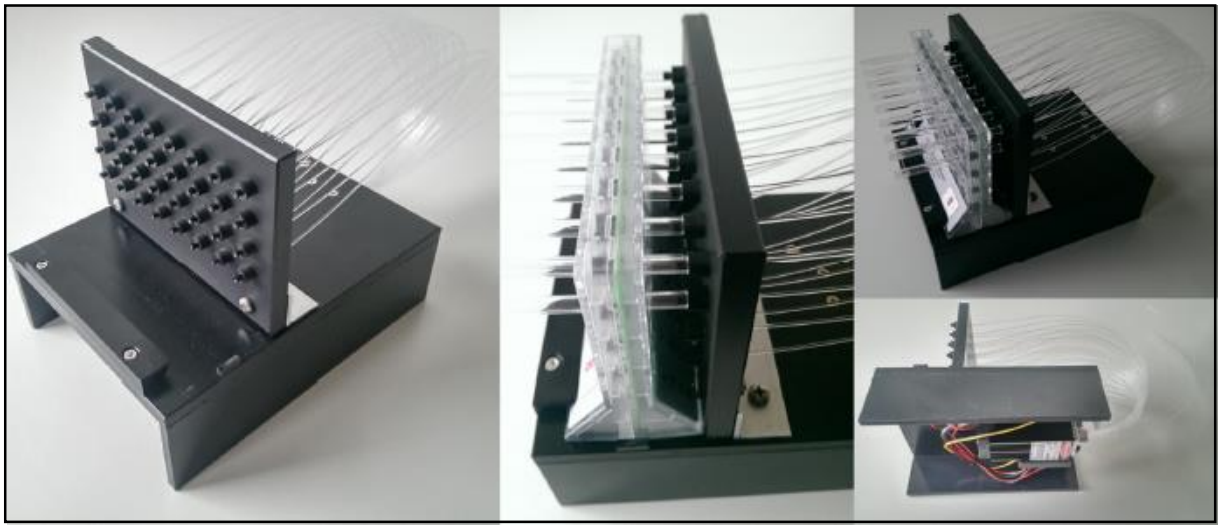

Figure 2.2. Depiction of the used laser application devices; glass fibres extend from the laser directly into the glass tubes, ensuring equal illumination angles; image taken from Dennis Segebarth, Bachelor's thesis [121]

Over the course of this thesis both approaches have been applied extensively and repeatedly. For each experiment described, it will be noted which approach had been used. Later during this thesis, the glass fibre devices were added another device, called PULSETRAIN, which made it possible to program even more precise light-pulses with a higher frequency than what had been possible with the previous programming. Phase shift experiments that were conducted during the later stages of this thesis were therefore able to employ more precise light-pulses. All light-pulses in this thesis were always applied as early as possible following the respective 12:12 LD or RD entrainment period. This was done in order to ensure that all recorded flies' circadian clocks would be depolarized at the same CT, or at least approximating the same CT for all flies as closely as possible. As the period length varies from each individual fly to the next, letting several days pass after the 12:12 entrainment period before applying the light pulse would result in every fly having its circadian neurons depolarized at a slightly or even vastly different CT, generating differing and incomparable phase shifts, according to the PRC (see Introduction 1.1.4.). An experimental protocol like this constitutes a modification of Aschoff's type II method for determining phase shifts and phase response curves (PRCs) [139].

2.8. Locomotor activity data analysis

The locomotor activity of the flies was recorded as text files and displayed as an actogram using the Fiji plugin ActogramJ [140]. Every time a fly seated in a monitor crossed the infrared beam in the middle of the tube, the software would mark this event on the actogram, resulting in a graph-like dataset, displaying locomotor activity as a function of the time of day.

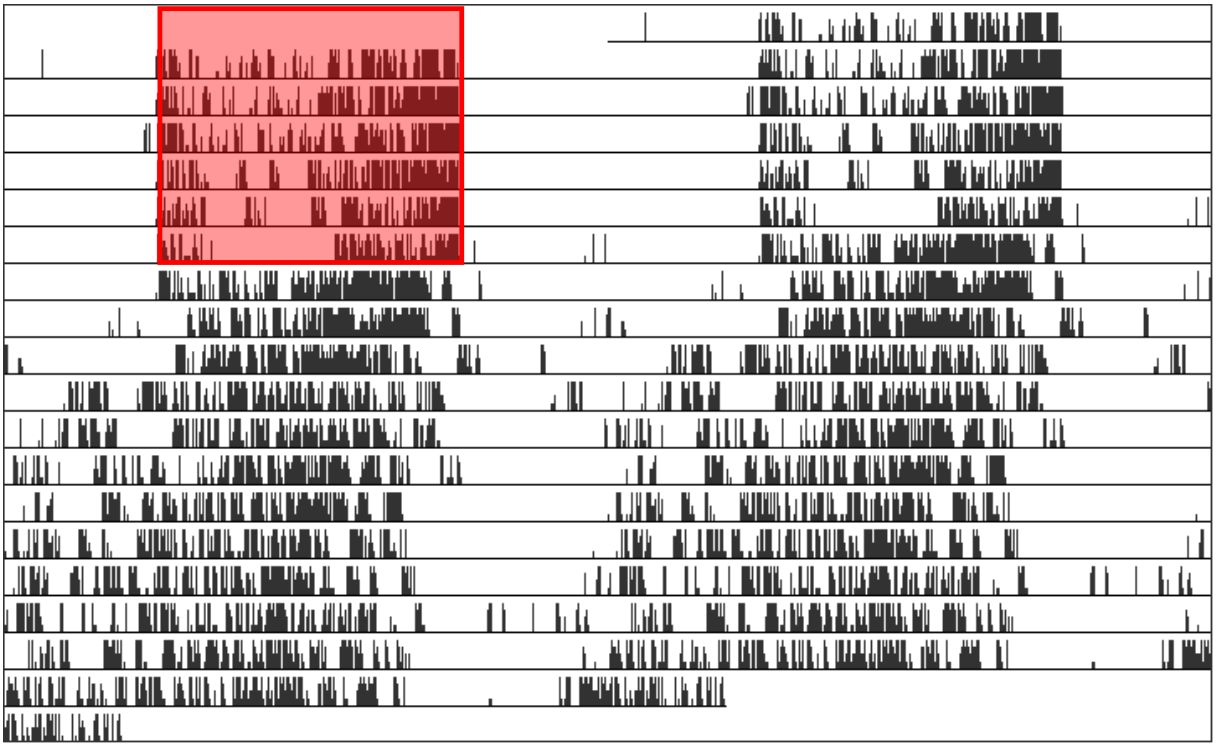

Figure 2.3: Exemplary actogram of a wildtype w^{1118} fly entrained by a 12:12 RD light regime; double-plotted, red shading indicates the 6-day 12:12 RD entrainment period.

For the sake of clearness, all actograms in this thesis are displayed without the time of day being indicated anywhere on the actogram. As the flies are sealed off from the outside world, the ZT set by the entrainment light is the only relevant time for these experiments. Usually the 12:12 RD entrainment regime that was used to synchronize the flies was programmed from 8 a.m. to 8 p.m. in order to continue the light regime that the flies were used to from the climate chambers. All actograms in this thesis are displayed as double plots, as demonstrated in Fig. 2.3. Double-plotted means that the right hand side column of the actogram is an exact copy of the left hand side column, except being advanced by 24 hours. This display makes it easier and more obvious to track endogenous periods that are longer or shorter than 24 hours. On a single-plot

such periods would “run” out of the frame on either side and “re-enter” the frame from the opposite side, making it difficult to track the endogenous period at a glance. Further, the double plot allows for a better graphic visualisation of all relevant entrainment data, while simultaneously providing the viewer with an unobstructed look at the locomotor data. All actograms in this thesis will be displayed as exemplified in Fig.2.3. and Fig 2.4., with all relevant data regarding light-entrainment period, light-pulses, temperature gradients or activity offsets being graphically indicated on the left hand side of the actogram, while the right hand side features no graphical indicators, providing an unobstructed view at the locomotor data.

Phase shifts were calculated using the automated ActogramJ software for calculating and displaying activity offsets. Activity offsets were calculated individually for the 12:12 RD or LD entrainment period and the DD period following the light pulse. The phase shift was then assessed optically using the ActogramJ eye fit tool (see Fig 2.4).

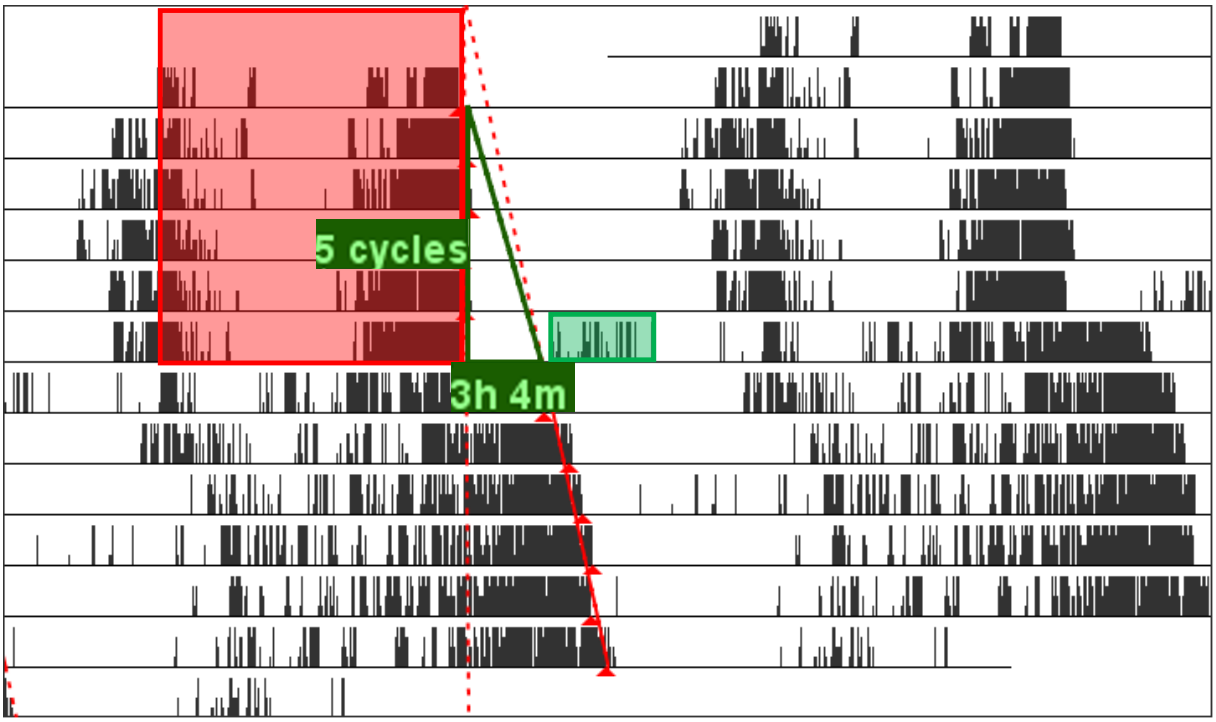

Figure 2.4: Exemplary actogram of a fly exhibiting a phase shift following a 2h green light pulse; Red shading indicates the 6-day 12:12 RD entrainment period; green shading indicates the 2h green light pulse; also indicated are the software-calculated activity offsets (red) and the phase shift assessed manually using the eye fit tool (green)

Averaged actograms were generated using a Microsoft Excel macro written by Pamela Menegazzi, which accessed the text files generated by the DAMS and drew a finalized graph in which the locomotor activity of the entire input sample group was averaged

for every minute of the day. To smooth out the finalized graph, each plot value (beam crosses per minute) was an average of five raw locomotor values, including the respective plot value itself, as well as the two plot values before and after.

2.9. FIMtrack larval assay

The larvae locomotion experiments in this thesis were done using the already established technology FIM [141, 142] and the accompanying processing software FIMtrack [142, 143]. The technology is an FTIR-based imaging method (frustrated total internal reflection), abbreviated as FIM [141]. In this setup, animals are only illuminated with infrared light at the very specific position of contact with the underlying crawling surface [141]. The larvae imaged for this assay were all reared in constant darkness, to avoid any exposure to light.

For the assay, 3 – 5 days old instar-3 larvae were placed on flat disc made from 1,5% agarose, 85 millimeters in diameter, which was seated atop the FIM recording device which contained the infrared light sources. The images were recorded from an infrared camera seated underneath the device, picking up the infrared light waves scattered by the agarose and the larva crawling on top. The recordings were taken at a frame rate of 1 frame per second. For the control light conditions, ambient red room light was used. For blue light illumination two LED arrays were used, one portable and one stationary, both at 470 nm wavelength, with the portable array having an effective light energy output of 25 µW/mm² and the stationary having an effective light energy output of 1,6 mW/mm². The larvae's movements were recorded under different conditions of illumination, varying both in intensity and exposure time. Two basic schemes of illumination and recording were deployed, one for measuring the maximal phenotype after long and strong illumination and one for observing the phenotype's recovery.

Maximal phenotype

- 30 seconds red light conditions
- 30 seconds blue light illumination (1,3 mW/mm²)
- 60 seconds full recording time

Phenotype recovery

- 30 seconds red light conditions
- Short blue light pulse (0,2 s – 2 s) (25 µW/mm²)
- Variable recording length until larva mobility was fully restored

The software used to process and evaluate the recordings was the established, free-to-use software FIMtrack, developed by the IT-department of the University Münster [143]. It can track individual larvae in the recorded material from frame to frame and calculate different parameters about the larva's size, movement and shape. In the context of this thesis and the accompanying published research paper [95], two tracked parameters were used to characterize the phenotypes of the optogenetic tools expressed in motor neurons of *Drosophila* larvae.

- "Momentum distance"
  The distance travelled by the larva's center of mass from one frame to the next, measured in pixels [143]. As the recording rate for all recordings was always one frame per second, the parameter "momentum distance" was equal to the velocity in pixels per second
- "Spine length"
  The body length of the larva measured from head to tail in pixels [143].

For the final evaluation of the data, all units were converted from pixels to micrometers, using the known diameter of the agarose disk in SI units (85 mm) and the diameter in pixels measured by the program as the value for the conversion.

2.10. Statistics

All statistical analysis in this thesis was conducted using R. Each dataset was first tested for normal gaussian distribution using a Shapiro-Wilk test. If all datasets followed a normal gaussian distribution, a pairwise-t-test was performed with Bonferroni correction. If one or more datasets did not follow normal gaussian distribution, a pairwise Wilcox-test was performed with Bonferroni correction. Differences were considered significant at p-values smaller than 0.05. One star (*) indicates a p-value smaller than 0.05, two stars (**) indicate a p-value smaller than 0.01 and three stars (***) indicate a p-value smaller than 0.001.

3. Results

3.1. Channelrhodopsin XXL

3.1.1. Shift experiments in a CRY-negative background

The very first shift experiments using Channelrhodopsin XXL were mostly based off of the data already assembled by Dennis Segebarth in his Bachelor's thesis [121]. Segebarth had used specimen of *Drosophila melanogaster* expressing Channelrhodopsin XXL, (see Introduction 1.2.1.), in different subsets of circadian neurons in order to influence the circadian clock with timed depolarization of the circadian neurons via a series of triggered light pulses [121]. Segebarth's experimental design was in turn largely based off of the work of Eck et al. who used the thermosensitive dTRPA1 channel to evoke phase shifts in *Drosophila* flies, expressing the channel in circadian neurons, using timed temperature pulses during the respective advance and delay zones of the phase response curve (see Introduction 1.1.4), in order to depolarize the respective neurons and trigger the shift [117].

Segebarth however was unable to replicate the significant phase shifts produced by Eck at al. with the ChR2-XXL test-lines. The phase shifts of the flies expressing ChR2-XXL were always as large, or even smaller in some instances, than those of the respective UAS- and GAL4-controls, basically showing no sign of any significant effect that the timed depolarization of ChR2-XXL might have had on the phase shifts of the circadian clock [121].

The first experiments conducted as part of this thesis, were designed around identifying the factors that had caused for Segebarth's experiments to not produce the desired results and eliminate them in any future experimental setups.

Segebarth had used a 12:12 RD entrainment to synchronize the flies, in order to avoid any light-triggered depolarization during entrainment prior to the programmed light pulse [121]. An RD light regime stalls the natural cycling of CRY, a blue light receptor, which is integral in resetting the circadian clock every morning, since red light is unable to activate CRY (see Introduction 1.1.3.) [51, 56]. We hypothesized that as a result, CRY levels in the circadian neurons slowly rise over time under an RD light regime and that upon illumination during the programmed light pulse, this elevated CRY level would then cause a massive degradation of the TIM:PER complex, resulting in a reset

of the circadian clock [5, 15], overriding or masking any effect that the neuronal depolarization, facilitated by the ChR2-XXL, might have had.

We decided that further shift experiments involving ChR2-XXL would be conducted in a CRY-negative background, using the *cry01* line, which has no CRY [128]. The rest of the experimental parameters were largely kept the same as in the experiments conducted by Segebarth, using a 12:12 RD entrainment and a two hour light pulse during the delay zone of the phase response curve [121]. The two hour light-pulse was programmed not as a continuous illumination, but rather as a series of two second light flashes every two minutes, as to minimize the light exposure while hopefully still triggering the maximal depolarizing effect of the ChR2-XXL, due its prolonged open state [86].

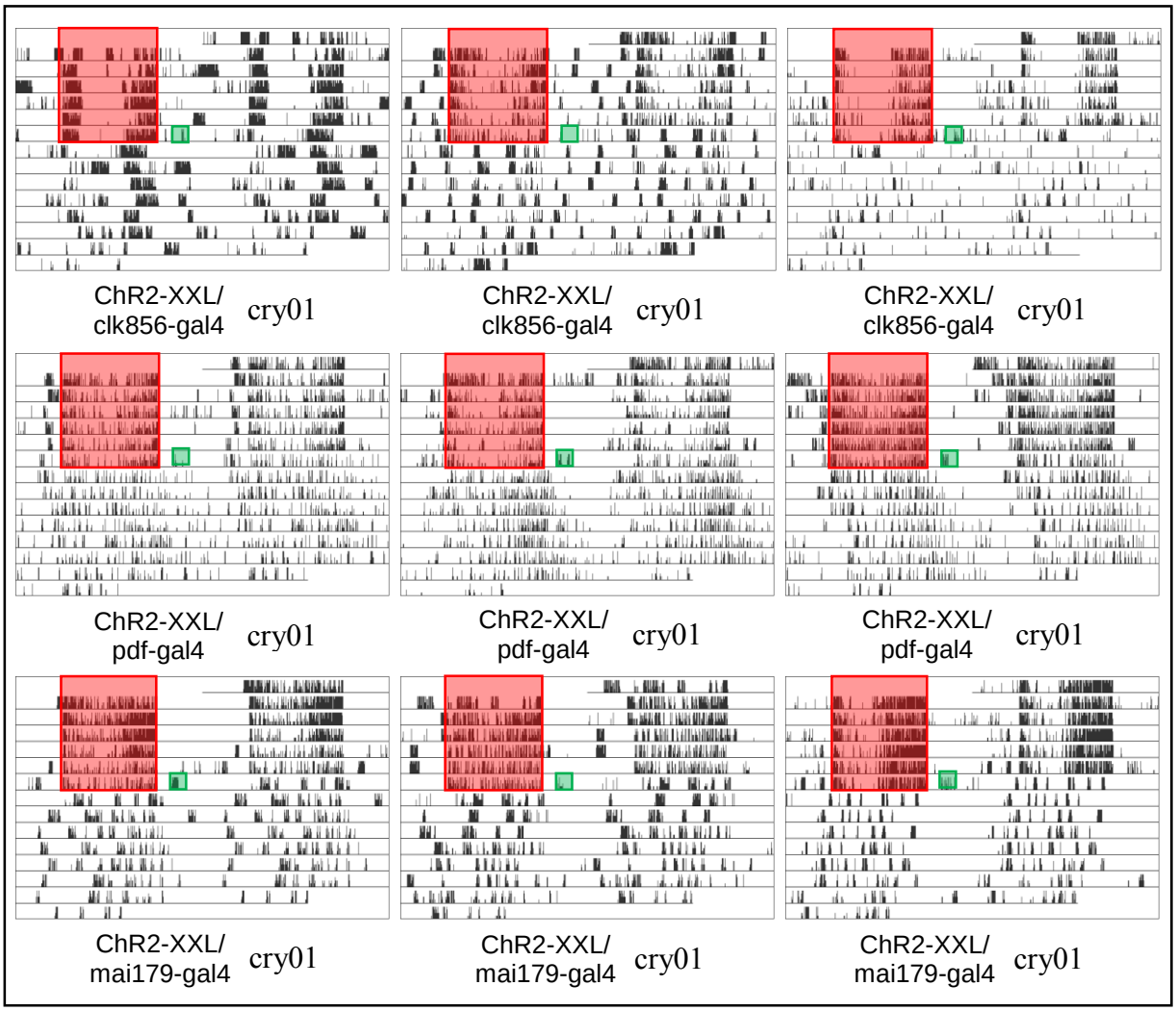

Figure 3.1.1a.: Sample actograms of flies expressing ChR2-XXL in all circadian neurons (clk856-gal4), all PDF-positive neurons (pdf-gal4) and the mai-subset (mai179-gal4) all in the homozygous *cry01*-background; red shading indicates 12:12 RD entrainment (620nm; ~5 µW/cm²) green shading indicates light pulse (532nm; ~0,1 - ~2 mW/mm²; pulse-interval: 2s flash every 2min for 2h); no shading indicates darkness; 25°C 60% RH

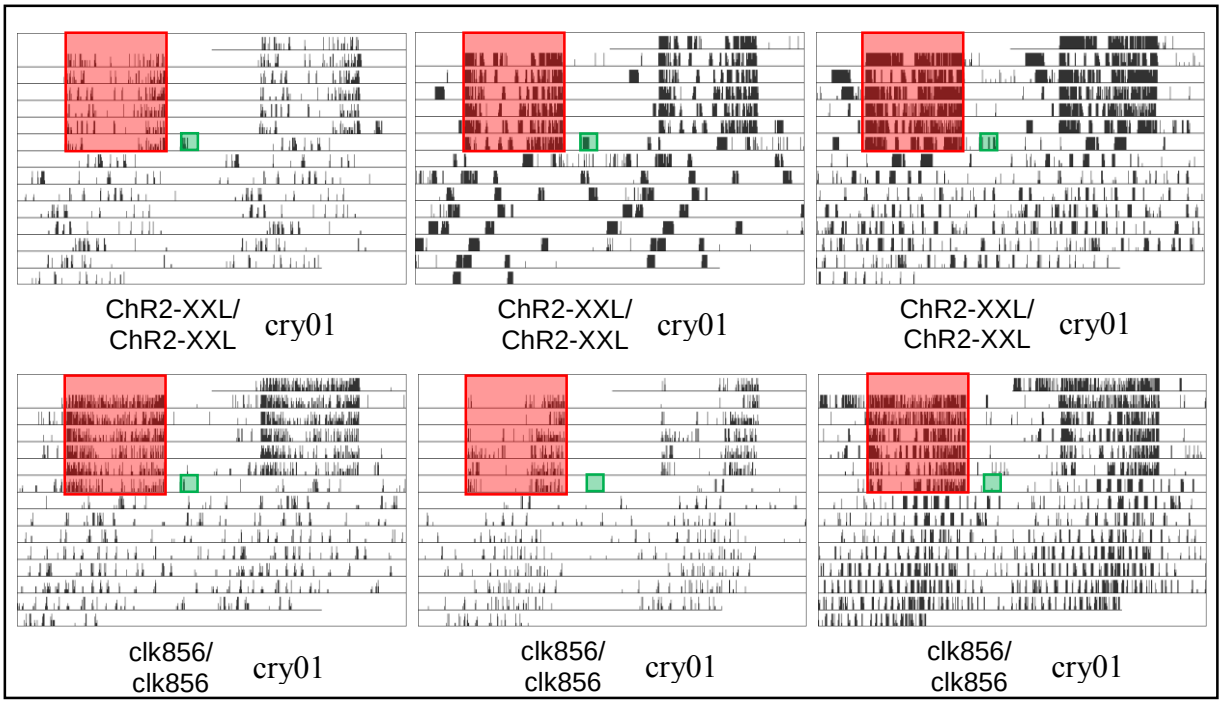

Figure 3.1.1b.: Sample actograms of flies expressing no ChR2-XXL anywhere, in the homozygous *cry01*-background (respective homozygous UAS- and gal4-controls to Fig 3.1.1a); red shading indicates 12:12 RD entrainment (620nm; 5 µW/cm²) green shading indicates light pulse (532nm; ~0,1 - ~2 mW/mm²; pulse-interval: 2s flash every 2min for 2h); no shading indicates darkness; 25°C 60% RH

The shift experiments with flies expressing ChR2-XXL in circadian neurons in a CRY-negative background yielded very poor results. It appeared that introducing the *cry01* background into the respective GAL4- and UAS-lines rendered almost all the tested lines arrhythmic or at least caused the specimen to display an extremely poor rhythmicity in DD (see Fig. 3.1.1a & Fig. 3.1.1b). Flies expressing ChR2-XXL in all circadian neurons (clk856-gal4) appeared to be almost completely arrhythmic while flies expressing ChR2-XXL in the PDF-positive neurons (pdf-gal4) and in the mai-subset (mai179-gal4) did display some residual rhythmic activity patterns, but no activity offsets that were clear and distinct enough in order to calculate any phase delays. The homozygous UAS- and clk856-GAL4-controls displayed a comparatively bad rhythmicity. The experiment was repeated twice more, with almost identic results, leading to the conclusion that a CRY-negative background was not the desired solution that had been hoped for. The experiments with the *cry01* lines were discontinued accordingly.

3.1.2. General functionality of ChR2-XXL

Before any new experiments using other light wavelengths for entrainment were conducted, it was tried to estimate the effect of white light on ChR2-XXL in the neurons. To this end, flies expressing ChR2-XXL in the motor neurons (ok6-gal4) were recorded in a 12:12 LD entrainment using white light of varying intensities. Doing this, it was tried to find an entrainment condition that would activate the expressed ChR2-XXL as little as possible, while at the same time still ensuring that the cryptochrome inside the circadian neurons was able to cycle naturally. As a readout for the activity of ChR2-XXL in the motor neurons of *Drosophila melanogaster*, it was decided to compare the activity rate of the tested flies under the different entrainment light-intensities.

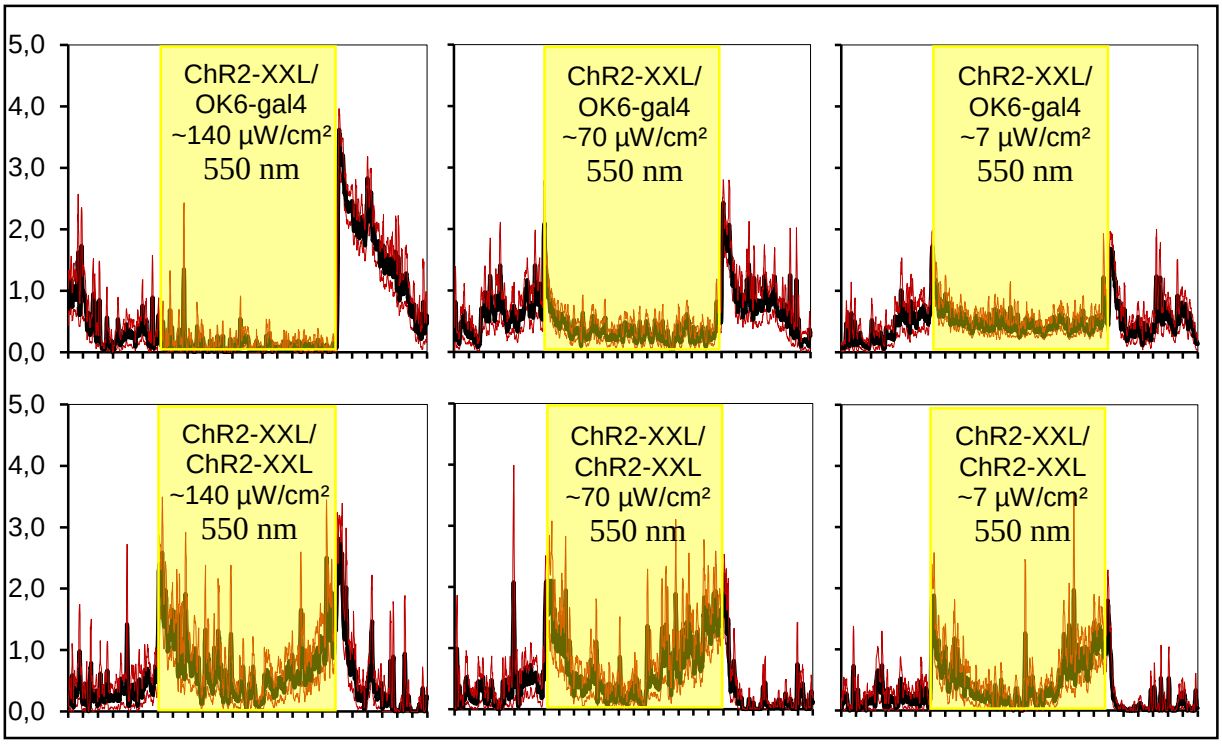

Figure 3.1.2.: Averaged actograms of flies expressing ChR2-XXL in the motor neurons (ok6-gal4) and the respective homozygous UAS-control; yellow shading represents cycle of 12:12 LD with indicated intensity; for each genotype three days were recorded under each respective light condition and used for data averaging; only flies that survived the 9 day experiment were used for data averaging; 25°C, 60% RH

The activity rate of the flies expressing ChR2-XXL in the motor neurons in comparison with the homozygous UAS-controls clearly demonstrates the strong effect of the ChR2-XXL on the flies' mobility. Under all three light intensities, the flies expressing ChR2-XXL displayed a clearly diminished activity rate compared to the controls (see Fig.

3.1.2.). At an intensity of roughly 140 µW/cm² the ChR2-XXL flies barely moved at all during illumination and appeared to be mostly paralyzed. At the end of the 12 hour illumination period the flies also displayed a large surge in activity lasting for a few hours. This activity surge could be seen as a sort of compensation for the 12 hours of paralysis that came before, during which the flies likely feed after having been starved for 12 hours. At light intensities 70 µW/cm² and 7 µW/cm² the flies expressing ChR2-XXL display a higher activity rate than at 140 µW/cm², but are still clearly inhibited in their movement. This is also noticeable when comparing the activity surges after the illumination period, which shrink with decreasing light intensity. While the flies apparently still compensate for the period of ChR2-XXL-induced paralysis or partial paralysis during the day, the need for compensation clearly diminishes as the light intensity decreases. It is also notable how the ChR2-XXL flies don't display a normal and wild type-like rhythmic behaviour under the 12:12 LD entrainment during the day. The activity throughout the day shows no recognizable rhythmic features like the midday siesta or the anticipatory increase of activity during the evening. The flies only display a constantly and equally low rate of activity throughout the day.

The activity rate of the controls on the other hand shows no apparent change between the different light conditions. Under all three light intensities the UAS-controls show a normal, wild type-like behaviour with the apparent rhythmic features (siesta, M peak, E peak), that the ChR2-XXL flies lacked.

Judging by these results, it can be concluded that ChR2-XXL has a strong and very noticeable effect on the flies' mobility when expressed in motor neurons and appears to be quite sensitive even under low light intensities. Accordingly, a white light condition which ensures for CRY to be able to cycle naturally throughout the day, without also activating ChR2-XXL, does not seem to be possible. Yet, it was decided to proceed with the phase shift experiments after LD entrainment regardless.

3.1.3. Shift experiments in a CRY-positive background

Since working with CRY-negative flies was no longer an option it was decided to return to working with the CRY-positive lines, used by Dennis Segebarth [121]. It was decided that in order to circumnavigate the hypothesized problem with the increasing CRY levels in the circadian neurons during an RD entrainment, an LD entrainment using white light was to be used in future experiments. This would allow the CRY levels to cycle naturally throughout the day. This in turn however, would also likely continuously activate the ChR2-XXL that was expressed in the circadian neurons, causing a continuous depolarization (see 3.1.2). This had been avoided in previous experiments as it was hypothesized that the circadian clock might start to compensate for such an ongoing input signal, which, as a consequence, might weaken or even completely negate any effect of a ChR2-XXL-medaited depolarization during the delay- or advance zones. But as no better option presented itself at the time, it was decided to test the deployment of an LD entrainment for the shift experiments.

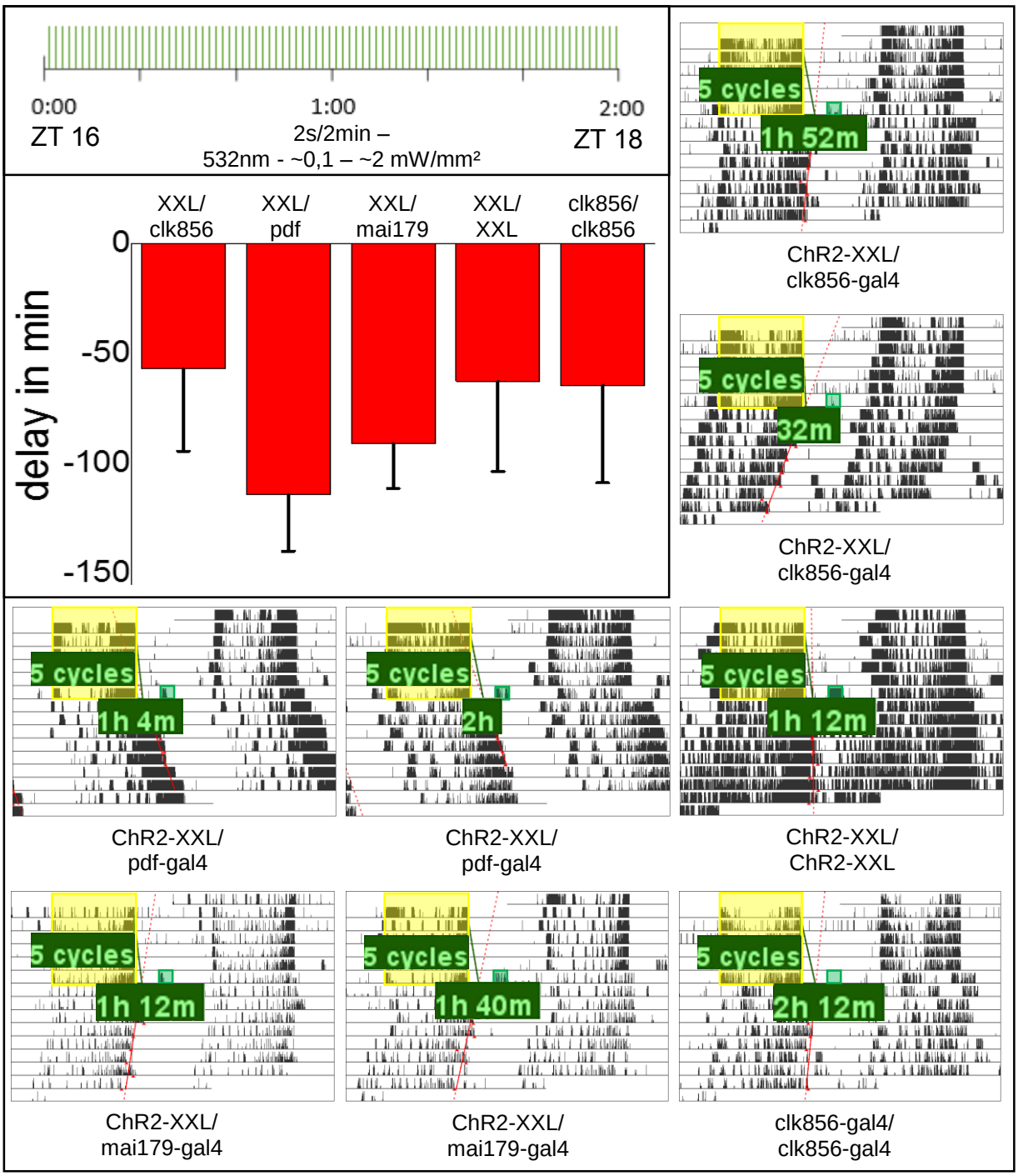

Figure 3.1.3. top left: visual representation of the programmed light pulse, indicating the time point (ZT) and the length and frequency of the individual light pulses; **left**: average phase delays of flies expressing ChR2-XXL in all circadian neurons (clk856-gal4), all PDF-positive neurons (pdf-gal4), the mai-subset (mai179-gal4) and the respective homozygous UAS- and GAL4-controls; error bars represent SEM; **bottom right:** sample actograms of flies expressing ChR2-XXL using the indicated GAL4-drivers and the respective homozygous UAS- and GAL4-controls; yellow shading indicates 12:12 LD entrainment (550nm; ~70 µW/cm²); green shading indicates light pulse; no shading indicates darkness; 25°C 60% RH; for a detailed analysis of the phase shift calculation see Material and Methods 2.8.

The shift experiment above, employing an LD-entrainment did not yield significant results. The flies displayed a good and robust rhythmicity with clear activity offsets, which allowed for the calculation of the phase-delays. No significantly higher phase-

delays were found in the test-lines compared to the controls, but there was a tendency towards slightly larger phase delays in the pdf-gal4 line and the mai179-gal4 line. (see Fig. 3.1.3.). The experiment was repeated with a lower entrainment light-intensity.

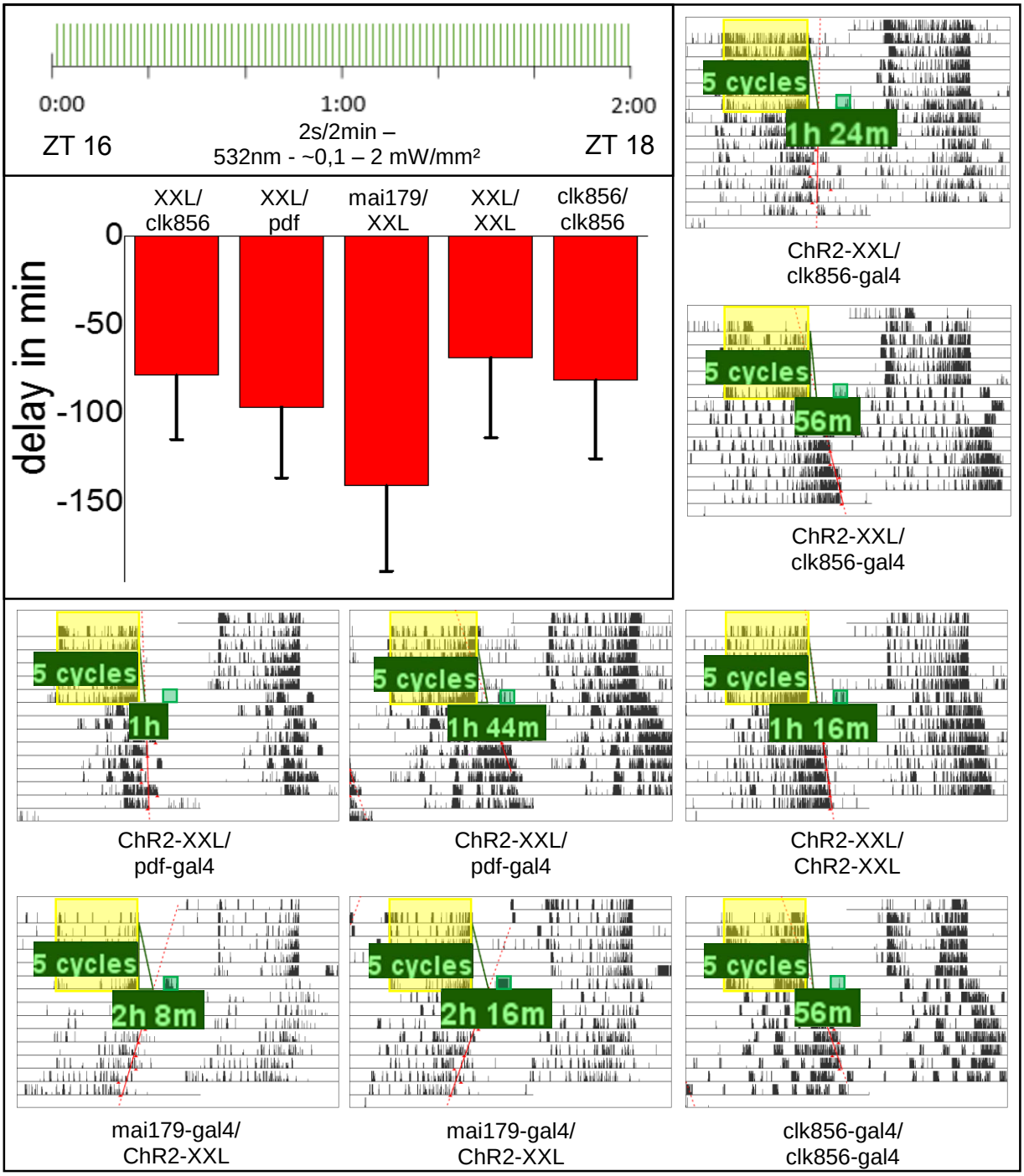

Figure 3.1.4. top left: visual representation of the programmed light pulse, indicating the time point (ZT) and the length and frequency of the individual light pulses; **left**: average phase delays of flies expressing ChR2-XXL in all circadian neurons (clk856-gal4), all PDF-positive neurons (pdf-gal4), the mai-subset (mai179-gal4) and the respective homozygous UAS- and GAL4-controls; error bars represent SEM; **bottom right:** sample actograms of flies expressing ChR2-XX using the indicated GAL4-drivers and the respective homozygous UAS- and GAL4-controls; yellow shading indicates 12:12 LD entrainment (550nm; ~7 µW/cm²); green shading indicates light pulse; no shading indicates darkness; 25°C 60% RH; for a detailed analysis of the phase shift calculation see Material and Methods 2.8.

Lowering the intensity of the white light used for the LD-entrainment did not affect the results of the phase-shift experiments significantly. The flies again displayed a good rhythmicity that allowed for a calculation of the phase shift (see Fig. 3.1.4.). Flies expressing ChR2-XXL under the clk856-gal4 driver and the pdf-gal4 driver did not display significantly larger phase shifts than the respective controls. Flies expressing ChR2-XXL under the mai179-gal4 driver however did on average show a noticeably larger phase delay than the two controls, but missed statistical significance. As neither one of the two controls is the proper and established heterozygous control however, these values are only to be taken as indicators, rather than as solid results.

It was also discovered during data analysis that the individual flies sometimes displayed large disparities and differences regarding the size of their phase shifts, also among genotypes (not shown in sample actograms). This had also been the case for the previous experiment (Fig 3.1.3.). It turned out that the output intensities of the laser-arrays (see Material and Methods 2.7.), that were used to apply the timed light-pulse, were not homogenous across the individual optical fibres. In some cases the difference in output intensity almost reached a factor of 10. While most of these experimental inaccuracies would be expected to average out for a large enough sample size, their effect on the results are still to be taken seriously. For future experiments, the individual positions of the tested flies were no longer disregarded, but carefully predetermined, to assure that the average light intensities for each genotype were as comparable to each other as possible.

Still, the results of these experiments were used to determine the experimental direction for the future. It was decided that the promising results of the flies expressing ChR2-XXL under the mai179-gal4 driver warranted further investigation. Another phase shift experiment was started, using only the mai179-gal4 driver and the proper and established, heterozygous controls. The other parameters, entrainment light intensity, length and frequency of the timed light-pulse were kept the same.

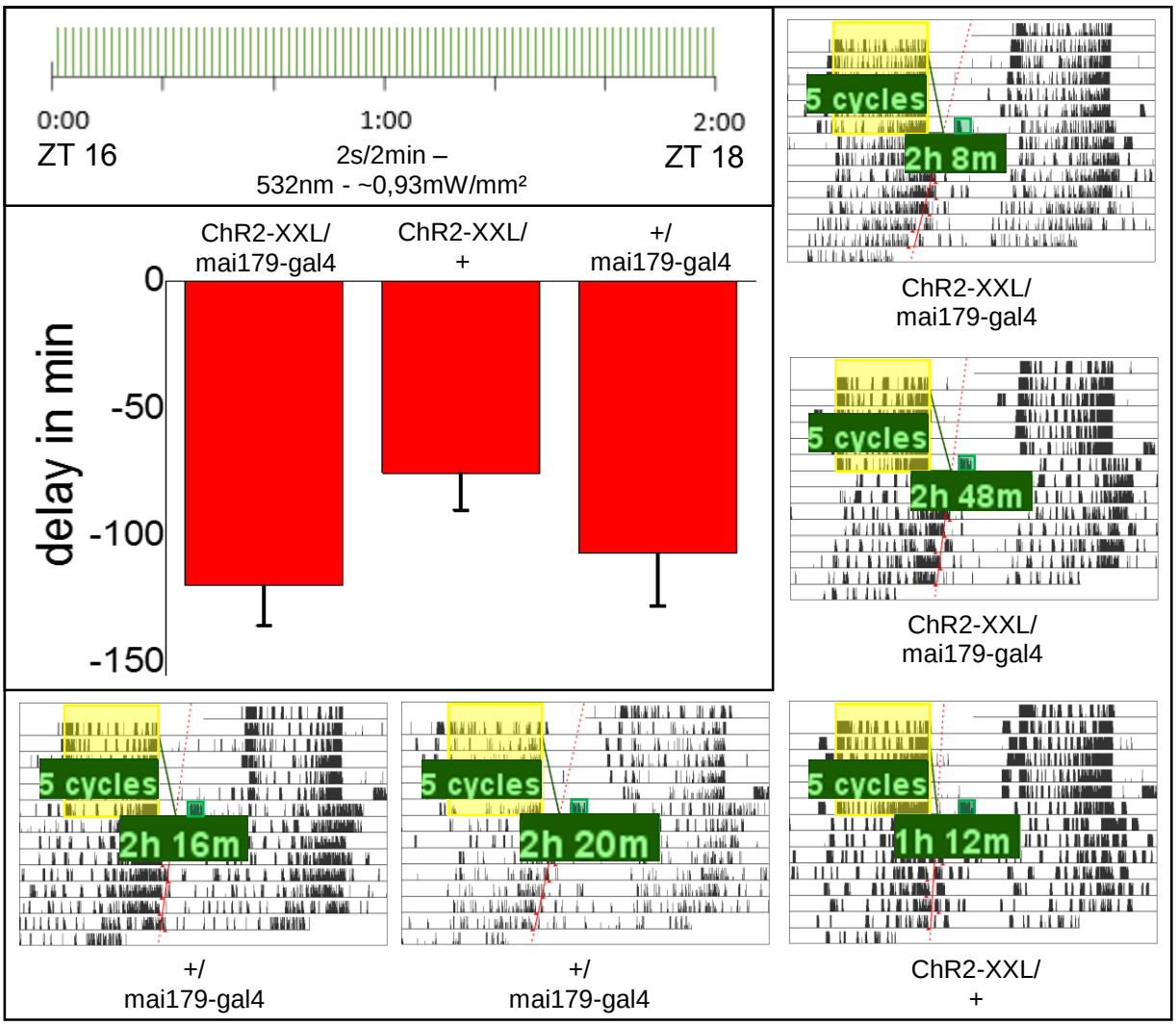

Figure 3.1.5. top left: visual representation of the programmed light pulse, indicating the time point (ZT) and the length and frequency of the individual light pulses; **left**: average phase delays of flies expressing ChR2-XXL in the mai-subset (mai179-gal4) and the respective UAS- and GAL4-controls; error bars represent SEM; **bottom right:** sample actograms of flies expressing ChR2-XXL in the mai-subset (mai179-gal4) the respective UAS- and GAL4-controls; yellow shading indicates 12:12 LD entrainment (550nm; ~7 µW/cm²); green shading indicates light pulse; no shading indicates darkness; 25°C 60% RH; for a detailed analysis of the phase shift calculation see Methods 2.8.

The shift experiment using only flies expressing ChR2-XXL in the mai-subset (mai179-gal4) delivered no positive results. The average phase delay of the flies expressing ChR2-XXL was not significantly larger than that of the GAL4-controls (see Fig. 3.1.5.). As the differences in the output intensity of the arrays' optical fibres had been taken into account this time and as the proper heterozygous controls had been used, the results of the experiment did not support the conclusion that the timed depolarization of circadian neurons using ChR2-XXL has any noticeable effect.

It was ultimately decided to discontinue the use of ChR2-XXL as the optogenetic tool of choice for accomplishing the thesis' goal and instead switch to using a construct that had more similar conductive properties as the dTRPA1 channel, which had been successfully used by Eck et al. to evoke significant phase shifts [117].

3.2. Olf-bPAC and SthK-bPAC

After obtaining no positive results by using ChR2-XXL as the optogenetic tool of choice and no real indication that influencing the circadian clock of *Drosophila melanogaster* might principally be possibly with said tool (see Results 3.1.), a new set of optogenetic tools was introduced, Olf-bPAC and SthK-bPAC. As detailed in Introduction 1.2.2., these tools are made up of the two cyclic nucleotide-gated ion channels Olf [98] and SthK [96] that are fused to the light activated adenylyl cyclase bPAC [102]. To allow for a direct detection of the construct under a confocal laser microscope, a yellow fluorescent protein (YFP) was fused in between the respective CNGC and the bPAC (see Fig. 1.7.). Since the conductive qualities of the two new channels differ widely from those of ChR2-XXL, with Olf being a lot more permeable for Ca^{+2} and as such resembling the conductive qualities of the dTRPA1 used by Eck et al. [117] much more closely [98, 118] and SthK being a highly selective K^{+}-channel [96], we assumed that these two tools might be more suited to evoke the desired effect of shifting the circadian clock of *Drosophila melanogaster*.

3.2.1. Olf-bPAC rhythmicity experiments

Before any actual shift experiments were conducted, the general rhythmicity of the flies under red-light control conditions was tested. 3 – 5 days old flies were collected and entrained under 12:12 RD conditions before being released into DD. For this experiment, flies were used that expressed Olf-bPAC in the entire clock neurons (clk856-gal4) as well as the PDF-neurons (pdf-gal4).

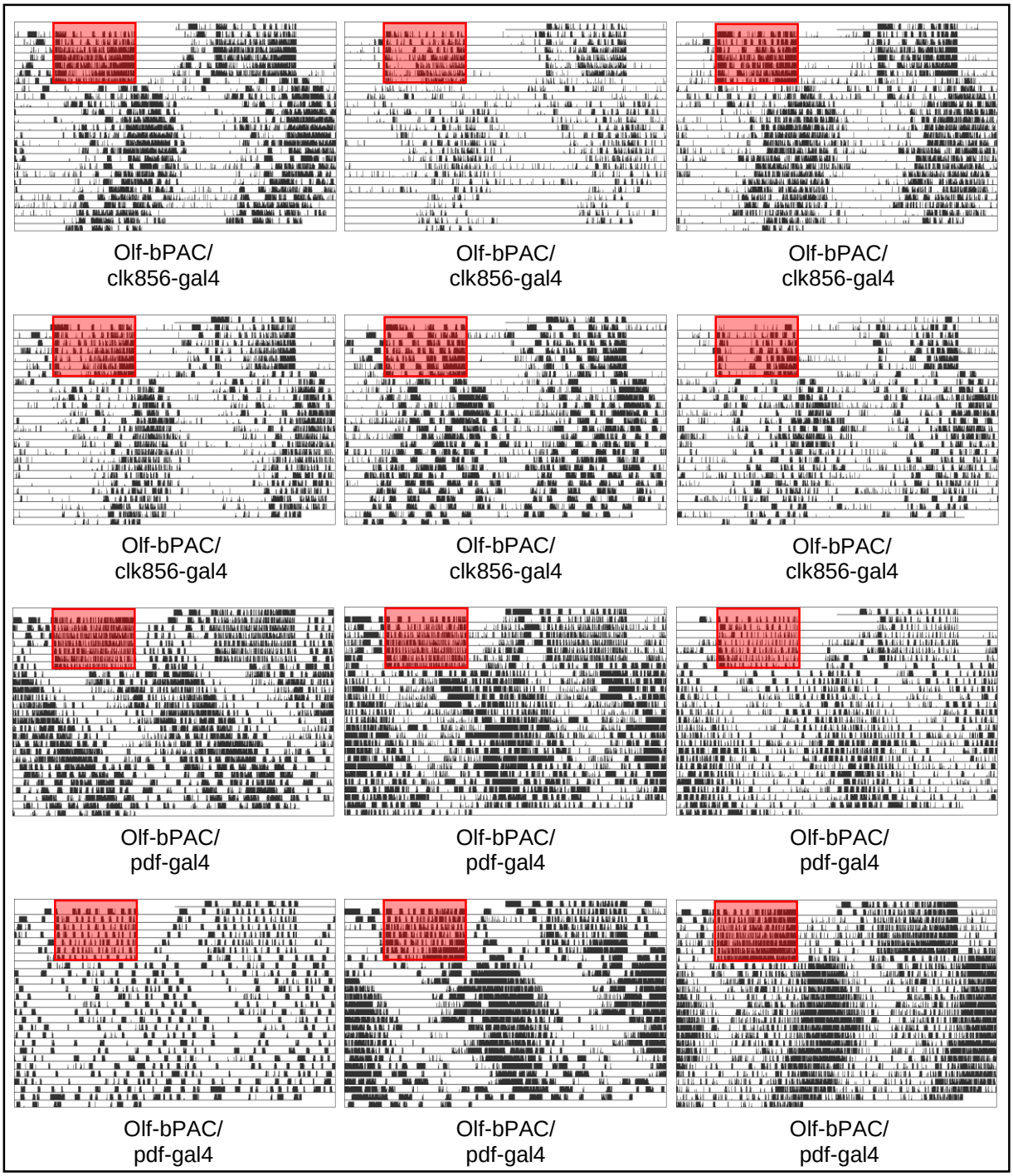

Figure 3.2.1a.: Sample actograms of flies expressing Olf-bPAC in all circadian clock neurons (clk856-gal4) and all PDF-positive neurons (pdf-gal4); double-plotted; red shading represent 7 day entrainment cycle of 12:12 RD (620nm, ~5 µW/cm²); no shading represents darkness; 20°C, 60% RH

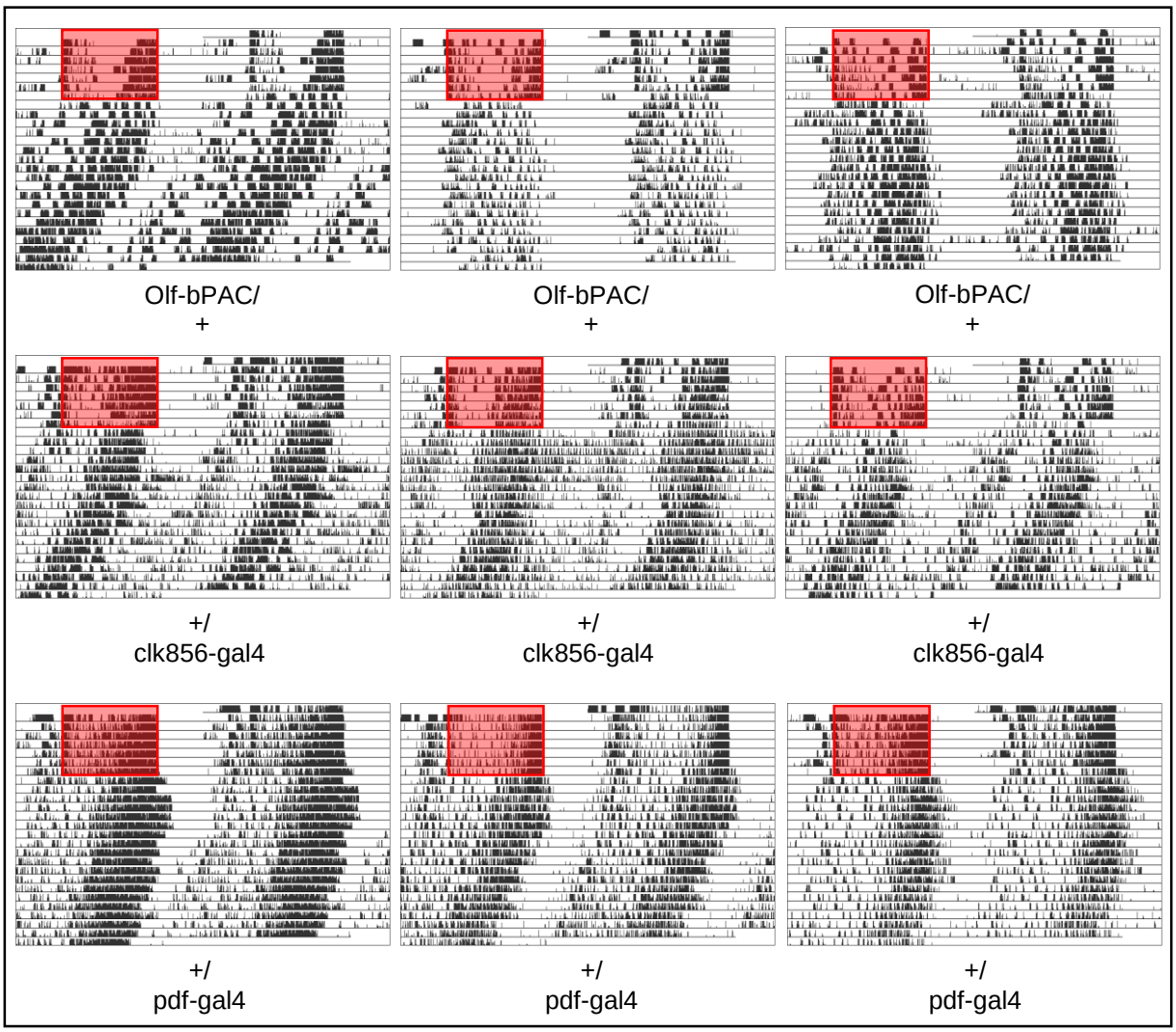

Figure 3.2.1b.: Sample actograms of flies expressing no Olf-bPAC anywhere (UAS-control and the two respective GAL4-controls), double-plotted; red shading represent 7 day entrainment cycle of 12:12 RD (620nm, ~5 µW/cm²); no shading represents darkness; 20°C, 60% RH

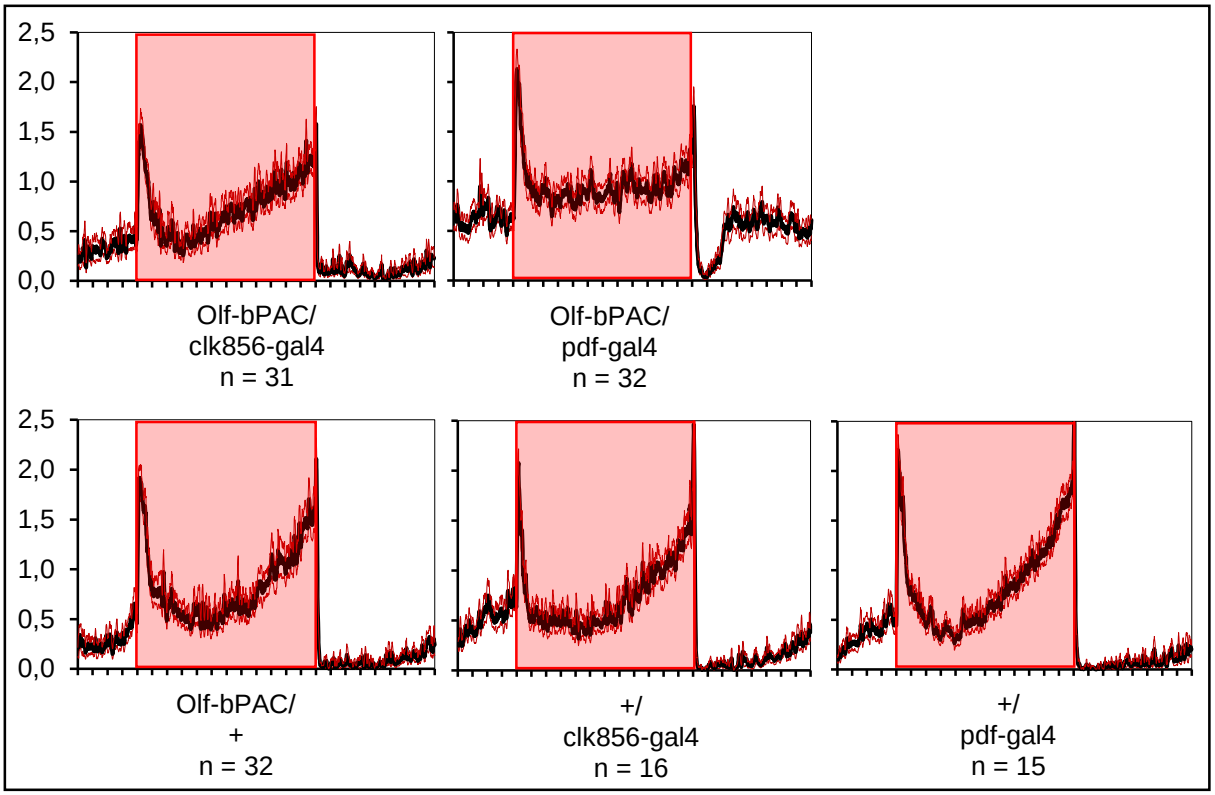

Figure 3.2.2.: Averaged actograms of flies expressing Olf-bPAC in all circadian clock neurons (clk856-gal4) and in all PDF-positive circadian clock neurons (pdf-gal4), as well as their respective UAS- and GAL4-controls; red shading represent entrainment cycle of 12:12 RD (620nm, ~5 µW/cm²); 20°C, 60% RH; no shading represents darkness; first 7 days of 12:12 RD entrainment were used for data averaging, no days in constant darkness were used for data averaging; for each genotype all flies that survived the 7 day entrainment cycle were used for data averaging;

Looking at the sample actograms of both flies expressing Olf-bPAC in either all circadian clock neurons (clk856-gal4), as well as only in all PDF-positive neurons (pdf-gal4), it is quite apparent that the presence of Olf-bPAC in either of those evokes a strong behavioural phenotype, while the respective controls exhibit a standard wild type-like bimodal activity pattern (see Fig 3.2.1.) .

When expressed in all circadian clock neurons (clk856-gal4), Olf-bPAC clearly disrupts wild type rhythmicity in DD. In many cases Olf-bPAC/clk856 flies lack clear M peaks and E peaks in DD, as well as a distinct siesta. All Olf-bPAC/clk856 flies do however exhibit rhythmic activity patterns, running on an intrinsic period, but they also appear to have had their phase be delayed by the onset of DD by several hours, which is clearly visible in the actograms. In some cases the activity patterns of the Olf-bPAC/clk856 flies also appear to be decoupled, with the M peak running on a longer (>24h) period and the E peak running on a shorter (<24h) period, up until the M peak merges into the E peak. The behaviour of Olf-bPAC flies during the 7 day 12:12 RD entrainment period however, displayed by the averaged actograms of each genotype,

closely resembles that of the respective controls, with a clearly observable siesta around noon and an E peak, recognizable by the anticipatory rise of activity approaching dusk (see Fig 3.2.2.).

Flies expressing Olf-bPAC in all PDF-positive neurons (pdf-gal4) also display heavily abnormal circadian behaviour. In DD Olf-bPAC/pdf flies maintain a semblance of rhythmicity, as the flies show rhythmic activity patterns, which do however lack all bimodal features like M peak, E peak and siesta (see Fig 3.2.1.). Olf-bPAC/pdf flies also appear to have had their phase be heavily delayed upon entering DD, much like the Olf-bPAC/clk856 flies. Looking at the averaged actograms, it is also evident that expressing Olf-bPAC in the PDF-positive clock neurons completely disrupts any bimodal rhythmicity during the RD entrainment period, which interestingly is not the case for the Olf-bPAC/clk856 flies (see Fig 3.2.2.). Olf-bPAC/pdf flies display no features of bimodal rhythmicity at all, no M or E peaks apart from a startle reaction towards the lights being turned on and off again. They also display no siesta and their activity rate remains constant throughout the entire day, suggesting a significant disability to entrain to the imposed 12:12 RD light regime.

Following these results, a new experiment was devised to further test the rhythmicity of this particular genotype and to see if it is even possible to entrain this genotype to a basic 12:12 RD light regime at all. In this new experiment, Olf-bPAC/pdf flies and their respective UAS- and GAL4-controls were first subjected to a 7 day 12:12 RD light regime, which was then switched to another 8 day 12:12 RD light regime, advanced by 8 hours compared to the first one. This was done to see if and how fast the flies were able to shift their circadian clocks to re-entrain to the new light regime.

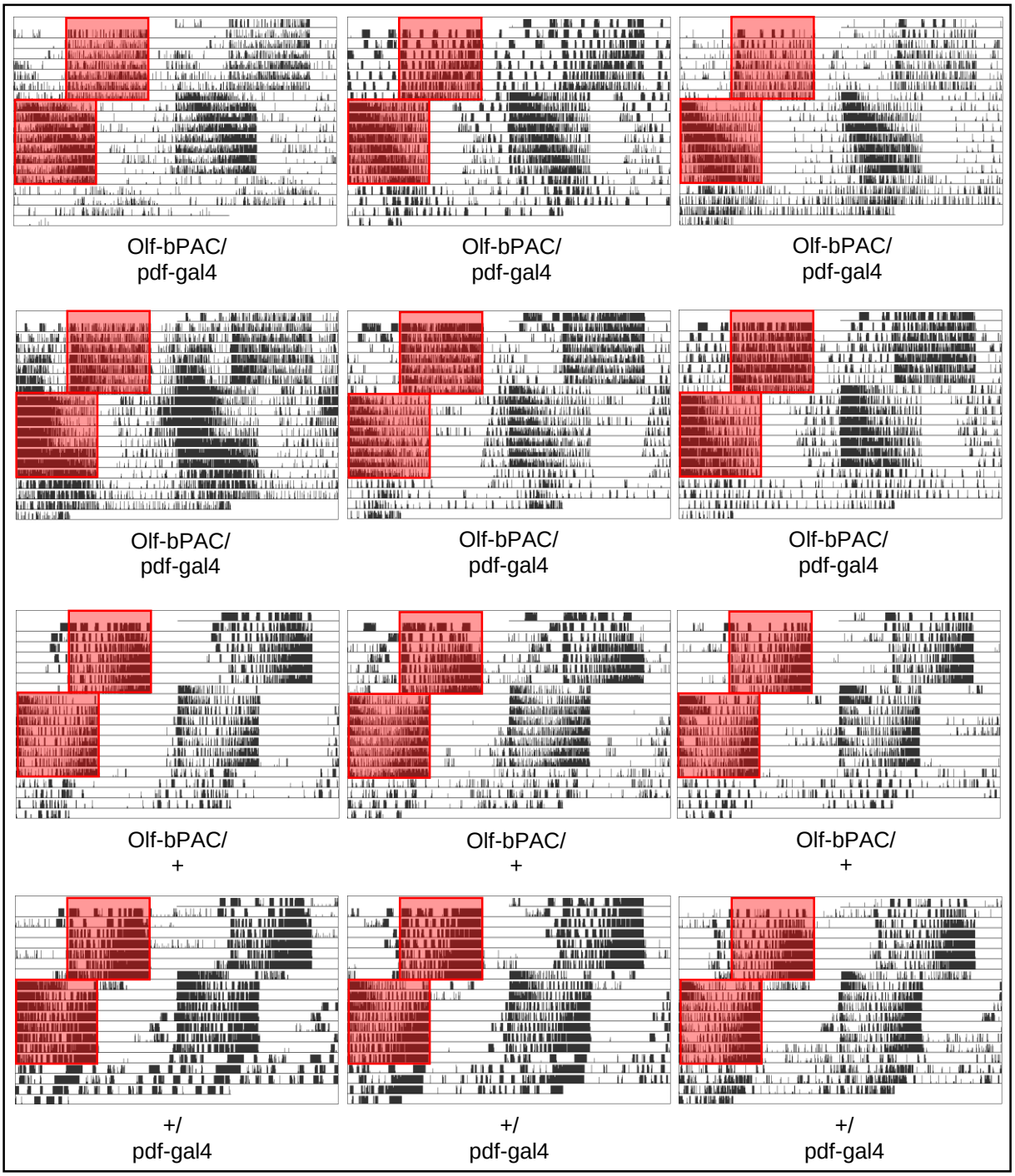

Figure 3.2.3.: Sample actograms of flies expressing Olf-bPAC in all PDF-positive clock neurons (pdf-gal4) and the respective UAS- and GAL4-controls, double-plotted; first red shading represents 7 day entrainment cycle of 12:12 RD from 8 a.m. to 8 p.m., second red shading represents second 8 day entrainment cycle of 12:12 RD from 12 p.m. to 12 a.m.; (620nm, 5 µW/cm²); no shading represents darkness; 20°C, 60% RH

The actograms of flies expressing Olf-bPAC in all PDF-positive clock neurons (pdf-gal4) strongly suggest that these flies are unable to entrain to a 12:12 RD light regime. While both the UAS-controls and the GAL4-controls adapt and re-entrain to the second advanced 12:12 RD light regime, the flies expressing Olf-bPAC are unable to do the same (see Fig. 3.2.3.). The controls clearly re-entrain to the advanced light regime,

which is evidenced by their periodically shifting bimodal activity pattern which steadily advances day by day, until it has caught up to the new RD cycle (see Fig. 3.2.3.). This is most clear when looking at the E peak and the siesta of the control flies, which both shift periodically, advancing roughly an hour per day. By the end of the second RD light regime, the control flies have been fully entrained to the new rhythm, as their locomotor behaviour in DD continues in phase with their behaviour during RD. Olf-bPAC flies on the other hand fail to re-entrain to the new RD regime and it is highly doubtful whether they had entrained to the first RD regime. They do display periodically rhythmic behaviour, which seems to be completely decoupled and independent of any of the two light regimes (see Fig. 3.2.3.). This can be most clearly seen by the flies' locomotor behaviour during the second, advanced 12:12 RD light regime. Here their clocks appear to be running on an independent and intrinsic cycle, with a long >24h period, steadily delaying day by day, instead of advancing. When entering DD, the Olf-bPAC flies seem to continue free-running on their intrinsic period. The only notable effect of the 12:12 RD light regime on the Olf-bPAC flies is a substantial increase in activity during the light phases.

3.2.2. SthK-bPAC rhythmicity experiments

Just like it was conducted for Olf-bPAC, the first thing to be assessed for SthK-bPAC was to test how flies, expressing the construct in various neurons of the circadian clock network, fared in basic and simple rhythmicity experiments. Therefore, 3 – 5 days old flies were collected and entrained under 12:12 RD conditions before being released into DD. For this experiment flies were used that expressed SthK-bPAC in the entire clock neurons (clk856-gal4) as well as the PDF-neurons (pdf-gal4).

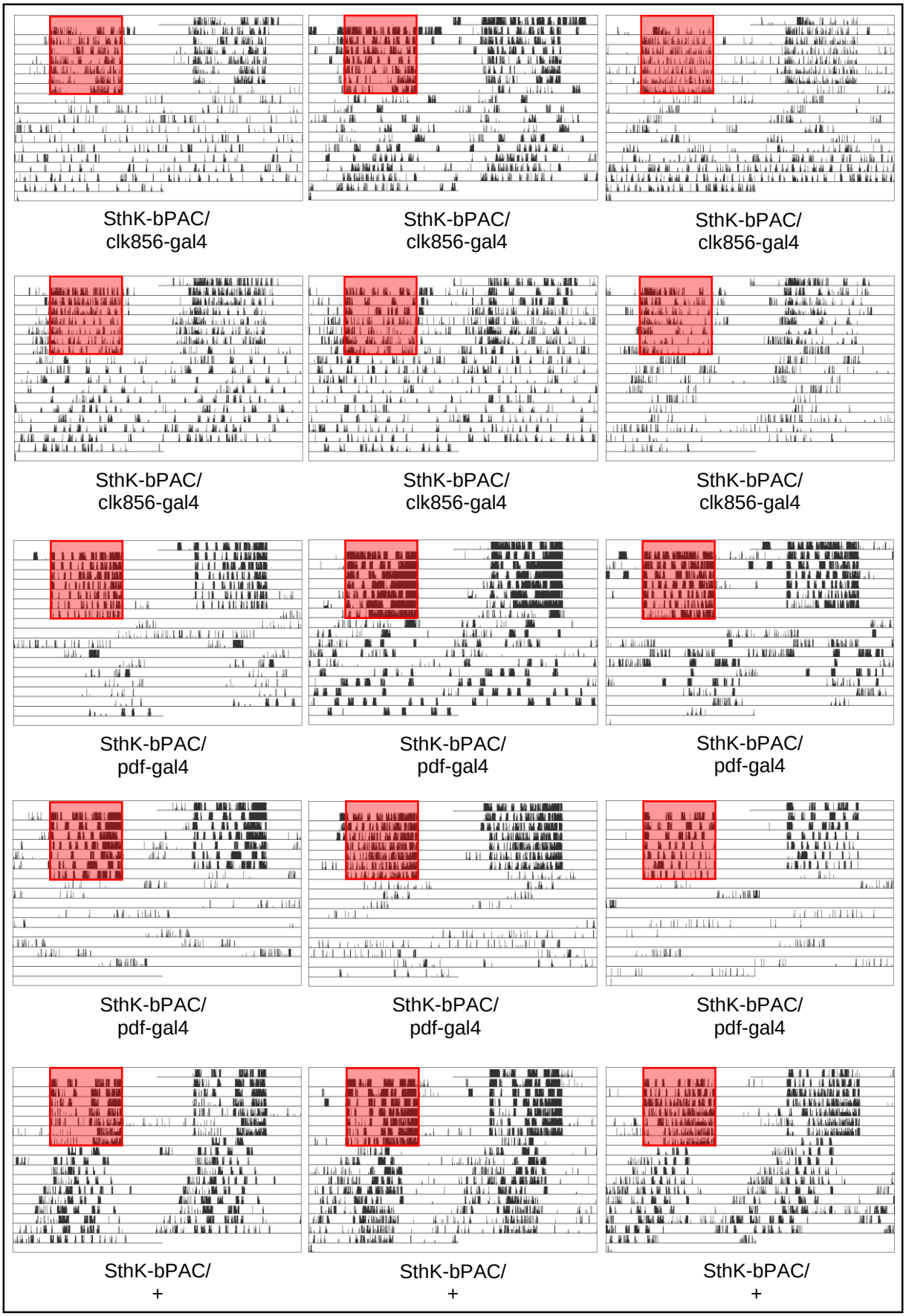

Figure 3.2.4.: Sample actograms of flies expressing SthK-bPAC in all clock neurons (clk856-gal4), in all PDF-positive clock neurons (pdf-gal4) and the respective UAS-control; double-plotted; red shading represent 7 day entrainment cycle of 12:12 RD (620 nm, 5 µW/cm²); no shading represents darkness; 20°C, 60% RH

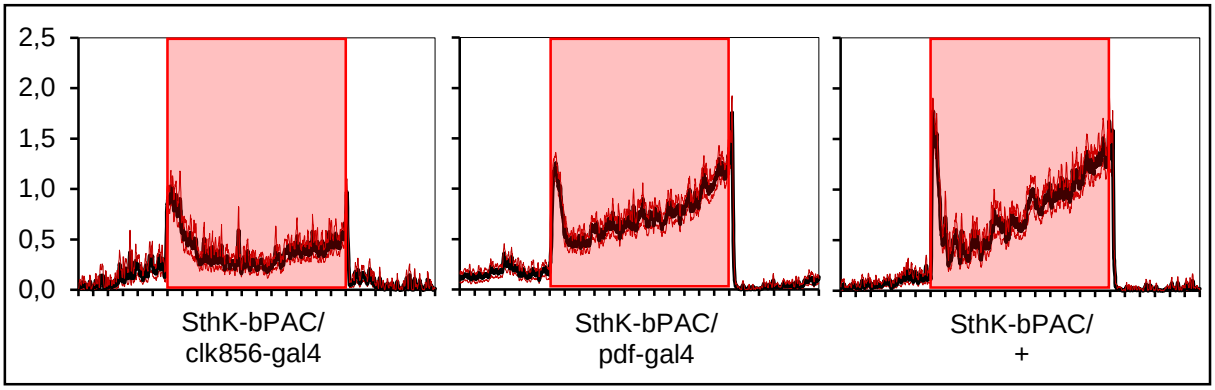

Figure 3.2.5.: Averaged actograms of flies expressing SthK-bPAC in all circadian clock neurons (clk856-gal4) and in all PDF-positive circadian clock neurons (pdf-gal4), as well as the respective UAS-control; red shading represent entrainment cycle of 12:12 RD (620 nm, 5 µW/cm²); 20°C, 60% RH; no shading represents darkness; first 7 days of 12:12 RD entrainment were used for data averaging, no days in constant darkness were used for data averaging; for each genotype all flies that survived the 7 day entrainment cycle were used for data averaging

The sample actograms of SthK-bPAC flies reveal that expressing SthK-bPAC in all clock neurons (clk856-gal4) or all PDF-positive clock neurons (pdf-gal4), heavily disrupts rhythmic behaviour (see Fig 3.2.4.). Flies expressing SthK-bPAC in all clock neurons appear to be almost completely arrhythmic in DD, with only a minor fraction of the sampled flies occasionally exhibiting weakly rhythmic activity patterns. Flies expressing SthK-bPAC in all PDF-positive neurons (pdf-gal4) are completely arrhythmic in DD with a noticeably low activity rate (see Fig 3.2.4.) and appear to be even worse affected than the clk856-flies. The UAS-controls display a robustly rhythmic behaviour in DD. Interestingly, when looking at the averaged actograms, it can be seen that flies expressing SthK-bPAC in the PDF-positive clock neurons exhibit a bimodal activity pattern during the 7 day 12:12 RD entrainment period, very similar to the UAS-control, with M peak, E peak and a midday siesta (see Fig. 3.2.5.). Those that express SthK-bPAC in all clock neurons however display an abnormal activity pattern in 12:12 RD, with no clear and pronounced E peak and only a weak anticipatory increase in activity approaching evening. Overall it appears that expressing SthK-bPAC disrupts the circadian clock of *Drosophila melanogaster* even more than Olf-bPAC (see 3.2.1.). Olf-bPAC flies do not display a wild type-like bimodal activity pattern in DD. With their circadian clocks being clearly affected by Olf-bPAC, they do exhibit rhythmic activity patterns in DD, while SthK-bPAC flies are overwhelmingly fully arrhythmic.

3.2.3. Immunostaining of flies expressing Olf-bPAC

After observing the unusual rhythmic phenotype of flies expressing Olf-bPAC, with pdf- flies being unable to entrain to a 12:12 RD light regime and the arrhythmicity of flies expressing SthK-bPAC (see 3.2.2.), it was contemplated whether the expression of Olf-bPAC as well as SthK-bPAC might also have an impact on the morphology of the respective neurons, given the drastic circadian phenotype. In order to address this hypothesis, a series of immunostaining experiments was started, focusing on displaying the morphology of the PDF-positive clock neurons. The neurons were stained using an anti-PDF antibody (see Material and Methods 2.5.), while the expression of the two constructs was assessed by making use of the yellow fluorescent protein (YFP), which is fused in between the respective CNGC and the bPAC (see Introduction 1.2.2.).

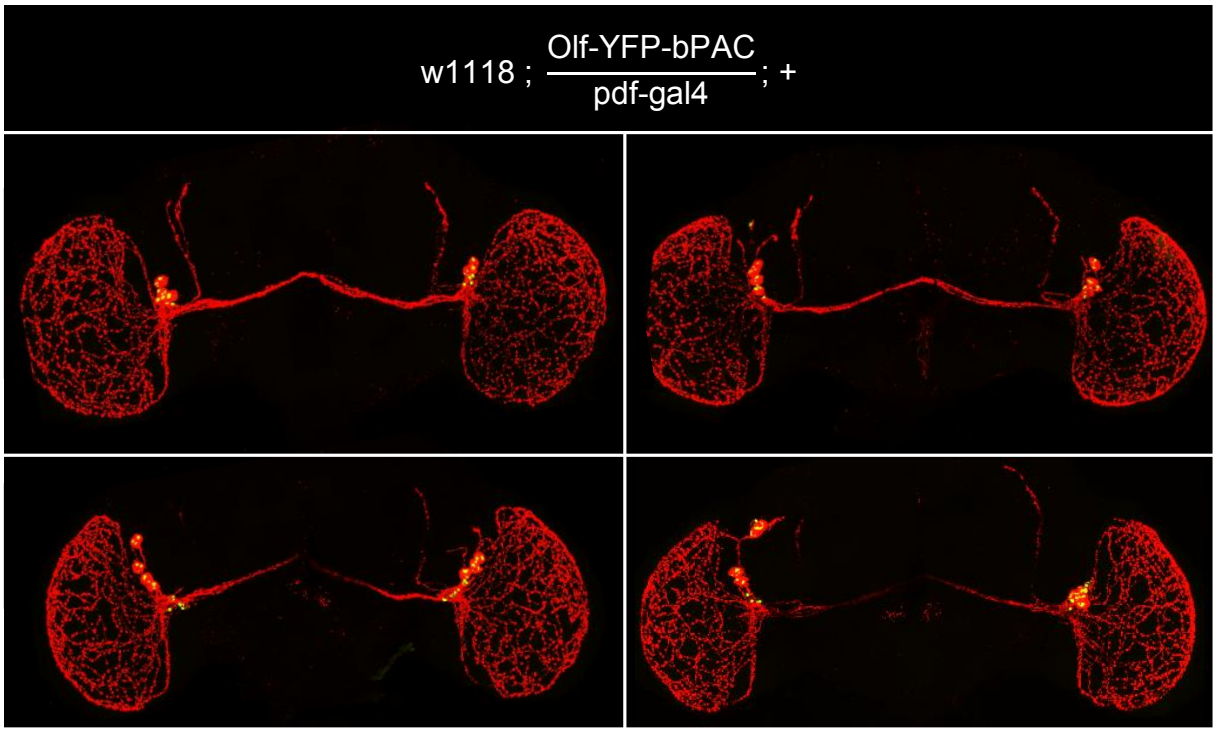

Figure 3.2.6a.: Prepared and immunostained brains of flies, expressing Olf-YFP-bPAC in the PDF-positive clock neurons; two-channel recording, laser-excitation with wavelengths 488 nm (green) and 532 nm (red), primary antibody: mouse anti-PDFc7; secondary antibody: Alexa Fluor 555 goat anti-mouse; all images in this section have been recorded with identical settings, incl. magnification, laser intensity, detector gain, frame average and resolution

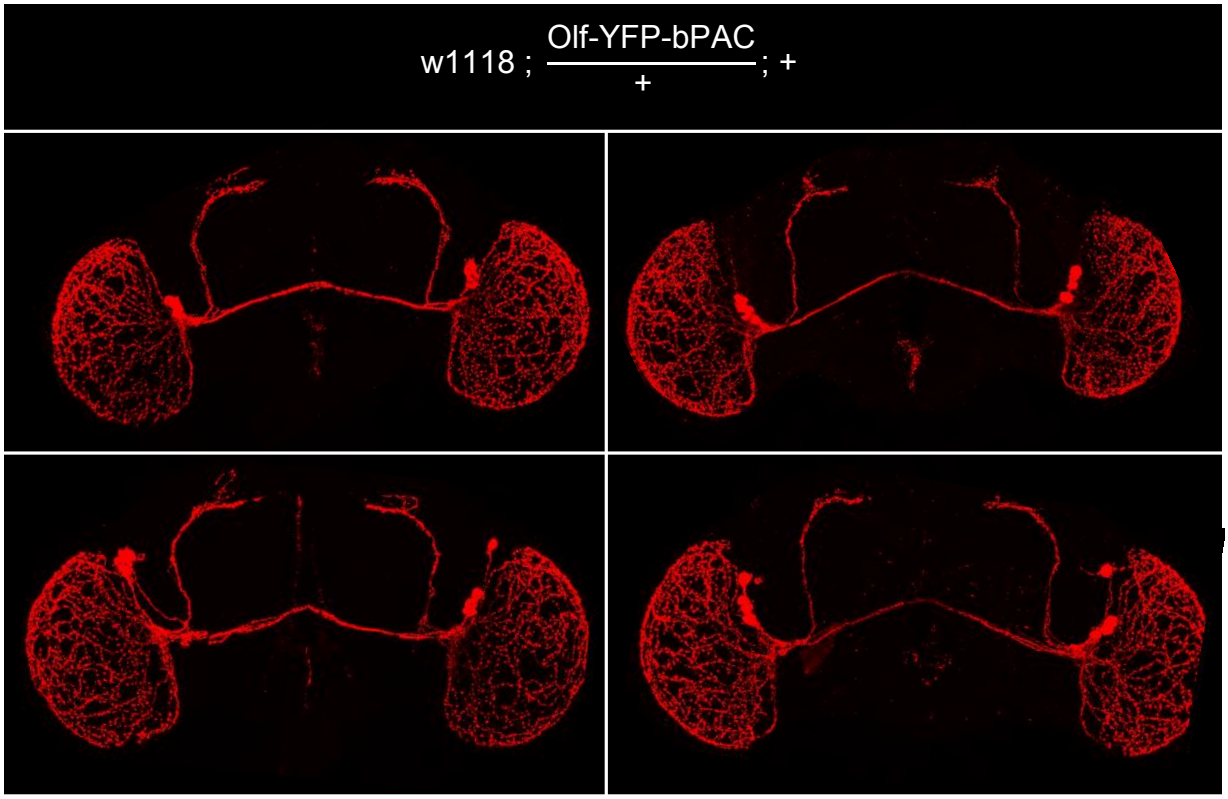

Figure 3.2.6b.: Prepared and immunostained brains of flies, expressing no Olf-YFP-bPAC anywhere (UAS-control); two-channel recording, laser-excitation with wavelengths 488 nm (green) and 532 nm (red), primary antibody: mouse anti-PDFc7; secondary antibody: Alexa Fluor 555 goat anti-mouse; all images in this section have been recorded with identical settings, incl. magnification, laser intensity, detector gain, frame average and resolution

Examining the immunostaining images of *Drosophila* brains expressing Olf-YFP-bPAC in the PDF-positive circadian neurons and the respective controls, it becomes evident at first glance, that expressing Olf-bPAC causes a massive and distinct morphological phenotype (see Fig. 3.2.6.). The arborisations of the small lateral ventral neurons (s-LN_vs), into the dorsal protocerebrum are significantly shortened, malformed and not fully developed, while those of the respective UAS-controls appear to be wild type-like. The arborisations of the large lateral ventral neurons (l-LN_vs) into the accessory medulla are seemingly unaffected by the expression of Olf-bPAC, however the complexity and intricacy of these arborisations make it impossible to definitively rule out any harmful effects of Olf-bPAC on the morphology of the l-LN_vs. The expression pattern of Olf-YFP-bPAC, visible in the YFP-channel of the recorded images, appears to be mainly centered around strong expression in the cell bodies of the respective neurons, rather than any axonal or dendritical expression, where expression seems rather low. After discovering the detrimental effect of Olf-bPAC on the morphology of the s-LNvs, it initially remained unclear whether the malformation of the neurons was a developmental effect, with the expression of the construct inhibiting the neurons from

developing properly during the larval stages or if it was a progressing phenotype, in which the initially well-developed neurons degraded slowly over time. To address this question, another series of immunostaining experiments was conducted, where flies of different ages were fixated and their brains prepared and immunostained with anti-PDF antibodies, to compare the morphology of the s-LNvs at varying ages.

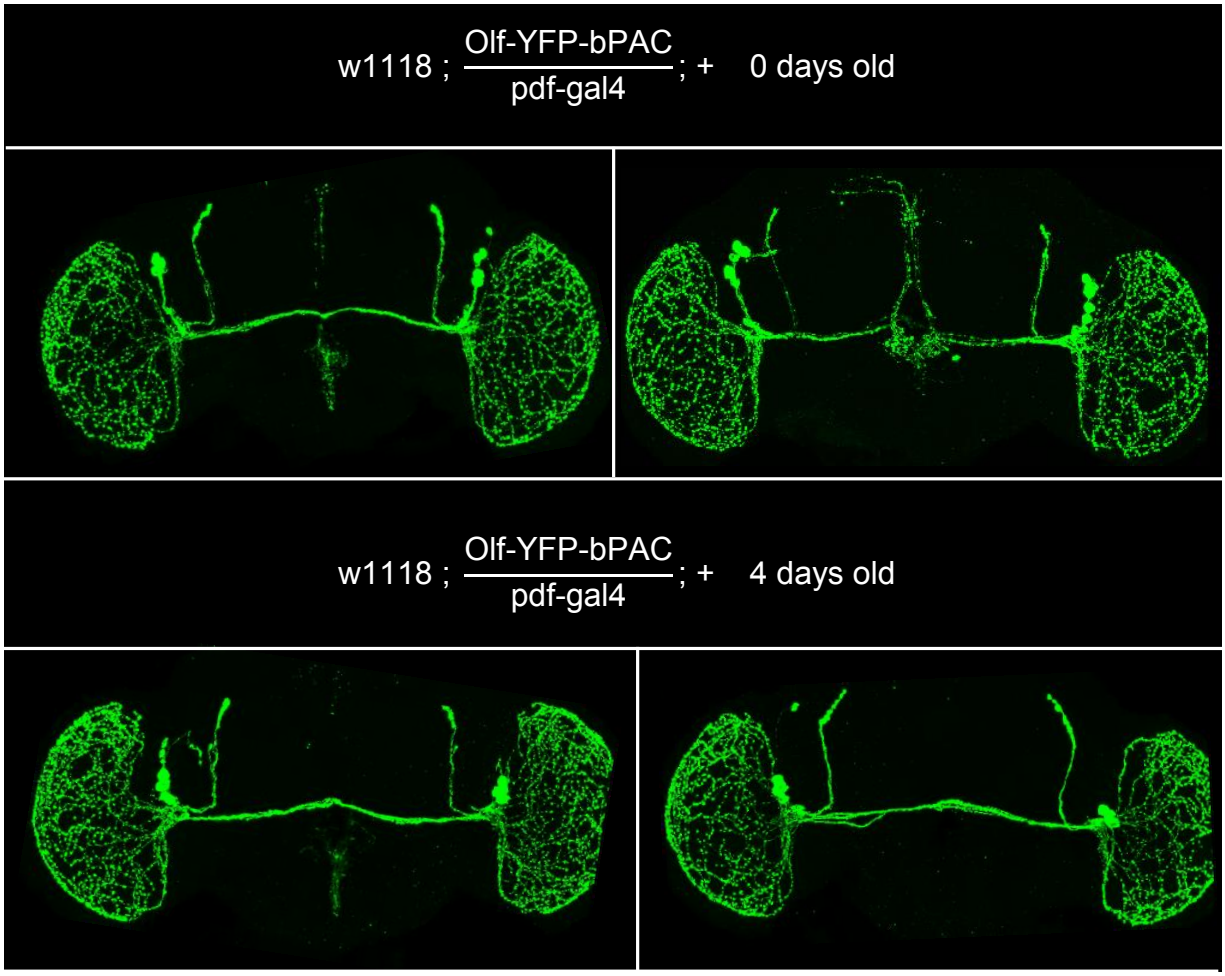

Figure 3.2.7a.: Prepared and immunostained brains of flies of different ages, expressing Olf-YFP-bPAC in the PDF-positive circadian neurons (pdf-gal4); single channel recording; laser-excitation with wavelength 488nm (green); primary antibody: mouse anti-PDFc7; secondary antibody: Alexa Fluor 488 goat anti-mouse; all images in this section have been recorded with identical settings, incl. magnification, laser intensity, detector gain, frame average and resolution

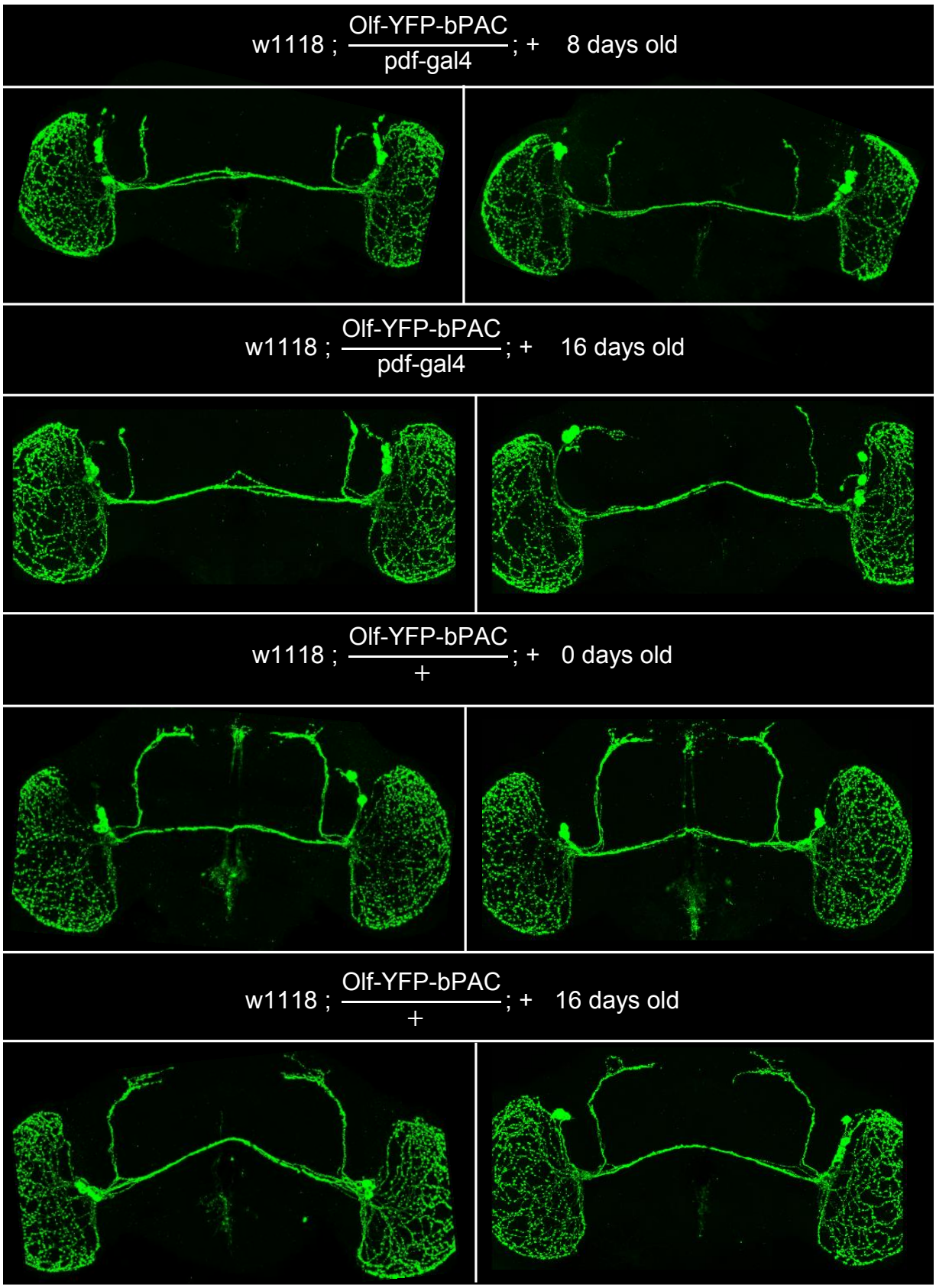

Figure 3.2.7b.:: Prepared and immunostained brains of flies of different ages, expressing Olf-YFP-bPAC in the PDF-positive circadian neurons (pdf-gal4) and the respective UAS-control; single channel recording; laser-excitation with wavelength 488nm (green); primary antibody: mouse anti-PDFc7; secondary antibody: Alexa Fluor 488 goat anti-mouse; all images in this section have been recorded with identical settings, incl. magnification, laser intensity, detector gain, frame average and resolution

The immunostaining images of flies of different age, expressing Olf-YFP-bPAC in the PDF-positive clock neurons clearly show that the severity of the phenotype of the shortened and malformed s-LN$_v$s does not progress with age, but is rather already established upon eclosion (see Fig. 3.2.7.). The s-LNvs of 16 days old flies, as well as those of 8 days old flies, expressing Olf-YFP-bPAC do not look significantly different from those of freshly hatched flies. This data suggests that this phenotype likely establishes itself during larval developmental, with Olf-YFP-bPAC likely inhibiting the s-LN$_v$s from developing properly.

3.2.4. Immunostaining of Instar-3 larvae expressing Olf-bPAC

Following up these results, a quick series of immunostaining experiments was conducted to conform this hypothesis. Instar-3 larvae expressing Olf-bPAC in the PDF-positive clock neurons were collected and fixated and their brains were prepared and stained with anti-PDF antibodies and imaged alongside the respective UAS-controls.

Figure 3.2.8a.: Prepared and immunostained brains of larvae expressing Olf-YFP-bPAC in the PDF-positive circadian neurons; two-channel recording, laser-excitation with wavelengths 488 nm (green) and 635 nm (red), primary antibody: mouse anti-PDFc7; secondary antibody: Alexa Fluor 635 goat anti-mouse; all images in this section have been recorded with identical settings, incl. magnification, laser intensity, detector gain, frame average and resolution

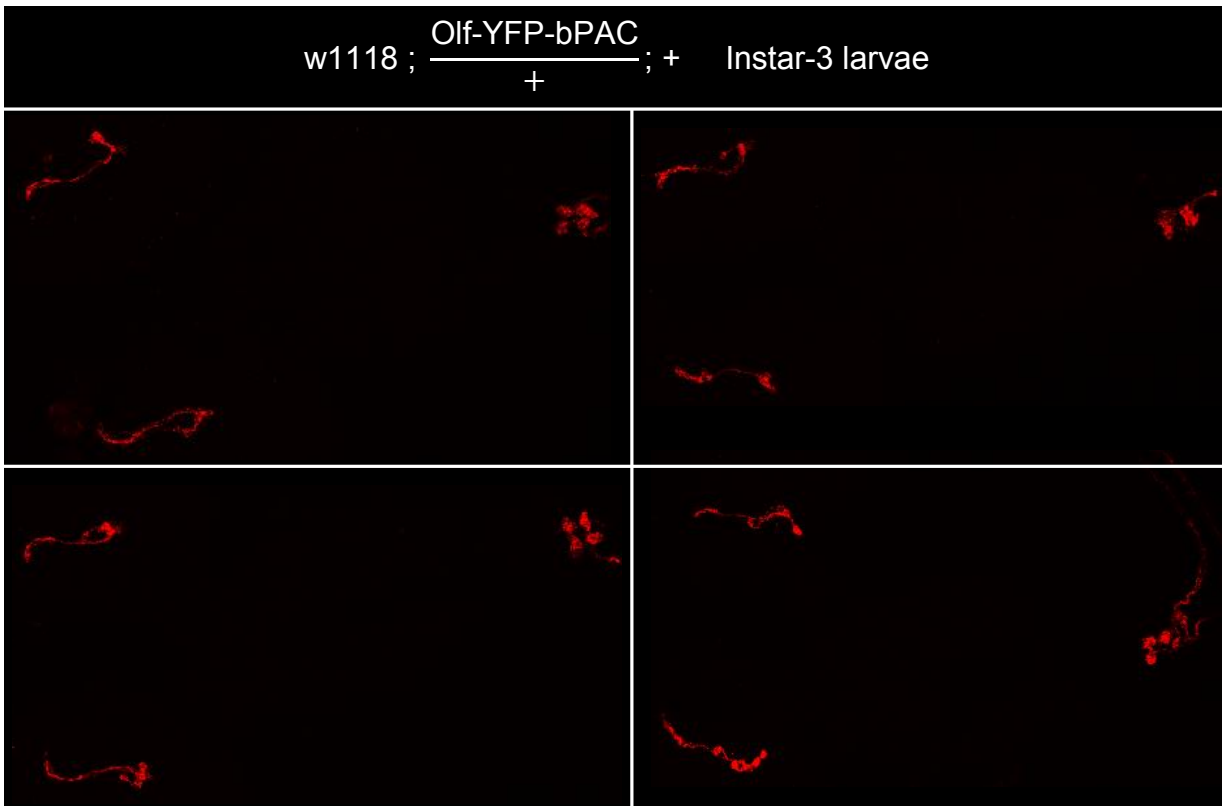

Figure 3.2.8b.: Prepared and immunostained brains of larvae expressing no Olf-YFP-bPAC anywhere (UAS-control); two-channel recording, laser-excitation with wavelengths 488nm (green) and 635 nm (red), primary antibody: mouse anti-PDFc7; secondary antibody: Alexa Fluor 635 goat anti-mouse; all images in this section have been recorded with identical settings, incl. magnification, laser intensity, detector gain, frame average and resolution

The immunostaining images of larvae expressing Olf-YFP-bPAC in the PDF-positive neurons confirm the hypothesis that the degradation of the s-LN$_v$s starts at the larval stages of development. As can be clearly seen in the YFP-channel, the channel is already well expressed at the larval stages, the cell bodies of the s-LN$_v$s can clearly be seen expressing the construct (see Fig. 3.2.8a.). This in turn appears to be hampering growth and development of the neuronal arborisations which would otherwise end up extending all the way into the dorsal protocerebrum of the adult fly [27]. The proper and unobstructed growth of the s-LN$_v$s at the Instar-3 larval stage can be seen in the staining of the UAS-control (see Fig 3.2.8b.).

3.2.5. Immunostaining of flies expressing SthK-bPAC

Given the similar nature of the constructs and the somewhat comparable circadian phenotypes regarding the poor rhythmicity of flies expressing either Olf-bPAC or SthK-bPAC in any clock neurons (see Results 3.2.1. & 3.2.2.), another series of immunostaining experiments was conducted to test whether the expression of SthK-bPAC has the same detrimental effect on the development of the s-LN$_v$s of *Drosophila melanogaster*. Flies expressing SthK-YFP-bPAC in the PDF-positive clock neurons (pdf-gal4) were fixated, prepared and subsequently imaged, along with the respective UAS-controls to assess the potential damage the expression of SthK-bPAC was likely doing on the morphology of the s-LN$_v$s.

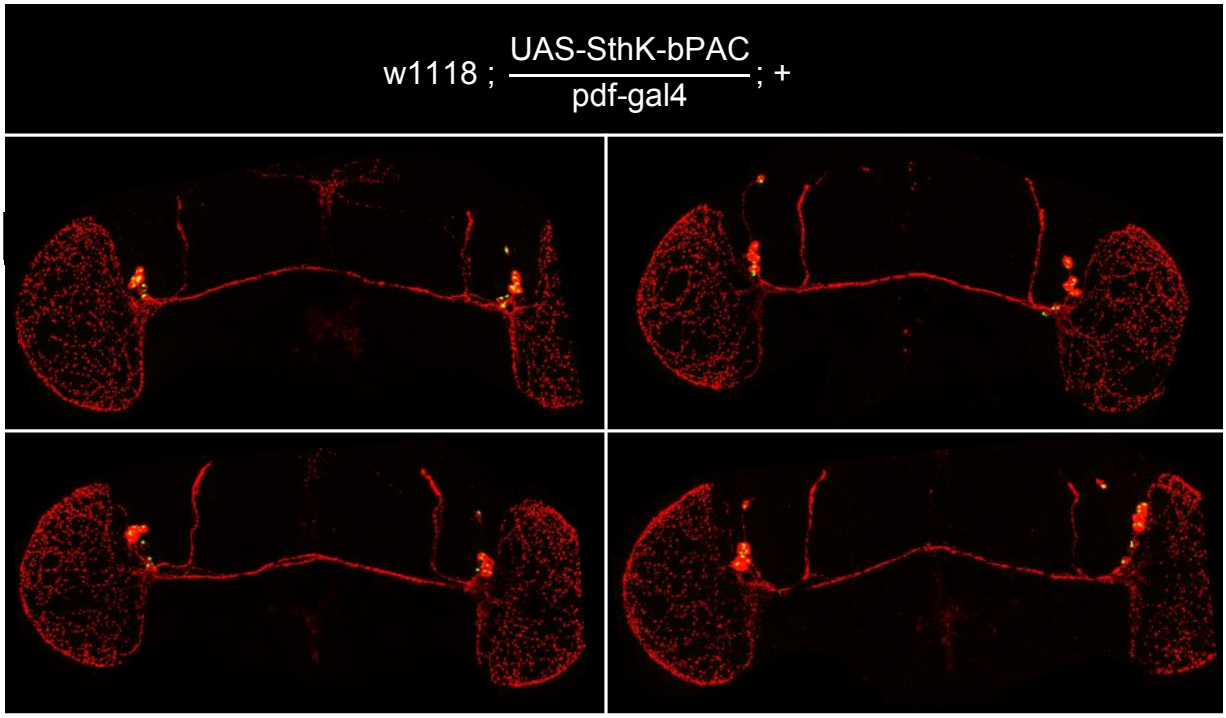

Figure 3.2.9a.: Prepared and immunostained brains of flies, expressing SthK-YFP-bPAC in the PDF-positive clock neurons (pdf-gal4); two-channel recording, laser-excitation with wavelengths 488 nm (green) and 532 nm (red), primary antibody: mouse anti-PDFc7; secondary antibody: Alexa Fluor 555 goat anti-mouse; all images in this section have been recorded with identical settings, incl. magnification, laser intensity, detector gain, frame average and resolution

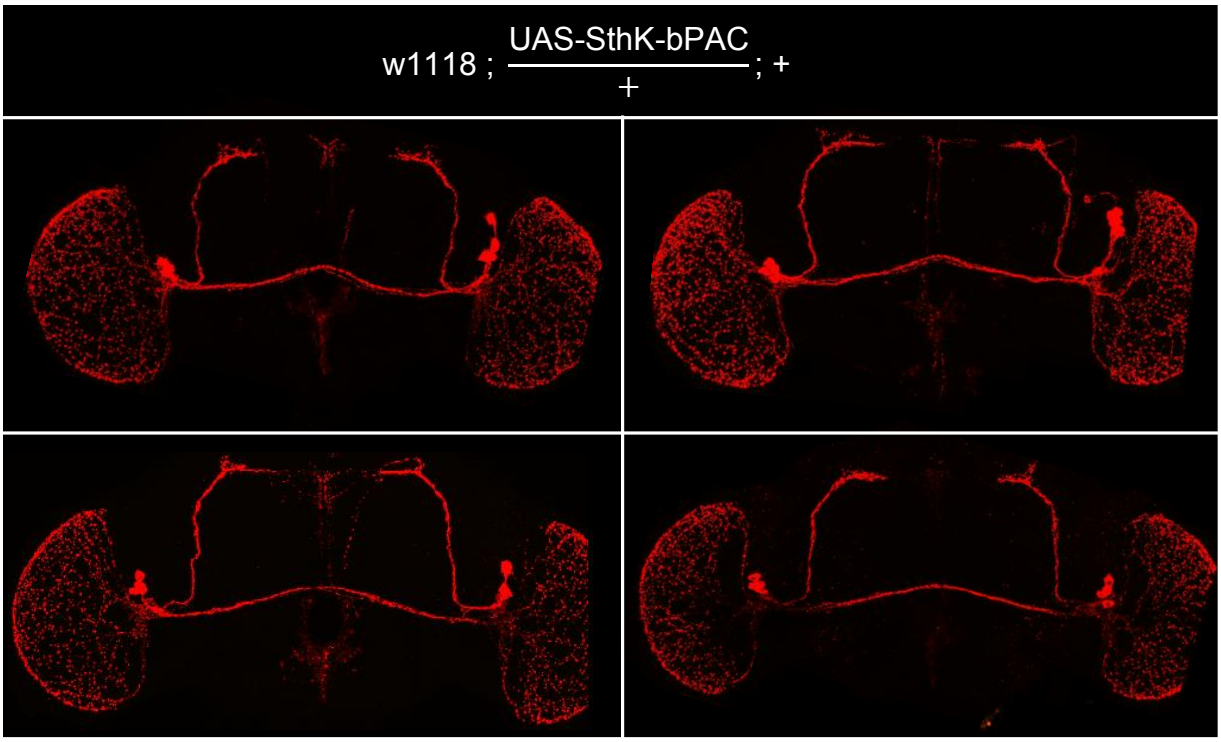

Figure 3.2.9b.: Prepared and immunostained brains of flies, expressing no SthK-YFP-bPAC anywhere (UAS-control); two-channel recording, laser-excitation with wavelengths 488nm (green) and 532 nm (red), primary antibody: mouse anti-PDFc7; secondary antibody: Alexa Fluor 555 goat anti-mouse; all images in this section have been recorded with identical settings, incl. magnification, laser intensity, detector gain, frame average and resolution

The immunostaining images of the *Drosophila melanogaster* flies expressing SthK-YFP-bPAC in the PDF-positive circadian neurons reveal that the small lateral ventral neurons (s-LN_vs) expressing the fusion construct are shortened and malformed, while the UAS-controls are unaffected (see Fig 3.2.9a. & 3.2.9b.), closely resembling the phenotype observed of expressing Olf-bPAC in the s-LN_vs (see Fig. 3.2.6a.). Judging by the immunostaining images of Instar-3 larvae expressing Olf-bPAC (see Fig 3.2.8a.), the neuronal damage resulting from the expression of SthK-bPAC is also very likely caused by the construct hampering neuronal development at an early larval stage, much like the phenotype observed with Olf-bPAC.

Mirroring the expression pattern of Olf-bPAC (see Fig. 3.2.6a.), SthK-bPAC is also heavily expressed in the cell bodies of the PDF-positive circadian neurons, while axonal and dendritic expression is undetectably low (see Fig 3.2.9a.).

3.2.6. Olf and bPAC rhythmicity control experiments

Next, the attention was focused on finding out which subunit of the expressed fusion constructs, Olf-bPAC and SthK-bPAC, was responsible for the observed phenotypes described in 3.2.1. - 3.2.5. (abnormal rhythmic behaviour and abnormal s-LN_v morphology of flies expressing either construct in clock neurons). It remained unclear if the Olf-channel and the SthK-channel were causing the described phenotypes, or if it was caused by the fused bPAC, or if in fact the phenotype could only be seen if both units were expressed together as a fusion construct. To answer this question, two new fly lines were tested, UAS-Olf-CNG(T537S)-YFP and UAS-bPAC (see Material and Methods 2.2.), one having a sequence under the regulatory expression control of the UAS coding only for the Olf-channel, the other coding only for the bPAC.

The easiest approach to test the influence of both constructs, Olf and bPAC individually was to repeat the experiment shown in Fig. 3.2.3., where a 7 day 12:12 RD light entrainment regime was then switched to another 7 day 12:12 RD light regime, advanced by 8 hours. Here flies that expressed Olf-bPAC in the PDF-positive clock neurons displayed a clear inability to entrain to the second, advanced light regime and were shown to be running on a light-independent period, rather than adjusting their circadian rhythm to the imposed light regime. If either of the two subunits, Olf or bPAC were to reproduce the observed phenotype when expressed alone, the problematic subunit could easily be identified. If neither of the two subunits were to reproduce the phenotype when expressed alone, its cause would then have to be attributed to the interaction of both constructs.

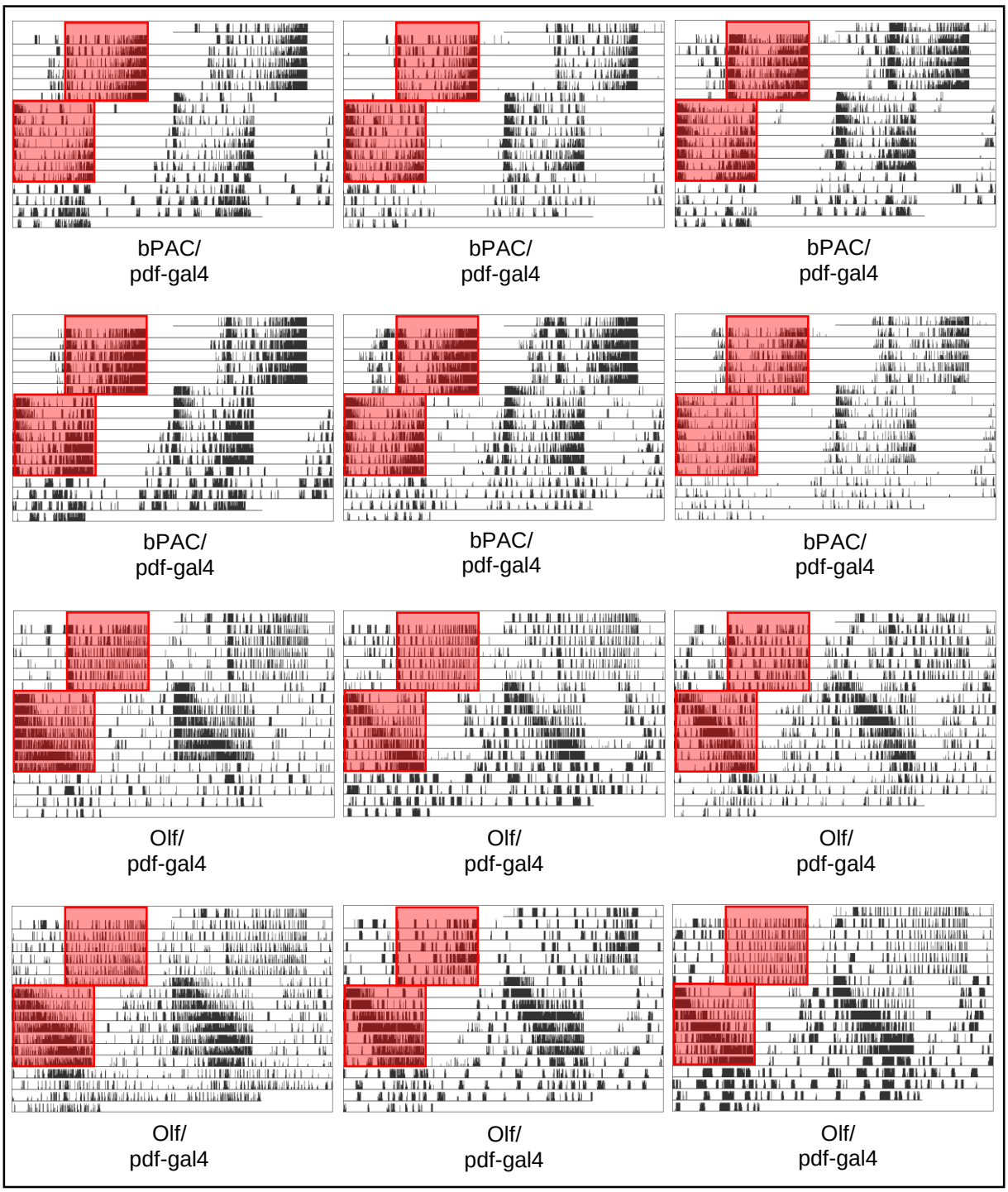

Figure 3.2.10.: Sample actograms of flies expressing bPAC or Olf in all PDF-positive clock neurons (pdf-gal4), double-plotted; first red shading represents 7 day entrainment cycle of 12:12 RD from 8 a.m. to 8 p.m., second red shading represents second 8 day entrainment cycle of 12:12 RD from 12 p.m. to 12 a.m. (660nm, ~5 µW/cm²); no shading represents darkness; 20°C, 60% RH

The experiments clearly show, that flies expressing only the Olf-channel in the PDF-positive clock neurons reproduce the behavioural phenotype exhibited by flies expressing Olf-bPAC (see Fig. 3.2.3.), being unable to re-entrain to the second advanced 12:12 RD light regime (see Fig. 3.2.10.). Like the Olf-bPAC flies their clocks apparently run on an intrinsic and light-independent period and the light's only

noticeable effect on the flies' locomotor behaviour is a substantial increase in their activity rate during light hours. Flies expressing only bPAC on the other hand behave similarly to the UAS-controls in Fig. 3.2.3., advancing their phase day after day until they are in phase with the light regime. These results clearly identify the Olf-channel as the singular cause for the abnormal rhythmic behaviour and the shortened and malformed arborisations of the s-LN$_v$s that were documented in all experiments involving the Olf and the Olf-bPAC constructs.

3.2.7. Immunostaining of flies expressing Olf and bPAC

In order to follow up on the behavioural experiments with the Olf and the bPAC controls (see 3.2.6.), a series of immunostaining experiments was conducted to further establish and confirm Olf as the sole cause of the abnormal and shortened arborisations of the s-LN$_v$s. The brains of flies expressing either bPAC or Olf under the pdf-gal4 driver were fixated, prepared and immunostained and subsequently imaged to assess the effects of their expression on the neuronal morphology.

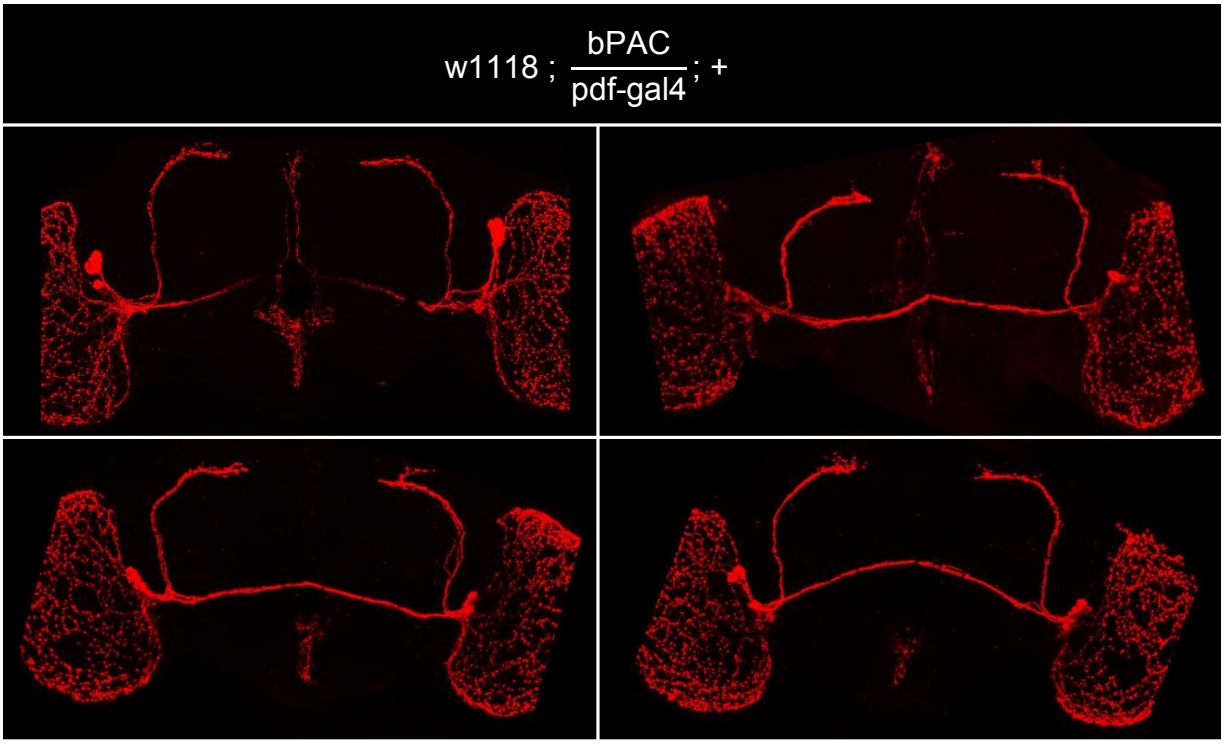

Figure 3.2.11a: Prepared and immunostained brains of flies, expressing bPAC in the PDF-positive clock neurons (pdf-gal4); single-channel recording, laser-excitation with wavelengths 532 nm (red), primary antibody: mouse anti-PDFc7; secondary antibody: Alexa Fluor 555 goat anti-mouse

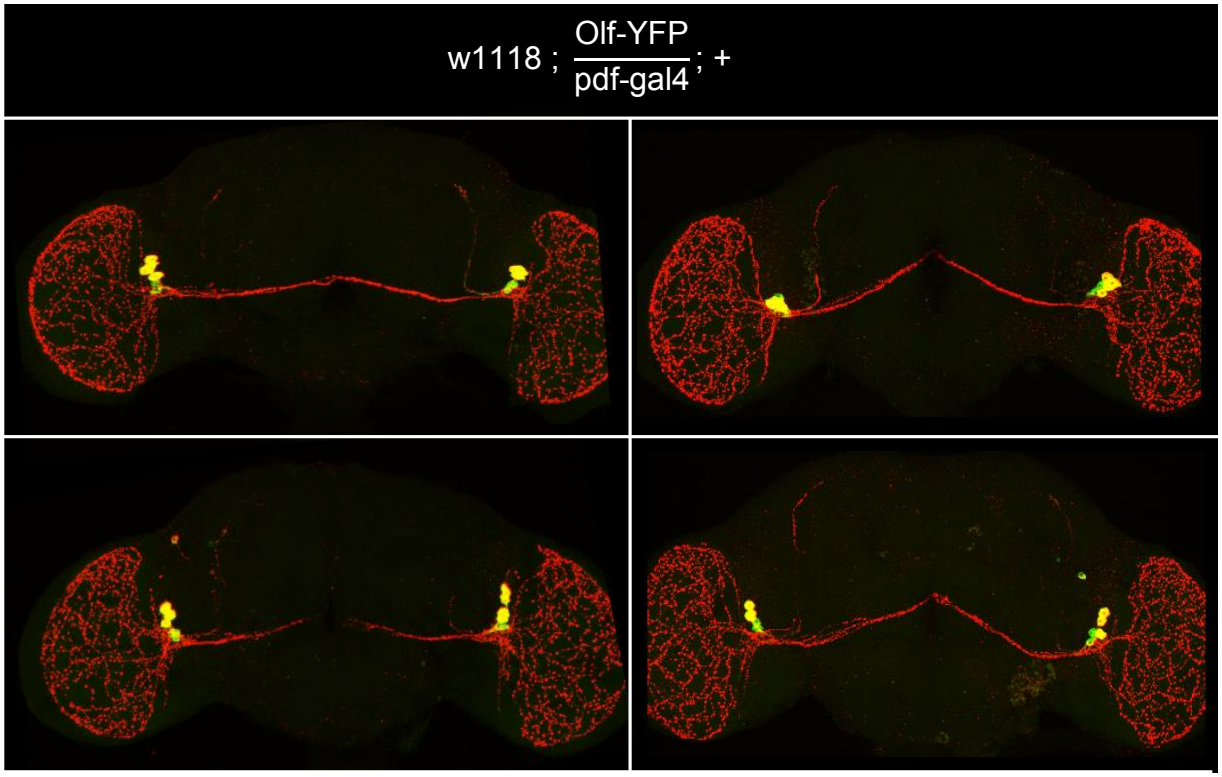

Figure 3.2.11b: Prepared and immunostained brains of flies, expressing Olf-YFP in the PDF-positive circadian neurons (pdf-gal4); two-channel recording, laser-excitation with wavelengths 488 nm (green) and 532 nm (red), primary antibody: mouse anti-PDFc7; secondary antibody: Alexa Fluor 555 goat anti-mouse

The immunostaining images of flies expressing either only bPAC or only Olf in the PDF-positive clock neurons confirm the results of the behavioural experiments (see 3.2.6.), with the Olf-channel alone being responsible for the shortened and underdeveloped s-LN_vs (see Fig. 3.2.11.). Brains expressing Olf in the PDF-positive clock neurons clearly exhibit the stunted and malformed s-LNvs, while brains expressing bPAC exhibit a rather wild type-like arborisation with projections of the s-LN_vs extending into the dorsal protocerebrum. It appears as if the damaging effects of expressing Olf-YFP alone are even worse than expressing Olf-bPAC or SthK-bPAC, as the s-LN_vs are barely even detectable in some images. The expression pattern of Olf-YFP is comparable to that of Olf-bPAC and SthK-bPAC (see 3.2.3 and 3.2.5), being centred mainly within the cell bodies with no detectable axonal expression. Brains expressing bPAC were not recorded with the YFP-channel, as the soluble bPAC has no fused YFP [105].

3.2.8. FIM-assay with *Drosophila* larvae expressing Olf-bPAC/SthK-bPAC

Trying to rear adult *Drosophila melanogaster*, expressing Olf-bPAC or SthK-bPAC in the motor neurons (ok6-gal4) produced no living flies, as the flies died during pupariation before eclosion. So the approach to characterize the two optogenetic tools within a living and moving model organism shifted away from trying to use adult *Drosophila* in favour of trying to use *Drosophila* larvae. It had already been shown that Olf-bPAC was already present in the larval stages when expression was driven using the pdf-gal4 driver (see 3.2.3) and larvae expressing Olf-bPAC in the motor neurons had already shown reactions towards light exposure in very early trial experiments (data not shown). So a method was devised involving the newly established FIM technology along with the accompanying analysis software FIMtrack (see Material and Methods 2.9.). Larvae expressing Olf-bPAC and SthK-bPAC in motor neurons were analysed for movement speed and body length in response to blue light illumination.

3.2.8.1. Assay with strong, long light exposure

To evaluate the applicability of the two optogenetic constructs Olf-bPAC and SthK-bPAC in *Drosophila* larvae, two standardized methods of testing were devised. One was devised to test the maximum possible effect evocable by illumination and featured a set recording time, a long light exposure time at a higher light intensity as well, while the other was meant to test the recoverability of the effects and featured shorter light exposure times at a lower light intensity and flexible recording times.
The assay with long and strong light exposure was always set to a full recording time of 60 seconds and consisted of a 30 second period in ambient red light, followed by a 30 second period of blue light illumination with an intensity of 1,6 mW/cm² at a wavelength of 470 nm.

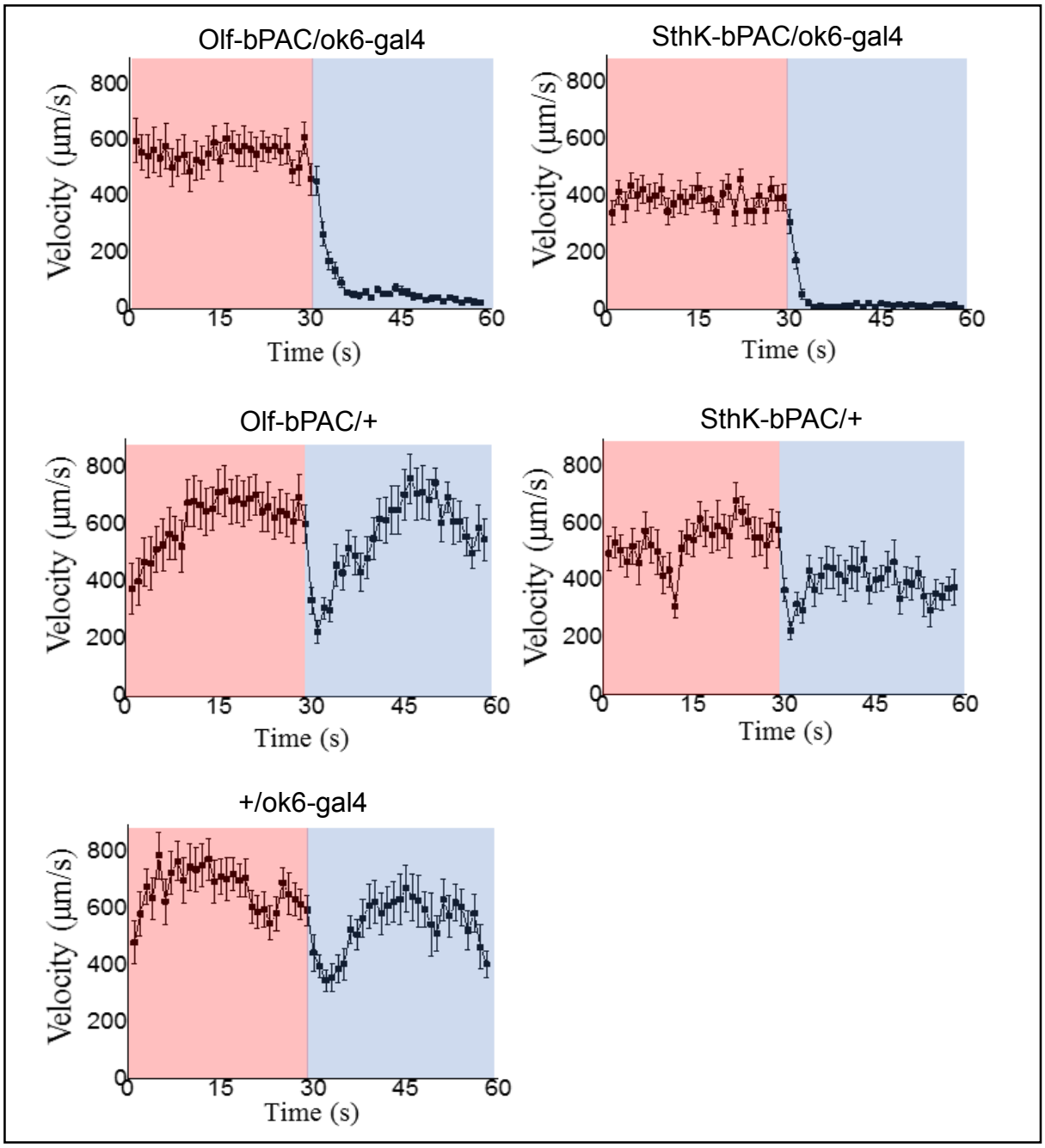

Figure 3.2.12: Velocity profiles of *Drosophila* larvae expressing either Olf-bPAC or SthK-bPAC in the motor neurons (ok6-gal4) and their respective controls under the influence of blue light illumination; red shading represents ambient red light conditions (0,1 µW/cm²), blue shading represents illumination period with blue light at 470nm wavelength and 1,6 mW/cm² intensity; n = 20 for each genotype, the velocity value at each second of the time graph consists of the averaged velocity values of each of the 20 recorded specimen at the overlapping time point of the recording; error bars represent SEM

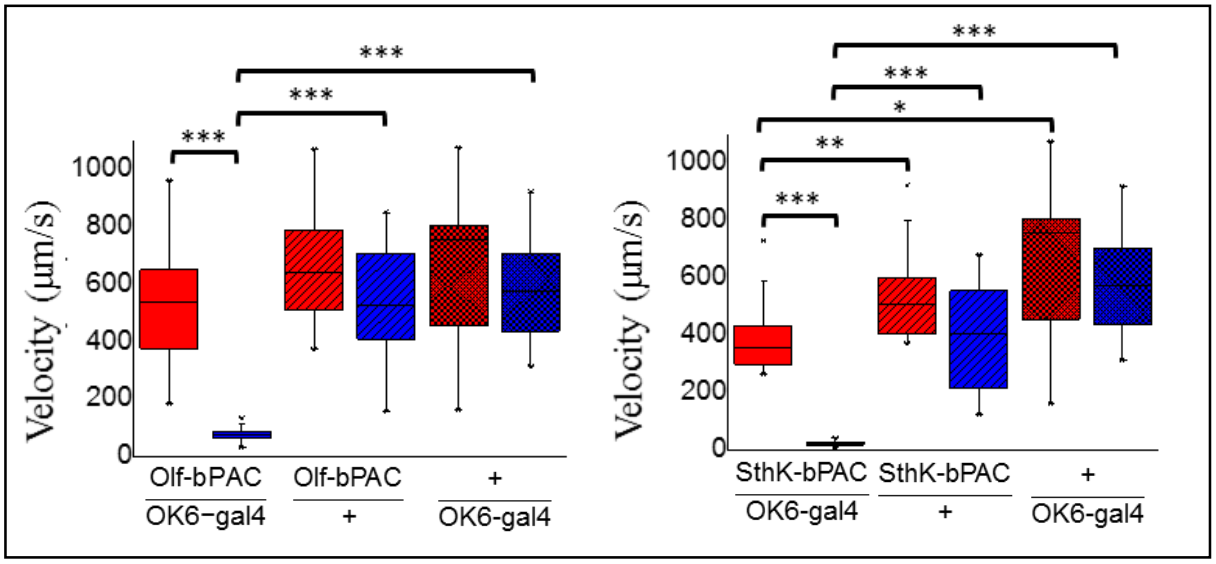

Figure 3.2.13: Average velocities of *drosophila* larvae expressing either Olf-bPAC or SthK-bPAC in the motor neurons (ok6-gal4) and their respective controls under the influence of blue light illumination; red plots represent ambient red light conditions (0,1 µW/cm²), blue plots represents illumination period with blue light at 470 nm wavelength and 1,6 mW/cm² intensity; n = 20 for each genotype, the boxplot velocity data for each genotype consists of the averaged velocity values of each of the 20 recorded specimen over the respective 30 second period of recording; Box line represents median, box square represents mean, box edges represent 25 and 75 percentiles, whiskers represent 1 and 99 percentiles

Drosophila larvae expressing either Olf-bPAC or SthK-bPAC in the motor neurons show a very strong and significant phenotype upon blue light illumination. Their respective velocities drop by over 95% when illuminated compared to their velocities under the ambient red light, rendering the larvae essentially motionless (see Fig 3.2.12). This drop in velocity is highly significant as evidenced by statistical analysis of the boxplot data (see Fig 3.2.13). The UAS-controls as well as the GAL4-controls are also initially affected by the changing of the light conditions, as their velocities briefly drop by roughly 50% for a couple of seconds before recovering. A notable exception here is the UAS-control for SthK-bPAC whose velocity never fully recovers but stays around 80% of its starting value. This effect is not statistically significant however. Another interesting and notable observation is the already significantly lower velocity of the SthK-bPAC/ok6 larvae under ambient red light, when compared to its respective UAS- and GAL4-controls, suggesting an effect of the construct already being noticeable even when not specifically activated.

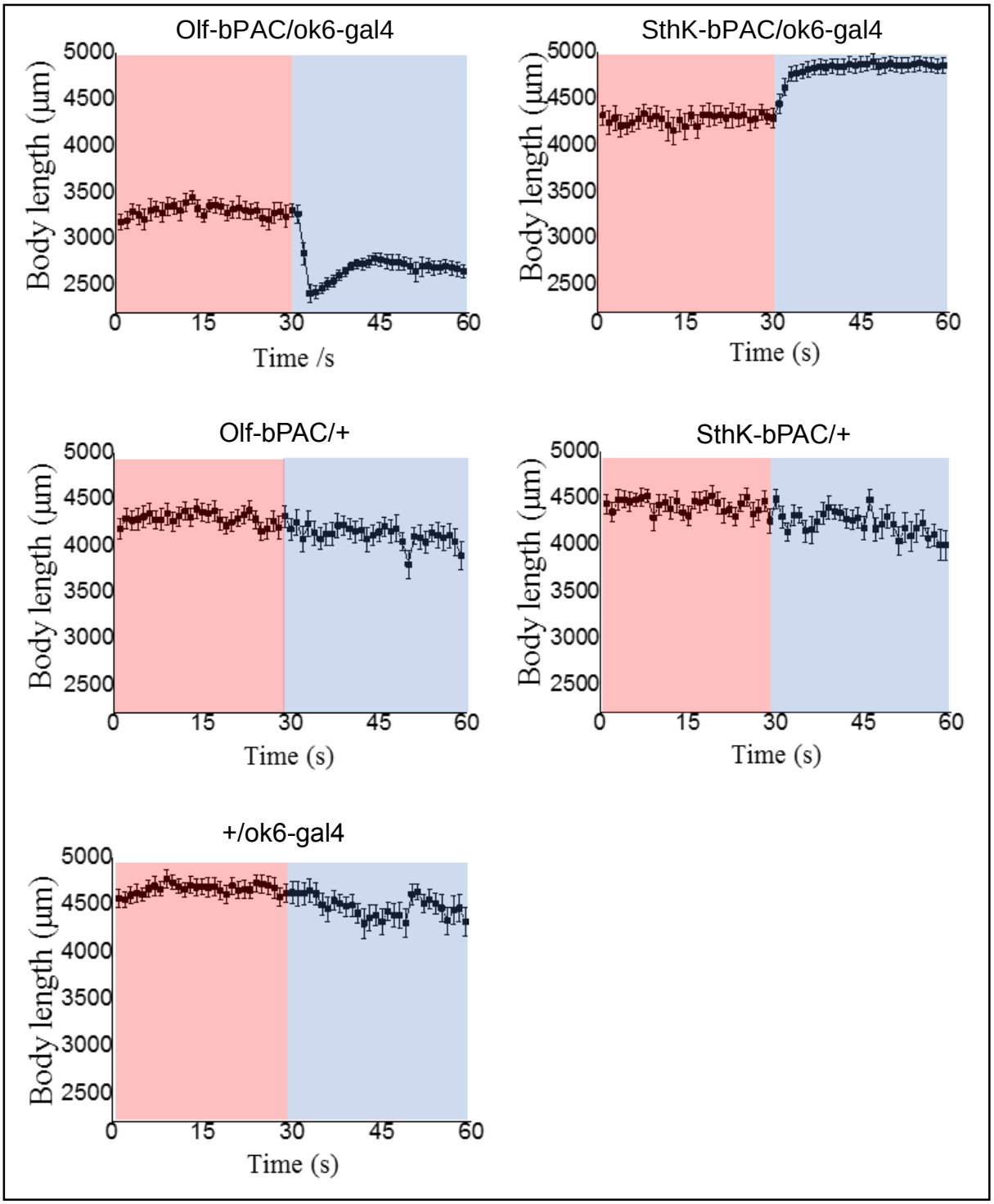

Figure 3.2.14: Body length profiles of *Drosophila* larvae expressing either Olf-bPAC or SthK-bPAC in the motor neurons (ok6-gal4) and their respective controls under the influence of blue light illumination; red shading represents ambient red light conditions (0,1 µW/cm²), blue shading represents illumination period with blue light at 470 nm wavelength and 1,6 mW/cm² intensity; n = 20 for each genotype, the velocity value at each second of the time graph consists of the averaged velocity values of each of the 20 recorded specimen at the overlapping time point of the recording; error bars represent SEM

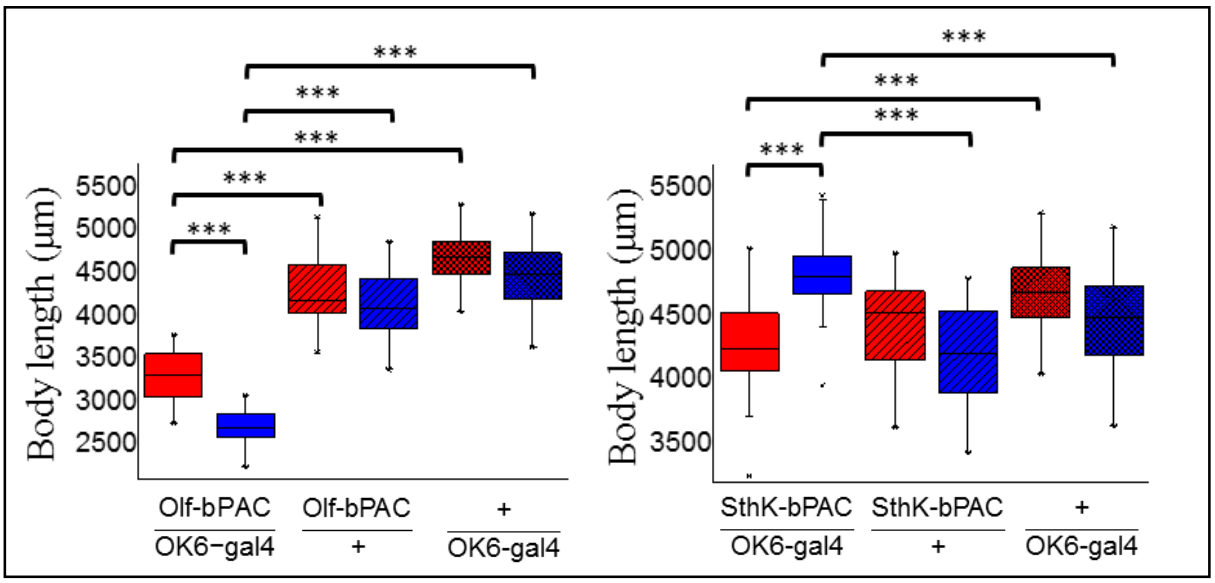

Figure 3.2.15: Average body length of *Drosophila* larvae expressing either Olf-bPAC or SthK-bPAC in the motor neurons (ok6-gal4) and their respective controls under the influence of blue light illumination; red plots represent ambient red light conditions, blue plots represents illumination period with blue light at 470 nm wavelength and 1,6 mW/cm² intensity; n = 20 for each genotype, the boxplot velocity data for each genotype consists of the averaged velocity values of each of the 20 recorded specimen over the respective 30 second period of recording; Box line represents median, box square represents mean, box edges represent 25 and 75 percentiles, whiskers represent 1 and 99 percentiles

The body length of both larvae expressing either Olf-bPAC or SthK-bPAC in their motor neurons is heavily affected upon blue light illumination, albeit in different respective ways. While larvae expressing Olf-bPAC heavily contract upon initial illumination, before slowly expanding again to about 70% of their initial body length, larvae expressing SthK-bPAC slowly expand to roughly 115% of their initial body length (see Fig. 3.2.14). All these changes in body length are also highly statistically significant as evidenced by the statistical comparison of the boxplot data (see Fig. 3.2.15). Both these changes in body size appear to be in congruence with the conductive qualities of the respective optogenetic tools at work, with Olf-bPAC likely having a depolarizing effect, while SthK-bPAC should have a hyperpolarizing effect [96, 98]. Unlike the velocity, the body length of the respective UAS- and GAL4-controls is not at all affected by the illumination, which stays exactly at its starting value, without even any initial startling reactions towards the light.

Also, larvae expressing Olf-bPAC are born significantly and a lot shorter and smaller than their respective controls, no matter the light conditions at roughly 75% comparative body length under ambient red light control conditions. SthK-larvae on the other hand are born a little bit, but still significantly shorter than the GAL4-control. These findings suggest strong effects of these tools even without being specifically triggered by illumination.

To test the influence that expressing only one subunit of the used CNGC-bPAC constructs might have on the *Drosophila* larvae, four separate control constructs were created and subsequently expressed in larval motor neurons to be assayed as well using the FIM assay. These four lines were the already established UAS-Olf (see 3.2.6. & 3.2.7.) and three newly created bPAC variants all trying to replicate the properties of the membrane-bound bPAC of the two fusion constructs as best as possible. One was the soluble bPAC-R278A, a bPAC-mutant with a point-mutation replacing the Arginine at position 278 with an Alanine, significantly reducing the cAMP production of the enzyme down to levels comparable to those of the membrane-bound bPAC in Olf-bPAC and SthK-bPAC, evidenced by recordings done in *Xenopus* oocytes (recordings by Dr. Shiqiang Gao, data not shown here). The others consisted of the two membrane-bound fusion constructs CD8-bPAC (bPAC fused to the membrane- bound lymphocyte marker CD8 [135]), and Glyco-bPAC (bPAC fused to the membrane-bound glycopetide Glycophorin [133]) (see Material and Methods 2.3).

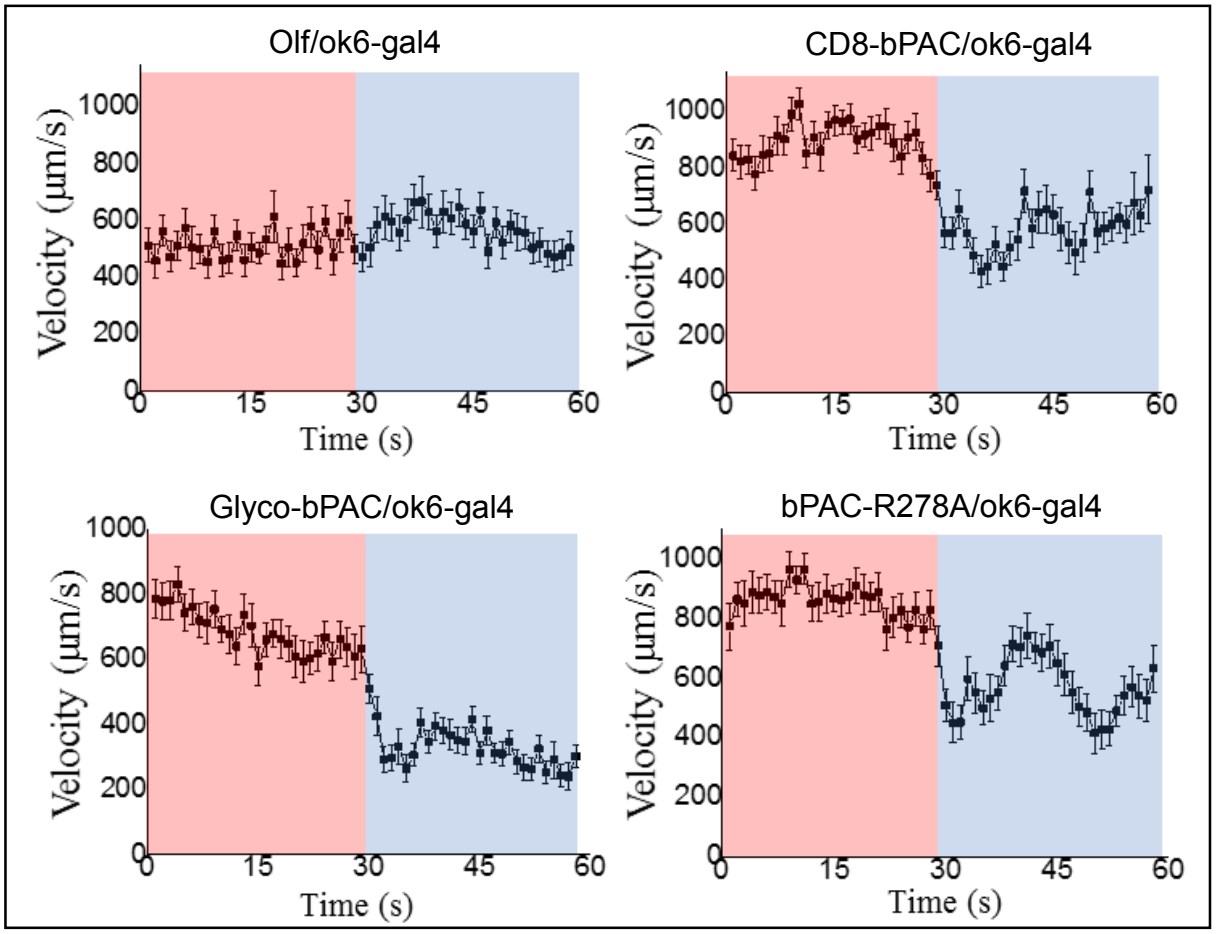

Figure 3.2.16: Velocity profiles of *Drosophila* larvae expressing either Olf, CD8-bPAC, Glyco-bPAC or bPAC-R278A in the motor neurons (ok6-gal4), under the influence of blue light illumination; red shading represents ambient red light conditions (0,1 µW/cm²), blue shading represents illumination period with blue light at 470nm wavelength and 1,6 mW/cm² intensity; n = 20 for each genotype, the velocity value at each second of the time graph consists of the averaged velocity values of each of the 20 recorded specimen at the overlapping time point of the recording; error bars represent SEM

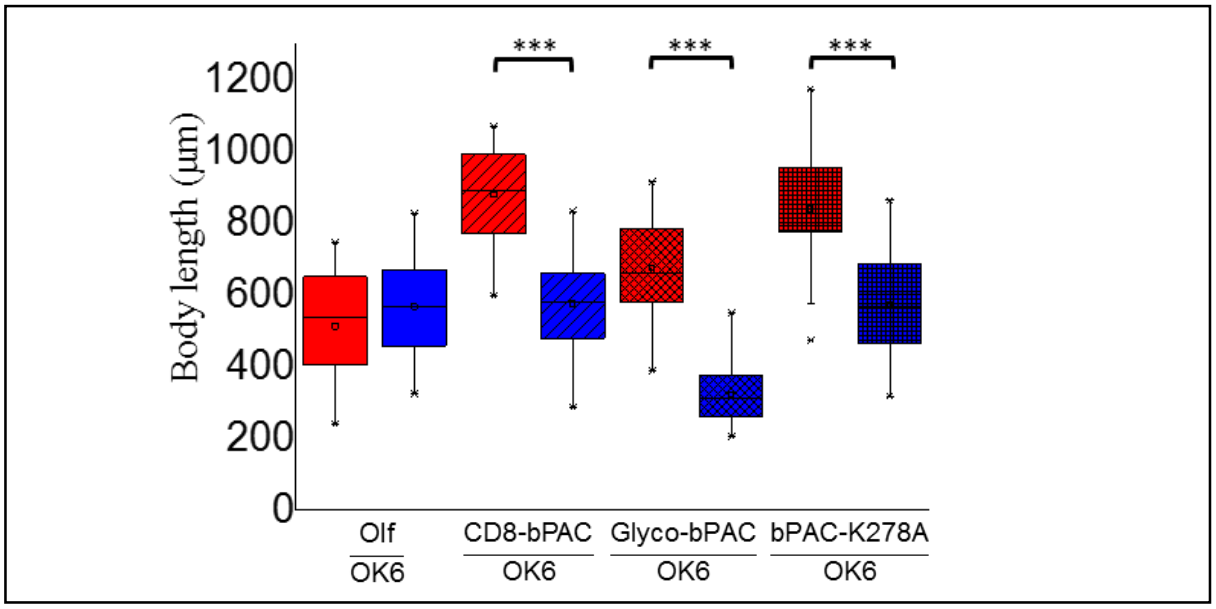

Figure 3.2.17: Average velocities of *Drosophila* larvae expressing either Olf, CD8-bPAC, Glyco-bPAC or bPAC-R278A in the motor neurons (ok6-gal4) under the influence of blue light illumination; red plots represent ambient red light conditions (0,1 µW/cm²), blue plots represents illumination period with blue light at 470nm wavelength and 1,6 mW/cm² intensity; n = 20 for each genotype, the boxplot velocity data for each genotype consists of the averaged velocity values of each of the 20 recorded specimen over the respective 30 second period of recording; Box line represents median, box square represents mean, box edges represent 25 and 75 percentiles, whiskers represent 1 and 99 percentiles

Apart from larvae expressing only Olf, all larvae expressing one of the three bPAC variants in their motor neurons react heavily to blue light illumination, with their respective velocities dropping by ~30% up to ~50% (see Fig 3.2.16). These drops in velocity are all also highly statistically significant, illustrated by the boxplot velocity data (see Fig 3.2.17). This suggests for cAMP to have a large and impactful role within motor neurons of *Drosophila* larvae. When combined with one of GNGCs however, the phenotype of the elevated cAMP levels is likely neglectable, as the CNGC-mediated and fully paralysing effect of the fusion construct takes precedence over the cAMP-mediated effect.

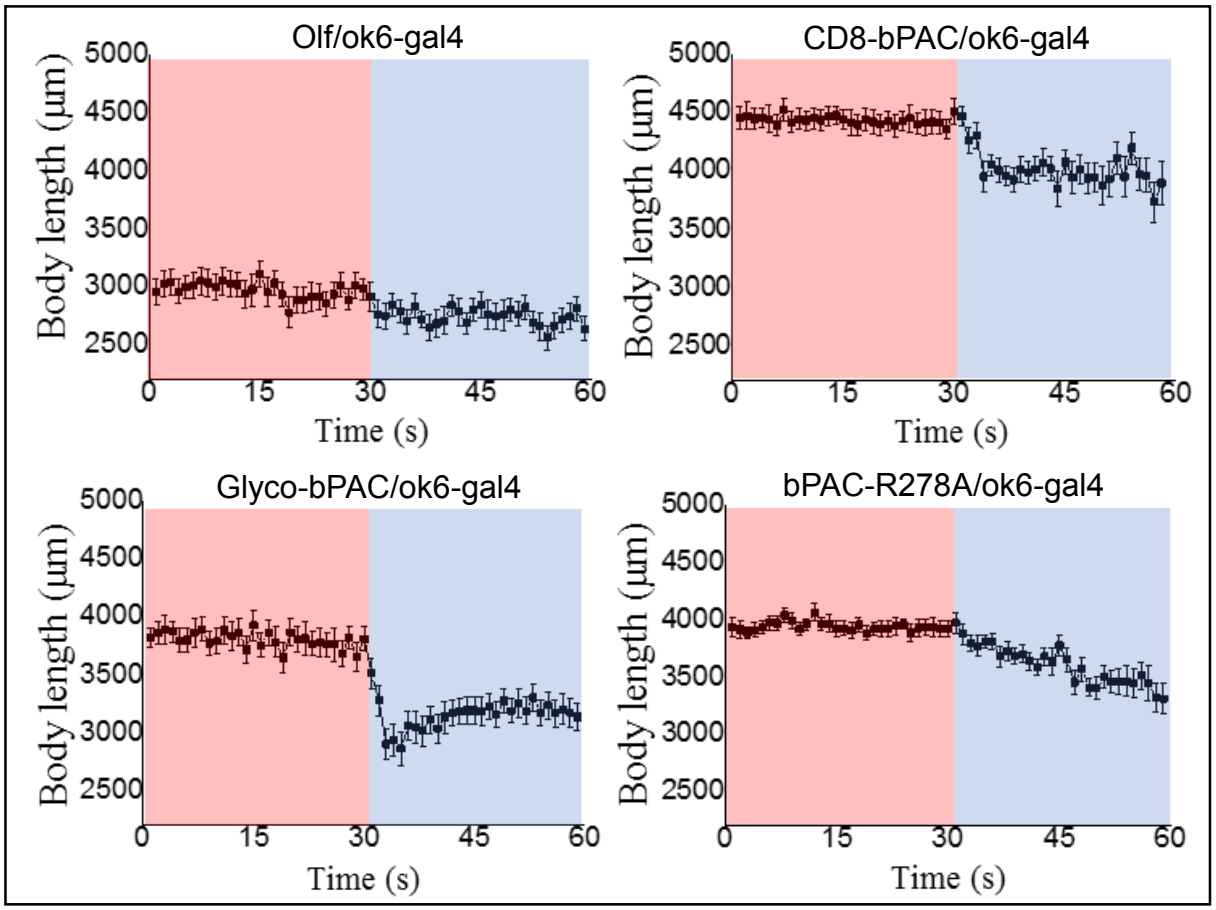

Figure 3.2.18: Body length profiles of *Drosophila* larvae expressing either Olf, CD8-bPAC, Glyco-bPAC or bPAC-R278A in the motor neurons (ok6-gal4), under the influence of blue light illumination; red shading represents ambient red light conditions (0,1 µW/cm²), blue shading represents illumination period with blue light at 470nm wavelength and 1,6 mW/cm² intensity; n = 20 for each genotype, the velocity value at each second of the time graph consists of the averaged velocity values of each of the 20 recorded specimen at the overlapping time point of the recording; error bars represent SEM

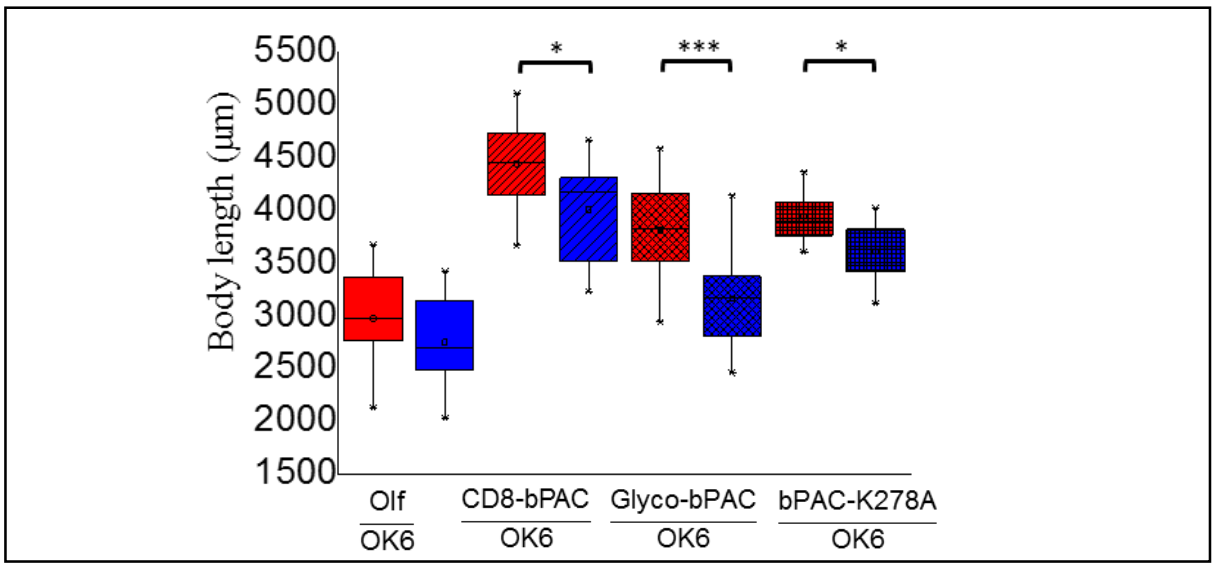

Figure 3.2.19: Average body length of *Drosophila* larvae expressing either Olf, CD8-bPAC, Glyco-bPAC or bPAC-R278A in the motor neurons (ok6-gal4) under the influence of blue light illumination; red plots represent ambient red light conditions (0,1 µW/cm²), blue plots represents illumination period with blue light at 470nm wavelength and 1,6 mW/cm² intensity; n = 20 for each genotype, the boxplot velocity data for each genotype consists of the averaged velocity values of each of the 20 recorded specimen over the respective 30 second period of recording; Box line represents median, box square represents mean, box edges represent 25 and 75 percentiles, whiskers represent 1 and 99 percentiles

All larvae expressing one of the three bPAC variants react quite strongly under blue light illumination, contracting to ~80% - ~90% of their initial body length (see Fig. 3.2.18). Larvae expressing Olf also contract very slightly. These reductions in body length are all statistically significant, except for the slight reduction in Olf-larvae (see Fig. 3.2.19). This data further confirms the strong and substantial effect of elevated of cAMP levels on larval mobility. Another notable observation is that larvae expressing Olf are born with drastically shorter bodies than those expressing one of the three bPAC variants. They very closely resemble the size and body shape of larvae expressing Olf-bPAC, proving the cause for this growth deficit to be due to the expression of the Olf channel (see Fig 3.2.14).

3.2.8.2. Assay with short, weak light exposure

To fully grasp the application frame of the two optogenetic tools Olf-bPAC and SthK-bPAC, it was necessary to evaluate the larvae's ability to recover from the CNGC-mediated paralysis after being illuminated. To test whether a recovery from the light induced effects was possible and to test the dependency of that recovery on illumination time, another assay was developed with different and shorter illumination times at a lower light intensity and also with a variable recording length to account for the varying durations of the larvae's recovery process.

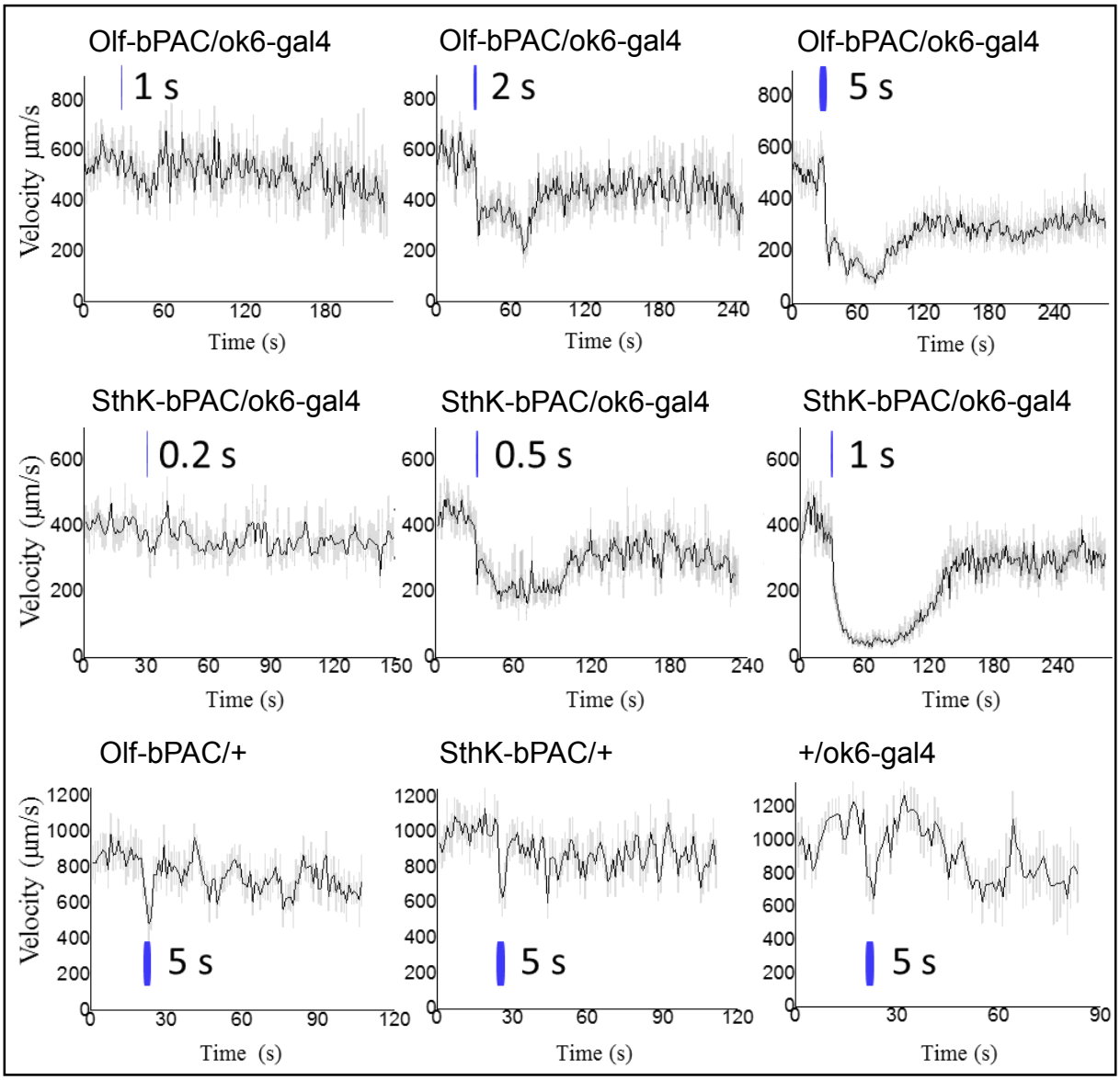

Figure 3.2.20: Velocity profiles of *Drosophila* larvae expressing Olf-bPAC or SthK-bPAC in the motor neurons (ok6-gal4) and their respective controls under the influence of blue light illumination; blue markings represent illumination with blue light at 470nm wavelength and 25 µW/cm² intensity for the indicated time period; n = 20 for each genotype, the velocity value at each second of the time graph consists of the averaged velocity values of each of the 20 recorded specimen at the respective time point of the recording; grey error bars represent SEM

The larvae tested in the short illumination assay, expressing Olf-bPAC and SthK-bPAC in motor neurons demonstrate that a recovery from the effects of the optogenetic fusion constructs is possible. Larvae expressing Olf-bPAC that were excited for 5 seconds are not able to fully recover their initial velocity however, unlike larvae expressing SthK-bPAC, which fully recover their initial velocity, even after a 5 second illumination period (see Fig. 3.2.20). Although apparently having longer lasting and less reversible effects on larval mobility, Olf-bPAC is less effective at reducing larval mobility at shorter illumination times. The longest illumination time that did not produce a recognizable effect on larval mobility was 1 second for Olf-bPAC and 0.2 seconds for SthK-bPAC.

The respective UAS- and GAL4-controls exhibit an initial startle response to a 5-second illumination, but did not remain affected for more than a few seconds.

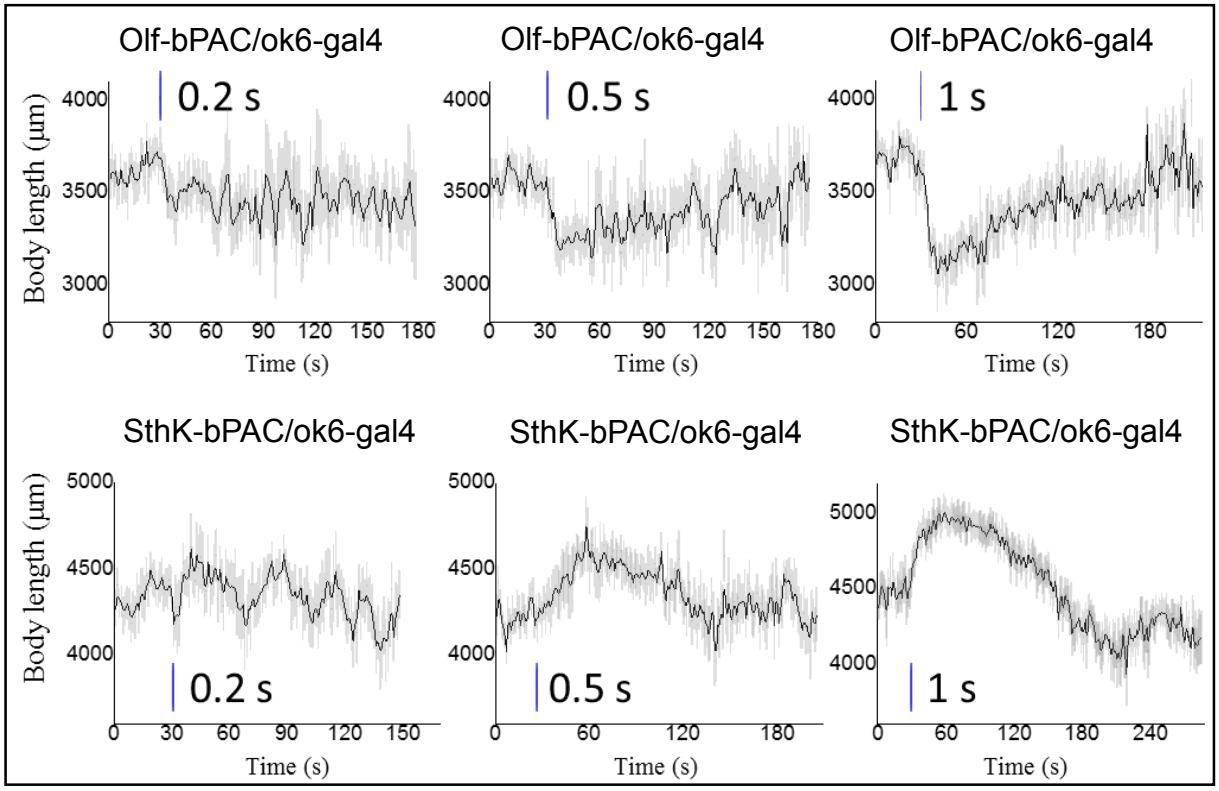

Figure 3.2.21: Body length profiles of *Drosophila* larvae expressing Olf-bPAC or SthK-bPAC in the motor neurons (ok6-gal4) under the influence of blue light illumination; blue markings represent illumination with blue light at 470nm wavelength and 25 µW/cm² intensity for the indicated time period; n = 20 for each genotype, the velocity value at each second of the time graph consists of the averaged velocity values of each of the 20 recorded specimen at the respective time point of the recording; grey error bars represent SEM

Observing the larvae's body length in reaction to the short light pulses, it becomes obvious that the light-induced effects of Olf-bPAC and SthK-bPAC can be much better evaluated when analysing the change in body length rather than in velocity. While Olf-bPAC-larvae exhibit unimpaired mobility when illuminated for 1 second (see Fig. 3.2.20), their bodies already clearly contract when illuminated for 0.5 seconds (see Fig. 3.2.21). In contrast to velocity, the body length of SthK-bPAC-larvae are also able to fully recover from the illumination effect, in the case of the 1 second illumination they appear even to overcompensate somewhat, closing out with a shorter overall body length than at the beginning of the recording. Since the body length of the UAS- and GAL4-control larvae are not affected at all by the strong 30 second illumination (see Fig. 3.2.14), the controls' FIM data was not analysed for that parameter in this assay.

3.3. Temperature-controlled expression of Olf-bPAC and SthK-bPAC

After the unsuccessful attempt to apply the optogenetic tools Olf-bPAC and SthK-bPAC in clock neurons of *Drosophila* and use them to reliably and predictably influence the circadian clock, alternative methods had to be considered. It became evident that expressing Olf-bPAC and SthK-bPAC with an ordinary GAL-4 driver, like pdf-gal4 or clk856-gal4, causes arrhythmicity and dysfunctional and underdeveloped s-LN_vs (see Results 3.2). To circumnavigate these issues, a new expression system was chosen that would halt the expression of the construct until adulthood, where expression could then be externally induced. We combined the two GAL4-driver lines (pdf-gal4 and clk856-gal4) with the temperature-sensitive tub-gal80^{ts}-line (see Material and Methods 2.4). GAL80^{ts} acts as an inhibitor to GAL4, binding and preventing it from interacting with the UAS-sequence to initiate transcription of the target gene. GAL80^{ts}, a temperature-sensitive splicing variant of GAL80 becomes inactive at temperatures above 28°C, providing us with a way of externally inducing the expression of Olf-PAC and SthK-bPAC (see Material and Methods 2.1) [126].

3.3.1. Assessment of functionality

The two newly crossed lines *w; clk856GAL4; tubGAL80ts/TM6B* and *y w; pdfGAL4; tubGAL80ts/TM6B* were first tested for basic functionality, to see if the expression of the optogenetic tools could indeed be induced by exposing the flies to a temperature of 29°C and to see whether the expression was also sufficiently suppressed when raising and keeping the flies at a temperature of 18°C. In order to test this, flies expressing Olf-bPAC and SthK-bPAC under control of the pdf-gal4/tub-gal80ts and clk856-gal4/tub-gal80ts were raised both at 18°C and at 29°C and had their brains immediately prepared, fixated and immunostained with an anti-PDF antibody after eclosion. Flies were also raised at 18°C and then exposed to 29°C for a certain period after they had reached adulthood.

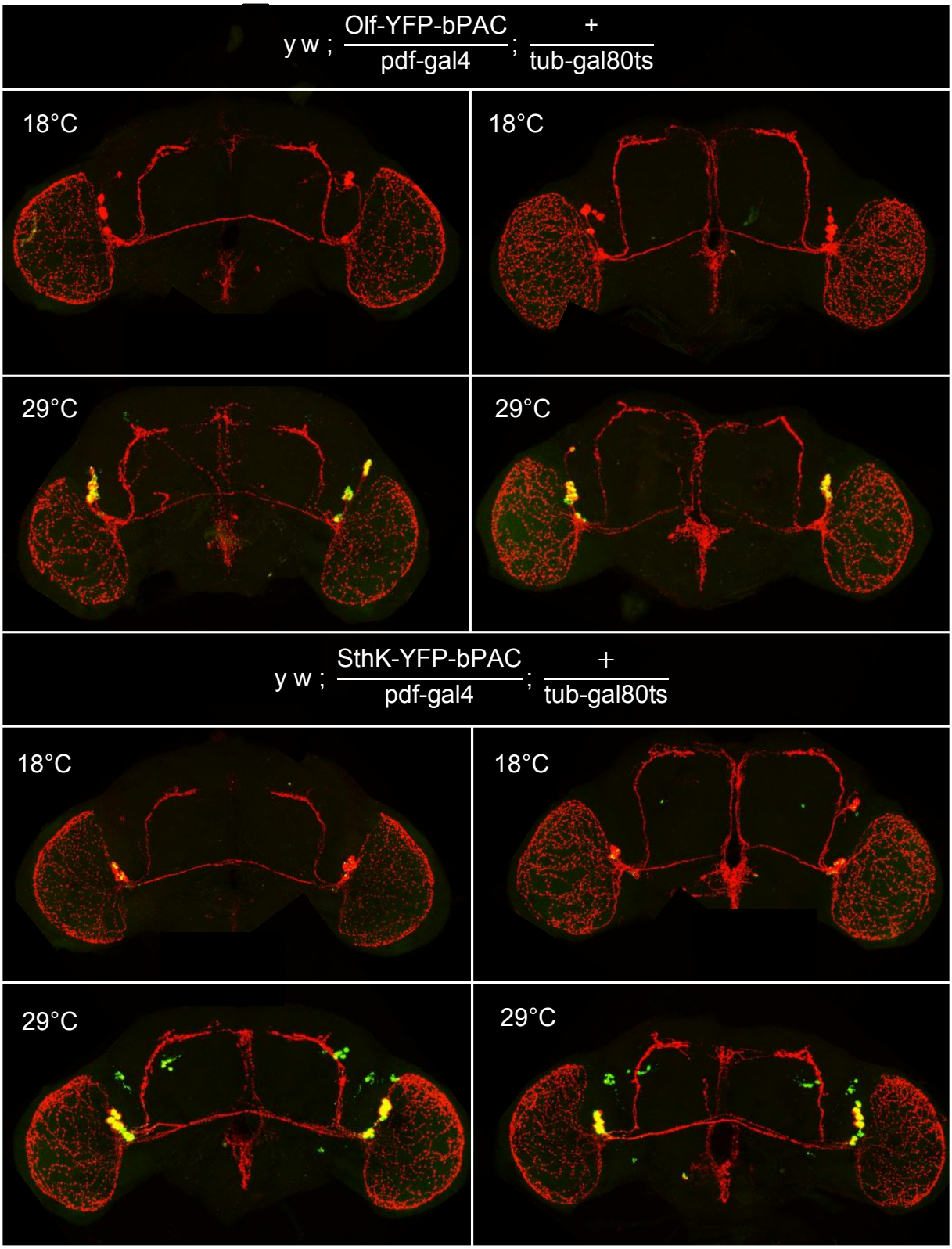

Figure 3.3.1: Prepared and immunostained brains of flies, expressing Olf-YFP-bPAC and SthK-YFP-bPAC in PDF-positive clock neurons (pdf-gal4) under the control of the temperature-sensitive tab-gal80ts, annotated with the respective temperatures the flies had been raised at; two-channel recording, laser-excitation with wavelengths 488 nm (green) and 635 nm (red), primary antibody: mouse anti-PDFc7; secondary antibody: Alexa Fluor 635 goat anti-mouse; all images in this section have been recorded with identical settings, incl. magnification, laser intensity, detector gain, frame average and resolution

The immunostaining experiments with the tub-gal80ts lines show that the temperature-sensitive transcriptional suppression works as intended with only minor side effects. Images of flies raised at 18°C show no sign of any expression for Olf-bPAC in the YFP-channel (488 nm), while those raised at 29°C show a strong signal located around the cell bodies of the LN_vs, signifying a strong expression of Olf-bPAC (see Fig. 3.3.1). In the case of SthK-bPAC the transcriptional suppression at 18°C by $GAL80^{ts}$ also seems to work, however not as effective as for Olf-bPAC, evidenced by the faint but noticeable signal given off by the LN_vs in the YFP-channel. SthK-bPAC flies raised at 29°C show an extremely strong YFP-signal, signifying strong expression of SthK-bPAC. Interestingly the s-LNvs of the flies raised at 29°C show almost no morphologic damages or abnormalities. This is rather unexpected, as it was expected that continuous expression of Olf-bPAC and SthK-bPAC would recreate the underdeveloped and malformed s-LN_vs that can be seen when these constructs are expressed without temperature-sensitive transcriptional control (see Results 3.2.3). Additionally, expression for SthK-bPAC at 29°C is not limited to the LN_vs, as other neurons in the protocerebrum, not stained by the anti-PDF immunostaining give off a strong signal in the YFP-channel. These neurons could not be identified however.

To further test the functionality of the $GAL80^{ts}$-lines, another experiment was run, raising flies at 18°C and subjecting them to 29°C for 12 hours after the flies eclosed, in order to assess how effectively expression could be induced during adulthood.

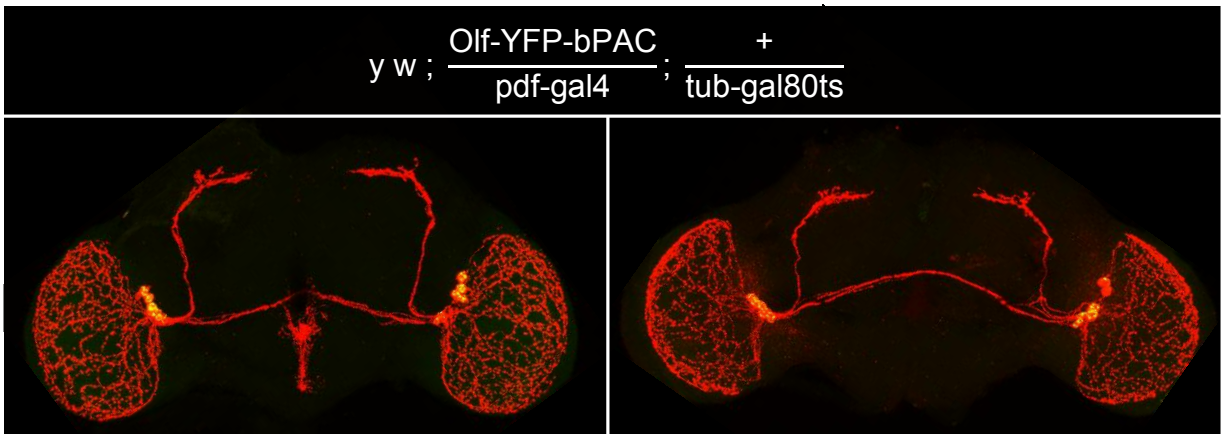

Figure 3.3.2: Prepared and immunostained brains of flies, raised at 18°C, expressing Olf-YFP-bPAC in the PDF-positive circadian neurons after having been subjected to 29°C for 12h; two-channel recording, laser-excitation with wavelengths 488 nm (green) and 635 nm (red), primary antibody: mouse anti-PDFc7; secondary antibody: Alexa Fluor 635 goat anti-mouse; all images in this section have been recorded with identical settings, incl. magnification, laser intensity, detector gain, frame average and resolution

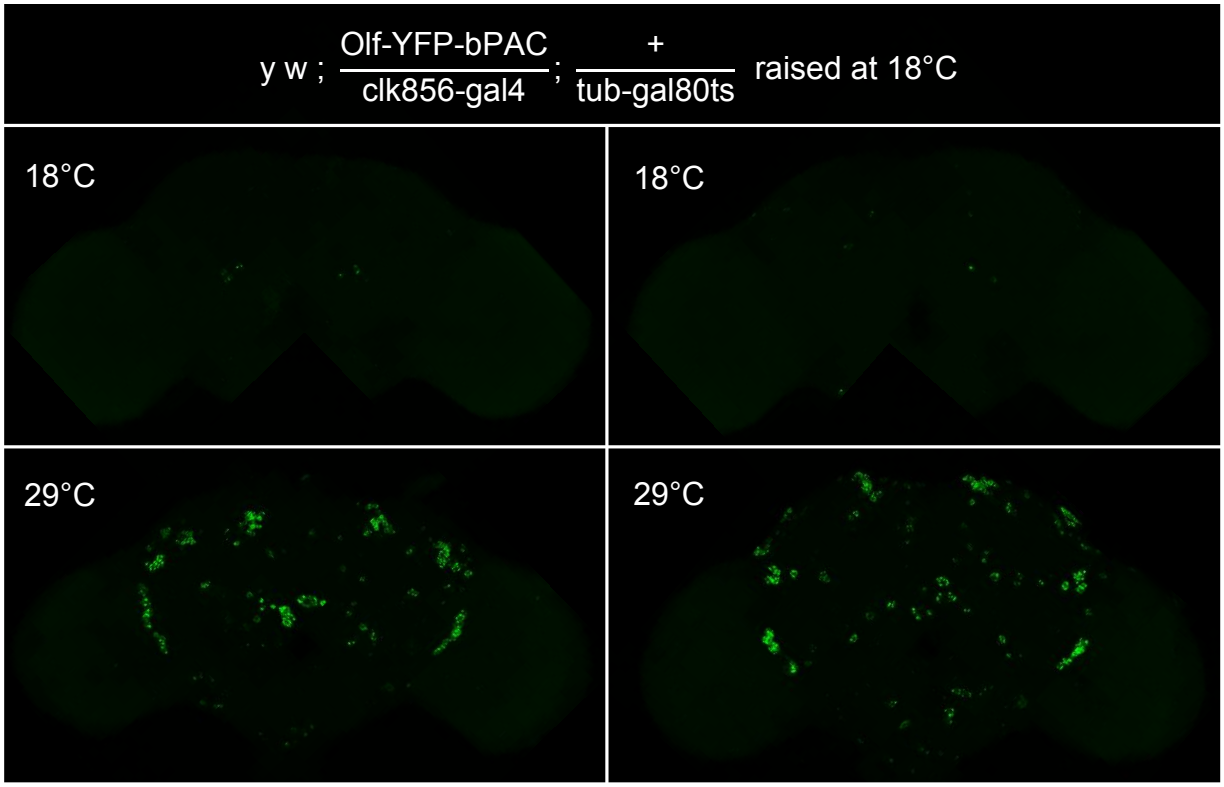

Figure 3.3.3: Prepared and fixated brains of flies, raised at 18°C, expressing Olf-YFP-bPAC in all clock neurons (clk856-gal4) after having been subjected to 29°C for 12h (bottom); no immunostaining; single-channel recording, laser-excitation with wavelength 488 nm (green); all images in this section have been recorded with identical settings, incl. magnification, laser intensity, detector gain, frame average and resolution

Judging by these images, it can be concluded that both GAL80^{ts}-lines function as intended, reliably triggering the expression of the target protein in adult flies of *Drosophila melanogaster* after having been subjected to 29°C for 12 hours. The YFP-channel (488 nm) in the images of flies expressing Olf-bPAC in the PDF-positive clock neurons shows a strong signal located around the LN$_v$s, signifying a successful expression of Olf-bPAC (see Fig. 3.3.2). Brains expressing Olf-bPAC in all clock neurons (clk856-gal4) also show a strong signal located around the cell bodies of these neurons (see Fig. 3.3.3), providing an anatomical overview of all cells of the neuronal clock network (see Introduction 1.1.2).

In conclusion it can be said that the overall functionality of the GAL80^{ts}-lines had been established and the flies were ready to be tested in behavioural experiments.

3.3.2. Rhythmicity experiments

To test the effects that inducing the temperature-controlled expression of Olf-bPAC and SthK-bPAC would have on the rhythmic behaviour of *Drosophila* after eclosion, a series of behavioural experiments was started. The experiments were designed to assess in what way the expression of the constructs themselves would have on the flies' circadian clock, as well as the rise in temperature. Different light regimes were tested as well, one which would not activate the fused bPAC (i.e. RD, red), compared to one that would (i.e. LD, white/blue). In the first experiment flies were entrained for 22 days by a 12:12 RD light regime. The first 8 days the flies were recorded at a temperature of 20°C. From day 9 to day 15, a temperature gradient was introduced, raising the temperature to 29°C in the morning and lowering it back down to 20°C in the evening, in phase with the 12:12 RD light entrainment. This setup was meant to use the periodical increase in temperature as a second Zeitgeber in addition to the light, strengthening entrainment. From day 16 onward, the temperature was kept at 20°C again. The experiment was designed to directly compare the two periods at 20°C with each other, one pre- and the other post-expression, to test for any background effects of the constructs on the flies' circadian clocks.

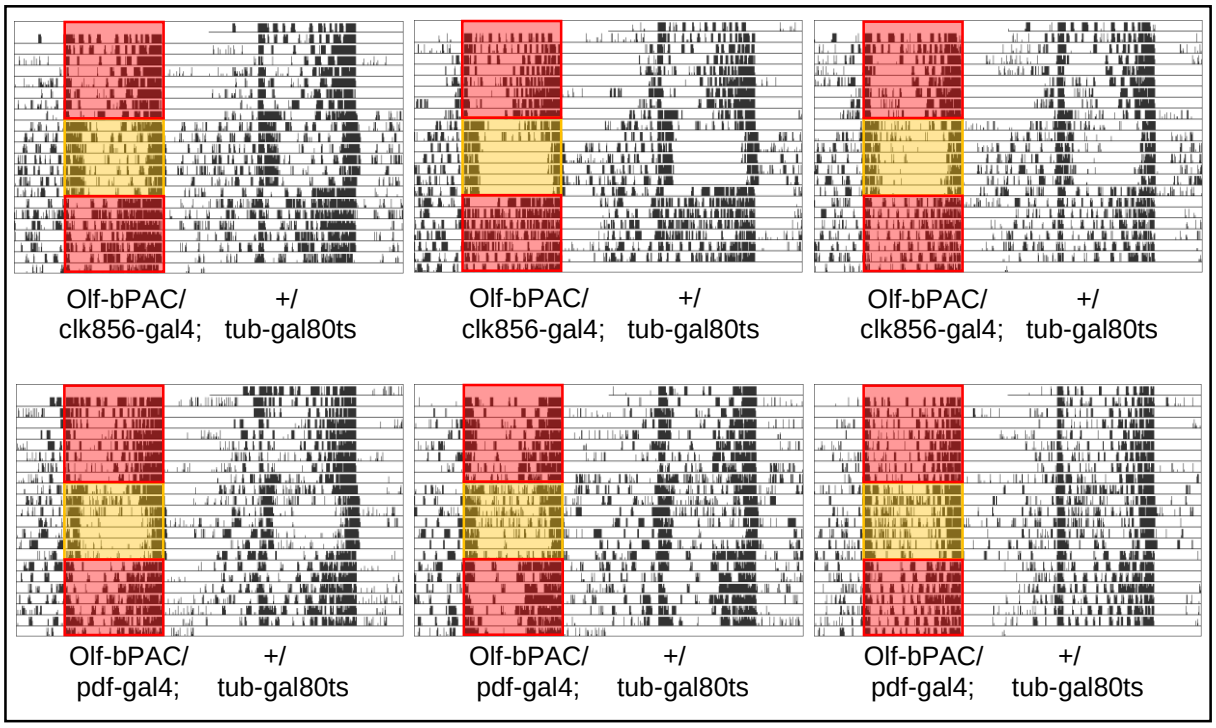

Figure 3.3.4a: Sample actograms of flies expressing Olf-bPAC in all clock neurons (clk856-gal4) and all PDF-positive clock neurons (pdf-gal4), temperature-controlled expression by GAL80ts, double-plotted; red shading represents 22 day entrainment cycle of 12:12 RD (620 nm, ~5 µW/cm²), orange shading represents 7 day 12:12 temperature cycle, 20°C during lights off, 29°C during lights on; no shading represents darkness; 60% RH

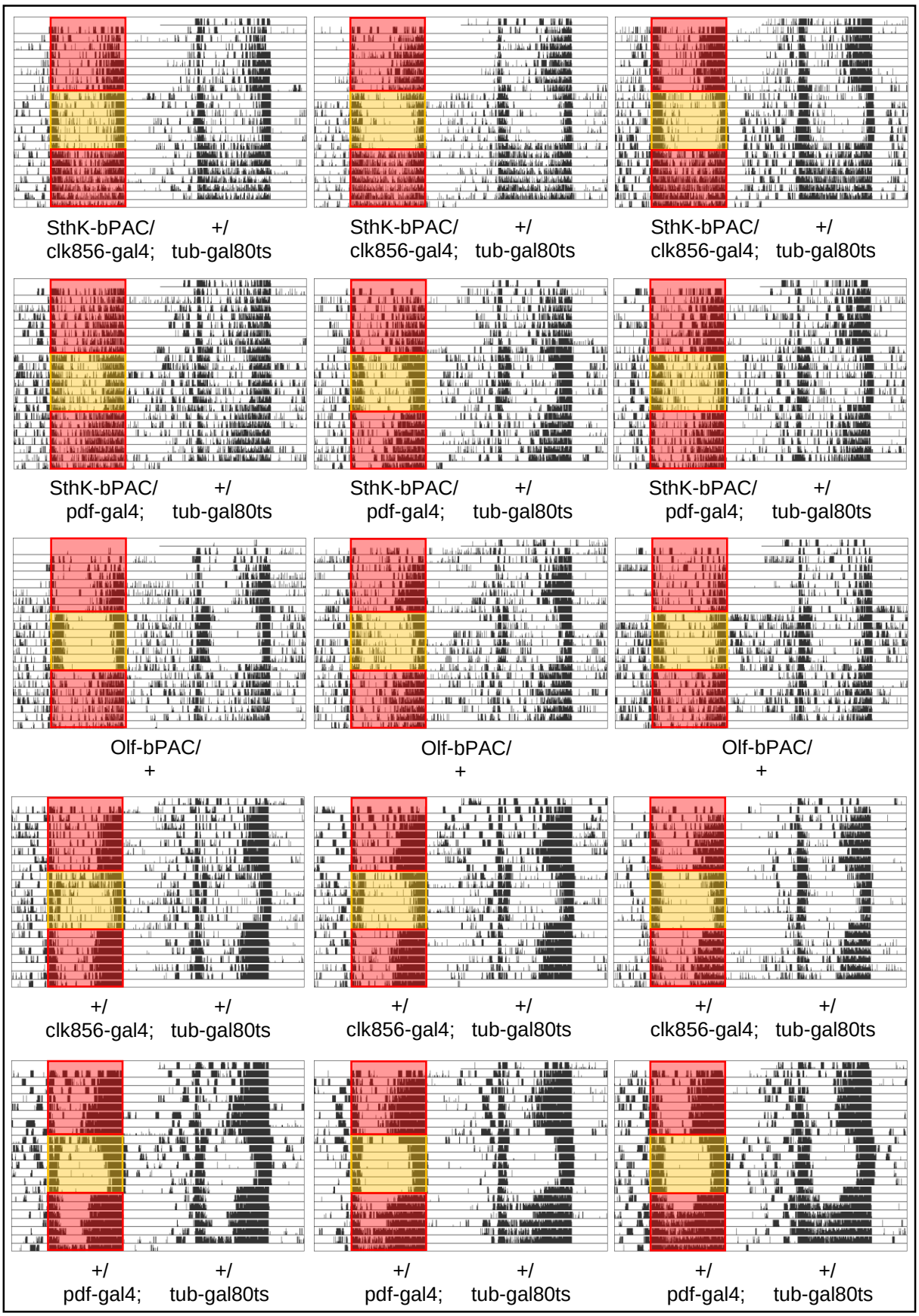

Figure 3.3.4b: Sample actograms of flies expressing SthK-bPAC in all clock neurons (clk856-gal4) and all PDF-positive clock neurons (pdf-gal4), temperature-controlled expression by GAL80ts, and the respective UAS- and GAL4-controls; double-plotted; red shading represents 22 day entrainment cycle of 12:12 RD (620 nm, ~5 µW/cm²), orange shading represents 7 day 12:12 temperature cycle, 20°C during lights off, 29°C during lights on; no shading represents darkness; 60% RH

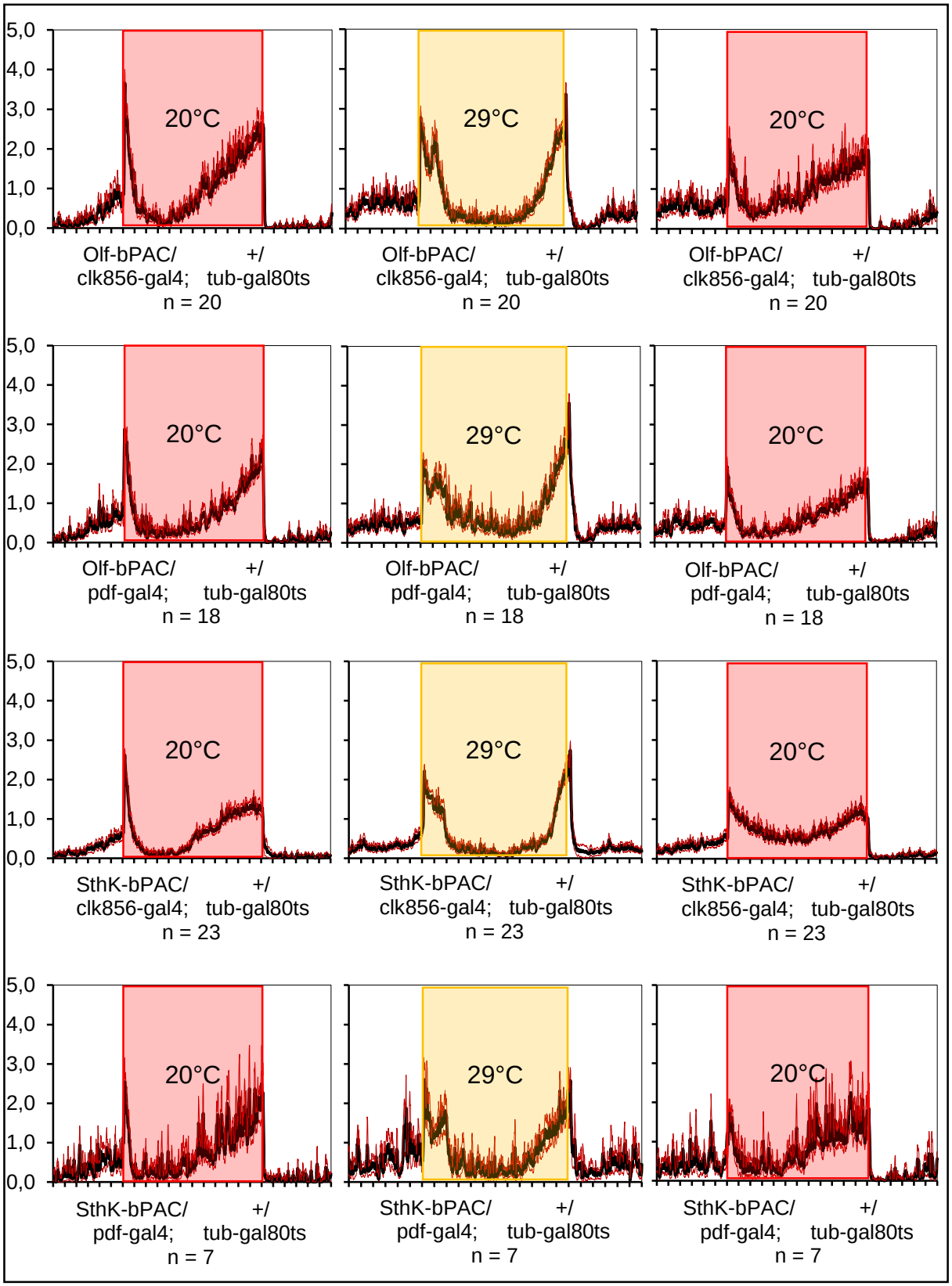

Figure 3.3.5a: Averaged actograms of flies expressing Olf-bPAC or SthK-bPAC in all circadian clock neurons (clk856-gal4) and all PDF-positive clock neurons (pdf-gal4); red shading represents entrainment cycle of 12:12 RD (620 nm, ~5 µW/cm²) at 20°C; orange shading represents entrainment cycle of 12:12 RD and 12:12 temperature cycle 20°C/29°C; 60% RH; for each genotype all available days recorded under the respective conditions were used for data averaging; for each genotype all flies that survived the 22 day experiment were used for data averaging

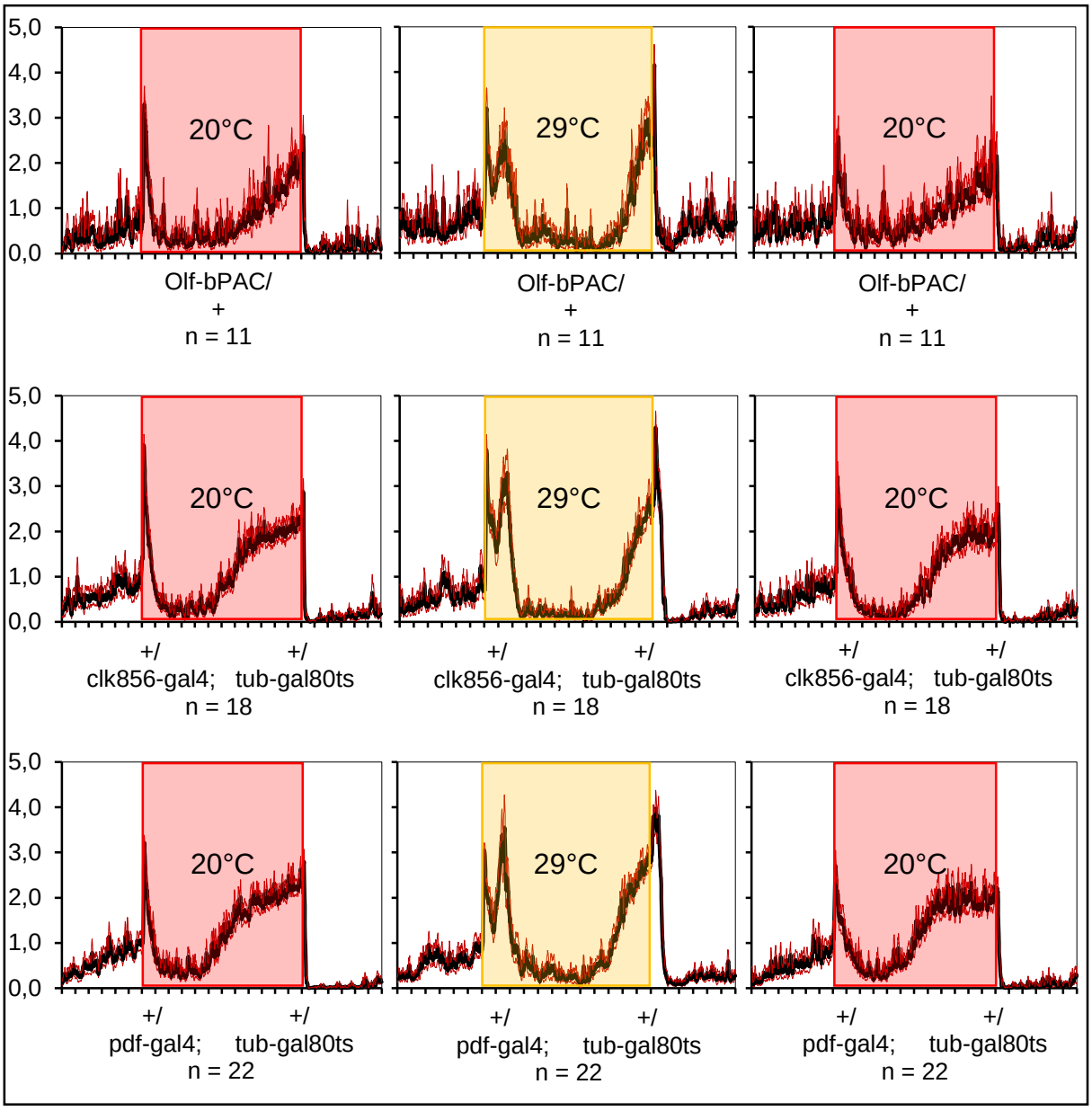

Figure 3.3.5b: Averaged actograms of flies expressing no Olf-bPAC or SthK-bPAC anywhere, (respective UAS- and GAL4-controls to Fig 3.3.5a); red shading represents entrainment cycle of 12:12 RD (620 nm, ~5 µW/cm²) at 20°C; orange shading represents entrainment cycle of 12:12 RD and 12:12 temperature cycle 20°C/29°C; 60% RH; for each genotype all available days recorded under the respective conditions were used for data averaging; for each genotype all flies that survived the 22 day experiment were used for data averaging

The experiment demonstrates that most of the flies still possess a functioning circadian clock and exhibit a bimodal, rhythmic activity pattern in 12:12 RD after the expression of Olf-bPAC or SthK-bPAC has been induced by increasing the temperature to 29°C. For Olf-bPAC, expression of the construct appears to not interfere with the circadian clock, even when expressed in all clock neurons, as long as the construct is not activated by blue light. The expression of SthK-bPAC however does seem to influence the circadian clock when expressed in all clock neurons, even under red-light conditions. Flies expressing SthK-bPAC in all clock neurons are the only strain to not

follow a wild type-like bimodal activity pattern in 12:12 RD, after the expression of the constructs had been induced (see Fig. 3.3.4 and 3.3.5). While the other flies along with the controls continue to exhibit an M peak, a siesta and an E peak, the bimodal activity pattern of the flies expressing SthK-bPAC in all clock neurons (clk856-gal4) breaks down after induction of expression at 29°C. This is clearly visible in both the sample actograms as well as the averaged actograms, where the differences in locomotor behaviour can easily be identified when comparing the two periods at 20°C before and after induction at 29°C (see Fig. 3.3.4 and 3.3.5). This hints at SthK-bPAC already being active in the absence of blue light, negatively impacting the rhythmicity of the circadian clock. At 29°C, flies expressing SthK-bPAC in all clock neurons do exhibit a bimodal activity pattern, likely because of the temperature cycle acting as a second Zeitgeber. All of the actograms recorded at 29°C, of both test-flies and controls alike, show a second M peak, visible both in the sample actograms as well as in the averaged actograms (see Fig. 3.3.4 and Fig. 3.3.5). Roughly at ZT 2, the flies' activity increases abruptly. This second peak in activity is due to the increase in temperature from 20°C to 29°C, which apparently has not been programmed to be perfectly in phase with the 12:12 RD light regime. The overall activity of flies in the experiment also decreases as the experiment progresses due to the flies' increasing age.

The same type of experiment was then repeated, only with a strong source of white light used for a 12:12 LD entrainment, to see the effects on the flies' rhythmic behaviour when the expressed optogenetic constructs were specifically activated by the light source.

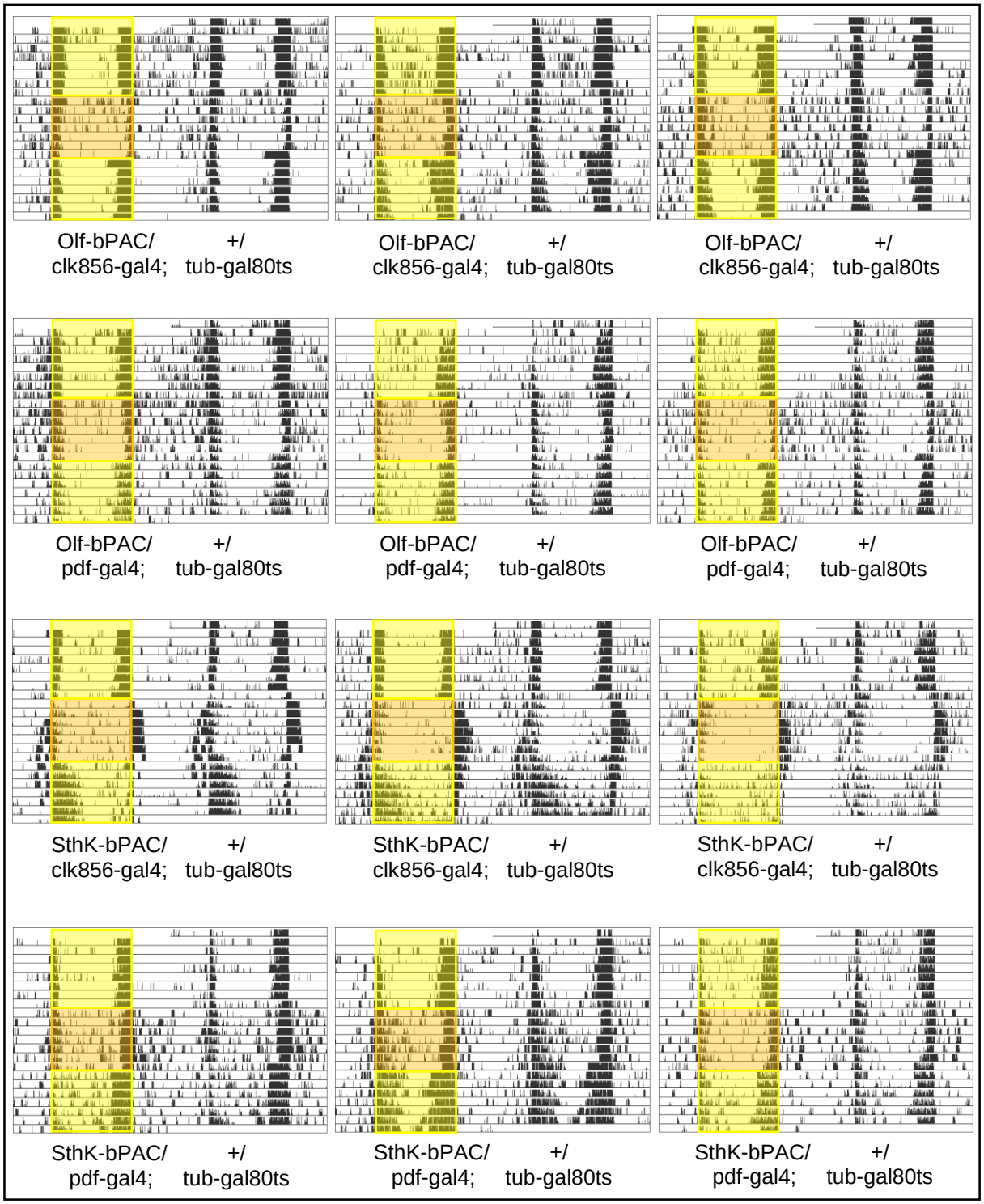

Figure 3.3.6a: Sample actograms of flies expressing Olf-bPAC and SthK-bPAC in all clock neurons (clk856-gal4) and all PDF-positive clock neurons (pdf-gal4), temperature-controlled expression by GAL80ts, double-plotted; yellow shading represents 22 day entrainment cycle of 12:12 RD (550 nm, ~90 µW/cm²), orange shading represents 7 day 12:12 temperature cycle, 20°C during lights off, 29°C during lights on; no shading represents darkness; 60% RH

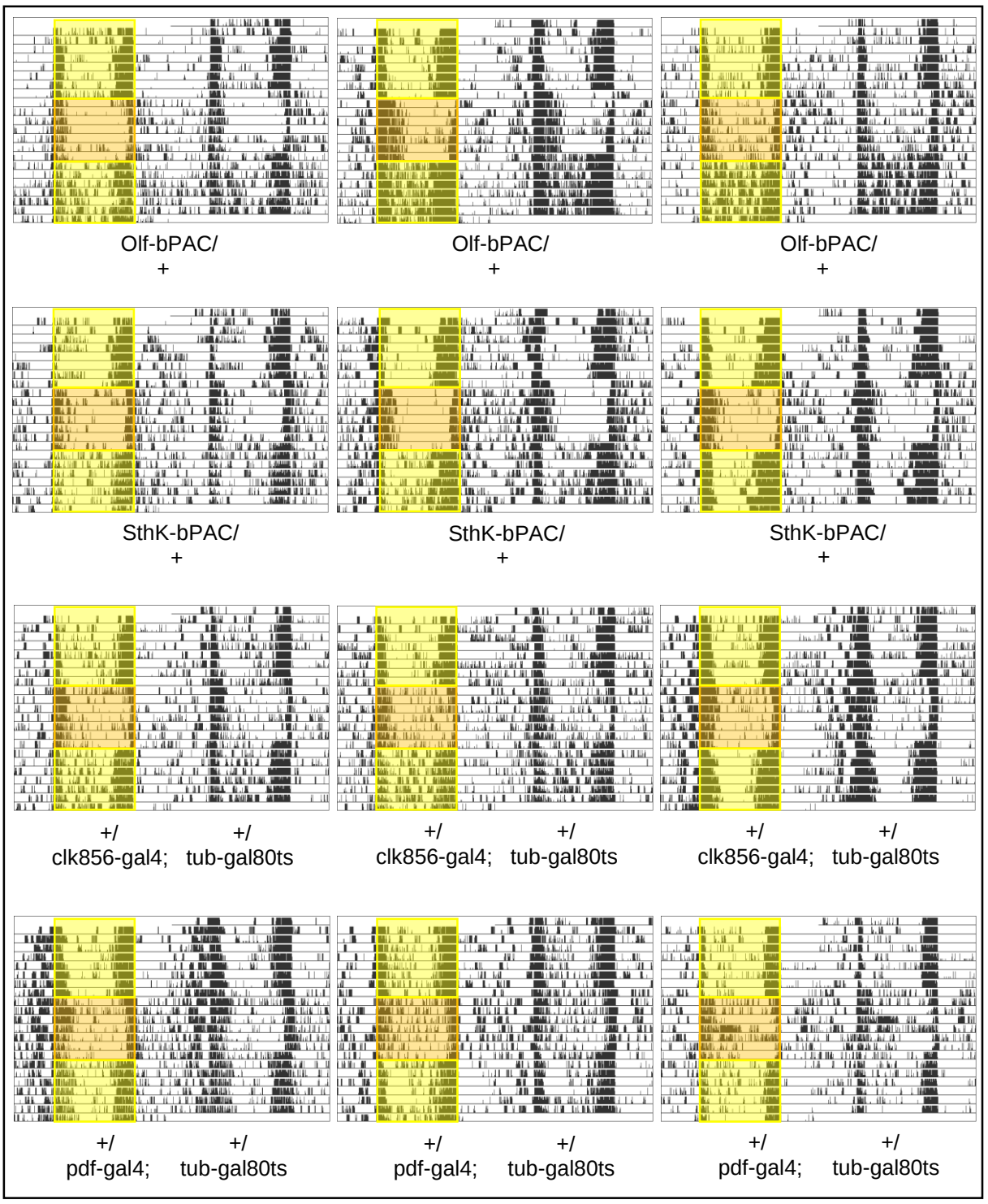

Figure 3.3.6b: Sample actograms of flies expressing no Olf-bPAC or SthK-bPAC anywhere (respective UAS- and GAL4-controls to Fig. 3.3.6b); double-plotted; yellow shading represents 22 day entrainment cycle of 12:12 RD (550 nm, ~90 µW/cm²), orange shading represents 7 day 12:12 temperature cycle, 20°C during lights off, 29°C during lights on; no shading represents darkness; 60% RH

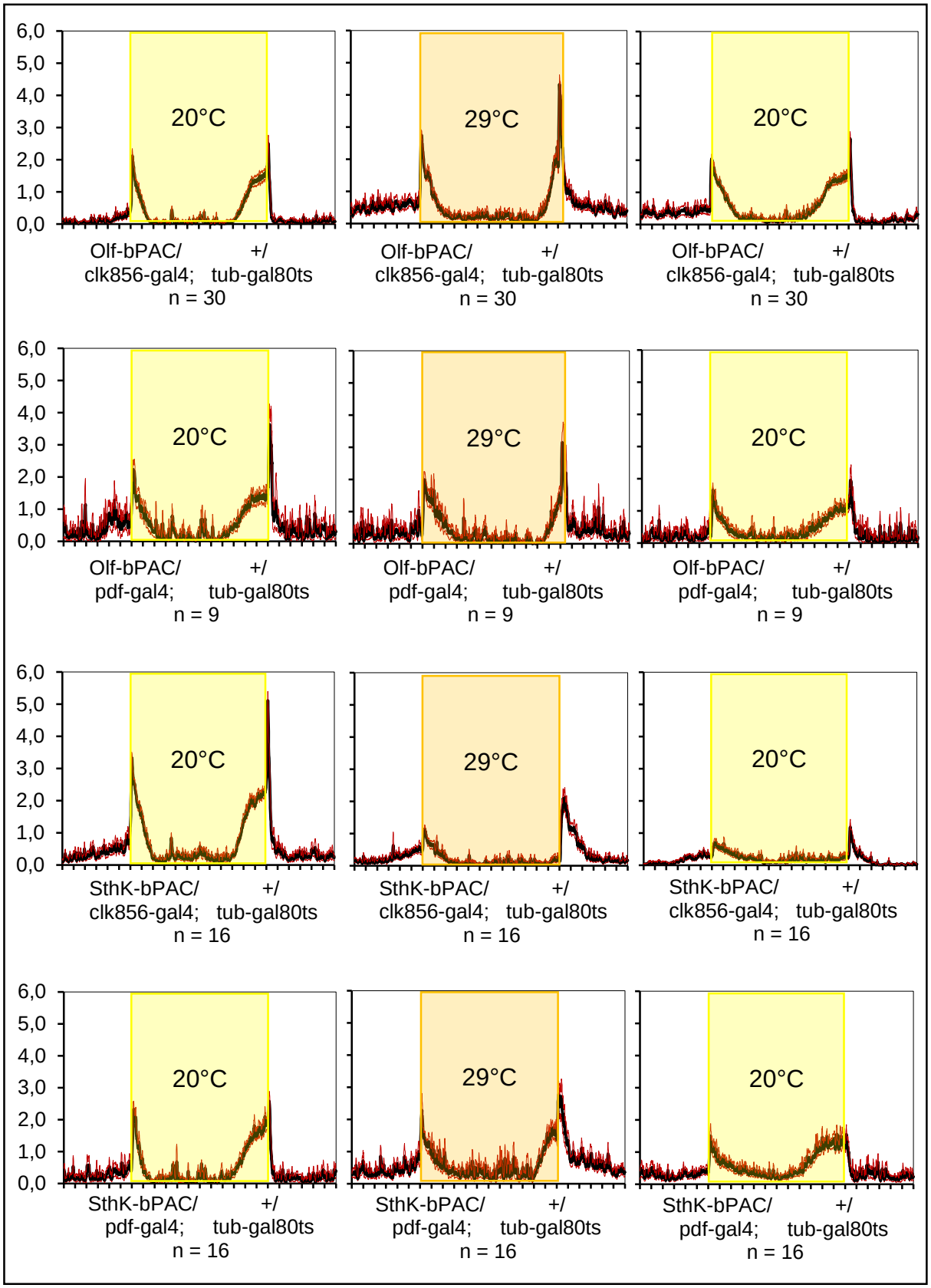

Figure 3.3.7a: Averaged actograms of flies expressing Olf-bPAC or SthK-bPAC in all circadian clock neurons (clk856-gal4) and all PDF-positive clock neurons (pdf-gal4); yellow shading represents entrainment cycle of 12:12 RD (550 nm, ~90 µW/cm²) at 20°C; orange shading represents entrainment cycle of 12:12 RD and 12:12 temperature cycle 20°C/29°C; 60% RH; for each genotype all available days recorded under the respective conditions were used for data averaging; for each genotype all flies that survived the 22 day experiment were used for data averaging

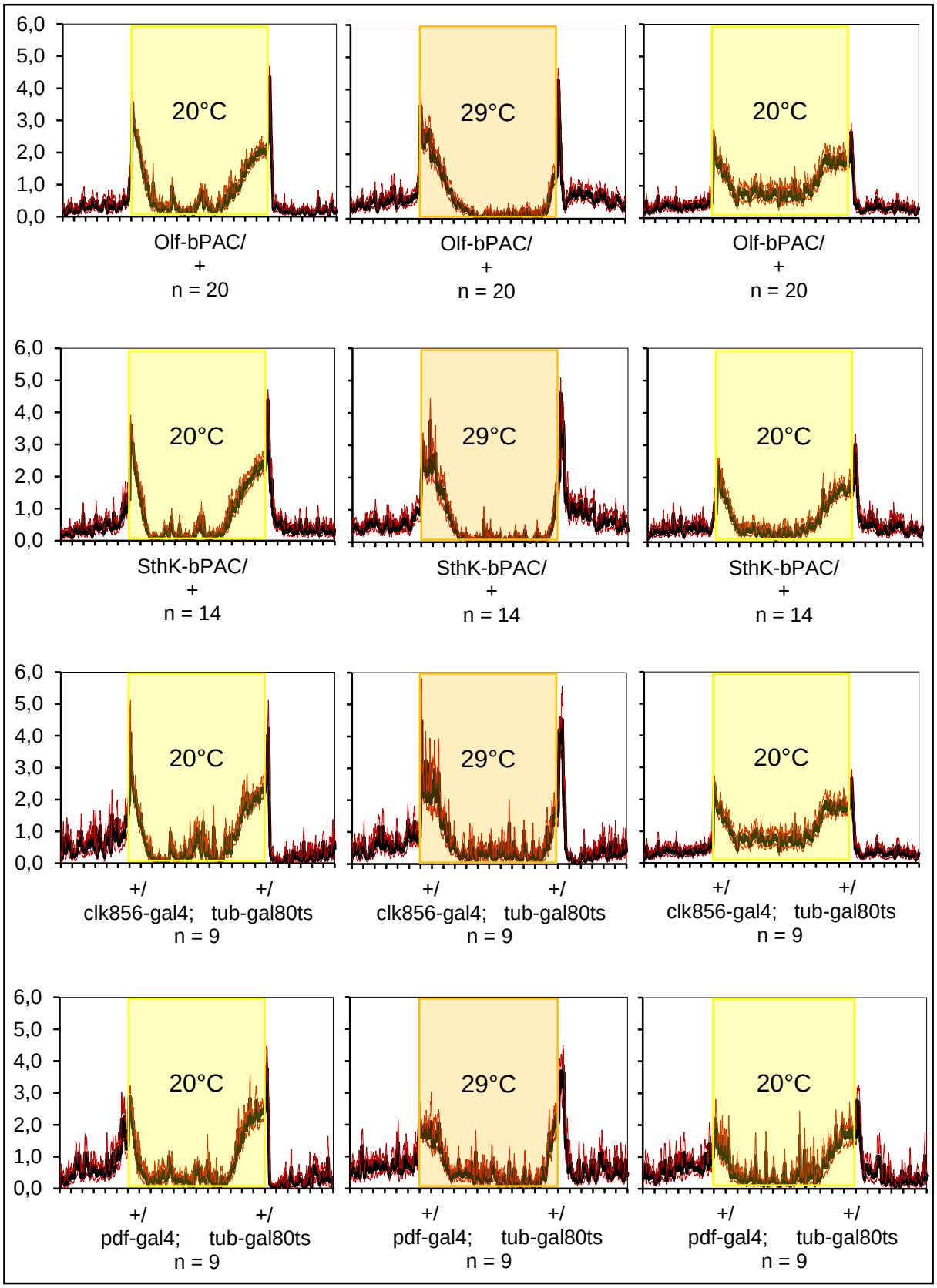

Figure 3.3.7b: Averaged actograms of flies expressing no Olf-bPAC or SthK-bPAC anywhere, (respective UAS- and gal4-controls to Fig 3.3.5a); yellow shading represents entrainment cycle of 12:12 LD (550 nm, ~90 µW/cm²) at 20°C; orange shading represents entrainment cycle of 12:12 RD and 12:12 temperature cycle 20°C/29°C; 60% RH; for each genotype all available days recorded under the respective conditions were used for data averaging; for each genotype all flies that survived the 22 day experiment were used for data averaging

The results of the experiment above successfully demonstrate a general applicability of the two optogenetic constructs Olf-bPAC and SthK-bPAC within the neurons of the circadian clock of *Drosophila melanogaster*.
The individual sample actograms (see Fig. 3.3.6), as well as the averaged actograms (see Fig. 3.3.7) show a much clearer bimodal activity pattern, compared to the previous experiment, conducted under RD conditions (see Fig. 3.3.4 and 3.3.5), likely because white light is a much stronger Zeitgeber than red light. When the expression of SthK-bPAC is induced in all circadian clock neurons (clk856-gal4) the flies start showing a clear and distinct reaction towards the white light by showing no activity during the evening, for as long as the light is turned on. When the light is turned off at ZT 12, locomotor activity surges, before slowly declining again in the hours following, as if the white light had a suppressive effect on the flies' activity. This effect persists far into the second 20°C-period, likely due to the stability of SthK-bPAC, staying expressed until after transcription is blocked again at 20°C. Flies expressing Olf-bPAC or flies expressing SthK-bPAC only in PDF-positive clock neurons seem not affected by the induction of expression and the white light, as their bimodal activity pattern continues unchanged. This yet doesn't rule out the possibility of all these three genotypes being affected at all, only that these effects apparently don't impact the locomotor behaviour, or can be compensated by the circadian clock. In conclusion, these two behavioural experiments with temperature-controlled expression of Olf-bPAC and SthK-bPAC have so far convincingly demonstrated that these two optogenetic constructs are, in principal, capable of influencing the circadian clock in a light-dependant manner.

3.3.3. Phase shift experiments

After the behavioural experiments shown in Results 3.3.2 had successfully demonstrated that the method of expressing SthK-bPAC and Olf-bPAC under the control of the temperature-sensitive tubgal80ts-gene could be a promising way of tackling the goal of the thesis, the newly crossed fly lines were then used for shift experiments, where the aim was now to shift the circadian clock of *Drosophila melanogaster.* The first experiment was designed to delay the phase of the clock with the experimental setup consisting of an 8 day 12:12 RD entrainment period, split up into 6 days at 20°C, blocking the transcription of the target gene, followed by 2 days at

29°C, inducing the expression. The 12:12 temperature cycle was again supposed to reinforce the light entrainment as a second Zeitgeber. The blue light pulse at 450 nm wavelength (~100 µW/mm²) was programmed for day 9 from ZT 15 to ZT 18 and was pulsed, firing a 20 ms light flash every 2 seconds. Due to a programming error however, the light pulse was administered 24h delayed, when the flies' individual CTs might have already diverged slightly.

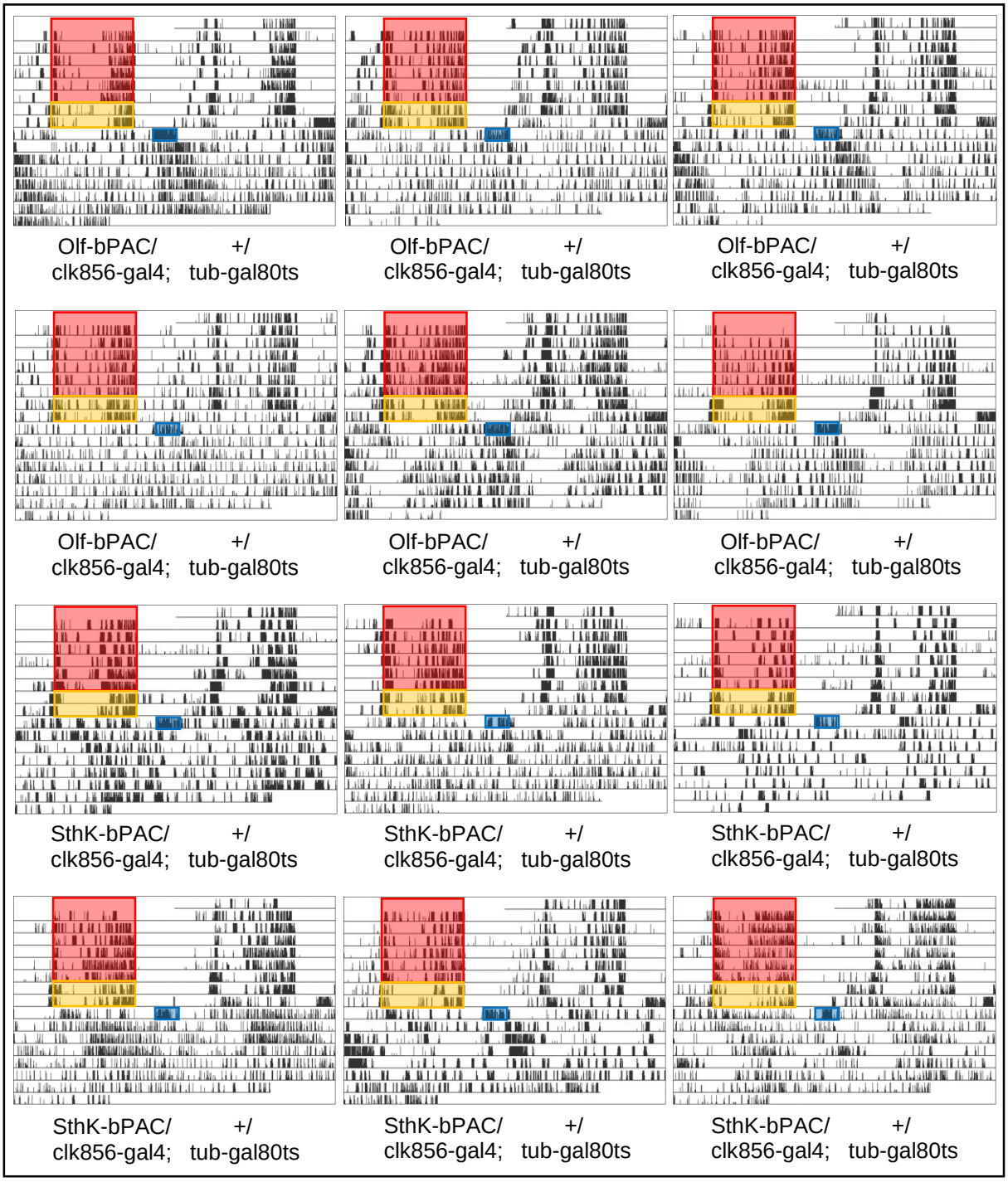

Figure 3.3.8a: Sample actograms of flies expressing Olf-bPAC and SthK-bPAC in all clock neurons (clk856-gal4); temperature-controlled expression by GAL80ts; red shading indicates 12:12 RD entrainment (620nm; ~5 µW/cm²); orange shading indicates 12:12 temperature cycle of 20°C/29°C; blue shading indicates light pulse (450 nm, 100 µW/mm², 20 ms/20 s); no shading indicates darkness

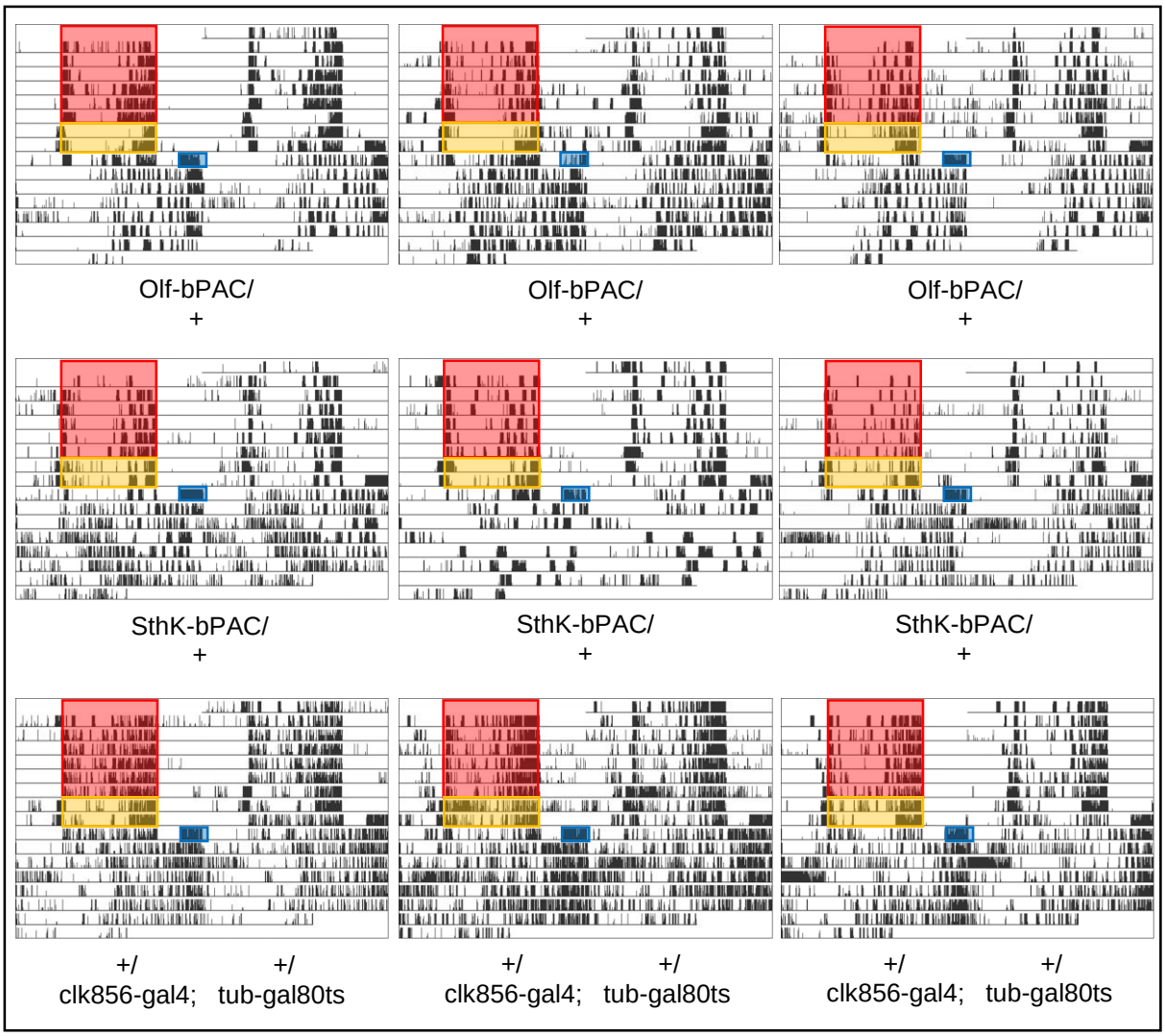

Figure 3.3.8b: Sample actograms of flies expressing no Olf-bPAC and SthK-bPAC anywhere (respective UAS- and GAL4-controls to Fig. 3.3.8a); red shading indicates 12:12 RD entrainment (620nm; ~5 µW/cm²); orange shading indicates 12:12 temperature cycle of 20°C/29°C; blue shading indicates light pulse (450 nm, 100 µW/mm², 20 ms/20 s); no shading indicates darkness

The experiment did not succeed. Most of the flies expressing Olf-bPAC or SthK-bPAC exhibit a very poor rhythmicity and produce largely unusable actograms that can not be evaluated for their phase delays in ActogramJ due to indistinct activity offsets (see Fig. 3.3.8a). Observing and gauging the actograms, it is evident that a phase delay had indeed been produced across all genotypes, including controls (see Fig. 3.3.8b). Even some of the largely arrhythmic test-genotypes, expressing the two constructs, display activity patterns that clearly indicate that a phase delay had been caused, by the way the bulk of the activity shifts into the subjective night. As this however is also true for the controls, no final conclusion regarding the applicability of Olf-bPAC and SthK-bPAC for this experimental setup can be drawn. The experiment was repeated twice more, adapting frequency and length of the light pulse, but both were cancelled

prematurely a few days after the light-pulse due to unusable actograms and a high degree of arrhythmicity. As a result it was decided to discontinue the experiments with the clk856-gal4/tubgal80ts line and to switch to using the pdf-gal4/tubgal80ts lines. Leaning on the work of Saskia Eck et al. [117] and the results obtained using the temperature sensitive TRPA1-channel, it was decided to try and evoke a phase advance in the pdf-gal4 lines, since triggering dTRPA1 in the PDF-positive clock neurons via “temperature pulse” had caused the flies to exhibit significant phase advances. It was decided to solely use Olf-bPAC for the advance experiments, as it is very similar to dTRPA1 in its conductive qualities. Again, a 12:12 RD entrainment was chosen, coupled with a 12:12 temperature cycle between 20°C and 29°C during the last 2 days of entrainment, to induce expression and function as an additional Zeitgeber. The light pulse was given in the advance zone between ZT 20 and ZT 22 and consisted of 20 ms light flashes every 2,5 seconds at 450 nm wavelength and 100 µW/mm².

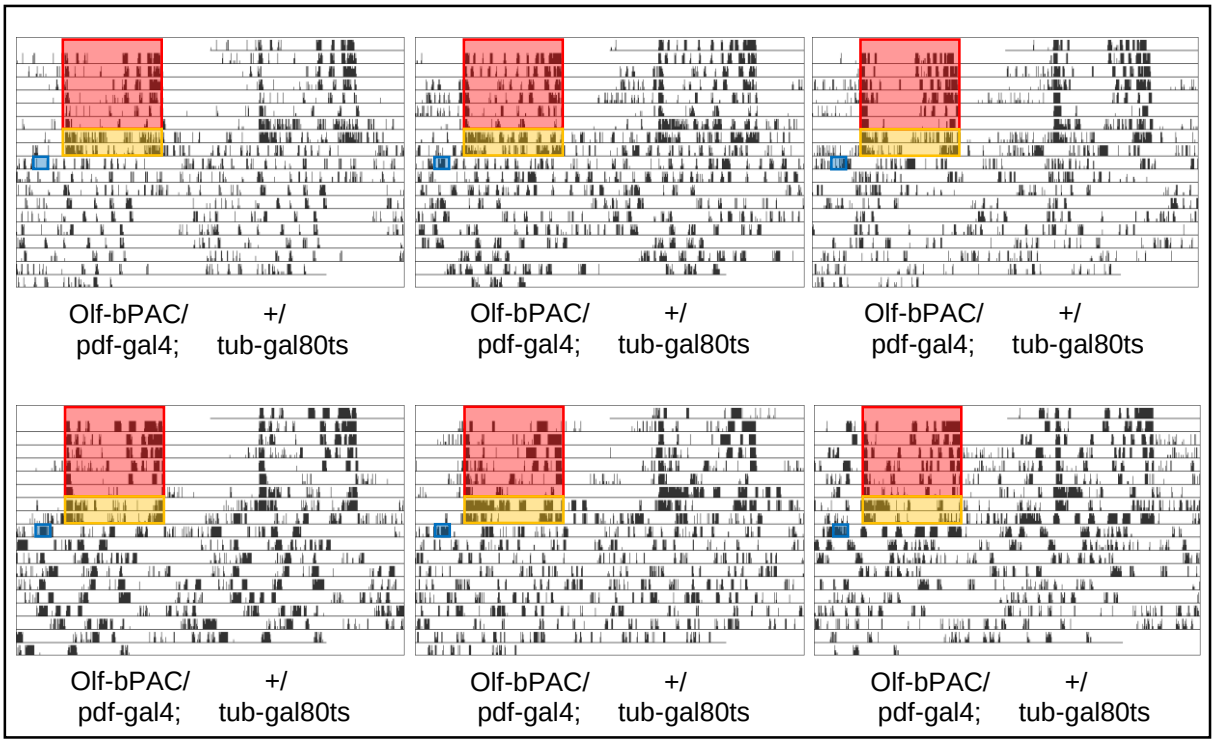

Figure 3.3.9a: Sample actograms of flies expressing Olf-bPAC in the PDF-positive clock neurons (pdf-gal4); temperature-controlled expression by GAL80ts; red shading indicates 12:12 RD entrainment (620nm; ~ 5 µW/cm²); orange shading indicates 12:12 temperature cycle of 20°C/29°C; blue shading indicates light pulse (450 nm, 100 µW/mm², 20 ms/20 s); no shading indicates darkness

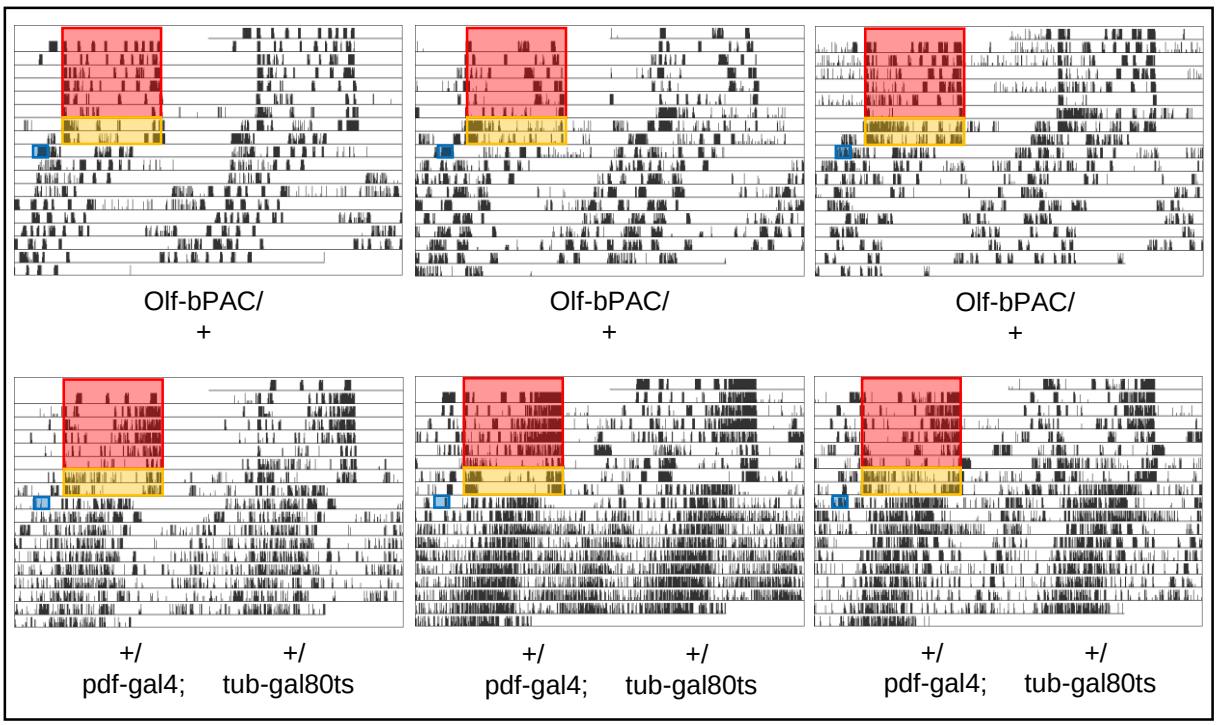

Figure 3.3.9b: Sample actograms of flies expressing no Olf-bPAC anywhere (respective UAS- and gal4-controls to Fig. 3.3.9a); red shading indicates 12:12 RD entrainment (620nm; ~5 µW/cm²); orange shading indicates 12:12 temperature cycle of 20°C/29°C; blue shading indicates light pulse (450 nm, 100 µW/mm², 20 ms/20 s); no shading indicates darkness

Much like the previous experiment in which it was tried to evoke a phase delay, the experiment trying to evoke a phase advance also ended up being unsuccesful. Again, flies expressing Olf-bPAC exhibit extremely poor rhythmicity, producing entirely unusable actograms for quantifying phase shifts. The flies' rhythmicity appears to be even worse than in the previous experiment, displaying almost no rhytmic patterns at all during DD (see Fig. 3.3.9a). The controls on the other hand exhibit rhythmic locomotor activity and also seem to have had their phase advanced, which can be seen most clearly in sample actograms of the UAS-control (see Fig. 3.3.9b). Following the repeated setbacks with the tub-gal80ts lines, the phase shift experiments with those lines were discontinued and other alternatives were considered.

3.4. CNGC-CyclOp

After the experiments with the temperature-sensitive tubgal80ts-lines had been discontinued, another novel approach was chosen. It was ultimately decided that the wild type Olf and wild type SthK channels were too potent and strong when used as optogenetic fusion-tools in neurons of the circadian clock of *Drosophila melanogaster.* Using a regular GAL4-driver, the constructs had a detrimental effect on the development of the circadian neurons during the larval stages (see Results 3.2.) and when expression was delayed until adulthood, via $GAL80^{ts}$, no usable actograms could be obtained in experiments trying to evoke a phase shift (see Results 3.3.).

It was then decided to use less potent ion channels with weaker currents at similar expression levels when compared to Olf. It was also decided to move away from bPAC as the light-sensitive domain, because the blue-shifted action spectrum of bPAC was considered a problem, due to the overlap with the action spectrum of CRY [77, 101]. The tool of choice was ultimately decided to be the newly published CyclOp, a membrane-bound, green light-dependant guanylyl cyclase with an ATR as chromophore [105]. The published action spectrum for the CyclOp locates the absorption maximum of the cyclase at roughly 550 nm wavelength, away from the absorption maximum of CRY. To allow for both membrane bound proteins Olf and CyclOp to be expressed from one transgene, the viral T2a ribosomal skip motif was introduced into the sequence, allowing two non-fused proteins to be translated from one singular open reading frame (see Material & Methods 2.3).

To reduce the cGMP-sensitivity of the co-expressed Olf and consequently its conductance relative to the light intensity, two point mutations were introduced into the channel sequence, replacing the arginine at position 532 with a lysine and a histidine respectively (R536K and R536H). The CyclOp was also co-expressed with the recently published canine CNGA3, which has similar conductive qualities like Olf [106]. Along with having reduced cGMP-sensitivity, the three new CNGC variants are also almost insensitive towards cAMP. As intrinsic cAMP was also believed to be responsible for possibly undesired side-effects caused by the expressed CNG channels, this quality appeared to be quite promising.

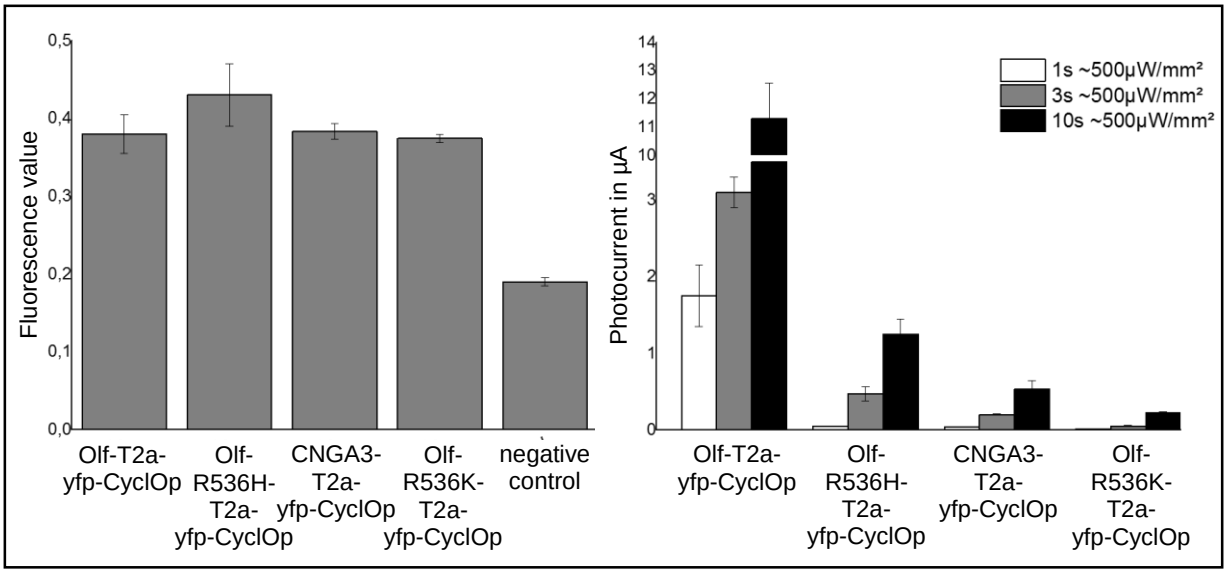

Figure 3.4.1 left: fluorescence assay of *Xenopus laevis* oocytes, expressing the labelled optogenetic constructs in the plasma membrane; relative fluorescence values were measured by homogenizing oocytes in a volume of 200µl ddH_2O and transferred to a 96-well-plate, which was then measured by a fluorescence plate reader, providing a relative value for the strength of expression; negative control represents oocytes expressing no construct; **right:** DEVC-measurements of *Xenopus laevis* oocytes, expressing the labelled optogenetic constructs in the plasma membrane; oocytes were voltage-clamped at -100mV and illuminated with blue light at 470 nm wavelength for the labelled durations and with the labelled intensity; error bars represent SEM, data produced by Jing Yu & Shang Yang

Figure 3.4.1 (experiments conducted and data provided by Jing Yu & Shang Yang) highlights the different conductive qualities of the new optogenetic constructs. To assess the height of the electrical current generated upon illumination, relative to the expression level, two different experiments were performed. First, oocytes of *Xenopus laevis,* expressing the optogenetic constructs in the plasma membrane, were recorded with the double-electrode-voltage-clamp method (DEVC) to quantify the current of each construct. Then those oocytes were homogenized in 200 µl water and transferred to a 96-well plate and recorded using a fluorescence plate reader, in order to quantify the relative expression level, by measuring the fluorescence of the co-expressed YFP. By assuring equal levels of protein expression, the DEVC recordings serve as a direct assessment of the conductive qualities of the expressed optogenetic constructs in terms of electric current. It becomes quite apparent that the three new channels, Olf-R536H, Olf-R536K and CNGA3 are a lot less sensitive towards cGMP than the Olf-536R that had been used so far and accordingly they generate a significantly weaker electrical current upon illumination. It was decided to generate new *Drosophila melanogaster* strains, carrying these new transgenes, in order to be used in circadian experiments.

3.4.1. Immunostaining experiments

To test if the expression of the new CNGC-CyclOp constructs would not interfere in neuronal development during the larval stages like Olf-bPAC and SthK-bPAC (see Results 3.2.), adult flies expressing Olf-R536H-CyclOp, Olf-R536K-CyclOp and CNGA3-CyclOp in the PDF-positive clock neurons (pdf-gal4) were raised under 12:12 RD conditions and collected after eclosion. The flies' brains were then fixated, prepared and subsequently immunostained to assess whether expressing these new constructs has a detrimental effect on the development of the s-LN_vs.

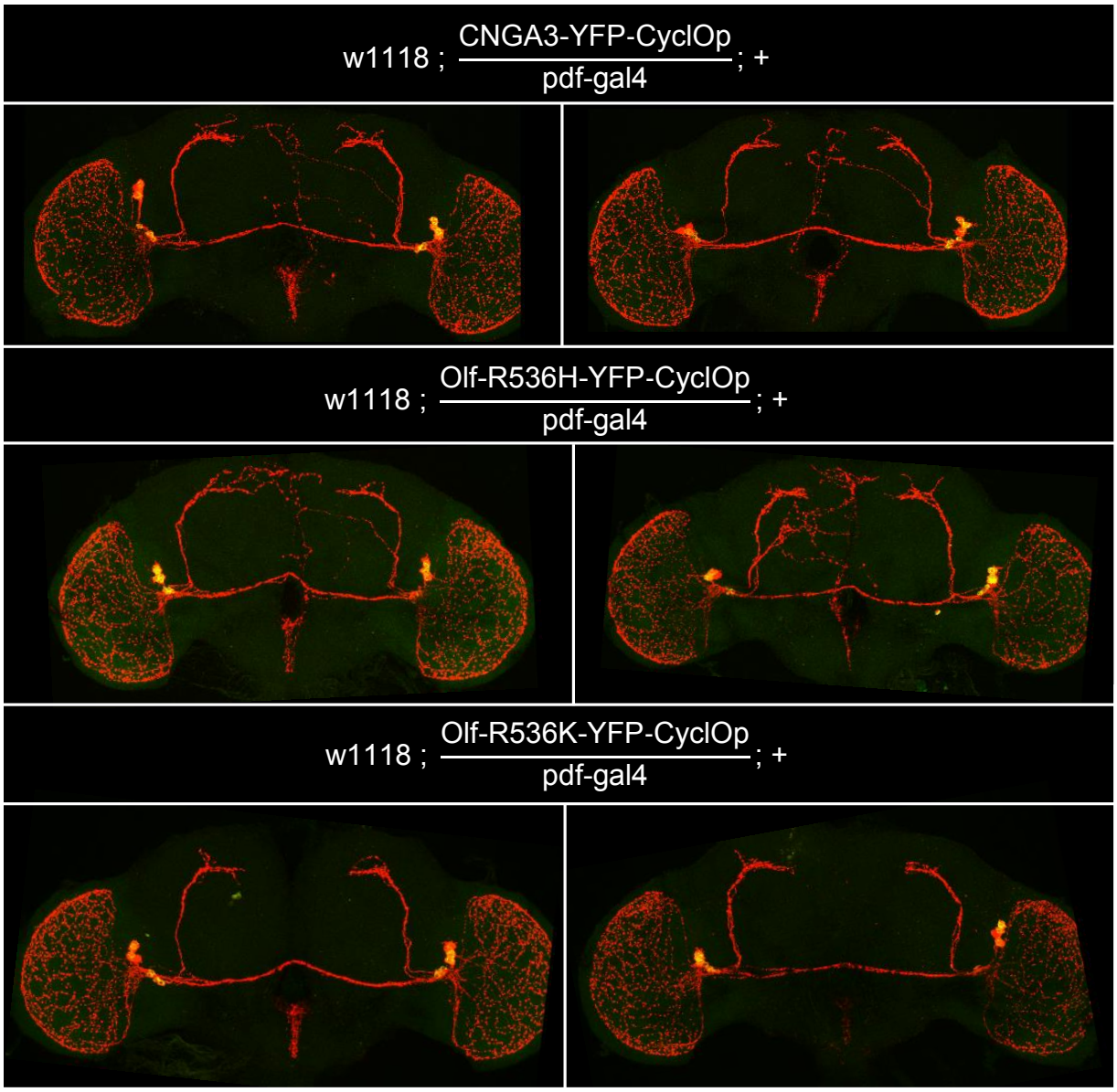

Figure 3.4.2a: Prepared and immunostained brains of flies, expressing CNGA3-YFP-CyclOp or Olf-R536H/K-YFP-CyclOp in the PDF-positive circadian neurons; two-channel recording, laser-excitation with wavelengths 488 nm (green) and 635 nm (red), primary antibody: mouse anti-PDFc7; secondary antibody: Alexa Fluor 647 goat anti-mouse

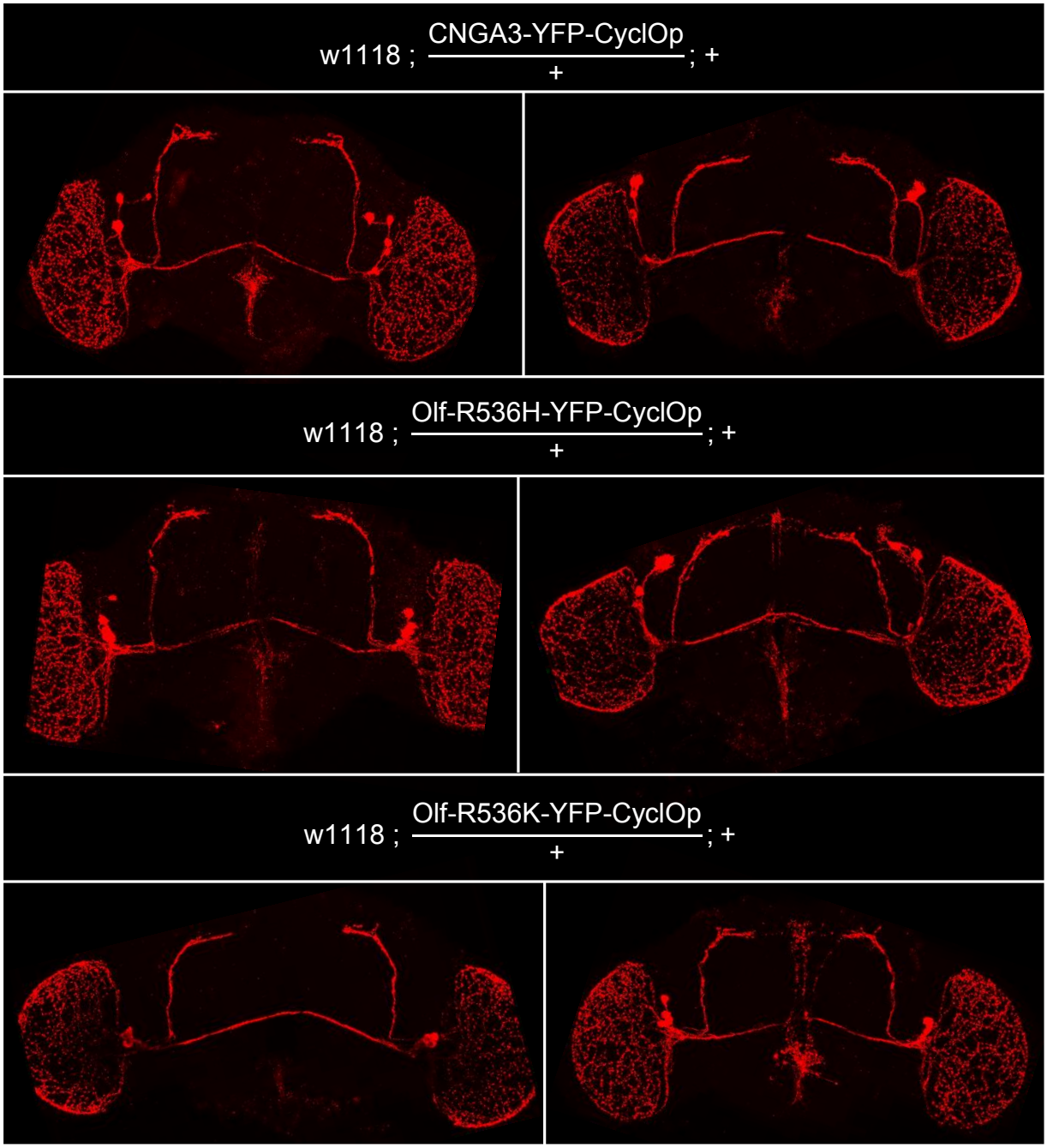

Figure 3.4.2b: Prepared and immunostained brains of flies, expressing no CNGC-CyclOp (UAS-control) single-channel recording, laser-excitation with wavelengths 635 nm, primary antibody: mouse anti-PDFc7; secondary antibody: Alexa Fluor 647 goat anti-mouse

The immunostaining images of *Drosophila* brains expressing CNGA3-CyclOp, Olf-R536H-CyclOp and Olf-R536K-CyclOp show that these new optogenetic tools apparently don't have the same harmful effect on the development of the s-LNvs that Olf-bPAC and SthK-bPAC have. The projections and the arborizations of the s-LNvs into the dorsal protocerebrum appear intact and fully grown and comparable to those of their respective UAS-controls (see Fig 3.4.2). However, in quite a substantial number of brains expressing CNGA3-Cyclop and Olf-R536H-Cyclop (~60% - 70%) at least one

of the s-LNvs in either brain hemisphere exhibits an abnormal growth pattern or abnormal path finding (see Fig. 3.4.2). This could also be observed in neurons expressing Olf-R536K-CyclOp, however at a much a much smaller percentage (~10%). The UAS-controls did not show any unusual growth of any sort. As these results suggest that the constructs still affect the development of the clock neurons, it was decided to further gauge the potency of these new optogenetic tools within the *Drosophila* circadian network. A new immunstaining experiment was designed, testing whether the three CNGC-Cyclop are also able to cause phenotype of shortened and malformed s-LNvs, like Olf-bPAC and SthK-bPAC (see Results 3.2), when the flies are illuminated during larval development. Flies expressing Olf-R536H-CyclOp, Olf-R536K-CyclOp and CNGA3-CyclOp in the PDF-positive clock neurons (pdf-gal4) were raised under constant and strong white light (90 µW/mm² at 530 nm) and collected after eclosion. The flies were then fixated, prepared and immunostained (anti-PDF) to see the effects a constant light activation of the new constructs would have.

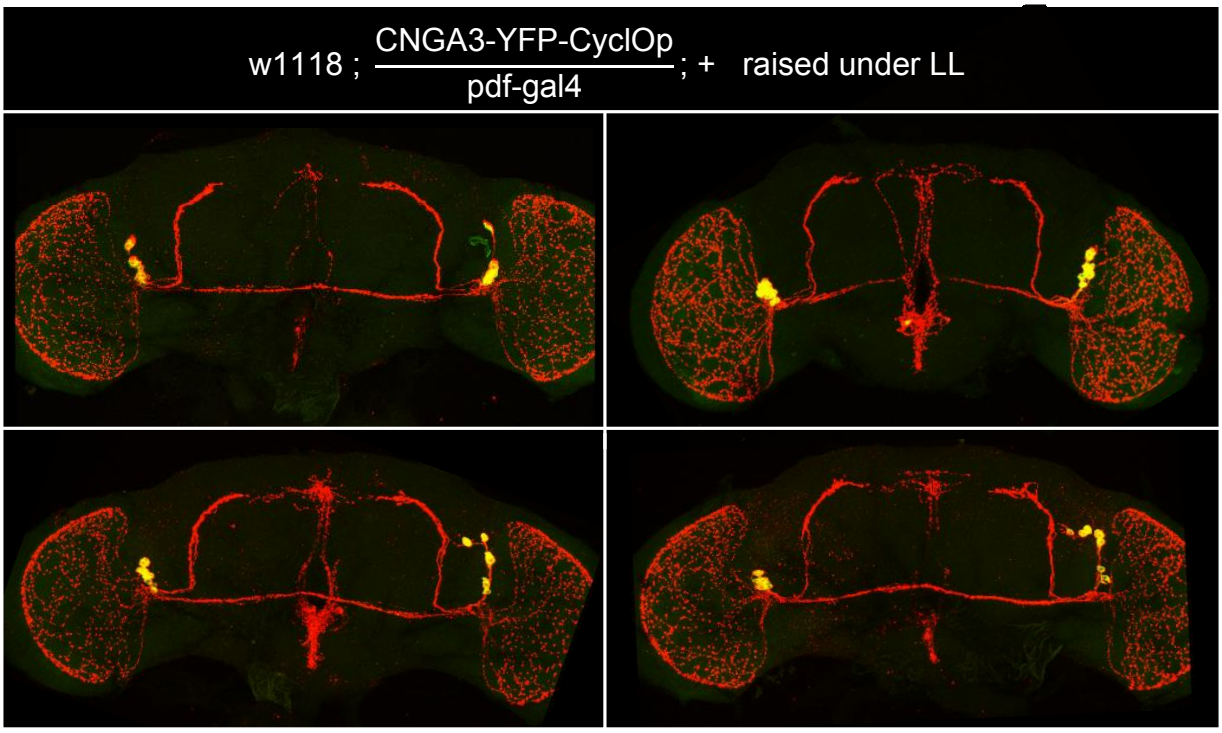

Figure 3.4.3a: Prepared and immunostained brains of flies, expressing CNGA3-YFP-CyclOp in the PDF-positive circadian neurons; two-channel recording, laser-excitation with wavelengths 488 nm (green) and 635 nm (red), primary antibody: mouse anti-PDFc7; secondary antibody: Alexa Fluor 647 goat anti-mouse

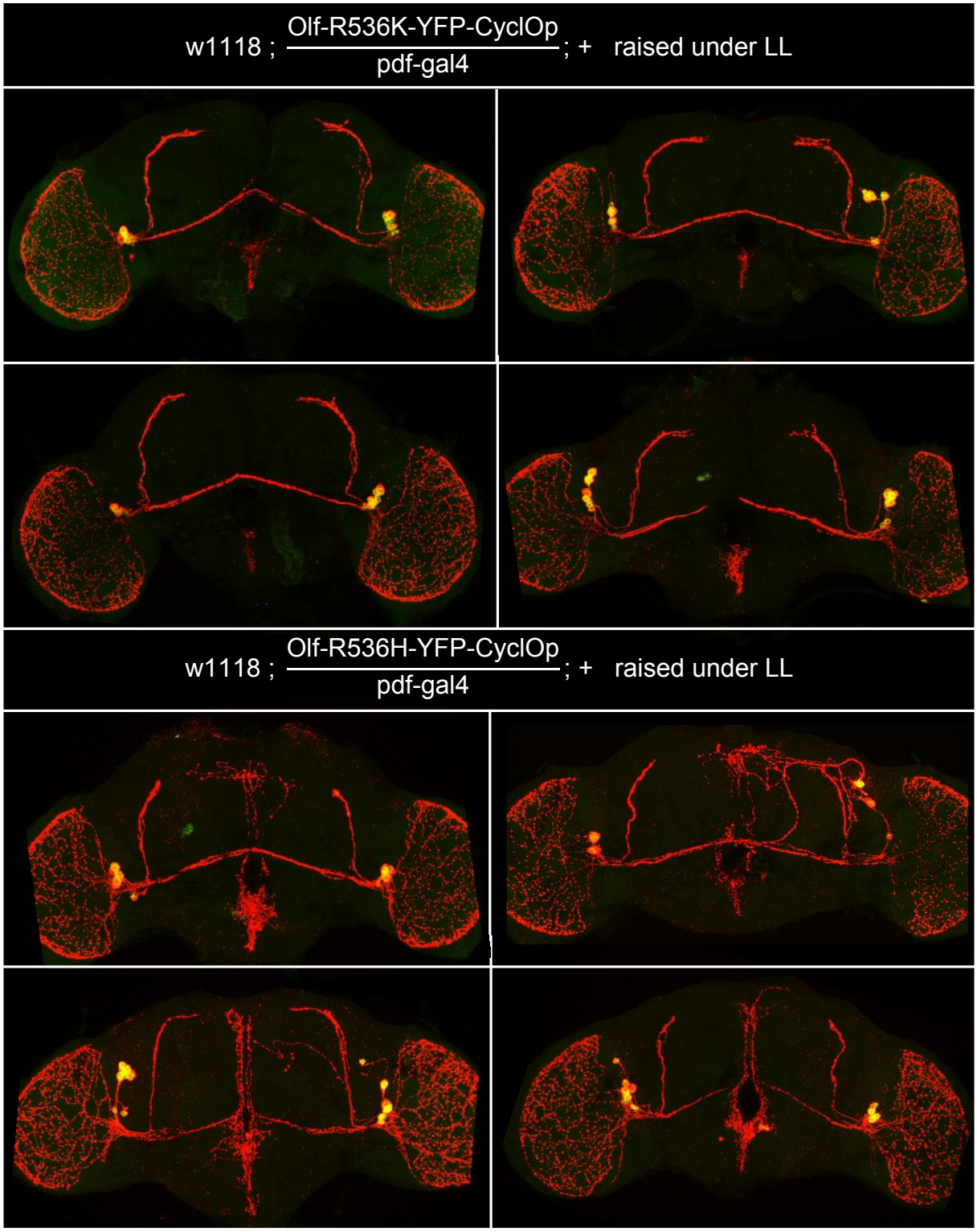

Figure 3.4.3b: Prepared and immunostained brains of flies, expressing Olf-R536H-YFP-CyclOp or Olf-R536K-YFP-CyclOp in the PDF-positive circadian neurons; two-channel recording, laser-excitation with wavelengths 488nm (green) and 635 nm (red), primary antibody: mouse anti-PDFc7; secondary antibody: Alexa Fluor 647 goat anti-mouse

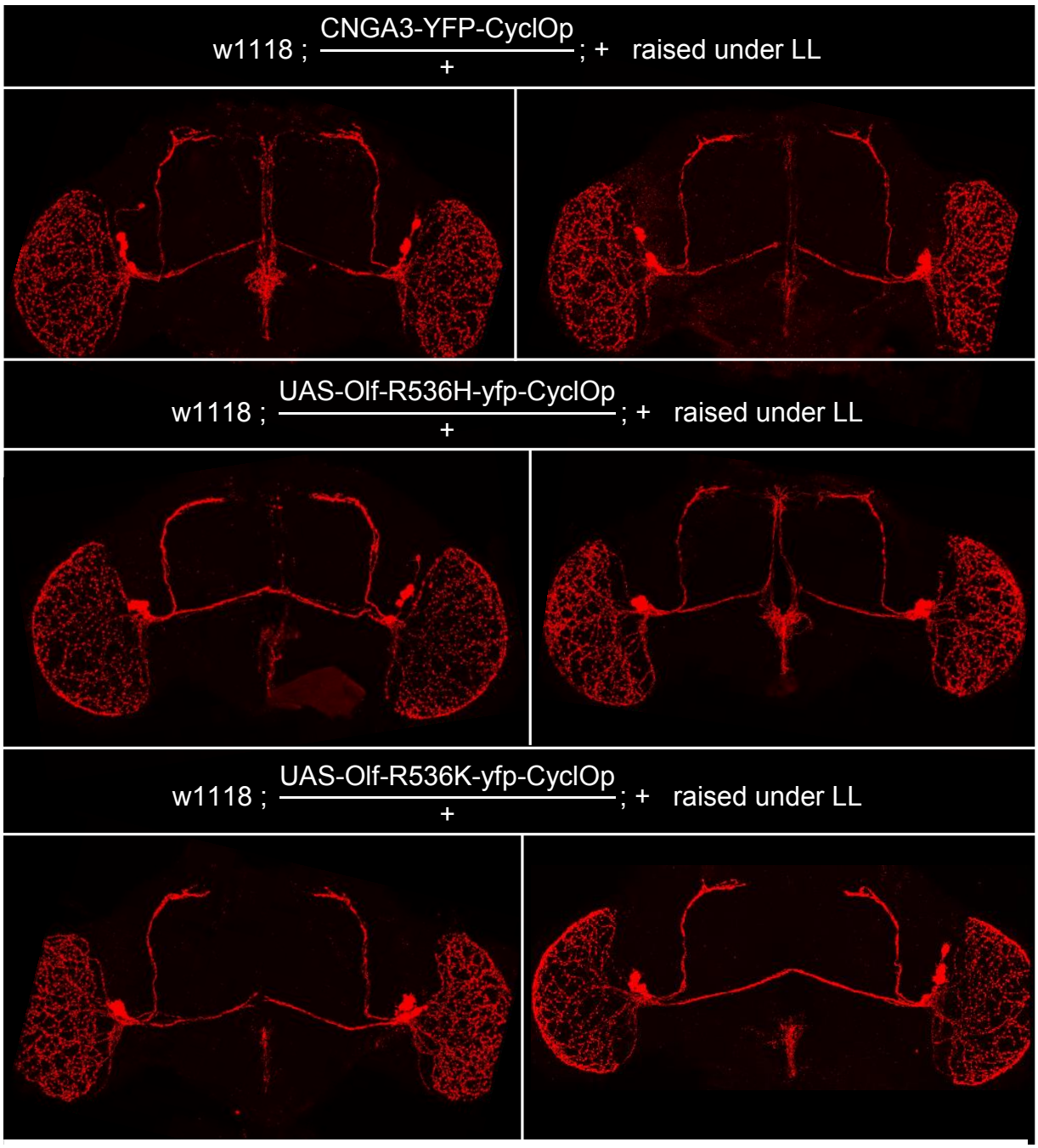

Figure 3.4.3c: Prepared and immunostained brains of flies, expressing no CNGC-CyclOp (UAS-control) single-channel recording, laser-excitation with wavelengths 635 nm, primary antibody: mouse anti-PDFc7; secondary antibody: Alexa Fluor 647 goat anti-mouse

The experiment successfully showcased the potential of the three new CNGC-CyclOp constructs. Flies expressing Olf-R536H-CyclOp in the PDF-positive neurons are clearly affected the most by the being raised under constant strong white light, as their s-LN$_v$s are heavily shortened and malformed across many sample brains (see Fig. 3.4.3b). Flies expressing CNGA3-CyclOp are also affected, as their s-LN$_v$s are also slightly shortened and less clearly defined when compared to the controls (see Fig. 3.4.3a and Fig 3.4.3c). Flies expressing Olf-R536K-CyclOp are least affected as they

have the most wild type-like and most well developed s-LN$_v$s out of the three genotypes expressing the CNGCs (see Fig. 3.4.3b). These results are also very much in congruence with the electrophysiological data gathered about the strength of the new constructs, as they appear to be more damaging for neuronal development, the higher their respective photocurrents in the DEVC-experiments had been (see Fig. 3.4.1).

3.4.2. Expressing CNGC-CyclOp in motor neurons

Before any behavioural experiments were started trying to use the CNGC-CyclOp constructs to influence the circadian clock in live adult *Drosophila*, another set of experiments was started, testing the CNGC-CyclOps' effect on motor neurons (ok6-gal4). Unlike Olf-bPAC and SthK-bPAC, which are lethal when expressed in motor neurons, flies expressing the CNGC-CyclOp survive the pupariation phase and are able to successfully eclose as living adult flies. These flies were recorded in three behavioural experiments, one under a 12:12 RD light regime, another under a 12:12 LD regime with strong white light and a last one again under a 12:12 LD strong white light regime, with the flies additionally having been fed ATR in the 24 hours leading up to the experiment (see Material and Methods 2.6). The actograms of all genotypes were then respectively averaged and compared. The CNGA3-CyclOp was omitted from this experiment, instead only the arguably the weakest and the strongest construct, Olf-R536K-CyclOp and Olf-R536H-CyclOp were recorded.

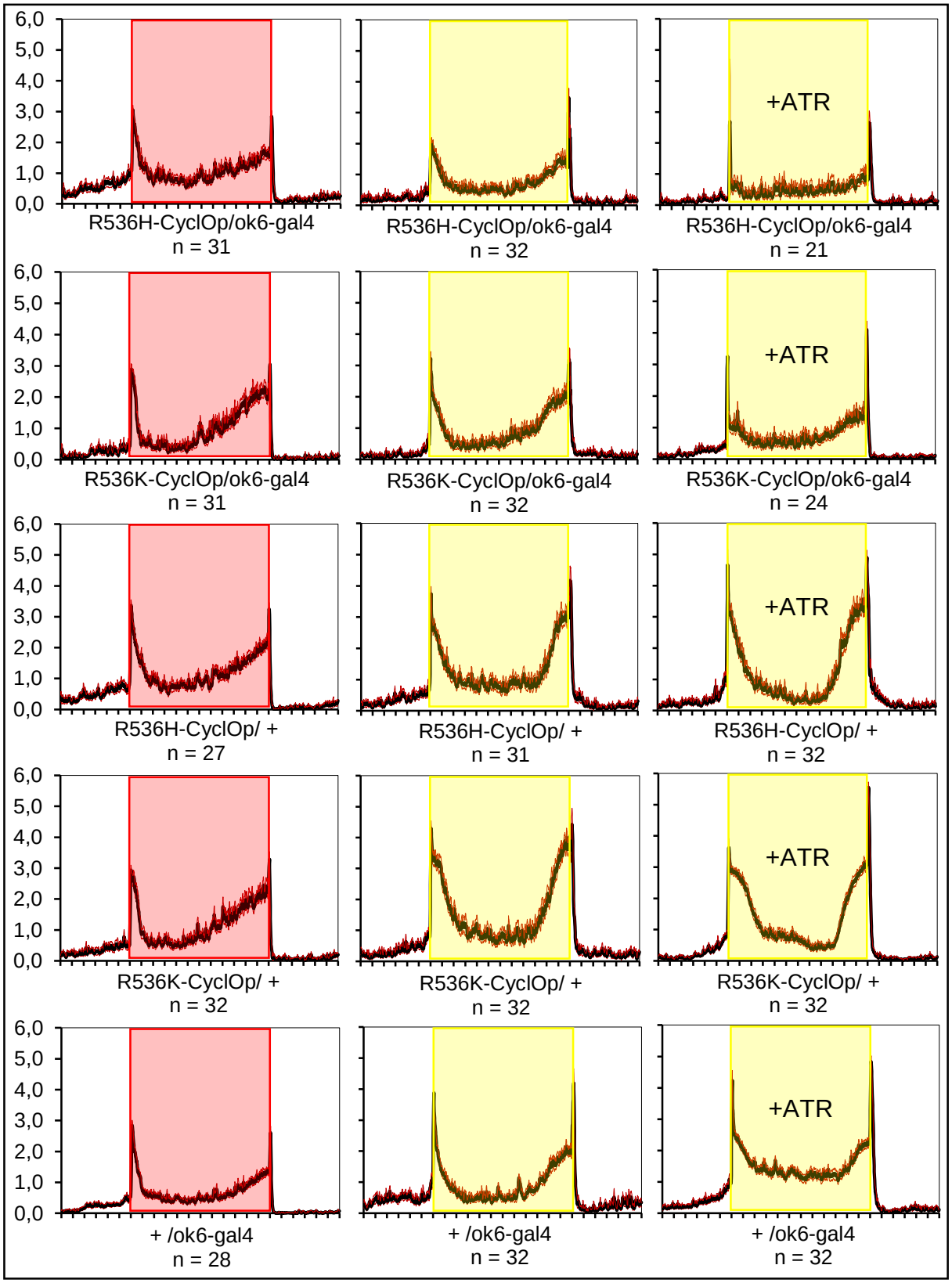

Figure 3.4.4: Averaged actograms of flies expressing Olf-R536H-CyclOp or Olf-R536K-CyclOp in the motor neurons (ok6-gal4) and the respective UAS- and GAL4-controls; red shading represents entrainment cycle of 12:12 RD (620 nm, ~5 µW/cm²); yellow shading represents entrainment cycle of 12:12 LD (550 nm, 90 µW/cm²), "+ATR" signifies that the flies had been fed all-trans-retinal for 24h prior to the experiment; for each genotype all available days recorded under the respective conditions were used for data averaging; for each genotype only flies that survived the 7 day experiment were used for data averaging

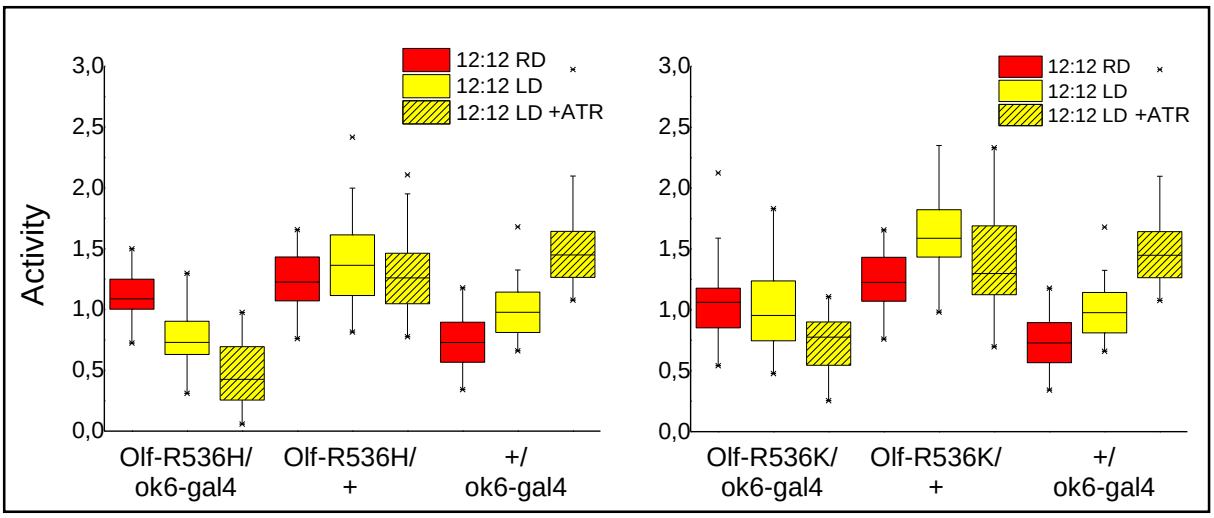

Figure 3.4.5: Adult male *Drosophila* flies' activity rate under 12:12 RD (red light 660 nm, ~5 µW/cm^2) indicated in red and 12:12 LD (550 nm, ~90 µW/cm^2) indicated in yellow; "+ATR" indicates feeding of ATR 24h prior; Boxplot data is composed of the 12 daylight hours of individual flies averaged over a 7 day period (see Fig. 3.4.4); Box line represents median, box square represents mean, box edges represent 25 and 75 percentiles, whiskers represent 1 and 99 percentiles

The averaged actograms and the boxplot data of the flies' activity rate clearly demonstrate the potency of the new CNGC-CyclOp constructs. As expected, the Olf-R536H-CyclOp construct has the strongest effect on *Drosophila* activity rate. The flies' activity rate (beam crosses per minute) drops significantly when the flies are entrained by strong white light rather than red light and drops even further when ATR has been fed prior (see Fig 3.4.4a and Fig 3.4.5). This is especially remarkable as both UAS- and GAL4-controls are visibly stimulated in their activity when being entrained by white light in comparison to red light, as well as by the feeding of ATR. The Olf-R536K-CyclOp was also noticeably affected by the LD entrainment. Although the activity rate did not drop when compared to the RD entrainment, the depolarisation seems to cancel out the stimulating effect of the white light that is visible in the controls (see Fig 3.4.5). The feeding of ATR then further amplified the activity reducing effect.

Following these promising results, behavioural experiments where started, trying to apply these constructs in the neurons of the circadian clock.

3.4.3. Behavioural experiments

In order to test the effect the new CNGC-CyclOp constructs have on the circadian network of *Drosophila melanogaster* when expressed in clock neurons, a series of behavioural experiments was started. Flies expressing the new constructs, in all PDF-positive circadian neurons (pdf-gal4), as well as all circadian neurons (clk856-gal4) were entrained both by a 12:12 RD light regime, as well as by a 12:12 LD light regime of very strong white light, to also test the effects of the constructs when constantly activated.

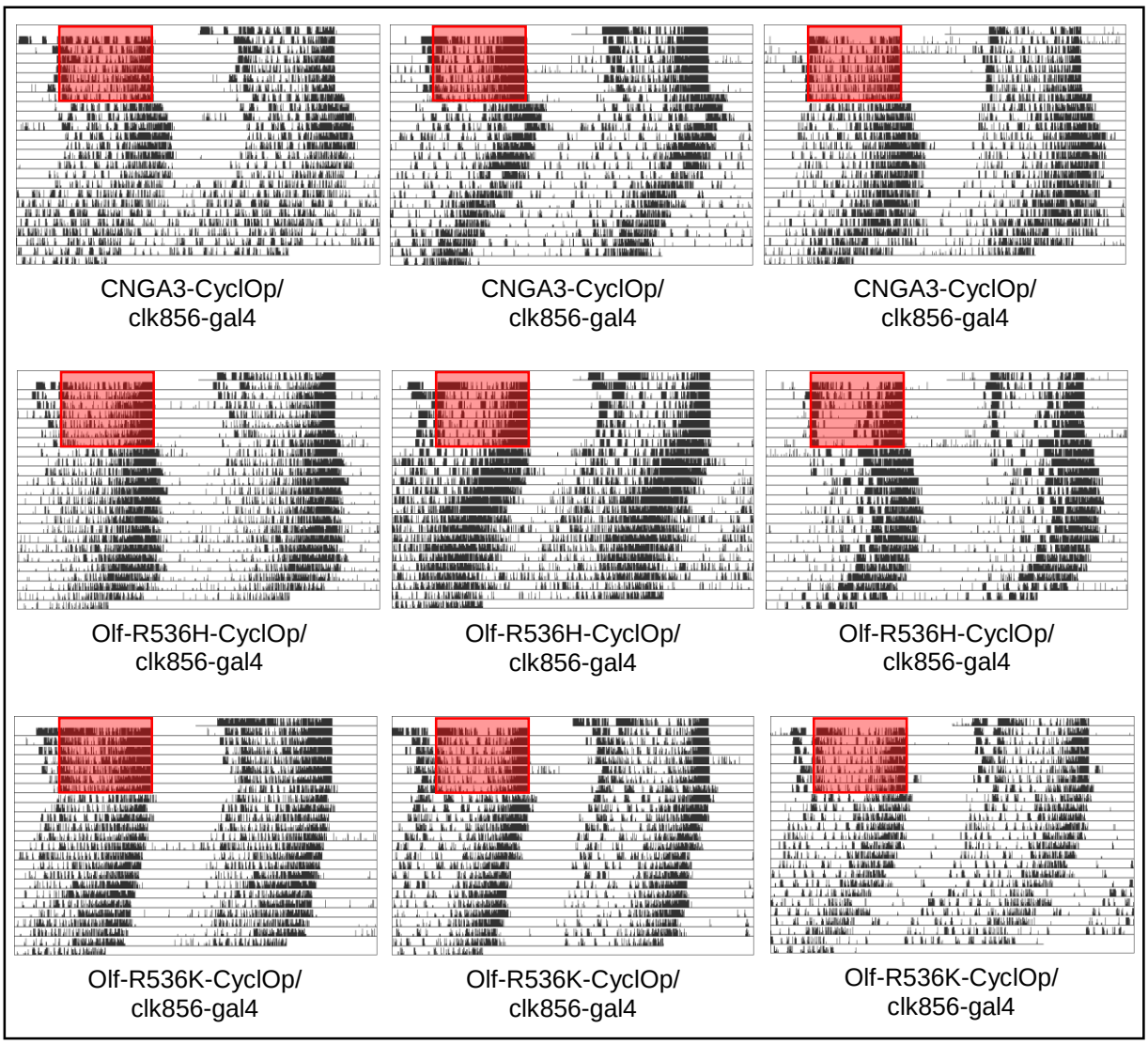

Figure 3.4.6a: Sample actograms of flies expressing CNGA3-CyclOp, Olf-R536H-CyclOp or Olf-R536K-CyclOp in all clock neurons (clk856-gal4); red shading represents entrainment cycle of 12:12 RD (660 nm, ~1,1 µW/cm²); no shading represents darkness; 20°C 60% RH;

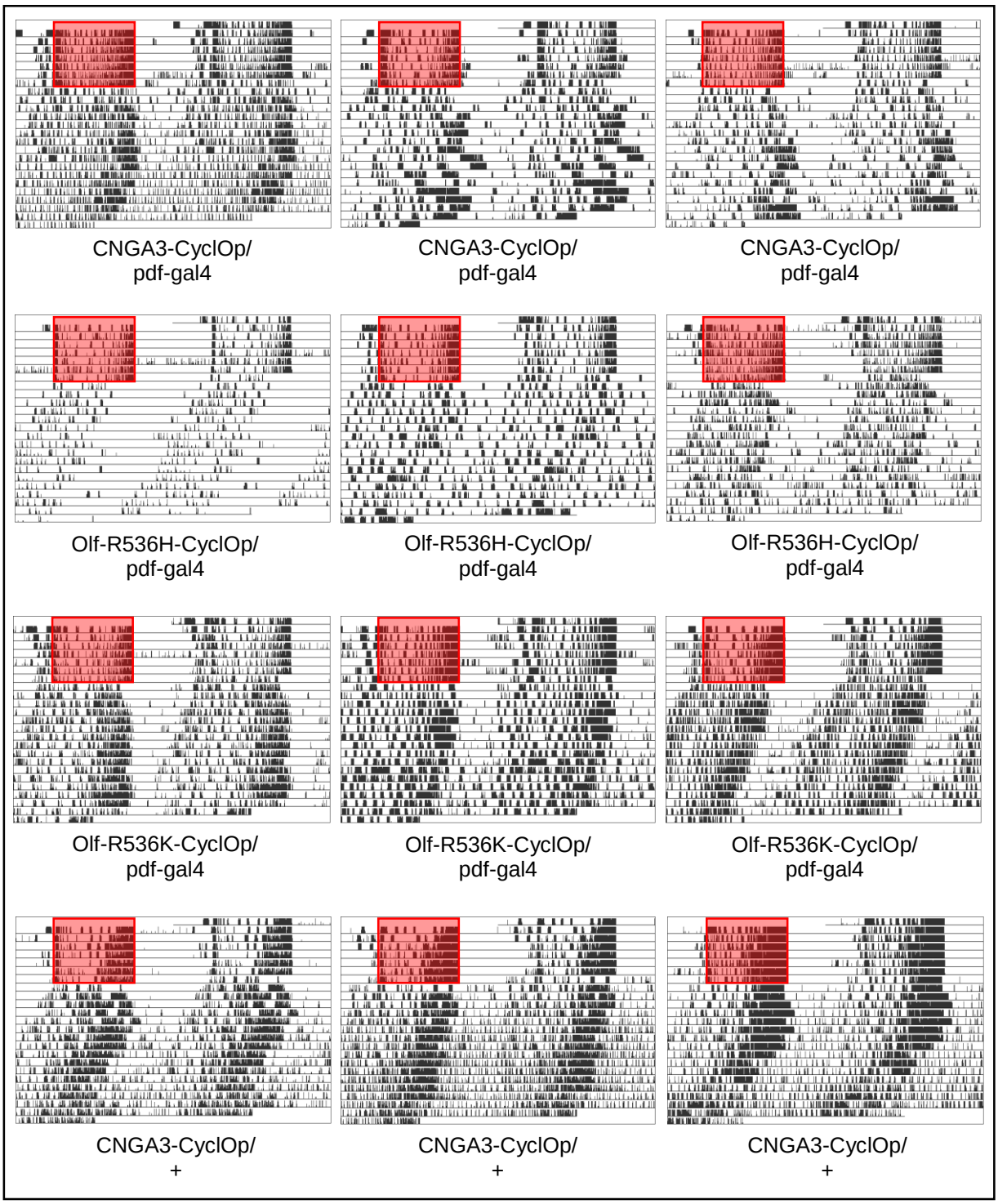

Figure 3.4.6b: Sample actograms of flies expressing CNGA3-CyclOp, Olf-R536H-CyclOp or Olf-R536K-CyclOp in all PDF-positive circadian clock neurons (pdf-gal4) and one respective UAS-control (CNGA3-CyclOp); red shading represents entrainment cycle of 12:12 RD (660 nm, ~1,1 µW/cm²); no shading represents darkness; 20°C 60% RH;

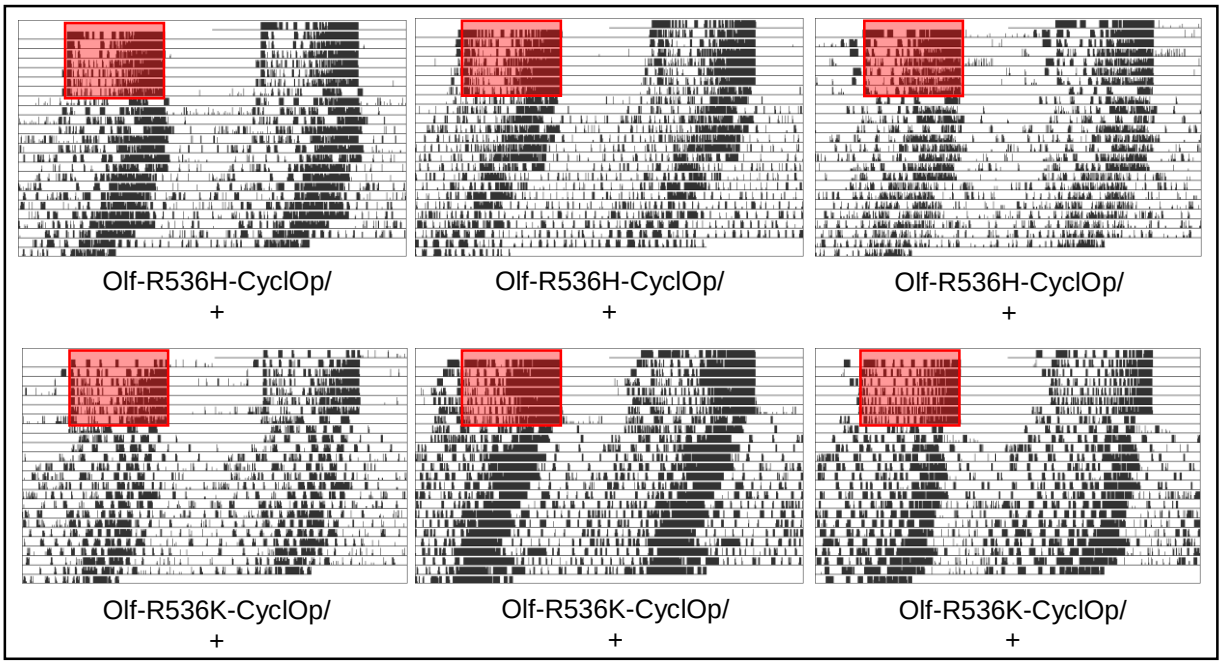

Figure 3.4.6c: Sample actograms of flies expressing no CNGC-CyclOp constructs anywhere; respective UAS-controls to Fig.3.4.6a&b; red shading represents entrainment cycle of 12:12 RD (660 nm, ~1,1 µW/cm²); no shading represents darkness; 20°C 60% RH

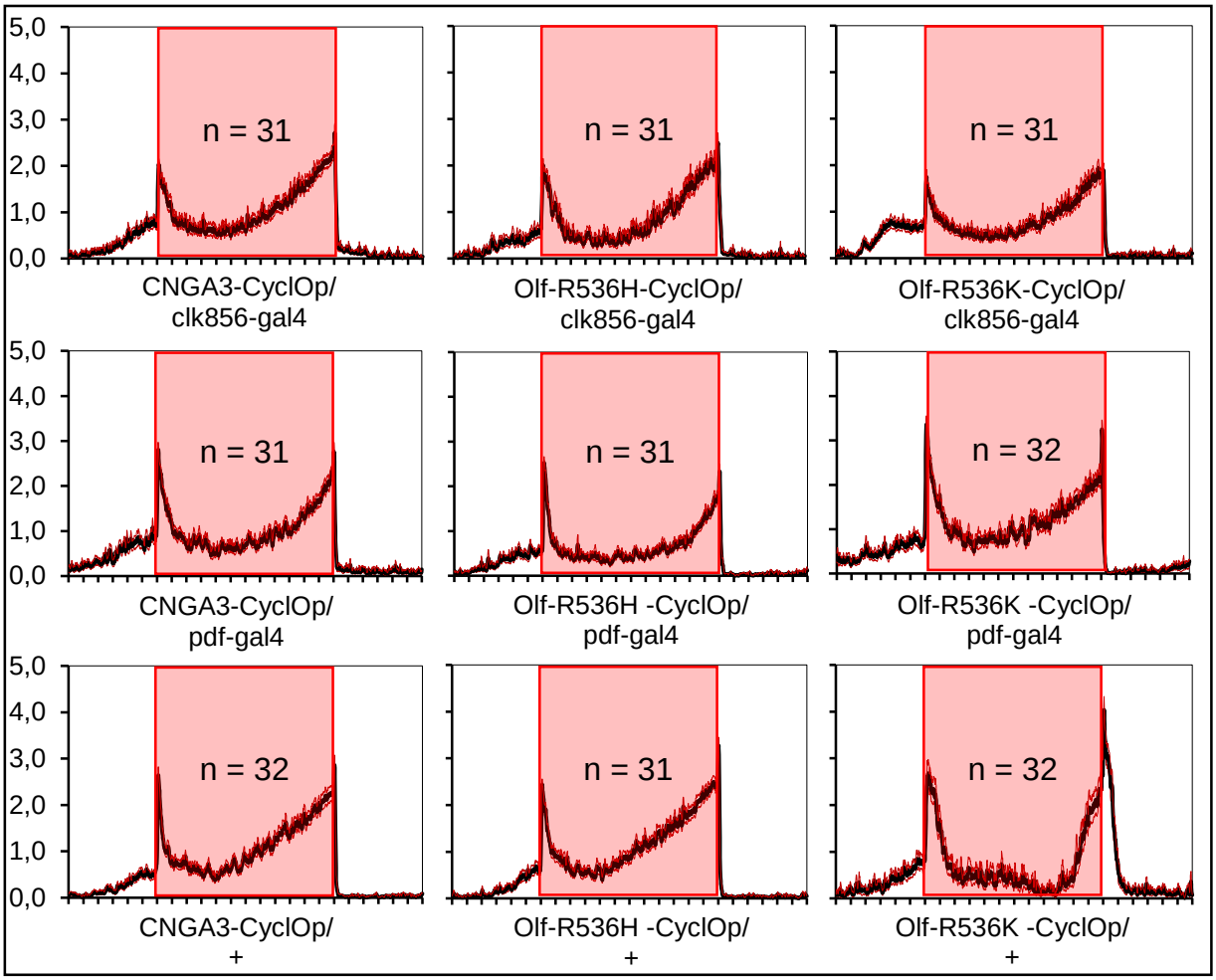

Figure 3.4.7: Averaged actograms of flies expressing CNGA3-CyclOp, Olf-R536H-CyclOp or Olf-R536K-CyclOp in PDF-positive clock neurons (pdf-gal4) and all circadian clock neurons (clk856); red shading represents entrainment cycle of 12:12 RD (660 nm, ~1,1 µW/cm²); for each genotype all available days recorded under the respective conditions were used for data averaging; for each genotype only flies that survived the 7 day experiment were used for data averaging

The 12:12 RD behavioural experiment with the three new CNGC-CyclOp constructs reveals that flies expressing any of the three constructs in all clock neurons (clk856-gal4) are largely unaffected in their circadian rhythm by the expression. Most sample actograms display clearly rhythmic behaviour which transitions into DD (see Fig. 3.4.6a). The averaged actograms of the respective genotypes confirm this as well, exhibiting wild type-like bimodal activity patterns (see Fig. 3.4.7). In the case of pdf-gal4 slight tendencies towards arrhythmicity show up in DD, with flies exhibiting increasingly arrhythmic activity patterns across all three constructs and some flies ending up fully arrhythmic while others exhibit no clear bimodal activity pattern (see Fig. 3.4.6b). During the 12:12 RD entrainment however, all three pdf-genotypes display wild type-like bimodal locomotor activity, which can be seen best in the averaged actograms (see Fig. 3.4.7). The UAS-controls exhibit wild type-like bimodal circadian rhythmicity (see Fig. 3.4.6c). Taken together these results indicate that the new CNGC-CyclOp tools do not disrupt the circadian clock of *Drosophila melanogaster* when expressed in circadian neurons. The tendencies towards arrhythmicity in the pdf-gal4 genotypes can be seen being exhibited by various controls throughout this thesis. Following this experiment under RD conditions, the experiment was repeated with a 12:12 LD entrainment regime, using very strong white light, to test the effect of the optogenetic constructs on the flies' rhythmic behaviour in a situation where the channels are constantly activated during the light period.

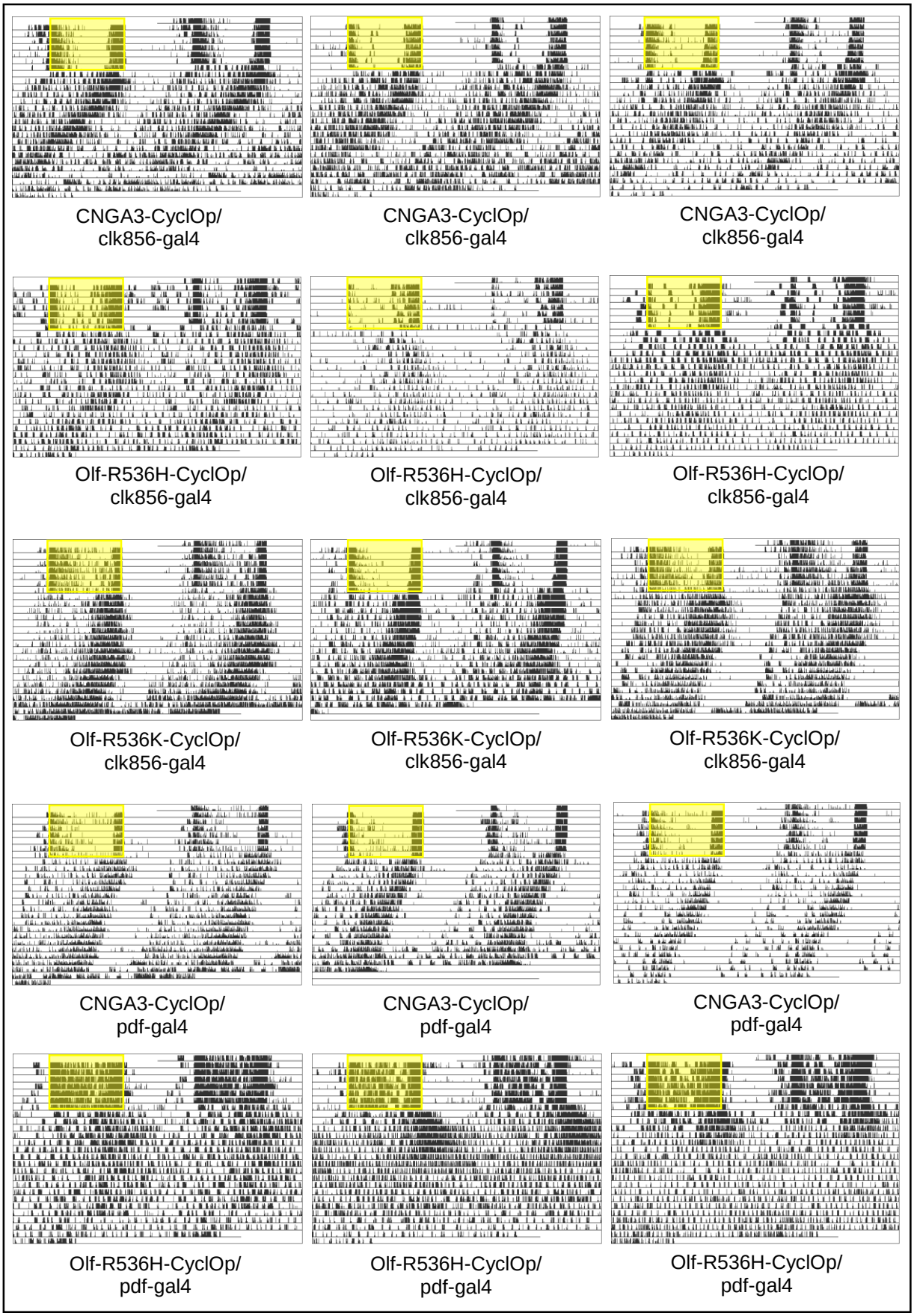

Figure 3.4.8a: Sample actograms of flies expressing CNGA3-CyclOp, Olf-R536H-CyclOp or Olf-R536K-CyclOp in all circadian clock neurons (clk856-gal4) or in PDF-positive clock neurons (pdf-gal4); yellow shading represents entrainment cycle of 12:12 LD (550 nm, 90 µW/cm²); no shading represents darkness; 20°C 60% RH

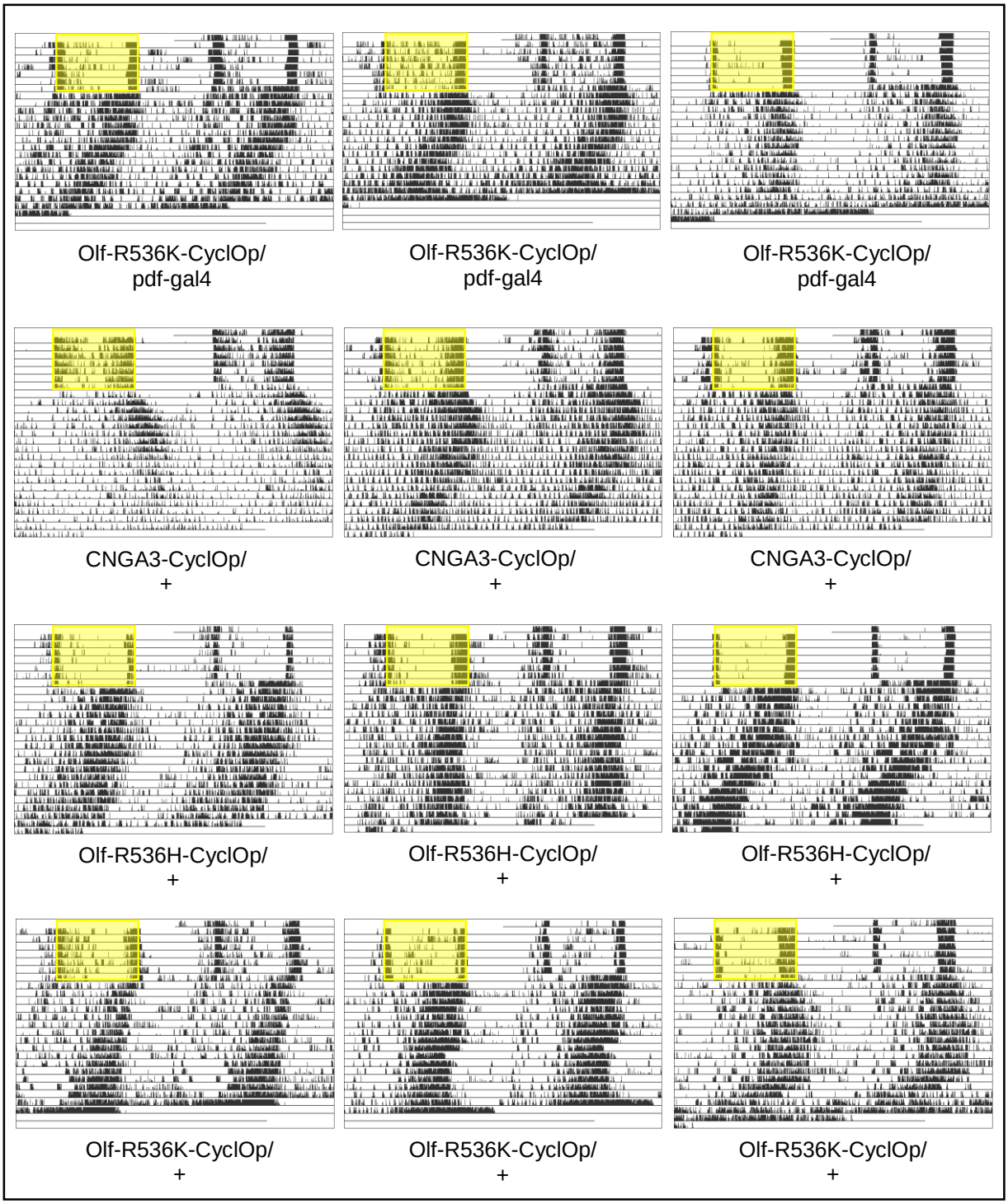

Figure 3.4.8b: Sample actograms of flies expressing Olf-R536K-CyclOp in PDF-positive clock neurons (pdf-gal4) and the respective UAS-controls to Fig. 3.4.8a; yellow shading represents entrainment cycle of 12:12 LD (550 nm, 90 µW/cm²); no shading represents darkness; 20°C 60% RH;

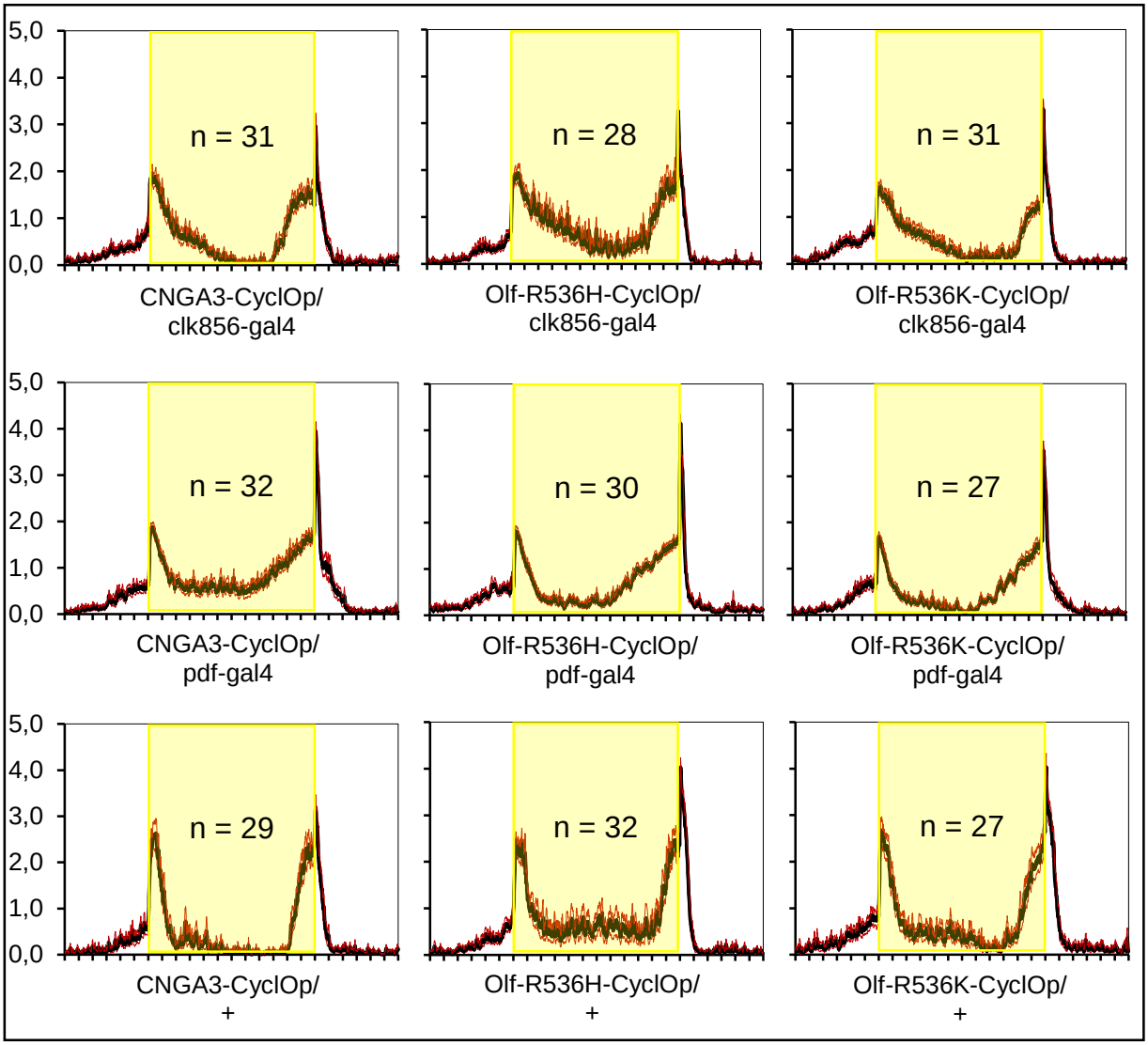

Figure 3.4.9: Averaged actograms of flies expressing CNGA3-CyclOp, Olf-R536H-CyclOp or Olf-R536K-CyclOp in PDF-positive clock neurons (pdf-gal4) and all circadian clock neurons (clk856-gal4); yellow shading represents entrainment cycle of 12:12 LD (550 nm, 90 µW/cm²); for each genotype all available days recorded under the respective conditions were used for data averaging; for each genotype only flies that survived the 7 day experiment were used for data averaging

The results of the behavioural experiment under strong 12:12 LD entrainment look quite comparable to the one done under 12:12 RD with a few exceptions. Flies expressing the three constructs in all clock neurons (clk856.gal4) appear to be affected by the constant activation of the constructs with Olf-R536H exhibiting tendencies towards arrhythmicity after transitioning into DD and CNGA3 displaying notably short periods, while Olf-R536K, the weakest channel exhibits perfectly rhythmic bimodal behaviour (see Fig. 3.4.8a). During the 12:12 LD entrainment however, all genotypes exhibit a wild type-like bimodal activity pattern, the flies expressing CNGC-CyclOp as well as the controls, which can clearly be seen in the averaged actograms (see Fig. 3.4.9). All genotypes show a very pronounced siesta, likely due to the high intensity of

the white light that was used for entrainment. Flies expressing the constructs in PDF-positive neurons are also affected in part, with Olf-R536H exhibiting almost arrhythmic behaviour in DD, while CNGA3 and Olf-R536K show no recognizable effect, as the flies exhibit robust and long-lasting rhythmicity in DD, along with the characteristic bimodal activity pattern (see Fig. 3.4.8a,b). In conclusion it can be stated that the strongest CNGC-CyclOp variant also has the most impactful effect on the circadian clock of *Drosophila melanogaster*, while the effects of the other two, judging by the locomotor data, appear to leave the workings of the clock intact. As these results were seen as a promising improvement to the detrimental effects of Olf-bPAC and SthK-bPAC (see Results 3.2) it was decided to use the new CNGC-CyclOp constructs for experiments aimed at shifting the phase of the circadian clock.

3.4.4. Phase shift experiments

Judging by the results of the previous behavioural experiments with the CNGC-CyclOp constructs, it was decided to focus the phase shift experiments on the two most potent constructs, the CNGA3-Cyclop and Olf-R536H-Cyclop and also to use the clk856-gal4 driver more prominently, since the pdf-gal4 driver had already produced actograms with unclear activity offsets after RD entrainment (see Results 3.4.3).
Following various issues with the climate chamber that had been used for the phase shift experiments in conjunction with the laser glass fibre devices (see Material and Methods 2.7), it was decided to conduct these phase shift experiments using the LED-entrainment boxes instead. The light-pulses to trigger the optogenetic tools to evoke the phase shifts were delivered using the boxes' built in LED units. Intensity, length wavelength and frequency of the light pulses were changed multiple times in between the following experiments, in order to find a setting that would not phase shift the controls by much, but at the same time evoke a significantly larger phase shift in the test-flies through the effects of the activated CNGC-CyclOp. Light entrainment was provided by a 12:12 RD light regime at 660 nm, combined with very faint blue light at 430 nm (12:12) to create light conditions in which the CRY levels in clock neurons could cycle naturally, without excessively activating the constructs.

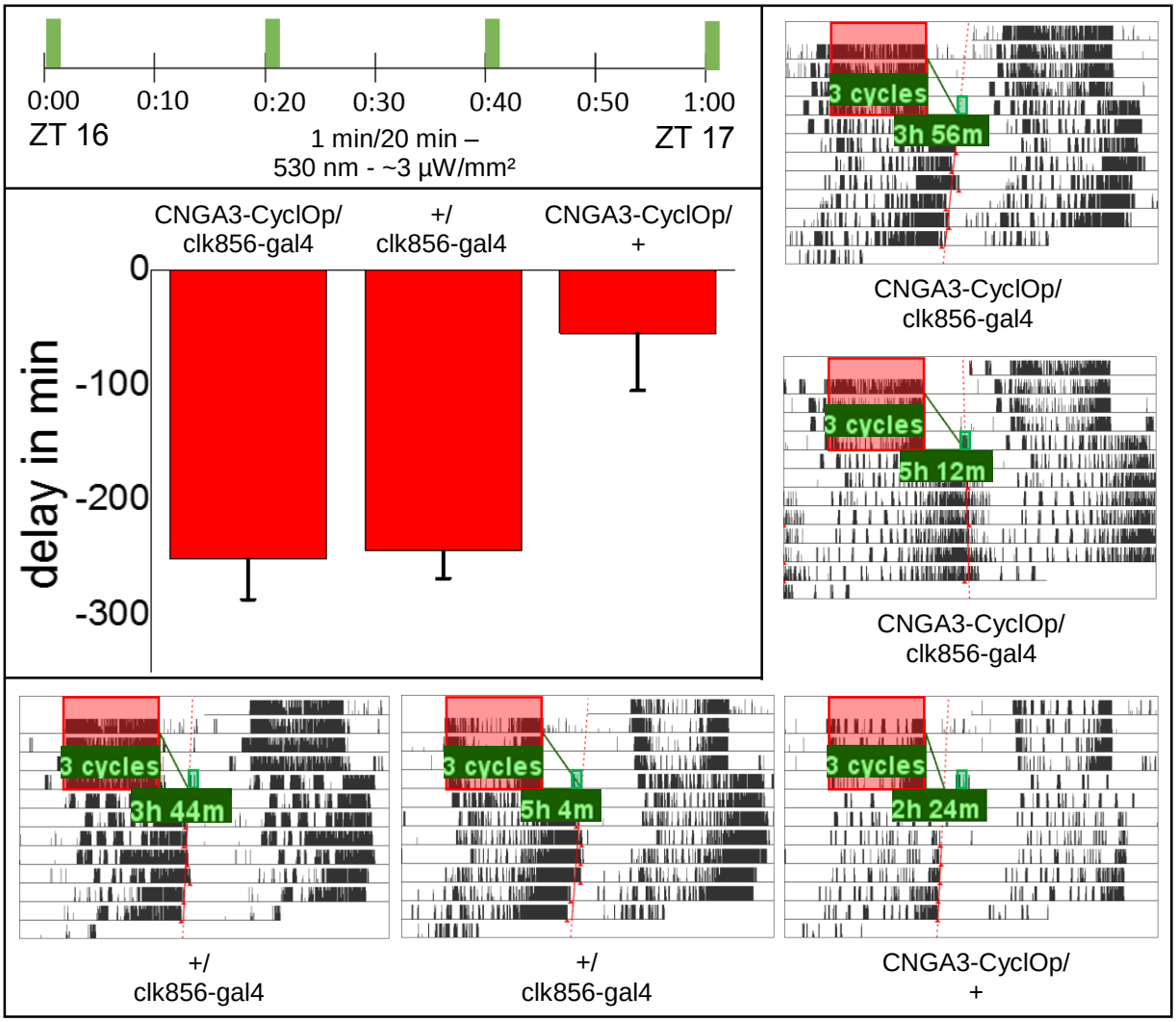

Fig 3.4.10, top left: visual representation of the programmed light pulse, indicating the ZT, the length and frequency of the individual light pulses; **left**: average phase delays of flies expressing CNGA3-CyclOp in all clock neurons (clk856-gal4) and the respective UAS- and GAL4-controls; error bars represent SEM; **bottom right:** sample actograms of flies expressing CNGA3-CyclOp in all clock neurons (clk856-gal4) and the respective UAS- and GAL4-controls; red shading indicates 12:12 RD entrainment (660 nm; ~1,1 µW/cm² + 430 nm 0,1 µW/cm²); green shading indicates light pulse; no shading indicates darkness; 20°C 60% RH; for analysis of the phase shift calculation see Material and Methods 2.7

The first shift experiment using the LED-boxes yielded negative results. The CNGA3-flies as well as the GAL4-control exhibited equally large phase delays after the light pulse, showing no observable and significant effect of the CNGA3-CyclOp construct on the phase shift (see Fig. 3.4.10). The UAS-control however produced a significantly smaller phase delay of only roughly one hour. Seeing this, it was concluded that the clk856-gal4 line apparently introduced a very high light sensitivity into the experimental lines, around which the intensity and length of the light pulse would have to be balanced, if any potential phase shifting effects of the expressed optogenetic constructs were to be demonstrated.

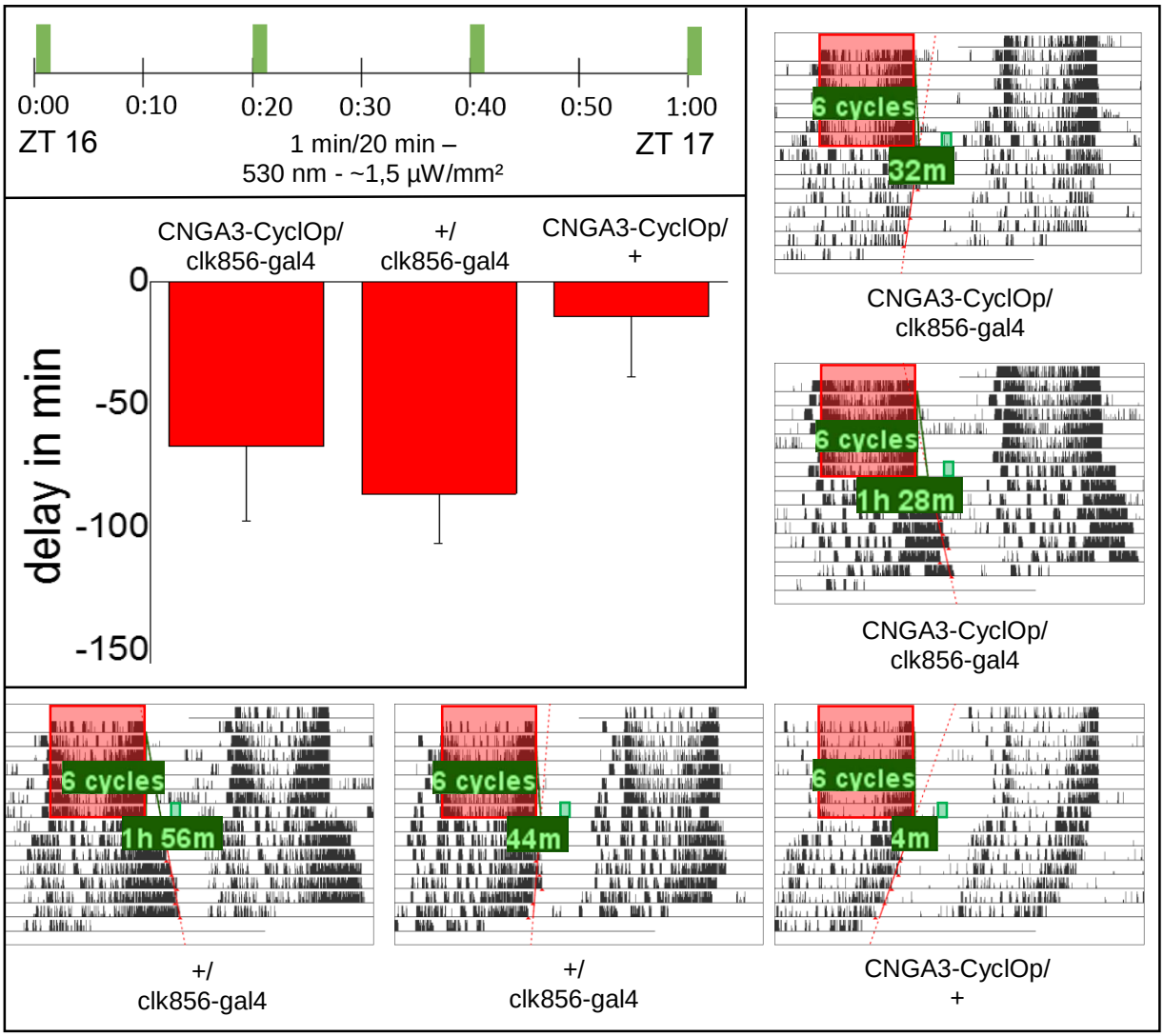

Fig 3.4.11, top left: visual representation of the programmed light pulse, indicating the ZT, the length and the frequency of the individual light pulses; **left**: average phase delays of flies expressing CNGA3-CyclOp in all clock neurons (clk856-gal4) and the respective UAS- and GAL4-controls; error bars represent SEM; **bottom right:** sample actograms of flies expressing CNGA3-CyclOp in all clock neurons (clk856-gal4) and the respective UAS- and GAL4-controls; red shading indicates 12:12 RD entrainment (660 nm; ~1,1 µW/cm² + 430 nm 0,1 µW/cm²); green shading indicates light pulse; no shading indicates darkness; 20°C 60% RH; for analysis of the phase shift calculation see Material and Methods 2.7

For the next shift experiment the intensity of the light pulse was lowered by 50% while keeping all other test parameters the same (see Fig. 3.4.11). This did lead to a massive reduction in the size of the phase delay of all flies, however again failed to produce any significant difference in the phase delays of the CNGA3-flies compared to the GAL4-control, as both again are of similar size. Also, the phase delays of the UAS-control are again significantly smaller than the other two. It was decided that the nature of the light pulse had to be altered further, opting for different wavelength for the next experiment.

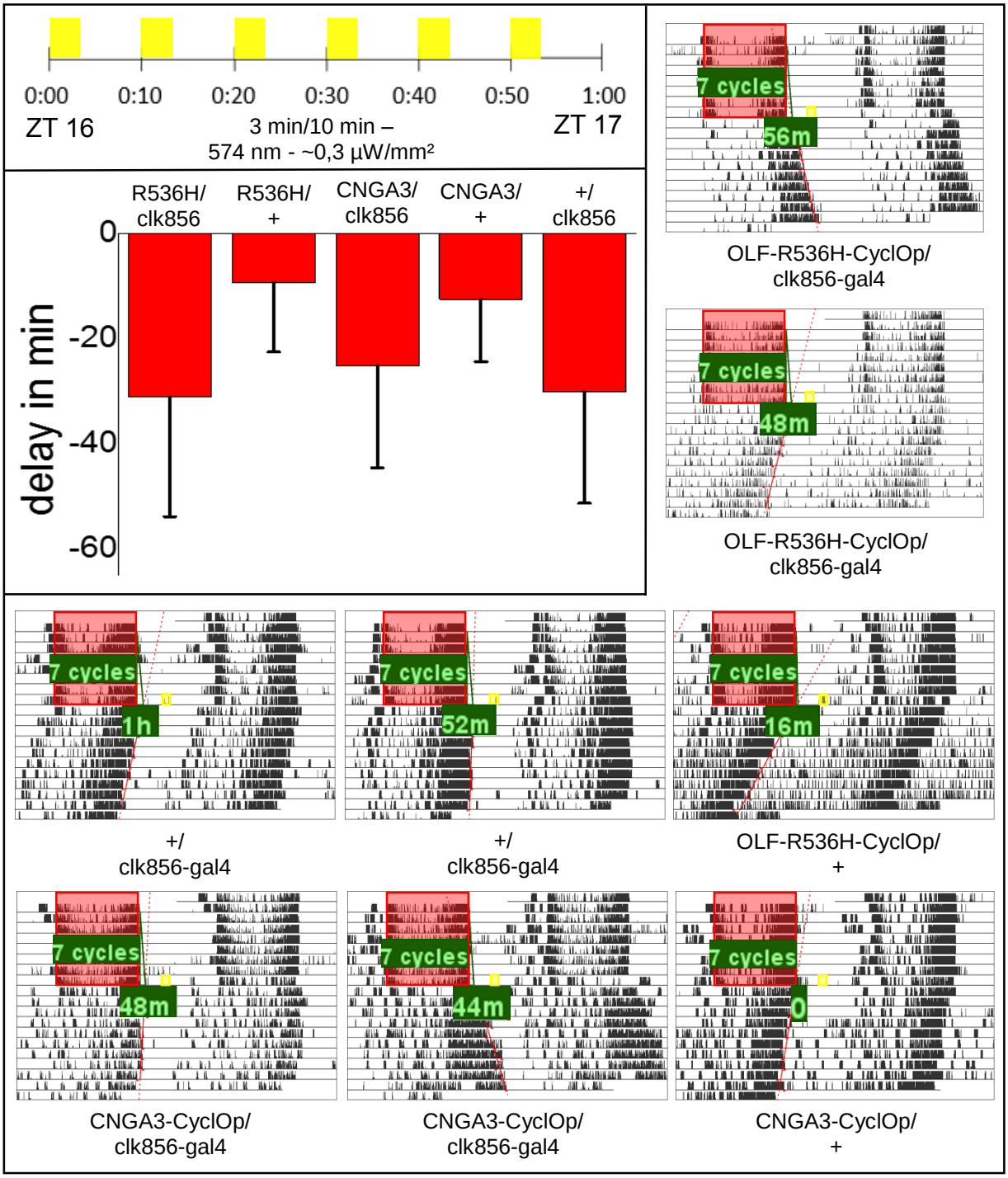

Fig 3.4.12, top left: visual representation of the programmed light pulse, indicating the ZT, the length and the frequency of the individual light pulses; **left**: average phase delays of flies expressing CNGA3-CyclOp or Olf-R536H-CyclOp in all clock neurons (clk856-gal4) and the respective UAS- and GAL4-controls; error bars represent SEM; **bottom right:** sample actograms of flies expressing CNGA3-CyclOp or Olf-R536H-CyclOp in all clock neurons (clk856-gal4) and the respective UAS- and GAL4-controls; red shading indicates 12:12 RD entrainment (660 nm; ~1,1 µW/cm² + 430 nm 0,1 µW/cm²); green shading indicates light pulse; no shading indicates darkness; 20°C 60% RH; for analysis of the phase shift calculation see Material and Methods 2.7

Changing the light pulse to employ a longer wavelength (yellow) and longer illumination times also did not produce any positive results (see Fig. 3.4.12). Once again the test-flies (adding Olf-R536H) showed equally large phase delays as the GAL4-control.

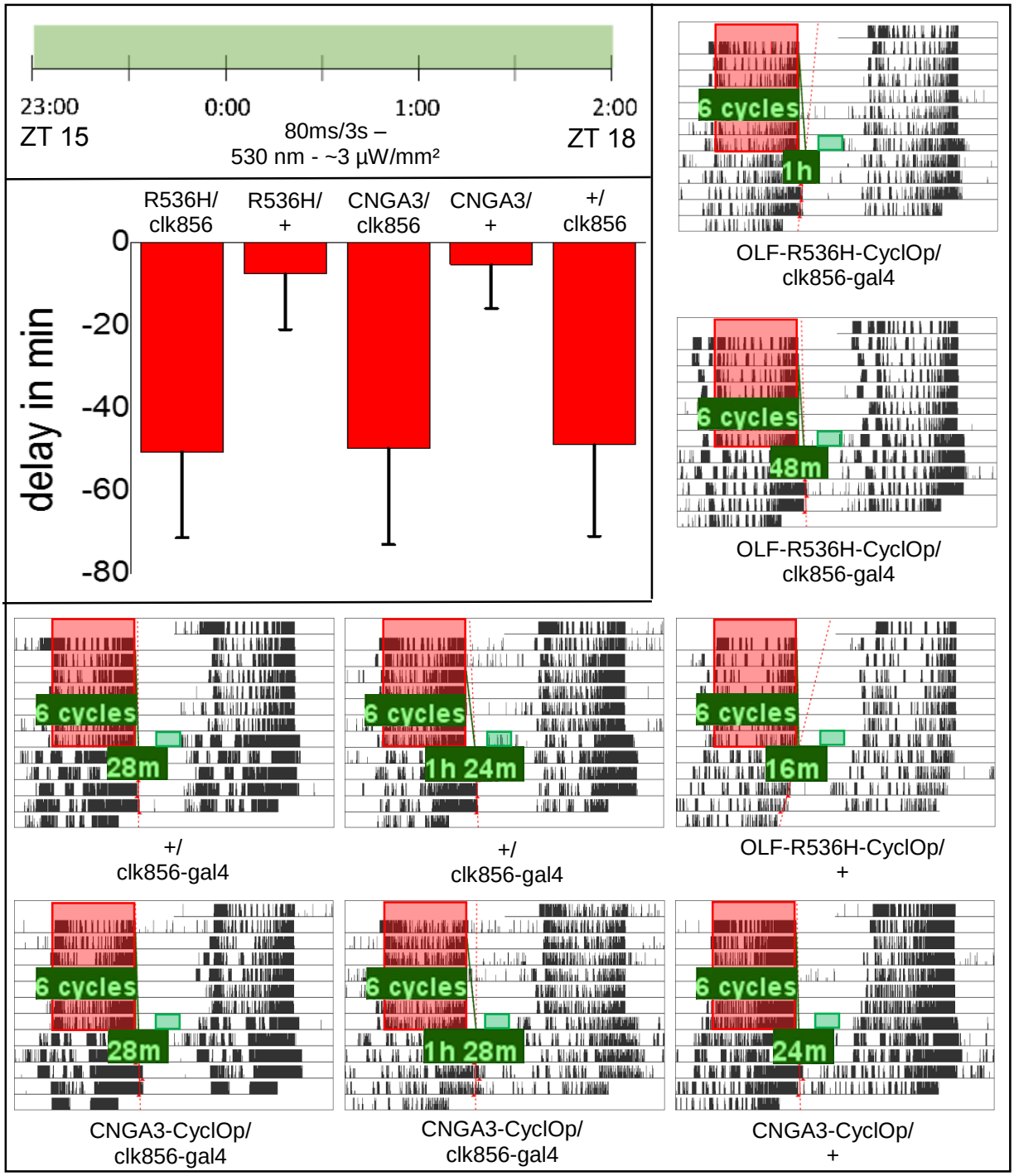

Fig 3.4.13, top left: visual representation of the programmed light pulse, indicating the ZT, the length and the frequency of the individual light pulses; **left**: average phase delays of flies expressing CNGA3-CyclOp or Olf-R536H-CyclOp in all clock neurons (clk856-gal4) and the respective UAS- and GAL4-controls; error bars represent SEM; **bottom right:** sample actograms of flies expressing CNGA3-CyclOp or Olf-R536H-CyclOp in all clock neurons (clk856-gal4) and the respective UAS- and GAL4-controls; red shading indicates 12:12 RD entrainment (660 nm; ~1,1 µW/cm² + 430 nm 0,1 µW/cm²); green shading indicates light pulse; no shading indicates darkness; 20°C 60% RH; for analysis of the phase shift calculation see Material and Methods 2.7

For the experiment above, the light pulse was changed to having the LEDs flash every 3 seconds for 80 milliseconds, for a period of 3 hours, reducing the total net illumination time, while also hopefully increasing the time of CNGC-CyclOp activation (see Fig. 3.4.13). However, this experiment does also not produce any significant results.

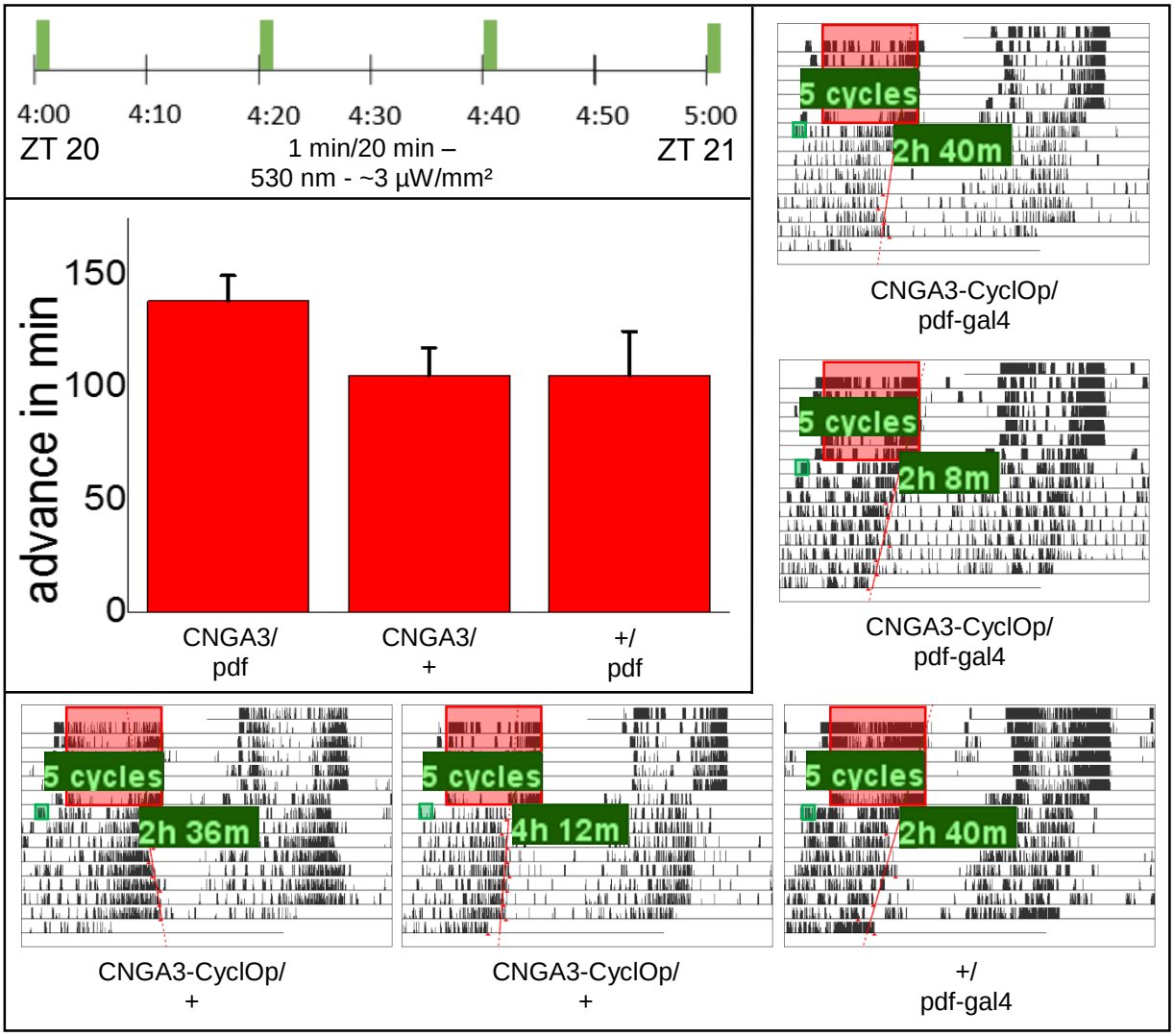

Fig 3.4.14, top left: visual representation of the programmed light pulse, indicating the ZT, the length and the frequency of the individual light pulses; **left**: average phase delays of flies expressing CNGA3-CyclOp in all clock neurons (clk856-gal4) and the respective UAS- and GAL4-controls; error bars represent SEM; **bottom right:** sample actograms of flies expressing CNGA3-CyclOp in all clock neurons (clk856-gal4) and the respective UAS- and GAL4-controls; red shading indicates 12:12 RD entrainment (660 nm; ~1,1 µW/cm² + 430 nm 0,1 µW/cm²); green shading indicates light pulse; no shading indicates darkness; 20°C 60% RH; for analysis of the phase shift calculation see Material and Methods 2.7

After many unsuccessful attempts using the clk856-gal4 driver, the experimental procedure was changed to now use the pdf-gal4 driver instead, attempting to produce a phase advance, mirroring the experimental setup of Eck et al., who used the dTRPA1 channel to produce significant phase advances, when expressed with pdf-gal4 [117]. While producing no results of statistical significance, the experiment looked more promising. The phase advances of the CNGA3-flies have a tendency towards being higher than those of the UAS- and GAL4-controls (see Fig. 3.4.14). The difference in the phase advances is not statistically significant however (p-value 0,094).

The next experiment then tried to expand on the attempt to produce a significant phase advance, by introducing the feeding of ATR prior to the experiment.

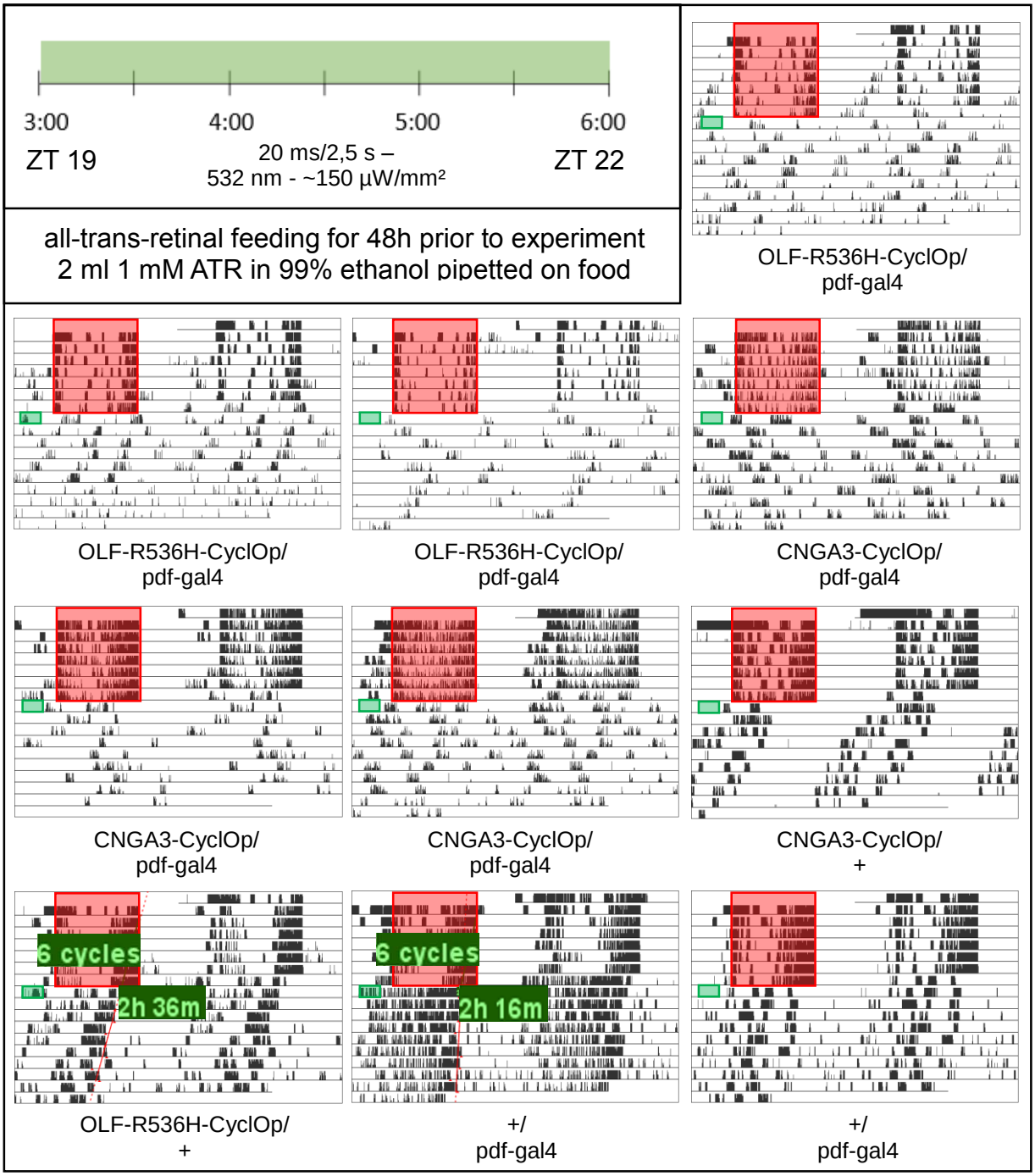

Fig 3.4.15, top left: visual representation of the programmed light pulse, indicating the ZT, the length and the frequency of the individual light pulses; **bottom right:** sample actograms of flies expressing CNGA3-CyclOp or Olf-R536H-CyclOp in all clock neurons (clk856-gal4) and the respective UAS- and GAL4-controls; red shading indicates 12:12 RD entrainment (660 nm; ~1,1 µW/cm² + 430 nm 0,1 µW/cm²); green shading indicates light pulse; no shading indicates darkness; 20°C 60% RH; for analysis of the phase shift calculation see Material and Methods 2.7

In order to increase the potential of the CNGC-CyclOp constructs, the decision was made to feed all assayed flies ATR for 48 hours before the experiment. As ATR is the chromophore of CyclOp, this was done in the hopes of ensuring higher levels of functional CyclOp being expressed, increasing the production of cGMP upon

illumination and increasing the depolarizing effect of the activated CNGCs. The experimental setup also returned to using the laser glass fibre devices, coupled with the PULSETRAIN, enabling the light pulse protocol to put out high frequency light flashes (see Material and Methods 2.7). This however did not end up having the desired effect. Instead of increasing any light-triggered phase shifts, the feeding of ATR apparently renders both CNGA3- and OLF-R536H-flies completely arrhythmic in DD (see Fig. 3.4.15). Almost all flies of both test lines don't show any rhythmicity or any rhythmic activity patterns after transitioning into DD. The UAS- and GAL4-controls on the other hand show sufficiently rhythmic patterns and in some cases even clear and distinct enough activity offsets that allow for the calculation of the phase advance. It is very likely that the increased strength of the CNGC-constructs due to higher cGMP levels causes the flies to become arrhythmic.

Because of time constraints, this experiment was the last one to be conducted, that was attempting to use the CNGC-constructs to invoke a light-triggered phase response of the circadian clock of *Drosophila melanogaster.*

4. Discussion

4.1. ChR2-XXL in neurons of the circadian clock of *D. melanogaster*

4.1.1. Behavioural experiments in a CRY-negative background

The exact reason for the poor rhythmicity displayed by the *cry01* flies in the shift experiments remains speculative. The *cry01* mutation in *Drosophila* has been reported to cause rhythm defects and exhibit two separate circadian components in LL, as if M oscillator and E oscillator were uncoupled [144, 145]. Judging by the actogram data of the *cry01* lines it can be concluded that while the rhythmicity exhibited by the flies may be poor, the flies do appear to be entrained to the 12:12 RD light regime, as they do display rhythmic activity patterns in DD, which are in phase with the RD entrainment regime (see Results 3.1.1). As most studies using CRY-negative flies have used experimental setups in which they tested the effects of CRY-activating light on the circadian clock in the absence of CRY, the exact state of the molecular clock of the *cry01* flies following the RD entrainment remains unaddressed. However, as the actogram data obtained by the *cry01* lines was unsuitable for the exact calculation of any putative phase shifts, due to the rhythmic activity patterns displaying neither clear nor distinct activity offsets, experiments with the *cry0*1 line were ultimately discontinued. The cause for the poor rhythmicity was not further investigated, as it was not a main goal of this thesis.

4.1.2. Behavioural experiments in a CRY-positive background

It can be concluded from the phase shift experiments with CRY-positive flies that ChR2-XXL was unable to evoke significant phase shifts in the flies expressing the construct in comparison to the respective controls (see Results 3.1.3). Judging by the actogram data obtained from experiments with flies expressing ChR2-XXL in motor neurons under control of the ok6-gal4 driver, it is also evident that ChR2-XXL is extremely effective at light-mediated neuronal depolarization, relative to light intensity (see Results 3.1.2). It appears as if the light-activated depolarization of the various clock neurons mediated by ChR2-XXL was not enough to cause the circadian clocks

of the tested flies to phase shift. The phase shifts that are visible in flies expressing ChR2-XXL, as well as in the controls, seem to have been caused by the light application itself, rather than any ChR2-XXL mediated depolarization. A study in which an optogenetic tool with similar conductive qualities like ChR2-XXL is used successfully to influence the circadian clock of *Drosophila melanogaster* does exist, however. Guo et al. used the red-shifted Channelrhodopsin variant Crimson [82] in a study aiming to research the sleep cycle of *Drosophila melanogaster* [116]. The experimental setup used by Guo et al. was however very different to the one used in this thesis. Guo et al. studied the effects of long-term red-light stimulation of flies expressing Crimson under the control of the r18h11-gal4 driver, which drives expression in the DN1s [146] and submitted flies to 17-hour periods of LED stimulation (0.08 mW/mm^2 at 627 nm), recording the flies' locomotor behaviour [116]. The constant red-light-mediated DN1-activation strongly affected fly behaviour, significantly suppressing locomotor activity and extending the siesta [116]. A subsequent study by the same authors repeated the experimental setup of using Crimson for red-light-mediated DN1 activation successfully [147]. It could be argued that the depolarization period of 2 hours used in this thesis was simply too short to lastingly effect the circadian clock of *Drosophila melanogaster.* Moreover, the effectiveness of the ChR2-mediated neuronal depolarization is not entirely certain. Dawydow et al. reported a closing time constant (τ_{off}) of roughly 76 seconds for ChR2-XXL in DEVC recordings of *Xenopus* oocytes [86]. The light-pulse in the discussed phase shift experiments using ChR2-XXL was designed to re-excite the optogenetic construct every 120 seconds, leaving a 2 minute time-gap during which the photocurrent of the ChR2-XXL was continuously diminishing. Thus, it is not entirely certain if ChR2-XXL was able to sustain a continuous depolarization of the respective clock neurons.

Another, more likely hypothesis is that any putative phase shifts caused by the light-activated depolarization were masked by CRY-mediated or also CRY-independent phase shifts that can be observed in the respective control flies. Due to the light-pulse illumination being facilitated by a strong green laser (0.4 mW/mm² at 532 nm), CRY-mediated phase shifts are quite possible even though *Drosophila*-CRY exhibits a very diminished residual absorption at 532 nm [148]. In addition CRY-negative flies have also been demonstrated to have their circadian clock phase shifted by white light pulses in the subjective night [56], which demonstrates that light-mediated CRY-

independent phase shifts could also be responsible for masking any putative phase shifts caused by ChR2-XXL.

Looking at the successful phase shift experiments conducted by Eck et al. using the thermogenetic dTRPA1 channel, the most likely cause for ChR2-XXL-mediated depolarization not being able to significantly phase shift the circadian clock, probably lies in the differences of conductivity between ChR2-XXL and dTRPA1, since the phase shift experiments conducted in this thesis were modelled after the successful experiments by Eck et al. [117]. A key difference in the conductivity of both channels is their conductivity for Ca^{+2}. While the dTRPA1 channel, belonging to the TRP superfamily of structurally related, non-selective cation channels, is highly conductive for Ca^{+2} [118, 149], ChR2-XXL like other Channelrhodopsin variants has a rather low conductivity for Ca^{+2} and other divalent cations [70], which has led to efforts trying to increase the Ca^{+2} conductivity of ChR2 by mutating key amino acid residues [84]. Studies suggest that intracellular Ca^{+2} plays an integral role in the function of the circadian clock. The buffering of intracellular Ca^{2+} in pacemaker neurons resulted in dose-dependent slowing of free-running behavioural rhythms and slowed the rhythmic nuclear accumulation of essential transcription factors [150], while glial-specific genetic manipulations, which among others, affected calcium signalling, lead to circadian arrhythmicity in adult *Drosophila* [151]. Also, Ca^{+2} levels in pacemaker neurons have been demonstrated to cycle rhythmically [147], with different groups of pacemaker neurons even displaying asynchronous rhythms of Ca^{+2} cycling [152]. A very recent study also showed that genetic manipulations that increased or decreased the levels of Ca^{+2} in the prothoracic gland, respectively shortened or lengthened the periodicity of emergence of *Drosophila* [153]. Accordingly it is quite likely that the phase shifts evoked by the timed depolarization of dTRPA conducted by Eck et al. [117], were due to the cytosolic manipulations of Ca^{+2} levels, rather than the neuronal depolarization by itself. Since ChR2-XXL is rather ineffective at manipulating cytosolic Ca^{+2} levels, mere ChR2-mediated neuronal depolarization would accordingly be unable to phase shift the circadian clock of *Drosophila melanogaster*. As this suggestion was considered to be the most likely explanation for the data obtained with ChR2-XXL, further experiments involving the Channelrhodopsin variant were discontinued and efforts were focused on finding a more suitable optogenetic approach.

4.2. Characterizing Olf-bPAC and SthK-bPAC in *D. melanogaster*

4.2.1. The harmful effects of Olf-bPAC and SthK-bPAC

From both locomotor activity and anti-PDF stainings it can undoubtedly be concluded that both the expression of Olf-bPAC and SthK-bPAC has a tremendously harmful effect on the development of the s-LNvs (see Results 3.2.1 – 3.2.5). Although no clear phenotypic indication of malformation or abnormal path finding can be found in the l-LNvs it stands to reason that the expression of both optogenetic constructs likely has a damaging effects on these clock neurons also, as well as other clock neurons, when expression is driven with the clk856-gal4 driver. The pdf-gal4 driver has been shown in this thesis to drive the expression of Olf-bPAC as early as the larval stages, where the expression of Olf-bPAC can already be seen to have a detrimental effect on neuronal growth (see Results 3.2.4), inarguably placing the origin of the observed phenotype during the larval stages of the flies. Upon eclosion, the flies already display the full phenotype. A gradual progression of the phenotype with age after eclosion was not recorded (see Results 3.2.3). The control experiments with flies expressing bPAC and the Olf channel each alone respectively, also revealed the Olf-channel to be responsible for the phenotype (see Results 3.2.6 & 3.2.7). Residual dark-activity by the bPAC, enhancing cAMP levels, can be ruled out accordingly as cause. This by extension also leads to the conclusion that the SthK channel is also responsible for the extremely similar phenotype observed in flies expressing SthK-bPAC under the control of the pdf-gal4 driver (see Results 3.2.2 & 3.2.5). A recent study found that several members of the TRP family can mediate a calcium-dependent cytotoxicity [154]. Either heterologously expressed in HEK cells or in native mouse dorsal root ganglion neurons, the two cation channels TRPV1 and TRPA1 both triggered a strong influx of external Ca^{+2} upon activation, accompanied by a strong Ca^{+2}-release from intracellular stores like the endoplasmic reticulum [154]. In the case of TRPV1, the activation additionally caused a probably lethal increase in mitochondrial Ca^{+2} leading to the death of the respective cells [154]. As Olf also belongs to the super-family of TRP channels and shares their conductive qualities [98], especially in regards to its Ca^{+2}-conductivity [99], it is possible that an Olf-mediated rise of intracellular Ca^{+2} is at least partially responsible for the observed phenotype of the malformed s-LNvs. As cAMP constitutes a ubiquitously present second-messenger molecule in neurons of

Drosophila melanogaster, where it is prominently involved in processes regulating synaptic plasticity [155–157] or memory formation [158, 159], it is likely that endogenous cAMP is responsible for activating the expressed Olf, triggering the influx of Ca^{+2}. Although cAMP levels within circadian clock neurons have never been explicitly assessed or monitored during the larval stages of development, a cAMP concentration high enough to activate the expressed Olf seems entirely plausible, given the fact that cAMP is directly involved in processes of the molecular clock mechanism, like enhancing PER stability [160], or affecting the circadian clock via the cAMP responsive element binding protein (CREB) [161]. While cGMP can't be ruled out as another contributor to the activation of the expressed CNGCs, no substantiated arguments can be made about the involvement of cGMP, as the role of cGMP within circadian neurons is unclear and unaddressed.

Increase in cytosolic Ca^{+2} levels however can't be the cause of the very similar phenotype, observed when expressing SthK-bPAC in circadian neurons, as SthK is a highly selective potassium channel [96]. Activation of SthK would not lead to an increase in cytosolic Ca^{+2}, but rather to continued hyperpolarization, like we demonstrated when light-activating SthK-bPAC in motor neurons of *Drosophila* larvae (see Results 3.2.8) [95]. It is however known that neuronal electric activity is an essential process in forming neuronal circuits and that processes like axon growth, axon branching, arborisation and refinements in axonal morphology are influenced by impulse activity, in mammals [162] as well as in *Drosophila* [163]. A recent study has shown that in zebrafish, heterologous expression of the inward rectifying K^+-channel Kir2.1 [164] strongly inhibits both net growth of retinal ganglion cell axons and the formation of new branches by individually transfected axon arbors [165]. It seems plausible that a similar phenotype can be observed here in *Drosophila*, when the also strictly inward rectifying K^+-channel SthK [96, 166] is activated by endogenous cAMP during larval development. Why different groups of clock neurons like the s-LN_vs are affected stronger than others is unclear, but could be due to different expression rates during larval development or varying endogenous cAMP levels.

The behavioural experiments with flies expressing Olf-bPAC and SthK-bPAC under the clk856-gal4 driver and the pdf-gal4-driver exhibited interesting rhythmic phenotypes, especially in the case of Olf-bPAC/pdf-gal4 (see Results 3.2.1 & 3.2.2). The importance of the LN_vs for a robust rhythmic circadian behaviour has been demonstrated in several studies. Flies that had their PDF-positive LN_vs completely

ablated, exhibited rhythmic behaviour under 12:12 LD entrainment but became mostly arrhythmic in DD [25]. A study of *disconnected* mutants showed that only flies that retained their LN_vs exhibited rhythmic behaviour, while flies lacking LN_vs were completely arrhythmic [26]. The actogram data acquired in this thesis of flies expressing Olf-bPAC and SthK-bPAC in the PDF-positive LN_vs supports these findings, further establishing the LN_vs as central pacemaker neurons. The exact effects of the malformed s-LN_vs, which lack the projections into the dorsal protocerebrum is difficult to assess, as these effects can't be separated from the effects of the likely continuous activation of the CNGCs by endogenous cAMP. The phenotype displayed by flies expressing Olf-bPAC and SthK-bPAC in all clock neurons (see Results 3.2.1 & 3.2.2) is also very difficult to describe in functional terms on the level of the clock network or even the molecular clock, as too many factors are to be considered. Moreover, any putative morphological damage to clock neurons other than the PDF-positive has not been researched, but is likely to be contributing to the final phenotype, given the damage caused by the CNGCs to the s-LN_vs (see Results 3.2.3 & 3.2.5). Interestingly, it has to be noted that flies expressing Olf-bPAC only in all PDF-positive clock neurons display a more drastic phenotype than those that express in all clock neurons. This is especially evident when comparing the average actograms under a 12:12 RD entrainment (see Figures 3.2.2 & 3.2.5). The clk856-flies exhibit a bimodal activity pattern with an anticipatory increase of activity during the evening, similar to the controls, while the pdf-flies are completely lacking in this regard. This phenomenon appears to be reversed for SthK-bPAC, in which case the pdf-flies exhibit a bimodal activity pattern during 12:12 RD that resembles the controls and the clk856-flies are the ones exhibiting a rather abnormal activity pattern. Due to more clock neurons being affected by the disruptive and damaging influence of the CNGCs, one would expect for the clk856-flies to exhibit a stronger impact on their rhythmicity than the pdf-flies, as is the case for SthK-bPAC, but not for Olf-bPAC. The exact cause of this phenomenon is impossible to decipher, as too many different factors are to be considered. The only genotype whose rhythmic phenotype was more closely researched in a follow-up experiment was Olf-bPAC/pdf-gal4 (see Figure 3.2.3). Here it was shown that flies that express Olf-bPAC in the PDF-positive neurons are completely unable to entrain to a 12:12 RD light regime and are free-running instead, a fact which was already suggested by the obtained data from the averaged actograms under 12:12 RD.

4.2.2. Characterizing Olf-bPAC and SthK-bPAC in larval motor neurons

Expressing Olf-bPAC and SthK-bPAC in motor neurons of *Drosophila* using the ok6-gal4-driver yielded no live adult animals, as 100% of flies died during pupariation. This further highlights the damaging effects of both Olf-bPAC and SthK-bPAC, already discussed in Discussion 4.2.1. Apart from that, the FIMtrack experiments with instar-3 larvae expressing Olf-bPAC and SthK-bPAC showed that both constructs have the potential to be valuable tools for further optogenetic research.

Both constructs reliably and reversibly paralyze *Drosophila* larvae upon illumination, which express the constructs in their motor neurons (see Results 3.2.8). In accordance with their conductive properties Olf-bPAC and SthK-bPAC both affecte the transient body length of the larvae. As Olf-bPAC increases membrane conductance for most monovalent and divalent cations upon, the light-induced depolarization triggers the firing of many subsequent action potentials along the neuronal membrane, causing muscles to contract, subsequently leading to a contraction of the entire larval body. As SthK-bPAC is a strictly selective and inward rectifying K^+-channel, the opening of SthK further hyperpolarizes the neuronal membrane and prevents action potentials from being fired. This, inversely to Olf-bPAC, causes muscles to relax and be unable to contract, leading to a slight lengthening of the larval body. The light-induced paralysis and change in body length are both reversible and light-dose-dependent, with SthK-bPAC being more light-sensitive than Olf-bPAC. This observation falls in line with the fact that SthK is more sensitive towards cAMP than Olf. The half maximal effective concentration (EC_{50}) of cAMP is roughly 3.7 µM for SthK [96] and roughly 14 µM for Olf-T537S [98]. The dependency on the light-dosage is due to fact that the closing of the channels relies on diffusion and hydrolysis of the intracellular cAMP, which takes longer when higher concentrations of cAMP had been produced by bPAC [95].

An interesting fact observed during the FIMtrack recording assay, was that larvae which expressed either Olf-bPAC or Olf alone as control, exhibited a 25% shorter body length than all controls, as well as larvae expressing SthK-bPAC (see Fig. 3.2.15 & 3.2.17). As this effect is specific for larvae expressing the Olf channel, it is likely due to the harmful effects of the channel during the instar-1 and instar-2 developmental stages, likely similar to the lethal effects during pupariation, as already discussed in Discussion 4.2.1. As larvae expressing SthK-bPAC do not exhibit any impaired body length, this also demonstrates that the channels' effects on neuronal morphology have

different causes regarding their molecular mechanics, even though the phenotypes are very similar in later developmental stages, as both end up causing the death of the larvae during pupariation or shortened and underdeveloped s-LN$_v$s in adult *Drosophila* when expressed with the pdf-gal4 driver. Larvae expressing SthK-bPAC on the other hand move significantly slower than their respective controls, as well as all other tested larvae, even under red light control conditions. This is likely due to SthK being already activated in red light by endogenous cAMP, or any cAMP produced by the fused bPAC due to its residual dark activity [105]. Given the fact that Olf already has a measurable effect on the larval body size, even when the larvae are reared in total darkness, it is likely that Olf is also activated to some degree by endogenous cAMP or by bPAC dark activity in these recordings, however apparently not to a degree where the larvae are slowed down measurably, likely due to the fact that SthK is more sensitive towards cAMP than Olf.

The bPAC controls CD8-bPAC, Glycophorin-bPAC and bPAC-R278A also all demonstrate that the increase of cAMP already heavily impacts larval motility as well as body length, even without a fused CNGC (see Fig 3.2.16 – 3.2.19). An effect like this was to be expected, as bPAC had already previously been shown to be able to efficiently stop *Drosophila* grooming behaviour upon illumination when expressed pan-neuronally using the elav-gal4 driver [105]. In regards to the acute effects of Olf-bPAC and SthK-bPAC on neurons, cAMP-associated effects can almost be neglected as they are completely masked by the much more pronounced CNGC-mediated effects. In terms of the viability of Olf-bPAC and SthK-bPAC as optogenetic tools however, these effects should be kept in mind and bPAC-only controls are recommended when applying these tools to new cell types or tissues, in order to address any possible long-term effects that the increased cAMP levels might have.

4.3. Temperature-controlled expression of Olf-bPAC and SthK-bPAC

Judging from all the data gathered by immunostaining *Drosophila* brains expressing Olf-bPAC or SthK-bPAC under control of the newly crossed lines clk856-gal4/tub-gal80ts and pdf-gal4/tub-gal80ts, it can be concluded that the desired goal of suppressing the expression of the two CNGC-constructs until adulthood was successful. *Drosophila* flies with the *tubgal80ts* transgene raised at 18°C, expressing both SthK-bPAC or Olf-bPAC under control of either the clk856-gal4 driver or the pdf-gal4-driver, have the expression of the CNGC-constructs successfully delayed until adulthood (see Results 3.3.1). This results in the flies exhibiting wild type-like arborisations of the s-LN_vs, very similar to the respective controls. Very interestingly, flies that express the *tubgal80ts* transgene combined with a pdf-gal4-controlled expression of either SthK-bPAC or Olf-bPAC also exhibited a near wild type-like s-LN_v-morphology even when reared at 29°C. This is surprising, as the function of GAL80,, suppressing GAL4-driven expression, should be inactivated at such temperatures. A phenotype very much like the one observed with a GAL4-driven expression without GAL80-mediated suppression would be expected, which should produce shortened and underdeveloped s-LN_vs (see Results 3.2.3). The reasons for this observation are speculative, but could be due to the respective transcription rates of the *gal4* and *gal80* transgenes. If the *tub-gal80* transgene were to be transcribed at a much higher rate than the *pdf-gal4* transgene during the critical period in larval development, it would be conceivable that an effective suppression could still be sustained. Also, when reared at 29°C, the pdf-gal4/tub-gal80 flies expressed SthK-bPAC in a number of unspecified neurons in the central brain (see Fig. 3.3.1). These neurons could not be identified and the exact nature of this unspecific expression could not be elucidated, but is apparently specific for the UAS-SthK-bPAC line, as no unspecific expression could be seen for the UAS-Olf-bPAC line. But since the temperature-controlled induction of expression worked reliably when flies were kept at 29°C for 12 hours, this unspecific expression of SthK-bPAC was not researched any further.

The behavioural experiments with temperature-controlled expression of the two CNGC-constructs revealed that except for flies expressing SthK-bPAC in all clock neurons, no discernible effects on the flies' rhythmic locomotor activity under a 12:12 RD entrainment could be seen (see Results 3.3.2). After the 7-day expression period, which introduced a 12:12 temperature cycle between 18°C and 29°C in phase with the

12:12 RD light entrainment, only flies that expressed SthK-bPAC in all clock neurons exhibited an unusual activity pattern in the 12:12 RD period. The aberrations in the flies' rhythmic locomotor behaviour can be clearly seen, both in the sample actograms, as well as the averaged data (see Fig. 3.3.4 & 3.3.5). Like is the case for the other off-target effects recorded so far when using these two CNGC-constructs, this effect is likely due to endogenous cAMP activating the SthK channel, along with bPAC dark-activity. Apparently, the circadian network is unable to compensate for the continuous hyperpolarization mediated by SthK, when entrained with a 12:12 RD light regime. Interestingly however, the circadian clock appears to be quite able to compensate for this effect when a 12:12 temperature gradient in phase with the 12:12 RD entrainment is introduced. During the 7 day expression period, the locomotor activity of the SthK-bPAC/clk856 flies follows the bimodal pattern that is also exhibited by the respective controls and the other tested lines during this period.

Another thing of note is the second M peak that is exhibited by all flies in the experiment during the expression period with the added 12:12 temperature gradient. This is most certainly because of the delayed ramping of the temperature compared the onset of light, which results in an increase of activity when peak temperature is reached during the early hours in the morning. After this second M peak all flies transitioned into a prolonged midday siesta, a well-documented adaption of the *Drosophila* circadian clock to avoid unnecessary exposure to heat during hot days [167, 168], regulated through thermal-sensitive splicing of the 3'-terminal intron in the *period* gene [169, 170].

When the experiment was repeated with a 12:12 LD entrainment with a strong white light source, the capabilities of the two CNGC-constructs in influencing the circadian clock and the rhythmic locomotor behavioural output was demonstrated. While all fly lines displayed a wild type-like bimodal activity pattern during the 7 day expression period, flies expressing SthK-bPAC in all clock neurons (clk856-gal4) clearly show strongly reduced locomotor activity during the evening, as soon as SthK-bPAC is expressed (see Fig. 3.3.6 & 3.3.7). This behaviour also persists once the temperature gradient is removed after the expression period, demonstrating that this is no temperature-mediated change in behaviour. Since studies successfully applying optogenetics to the circadian clock of *Drosophila melanogaster* haven't been published until very recently, no really comprehensive data exists yet, to which the phenotype caused by the light-controlled silencing of the entire circadian clock network could be compared to. Guo et al. used the newly discovered anion channelrhodospin GtACR

from the cryptophyte alga *Guillardia theta* [171], and thermo-induced expression of the inward rectifying K^+ channel Kir2.1 [164] to be able to silence specific circadian neurons [147]. Silencing three LN_ds along with the 5th PDF-negative s-LN_v (collectively referred to as evening “E” cells), resulted in behavioural phenotypes similar to those recorded here when using SthK-bPAC for light-induced silencing [147]. Flies that had the E cells silenced using either approach, exhibited significantly reduced locomotor activity during the subjective evening, with Kir2.1 producing a stronger phenotype than GtACR. Since Guo et al. only published processed locomotion data of the *Drosophila* flies, comparing sleep profiles rather than raw actogram data and didn’t publish any sample actograms alongside, it is difficult to directly compare their data to the data acquired here, when using SthK-bPAC for a similar purpose. But judging by the data provided, it could be argued that the effect of SthK-bPAC is at least as strong, if not even stronger than the effect obtained with Kir2.1. Another notable difference between the study by Guo et al. and the SthK-bPAC data here is obviously the expression profile of the constructs. While Guo et al. used quite specific drivers for their constructs, SthK-bPAC was expressed in all clock neurons. It is unclear for example, why SthK-bPAC only affects locomotor activity during the subjective evening, even though the clk856-gal4 driver also drives expression in the PDF-positive cells, which have been described as M cells in the dual oscillator model [41, 46, 47], opposed to the E cells silenced by Guo et al. Also, no significantly reduced morning activity was recorded for flies expressing SthK-bPAC exclusively in the PDF-positive neurons using the pdf-gal4 driver. However, as the light-induced silencing fully coincides with the 12:12 LD entrainment in this experiment, the effect of the neuronal silencing may be masked to some degree by a startled response to the light being turned on in the morning. The fact that SthK-bPAC/pdf-gal4 flies turn out arrhythmic in DD strongly suggests that the continuous silencing of these clock neurons heavily impacts the circadian clock.

Unfortunately, despite these first promising results, neither SthK-bPAC nor Olf-bPAC could be applied successfully when trying to evoke any phase shifts. As the actogram data of almost all fly lines recorded, including the controls, proved to be unsuitable for further analysis, there is no definite conclusion to be drawn about the general effectiveness of the experimental approach (see Results 3.3.3). It seems unlikely however, that the chosen setup was successful with its goal, as the intensity and length of the light pulse was almost certainly too high. Some of the controls exhibited quite a substantial phase delay or phase advance respectively, making it extremely dubitable

that any phase shifts potentially displayed by the test lines would have ended up being significantly greater than the ones of the controls (see Fig. 3.3.8 & 3.3.9). The reasons for the poor rhythmicity and unusable actogram data could partially be directly caused by the CNGC-mediated effects after the light-pulse, but seems to also be rooted to no small part within the genetic background of the fly strains, as a sizeable portion of the controls also produced actogram data unusable for further analysis. The fact that RD entrainment constitutes a weaker Zeitgeber than LD entrainment may have also added to the problem [172], as red light information is only mediated to the circadian clock through the two Rhodopsins 1 and 6 in the compound eye and is also independent of CRY [173]. The fact that both SthK-bPAC strains turned out arrhythmic is less of a surprise, as SthK-bPAC already had a strong effect on the flies in the previous two experiments, disrupting their rhythmicity (see Results 3.3.2). After it became obvious that it was very unlikely that the two CNGC-constructs could be ever be used successfully in trying to influence the circadian clock reliably and predictably, experiments involving the constructs were abandoned and further research into their effects on the circadian clock was not conducted. It was concluded that the cAMP sensitivity of both constructs is likely too high, leading to undesired off-target effects, which ultimately resulted in efforts trying to develop less cAMP- and cGMP-sensitive tools.

4.4. The effect of CNGC-CyclOp on the circadian clock

The efforts to make the new CNGC-constructs less sensitive towards cAMP and cGMP turned out successful. Fly strains expressing either of the three new constructs, CNGA3-Cyclop, Olf-R536H-Cyclop and Olf-R536K-Cyclop in the motor neurons all survived until adulthood instead of dying during pupariation, as was the case for Olf-bPAC and SthK-bPAC. The immunostaining images further supported these initial findings, proving that the new constructs have a lot less damaging effects on the arborisation and morphology of the s-LN_vs when the flies were raised under RD conditions (see Results 3.4.1). The fact that the damaging effects returned when the flies were raised under constant illumination with white light also showcased the light-dosage-dependency of the new constructs and their capabilities of actually transporting a light-triggered effect, mediated via depolarization and Ca^{+2} influx that

could be clearly distinguished from any undesired background or off-target effects, something which was not possible for SthK-bPAC and Olf-bPAC. As expected, the light-dependent effect of the constructs is able to be enhanced by the feeding of ATR, the chromophore of the co-expressed CyclOp [109, 111]. Adding ATR greatly and significantly increases the light-triggered cGMP-production, when CyclOp is heterologously expressed in *Xenopus* oocytes [111]. Likewise the addition of ATR to the standard agar/cornmeal medium of *Drosophila* increases the light-triggered reduction of the activity rate of flies expressing Olf-R536K-CyclOp and Olf-R536H-CyclOp in their motor neurons (see Results 3.4.2), adding more utility and range to the application possibilities of the new CNGC-constructs. Higher levels of cGMP production were proven to also lead to a higher activation rate of the co-expressed CNGC. It could also be shown that the expression of the new CNGC-constructs in circadian clock neurons of *Drosophila* has no detrimental effect on rhythmic locomotor behaviour, both under RD entrainment as well as under LD entrainment (see Results 3.4.3). This shows that the endogenous cAMP and cGMP levels were apparently not high enough to noticeably activate the transmembral CNGCs, unlike SthK-bPAC and Olf-bPAC. The results obtained when raising flies expressing Olf-R536H-CyclOp in the PDF-positive neurons under constant white light, strongly suggest that all three constructs are constantly active under a 12:12 LD entrainment. However, the circadian clock appears to either be able to compensate for the CNGC-mediated input into the system, or the CNGC-mediated signal might also function as an additional Zeitgeber, as the depolarization and $Ca^{+}2$ influx would be in phase with the 12:12 LD entrainment regime. The combination of all these results suggested that a suitable optogenetic tool for reliably and repeatedly influencing the circadian clock of *Drosophila melanogaster* had finally been found.

Unfortunately none of the shift experiments that followed yielded any positive results. The shifts evoked in the GAL4-controls are always as high as those evoked in the test strains for any experiment that had been run (see Results 3.4.4). The only outlier from this trend is the advance experiment with flies expressing the CNGC-constructs under control of the pdf-gal4-driver, in which the test strains exhibited a slightly increased phase advance compared to both controls, which was statistically insignificant however (see Fig. 3.4.14). It can be concluded from these experiments that any putative light-triggered and CNGC-mediated effect on the circadian clock of *Drosophila* was completely masked by the phase response that was mediated by CRY and/or other

light input pathways. Very notable are the significantly lower phase delays of the UAS-controls in all experiments involving the clk856-gal4 driver (see Fig. 3.4.10 – 3.4.13) Regardless of wavelength or light intensity, the GAL4-control always exhibit large phase delays, along with the test lines, while the UAS-controls show significantly smaller delays. It is possible that this is due the genetic background introduced by the clk856-gal4 strain. Different laboratory Canton-S and w^{1118} strains have been shown to exhibit significantly different circadian periods and sleep phenotypes, alongside other social parameters like mating status [174]. It seems plausible that due to spontaneous mutations, the w^{1118} background of the clk856-gal4 line introduced an increased light-sensitivity into the circadian clock of the assayed flies, altering their light-dependant phase responses as well as the whole PRC. A decreased sensitivity introduced by the UAS-lines seems less likely, as it would be expected for them to then also exhibit significantly decreased phase advances, which was not the case. Another possibility is that the network-wide expression of the GAL4 transcription factor itself alters the light-mediated phase response of the circadian clock. Expression of the GAL4 transcription factor has been shown to cause a wide array of off-target effects in *Drosophila*. Expressing GAL4 in the developing compound eye of Drosophila, using the GMR-gal4 driver [175], resulted in partial apoptosis and developmental defects [176]. Effects of GAL4 on stress and immune response pathways have also been reported [177]. Most interestingly however, accumulation of GAL4 in the PDF-positive LN_vs under the pdf-gal4 driver has been shown to be disorganising rhythmic locomotor behaviour in *Drosophila* [178]. This effect was also shown to be dosage-dependant as it was found that an increased *gal4* gene dose positively correlated with a decrease in behavioural rhythmicity, concluded from the fact that rhythmicity was more heavily impacted when GAL4 was expressed in a homozygous state, than when it was expressed in a heterozygous state [178]. These effects were ultimately found to be apoptosis-related as well [178]. Taken together, these results indicate that GAL4 could also be partially responsible for the increased phase response observed in these phase shift experiments, via apoptosis-related effects on certain clock neurons, which ultimately might alter the phase response of the entire system. The involvement of GAL4 is quite speculative however, especially as no phase response increasing effect was noted in experiments using the pdf-gal4 line (see Fig. 3.4.14 & 3.4.15). The one shift experiment using the pdf-gal4 line was also the only one which suggested that there might be some CNGC-mediated effect on the phase response of the flies, as flies

expressing the construct exhibited slightly increased phase advances. Also, the shift experiment in which additional ATR was mixed in with the food also suggests that light-triggered CNGC-mediated effects can impact the circadian clock, as flies from that experiment which expressed the construct turned arrhythmic in DD following the light-pulse. The causes for the light-triggered, CNGC-mediated arrhythmicity remain unclear however. Since Olf and dTRPA1 have similar conductive qualities, a channel-mediated depolarization and Ca^{+2} influx would be expected to have the same results, which is obviously not the case, as dTRPA was shown to be able to phase shift the circadian clock via timed temperature pulse [117], while Olf was not.

Ultimately it can be concluded that the CNGC-CyclOp constructs have been demonstrated as unable to cause a light-triggered phase shift. While it still seems obvious that timed CNGC activation does impact the circadian clock in some way, any putative phase shifting effects have ultimately been masked by the phase shifting effects of the light itself. A light-pulse setup which sufficiently activates the CNGC-constructs, while at the same time barely triggering any phase responses mediated by CRY or other light input pathways could not be found in this thesis.

4.5. Conclusion

This present PhD-thesis intended to develop an optogenetic tool that could be used to influence the circadian clock of *Drosophila melanogaster*, aiming for a high reliability and a high temporal resolution. The developed tool was believed to open up many possibilities of researching the ways circadian neurons communicate with each other. The tool was intended to be used in, for example, live imaging experiments of cultured *Drosophila* brains, monitoring the state of the molecular clock in specific neurons.

None of the used or developed tools were however able to deliver satisfactory results, due to a number of reasons, some of them speculative.

Channelrhodopsin XXL [86] was unable to elicit significant phase shifts in flies upon light activation, when expressed in clock neurons. This was thought to be due to the low Ca^{+2}-conduction of the ChR2-variant, which is the case for most channelrhodopsins [70, 84]. This issue was tried to be addressed by using newly designed optogenetic constructs, Olf-bPAC and SthK-bPAC, fusion proteins, fusing together the two CNGCs Olf [98] and SthK [96] with the light activated guanylyl-cyclase

bPAC [102]. Those constructs proved unsuitable as well, as they caused severe damages to the neurons expressing them, resulting in impaired axon growth, missing arborisations and substantial loss-of-function for the respective neurons, in the case of the motor neurons having even fatal consequences, very likely caused by endogenous cAMP, activating the CNGCs even in the absence of light. Using temperature-controlled ways of expression for these constructs mitigated the morphological damages to the neurons, but also did not deliver the desired results, as light-pulses delivered to the tested flies caused them to become arrhythmic, rather than phase shift the circadian clock in a controlled way. The final approach, using CNGC-variants which showed reduced cAMP- and cGMP-sensitivity [100] in combination with the light-activated guanylyl-cyclase CyclOp [109], also proved to be unsuccessful, as again no significant phase shifts could be triggered upon illumination. While the newly developed CNGC-bPAC and CNGC-CyclOp constructs work as expected, it appears rather questionable whether they can ever be used reliably or predictably for influencing the circadian clock of *Drosophila melanogaster.* The tools were shown to work in motor neurons of *Drosophila* larvae [95], controlling locomotion, as well as in the motor neurons of adult Drosophila, again influencing locomotion and rate of activity. The tools by themselves are useful additions to the optogenetic toolbox and are likely to see use in research involving cells and tissues with lower cAMP concentrations. In regards to the effects on the circadian clock of *Drosophila* it can be concluded that the CNGC-constructs do impact the clock in some way, as shown by the experiments involving temperature-controlled expression of SthK-bPAC, the results of which bore resemblance to the experiments conducted by Guo et al. using Kir2.1 [116, 147]. As all witnessed effects however are of a disruptive and destabilizing nature, negatively impacting the flies' rhythmicity, these tools appear to be unsuited for precise and reliable manipulation of the circadian clock. The exact reason for these destabilizing effects are not fully clear, especially in the case of the Olf-variants, since they belong to the same super-family of TRP-channels with similar conductive qualities like dTRPA1 [98, 100, 118, 149]. Another issue that complicated the aim of this thesis, were the comparatively short wavelengths that were needed to be used for the light-pulses, in order to activate the optogenetic tools. These light-pulses always had a profound phase shifting effect on the circadian clock by itself, causing large phase shifts in the controls as well as the test-flies, masking any putative CNGC-mediated phase shifting effects. Judging by these results, it seems doubtful that an optogenetic

tool requiring wavelengths below ~550 nm for efficient activation can ever be used in this context. The two studies that successfully used optogenetics to influence the circadian clock of *Drosophila* so far, used red light above 600 nm wavelength in combination with long illumination periods [116, 147]. Future research trying to combine optogenetics with circadian research should consider experimental approaches similar to those employed by Guo et al., combining strongly red-shifted optogenetic tools with long illumination times.

5. References

[1] Johnson, C. H. and Golden, S. S. 1999. Circadian programs in cyanobacteria: adaptiveness and mechanism. Annu Rev Microbiol 53, 389–409.

[2] Johnson, C. H., Golden, S. S., Ishiura, M., and Kondo, T. 1996. Circadian clocks in prokaryotes. Mol Microbiol 21, 1, 5–11.

[3] Mergenhagen, D. 1984. Circadian clock: genetic characterization of a short period mutant of Chlamydomonas reinhardii. Eur J Cell Biol 33, 1, 13–18.

[4] Carl Hirschie Johnson and J. Woodland Hastings. 1986. The Elusive Mechanism of the Circadian Clock: The quest for the chemical basis of the biological clock is beginning to yield tantalizing clues. American Scientist 74, 1, 29–37.

[5] Emery, P., So, W. V., Kaneko, M., Hall, J. C., and Rosbash, M. 1998. CRY, a Drosophila clock and light-regulated cryptochrome, is a major contributor to circadian rhythm resetting and photosensitivity. Cell 95, 5, 669–679.

[6] Pittendrigh, C., Bruce, V., and Kaus, P. 1958. ON THE SIGNIFICANCE OF TRANSIENTS IN DAILY RHYTHMS. Proc Natl Acad Sci U S A 44, 9, 965–973.

[7] Glaser, F. T. and Stanewsky, R. 2005. Temperature synchronization of the Drosophila circadian clock. Current biology : CB 15, 15, 1352–1363.

[8] Levine, J. D., Funes, P., Dowse, H. B., and Hall, J. C. 2002. Resetting the circadian clock by social experience in Drosophila melanogaster. Science 298, 5600, 2010–2012.

[9] Pittendrigh, C. S. 1960. Circadian rhythms and the circadian organization of living systems. Cold Spring Harbor symposia on quantitative biology 25, 159–184.

[10] Bruce, V. G. and Pittendrigh, C. S. 1956. TEMPERATURE INDEPENDENCE IN A UNICELLULAR "CLOCK". Proceedings of the National Academy of Sciences of the United States of America 42, 9, 676–682.

[11] ASCHOFF, J. 1960. Exogenous and endogenous components in circadian rhythms. Cold Spring Harbor symposia on quantitative biology 25, 11–28.

[12] Konopka, R. J. and Benzer, S. 1971. Clock mutants of Drosophila melanogaster. Proceedings of the National Academy of Sciences of the United States of America 68, 9, 2112–2116.

[13] Darlington, T. K., Wager-Smith, K., Ceriani, M. F., Staknis, D., Gekakis, N., Steeves, T. D., Weitz, C. J., Takahashi, J. S., and Kay, S. A. 1998. Closing the circadian loop: CLOCK-induced transcription of its own inhibitors per and tim. Science (New York, N.Y.) 280, 5369, 1599–1603.

[14] Rutila, J. E., Suri, V., Le, M., So, W. V., Rosbash, M., and Hall, J. C. 1998. CYCLE is a second bHLH-PAS clock protein essential for circadian rhythmicity and transcription of Drosophila period and timeless. Cell 93, 5, 805–814.

[15] Lin, F. J., Song, W., Meyer-Bernstein, E., Naidoo, N., and Sehgal, A. 2001. Photic signaling by cryptochrome in the Drosophila circadian system. Molecular and cellular biology 21, 21, 7287–7294.

[16] Price, J. L., Blau, J., Rothenfluh, A., Abodeely, M., Kloss, B., and Young, M. W. 1998. double-time is a novel Drosophila clock gene that regulates PERIOD protein accumulation. Cell 94, 1, 83–95.

[17] Martinek, S., Inonog, S., Manoukian, A. S., and Young, M. W. 2001. A role for the segment polarity gene shaggy/GSK-3 in the Drosophila circadian clock. Cell 105, 6, 769–779.

[18] Lee, C., Bae, K., and Edery, I. 1999. PER and TIM inhibit the DNA binding activity of a Drosophila CLOCK-CYC/dBMAL1 heterodimer without disrupting formation of the heterodimer: a basis for circadian transcription. Molecular and cellular biology 19, 8, 5316–5325.

[19] Yu, W., Zheng, H., Houl, J. H., Dauwalder, B., and Hardin, P. E. 2006. PER-dependent rhythms in CLK phosphorylation and E-box binding regulate circadian transcription. Genes & development 20, 6, 723–733.

[20] Cyran, S. A., Buchsbaum, A. M., Reddy, K. L., Lin, M.-C., Glossop, Nicholas R J, Hardin, P. E., Young, M. W., Storti, R. V., and Blau, J. 2003. vrille, Pdp1, and dClock form a second feedback loop in the Drosophila circadian clock. Cell 112, 3, 329–341.

[21] Glossop, Nicholas R J, Houl, J. H., Zheng, H., Ng, F. S., Dudek, S. M., and Hardin, P. E. 2003. VRILLE feeds back to control circadian transcription of Clock in the Drosophila circadian oscillator. Neuron 37, 2, 249–261.

[22] Collins, B. and Blau, J. 2007. Even a stopped clock tells the right time twice a day: circadian timekeeping in Drosophila. Pflugers Archiv : European journal of physiology 454, 5, 857–867.

[23] Zhang, L., Chung, B. Y., Lear, B. C., Kilman, V. L., Liu, Y., Mahesh, G., Meissner, R.-A., Hardin, P. E., and Allada, R. 2010. DN1(p) circadian neurons coordinate acute light and PDF inputs to produce robust daily behavior in Drosophila. Current biology : CB 20, 7, 591–599.

[24] Picot, M., Klarsfeld, A., Chelot, E., Malpel, S., and Rouyer, F. 2009. A role for blind DN2 clock neurons in temperature entrainment of the Drosophila larval brain. The Journal of neuroscience : the official journal of the Society for Neuroscience 29, 26, 8312–8320.

[25] Renn, S. C., Park, J. H., Rosbash, M., Hall, J. C., and Taghert, P. H. 1999. A pdf neuropeptide gene mutation and ablation of PDF neurons each cause severe abnormalities of behavioral circadian rhythms in Drosophila. Cell 99, 7, 791–802.

[26] Helfrich-Förster, C. 1998. Robust circadian rhythmicity of Drosophila melanogaster requires the presence of lateral neurons: a brain-behavioral study of disconnected mutants. Journal of comparative physiology. A, Sensory, neural, and behavioral physiology 182, 4, 435–453.

[27] Helfrich-Förster, C., Shafer, O. T., Wulbeck, C., Grieshaber, E., Rieger, D., and Taghert, P. 2007. Development and morphology of the clock-gene-expressing lateral neurons of Drosophila melanogaster. The Journal of comparative neurology 500, 1, 47–70.

[28] Homberg, U., Reischig, T., and Stengl, M. 2003. Neural organization of the circadian system of the cockroach Leucophaea maderae. Chronobiology international 20, 4, 577–591.

[29] Benito, J., Houl, J. H., Roman, G. W., and Hardin, P. E. 2008. The blue-light photoreceptor CRYPTOCHROME is expressed in a subset of circadian oscillator neurons in the Drosophila CNS. Journal of biological rhythms 23, 4, 296–307.

[30] Shang, Y., Griffith, L. C., and Rosbash, M. 2008. Light-arousal and circadian photoreception circuits intersect at the large PDF cells of the Drosophila brain. Proceedings of the National Academy of Sciences of the United States of America 105, 50, 19587–19594.

[31] Fogle, K. J., Parson, K. G., Dahm, N. A., and Holmes, T. C. 2011. CRYPTOCHROME is a blue-light sensor that regulates neuronal firing rate. Science (New York, N.Y.) 331, 6023, 1409–1413.

[32] Veleri, S., Rieger, D., Helfrich-Forster, C., and Stanewsky, R. 2007. Hofbauer-Buchner eyelet affects circadian photosensitivity and coordinates TIM and PER expression in Drosophila clock neurons. Journal of biological rhythms 22, 1, 29–42.

[33] Im, S. H. and Taghert, P. H. 2010. PDF receptor expression reveals direct interactions between circadian oscillators in Drosophila. The Journal of comparative neurology 518, 11, 1925–1945.

[34] Klarsfeld, A., Malpel, S., Michard-Vanhee, C., Picot, M., Chelot, E., and Rouyer, F. 2004. Novel features of cryptochrome-mediated photoreception in the brain circadian clock of Drosophila. The Journal of neuroscience : the official journal of the Society for Neuroscience 24, 6, 1468–1477.

[35] Lin, Y., Stormo, G. D., and Taghert, P. H. 2004. The neuropeptide pigment-dispersing factor coordinates pacemaker interactions in the Drosophila circadian system. The Journal of neuroscience : the official journal of the Society for Neuroscience 24, 36, 7951–7957.

[36] Peng, Y., Stoleru, D., Levine, J. D., Hall, J. C., and Rosbash, M. 2003. Drosophila free-running rhythms require intercellular communication. PLoS biology 1, 1, E13.

[37] Helfrich-Forster, C., Yoshii, T., Wulbeck, C., Grieshaber, E., Rieger, D., Bachleitner, W., Cusumano, P., and Rouyer, F. 2007. The lateral and dorsal neurons of Drosophila melanogaster: new insights about their morphology and function. Cold Spring Harbor symposia on quantitative biology 72, 517–525.

[38] Taghert, P. H. and Shafer, O. T. 2006. Mechanisms of clock output in the Drosophila circadian pacemaker system. Journal of biological rhythms 21, 6, 445–457.

[39] Nitabach, M. N., Blau, J., and Holmes, T. C. 2002. Electrical silencing of Drosophila pacemaker neurons stops the free-running circadian clock. Cell 109, 4, 485–495.

[40] Blanchardon, E., Grima, B., Klarsfeld, A., Chelot, E., Hardin, P. E., Preat, T., and Rouyer, F. 2001. Defining the role of Drosophila lateral neurons in the control of circadian rhythms in motor activity and eclosion by targeted genetic ablation and PERIOD protein overexpression. The European journal of neuroscience 13, 5, 871–888.

[41] Rieger, D., Shafer, O. T., Tomioka, K., and Helfrich-Forster, C. 2006. Functional analysis of circadian pacemaker neurons in Drosophila melanogaster. The Journal of neuroscience : the official journal of the Society for Neuroscience 26, 9, 2531–2543.

[42] Kaneko, M. and Hall, J. C. 2000. Neuroanatomy of cells expressing clock genes in Drosophila: transgenic manipulation of the period and timeless genes to mark the perikarya of circadian pacemaker neurons and their projections. The Journal of comparative neurology 422, 1, 66–94.

[43] Yoshii, T., Hermann, C., and Helfrich-Forster, C. 2010. Cryptochrome-positive and -negative clock neurons in Drosophila entrain differentially to light and temperature. Journal of biological rhythms 25, 6, 387–398.

[44] Johard, Helena A D, Yoishii, T., Dircksen, H., Cusumano, P., Rouyer, F., Helfrich-Forster, C., and Nassel, D. R. 2009. Peptidergic clock neurons in Drosophila: ion transport peptide and short neuropeptide F in subsets of dorsal and ventral lateral neurons. The Journal of comparative neurology 516, 1, 59–73.

[45] Pittendrigh, C. S. and Daan, S. 1976. A functional analysis of circadian pacemakers in nocturnal rodents. Journal of comparative physiology 106, 3, 333–355.

[46] Stoleru, D., Peng, Y., Agosto, J., and Rosbash, M. 2004. Coupled oscillators control morning and evening locomotor behaviour of Drosophila. Nature 431, 7010, 862–868.

[47] Grima, B., Chelot, E., Xia, R., and Rouyer, F. 2004. Morning and evening peaks of activity rely on different clock neurons of the Drosophila brain. Nature 431, 7010, 869–873.

[48] Rieger, D., Wulbeck, C., Rouyer, F., and Helfrich-Forster, C. 2009. Period gene expression in four neurons is sufficient for rhythmic activity of Drosophila melanogaster under dim light conditions. Journal of biological rhythms 24, 4, 271–282.

[49] Yoshii, T., Rieger, D., and Helfrich-Forster, C. 2012. Two clocks in the brain: an update of the morning and evening oscillator model in Drosophila. Progress in brain research 199, 59–82.

[50] Bywalez, W., Menegazzi, P., Rieger, D., Schmid, B., Helfrich-Forster, C., and Yoshii, T. 2012. The dual-oscillator system of Drosophila melanogaster under natural-like temperature cycles. Chronobiology international 29, 4, 395–407.

[51] Yu, X., Liu, H., Klejnot, J., and Lin, C. 2010. The Cryptochrome Blue Light Receptors. The arabidopsis book 8, e0135.

[52] Yoshii, T., Todo, T., Wulbeck, C., Stanewsky, R., and Helfrich-Forster, C. 2008. Cryptochrome is present in the compound eyes and a subset of Drosophila's clock neurons. The Journal of comparative neurology 508, 6, 952–966.

[53] Schlichting, M., Rieger, D., Cusumano, P., Grebler, R., Costa, R., Mazzotta, G. M., and Helfrich-Forster, C. 2018. Cryptochrome Interacts With Actin and Enhances Eye-Mediated Light Sensitivity of the Circadian Clock in Drosophila melanogaster. Frontiers in molecular neuroscience 11, 238.

[54] Koh, K., Zheng, X., and Sehgal, A. 2006. JETLAG resets the Drosophila circadian clock by promoting light-induced degradation of TIMELESS. Science (New York, N.Y.) 312, 5781, 1809–1812.

[55] Peschel, N., Chen, K. F., Szabo, G., and Stanewsky, R. 2009. Light-dependent interactions between the Drosophila circadian clock factors cryptochrome, jetlag, and timeless. Current biology : CB 19, 3, 241–247.

[56] Kistenpfennig, C., Hirsh, J., Yoshii, T., and Helfrich-Forster, C. 2012. Phase-shifting the fruit fly clock without cryptochrome. Journal of biological rhythms 27, 2, 117–125.

[57] Lamba, P., Bilodeau-Wentworth, D., Emery, P., and Zhang, Y. 2014. Morning and evening oscillators cooperate to reset circadian behavior in response to light input. Cell reports 7, 3, 601–608.

[58] Busza, A., Emery-Le, M., Rosbash, M., and Emery, P. 2004. Roles of the two Drosophila CRYPTOCHROME structural domains in circadian photoreception. Science (New York, N.Y.) 304, 5676, 1503–1506.

[59] Konopka, R. J., Pittendrigh, C., and Orr, D. 1989. Reciprocal behaviour associated with altered homeostasis and photosensitivity of Drosophila clock mutants. Journal of neurogenetics 6, 1, 1–10.

[60] Johnson, C. H. 1999. Forty years of PRCs--what have we learned? Chronobiology international 16, 6, 711–743.

[61] Golombek, D. A. and Rosenstein, R. E. 2010. Physiology of circadian entrainment. Physiological reviews 90, 3, 1063–1102.

[62] Glass, L. and Winfree, A. T. 1984. Discontinuities in phase-resetting experiments. The American journal of physiology 246, 2 Pt 2, R251-8.

[63] Varma, V., Mukherjee, N., Kannan, N. N., and Sharma, V. K. 2013. Strong (type 0) phase resetting of activity-rest rhythm in fruit flies, Drosophila melanogaster, at low temperature. Journal of biological rhythms 28, 6, 380–389.

[64] Oesterhelt, D. and Stoeckenius, W. 1971. Rhodopsin-like protein from the purple membrane of Halobacterium halobium. Nature: New biology 233, 39, 149–152.

[65] Matsuno-Yagi, A. and Mukohata, Y. 1977. Two possible roles of bacteriorhodopsin; a comparative study of strains of Halobacterium halobium differing in pigmentation. Biochemical and biophysical research communications 78, 1, 237–243.

[66] HILDEBRAND, E. and DENCHER, N. 1975. Two photosystems controlling behavioural responses of Halobacterium halobium. Nature 257, 46 EP -.

[67] Takahashi, T., Tomioka, H., Kamo, N., and Kobatake, Y. 1985. A photosystem other than PS370 also mediates the negative phototaxis of Halobacterium halobium. FEMS Microbiology Letters 28, 2, 161–164.

[68] Marwan, W. and Oesterhelt, D. 1987. Signal formation in the halobacterial photophobic response mediated by a fourth retinal protein (P480). Journal of Molecular Biology 195, 2, 333–342.

[69] Nagel, G., Ollig, D., Fuhrmann, M., Kateriya, S., Musti, A. M., Bamberg, E., and Hegemann, P. 2002. Channelrhodopsin-1: a light-gated proton channel in green algae. Science (New York, N.Y.) 296, 5577, 2395–2398.

[70] Nagel, G., Szellas, T., Huhn, W., Kateriya, S., Adeishvili, N., Berthold, P., Ollig, D., Hegemann, P., and Bamberg, E. 2003. Channelrhodopsin-2, a directly light-gated cation-selective membrane channel. Proc Natl Acad Sci U S A 100, 24, 13940–13945.

[71] Boyden, E. S., Zhang, F., Bamberg, E., Nagel, G., and Deisseroth, K. 2005. Millisecond-timescale, genetically targeted optical control of neural activity. Nature Neuroscience 8, 1263 EP -.

[72] Nagel, G., Brauner, M., Liewald, J. F., Adeishvili, N., Bamberg, E., and Gottschalk, A. 2005. Light activation of channelrhodopsin-2 in excitable cells of Caenorhabditis elegans triggers rapid behavioral responses. Curr Biol 15, 24, 2279–2284.

[73] Bi, A., Cui, J., Ma, Y.-P., Olshevskaya, E., Pu, M., Dizhoor, A. M., and Pan, Z.-H. 2006. Ectopic Expression of a Microbial-Type Rhodopsin Restores Visual Responses in Mice with Photoreceptor Degeneration. Neuron 50, 1, 23–33.

[74] Nature Methods Editorial. 2010. Method of the Year 2010. Nat Meth 8, 1, 1.

[75] Chen, M. and Bi, L.-L. 2018. Optogenetic Long-Term Depression Induction in the PVT-CeL Circuitry Mediates Decreased Fear Memory. Molecular neurobiology.

[76] Keppeler, D., Merino, R. M., Lopez de la Morena, David, Bali, B., Huet, A. T., Gehrt, A., Wrobel, C., Subramanian, S., Dombrowski, T., Wolf, F., Rankovic, V., Neef, A., and Moser, T. 2018. Ultrafast optogenetic stimulation of the auditory pathway by targeting-optimized Chronos. The EMBO journal.

[77] Wu, G.-Y., Liu, S.-L., Yao, J., Li, X., Wu, B., Ye, J.-N., and Sui, J.-F. 2018. Optogenetic Inhibition of Medial Prefrontal Cortex-Pontine Nuclei Projections During the Stimulus-free Trace Interval Impairs Temporal Associative Motor Learning. Cerebral cortex (New York, N.Y. : 1991) 28, 11, 3753–3763.

[78] Lorenz-Fonfria, V. A., Resler, T., Krause, N., Nack, M., Gossing, M., Fischer von Mollard, Gabriele, Bamann, C., Bamberg, E., Schlesinger, R., and Heberle, J. 2013. Transient protonation changes in channelrhodopsin-2 and their relevance to channel gating. Proc Natl Acad Sci U S A 110, 14, E1273-81.

[79] Bamann, C., Kirsch, T., Nagel, G., and Bamberg, E. 2008. Spectral characteristics of the photocycle of channelrhodopsin-2 and its implication for channel function. J Mol Biol 375, 3, 686–694.

[80] Feldbauer, K., Zimmermann, D., Pintschovius, V., Spitz, J., Bamann, C., and Bamberg, E. 2009. Channelrhodopsin-2 is a leaky proton pump. Proc Natl Acad Sci U S A 106, 30, 12317–12322.

[81] Kato, H. E., Zhang, F., Yizhar, O., Ramakrishnan, C., Nishizawa, T., Hirata, K., Ito, J., Aita, Y., Tsukazaki, T., Hayashi, S., Hegemann, P., Maturana, A. D., Ishitani, R., Deisseroth, K., and Nureki, O. 2012. Crystal structure of the channelrhodopsin light-gated cation channel. Nature 482, 7385, 369–374.

[82] Klapoetke, N. C., Murata, Y., Kim, S. S., Pulver, S. R., Birdsey-Benson, A., Cho, Y. K., Morimoto, T. K., Chuong, A. S., Carpenter, E. J., Tian, Z., Wang, J., Xie, Y., Yan, Z., Zhang, Y., Chow, B. Y., Surek, B., Melkonian, M., Jayaraman, V., Constantine-Paton, M., Wong, G. K.-S., and Boyden, E. S. 2014. Independent optical excitation of distinct neural populations. Nature methods 11, 3, 338–346.

[83] Gunaydin, L. A., Yizhar, O., Berndt, A., Sohal, V. S., Deisseroth, K., and Hegemann, P. 2010. Ultrafast optogenetic control. Nat Neurosci 13, 3, 387–392.

[84] Kleinlogel, S., Feldbauer, K., Dempski, R. E., Fotis, H., Wood, P. G., Bamann, C., and Bamberg, E. 2011. Ultra light-sensitive and fast neuronal activation with the Ca(2)+-permeable channelrhodopsin CatCh. Nat Neurosci 14, 4, 513–518.

[85] Pan, Z.-H., Ganjawala, T. H., Lu, Q., Ivanova, E., and Zhang, Z. 2014. ChR2 mutants at L132 and T159 with improved operational light sensitivity for vision restoration. PLoS One 9, 6, e98924.

[86] Dawydow, A., Gueta, R., Ljaschenko, D., Ullrich, S., Hermann, M., Ehmann, N., Gao, S., Fiala, A., Langenhan, T., Nagel, G., and Kittel, R. J. 2014. Channelrhodopsin-2-XXL, a powerful optogenetic tool for low-light applications. Proc Natl Acad Sci U S A 111, 38, 13972–13977.

[87] Stockinger, P., Kvitsiani, D., Rotkopf, S., Tirian, L., and Dickson, B. J. 2005. Neural circuitry that governs Drosophila male courtship behavior. Cell 121, 5, 795–807.

[88] Hall, J. C. 1994. The mating of a fly. Science 264, 5166, 1702–1714.

[89] Kyung, T., Lee, S., Kim, J. E., Cho, T., Park, H., Jeong, Y.-M., Kim, D., Shin, A., Kim, S., Baek, J., Kim, J., Kim, N. Y., Woo, D., Chae, S., Kim, C.-H., Shin, H.-S., Han, Y.-M., Kim, D., and Heo, W. D. 2015. Optogenetic control of endogenous Ca(2+) channels in vivo. Nature biotechnology 33, 10, 1092–1096.

[90] He, L., Zhang, Y., Ma, G., Tan, P., Li, Z., Zang, S., Wu, X., Jing, J., Fang, S., Zhou, L., Wang, Y., Huang, Y., Hogan, P. G., Han, G., and Zhou, Y. 2015. Near-infrared photoactivatable control of Ca(2+) signaling and optogenetic immunomodulation. eLife 4.

[91] Govorunova, E. G., Sineshchekov, O. A., Janz, R., Liu, X., and Spudich, J. L. 2015. NEUROSCIENCE. Natural light-gated anion channels: A family of microbial rhodopsins for advanced optogenetics. Science 349, 6248, 647–650.

[92] Mahn, M., Prigge, M., Ron, S., Levy, R., and Yizhar, O. 2016. Biophysical constraints of optogenetic inhibition at presynaptic terminals. Nat Neurosci 19, 4, 554–556.

[93] Banghart, M., Borges, K., Isacoff, E., Trauner, D., and Kramer, R. H. 2004. Light-activated ion channels for remote control of neuronal firing. Nat Neurosci 7, 1381 EP -.

[94] Cosentino, C., Alberio, L., Gazzarrini, S., Aquila, M., Romano, E., Cermenati, S., Zuccolini, P., Petersen, J., Beltrame, M., van Etten, J. L., Christie, J. M., Thiel, G., and Moroni, A. 2015. Optogenetics. Engineering of a light-gated potassium channel. Science 348, 6235, 707–710.

[95] Beck, S., Yu-Strzelczyk, J., Pauls, D., Constantin, O. M., Gee, C. E., Ehmann, N., Kittel, R. J., Nagel, G., and Gao, S. 2018. Synthetic Light-Activated Ion Channels for Optogenetic Activation and Inhibition. Frontiers in neuroscience 12, 643.

[96] Brams, M., Kusch, J., Spurny, R., Benndorf, K., and Ulens, C. 2014. Family of prokaryote cyclic nucleotide-modulated ion channels. Proc Natl Acad Sci U S A 111, 21, 7855–7860.

[97] Kesters, D., Brams, M., Nys, M., Wijckmans, E., Spurny, R., Voets, T., Tytgat, J., Kusch, J., and Ulens, C. 2015. Structure of the SthK carboxy-terminal region reveals a gating mechanism for cyclic nucleotide-modulated ion channels. PloS one 10, 1, e0116369.

[98] Altenhofen, W., Ludwig, J., Eismann, E., Kraus, W., Bönigk, W., and Kaupp, U. B. 1991. Control of ligand specificity in cyclic nucleotide-gated channels from rod photoreceptors and olfactory epithelium. Proceedings of the National Academy of Sciences 88, 21, 9868.

[99] Frings, S., Seifert, R., Godde, M., and Kaupp, U. B. 1995. Profoundly different calcium permeation and blockage determine the specific function of distinct cyclic nucleotide-gated channels. Neuron 15, 1, 169–179.

[100] Tanaka, N., Dutrow, E. V., Miyadera, K., Delemotte, L., MacDermaid, C. M., Reinstein, S. L., Crumley, W. R., Dixon, C. J., Casal, M. L., Klein, M. L., Aguirre, G. D., Tanaka, J. C., and Guziewicz, K. E. 2015. Canine CNGA3 Gene Mutations Provide Novel Insights into Human Achromatopsia-Associated Channelopathies and Treatment. PloS one 10, 9, e0138943.

[101] Lolicato, M., Nardini, M., Gazzarrini, S., Moller, S., Bertinetti, D., Herberg, F. W., Bolognesi, M., Martin, H., Fasolini, M., Bertrand, J. A., Arrigoni, C., Thiel, G., and Moroni, A. 2011. Tetramerization dynamics of C-terminal domain underlies isoform-specific cAMP gating in hyperpolarization-activated cyclic nucleotide-gated channels. The Journal of biological chemistry 286, 52, 44811–44820.

[102] Iseki, M., Matsunaga, S., Murakami, A., Ohno, K., Shiga, K., Yoshida, K., Sugai, M., Takahashi, T., Hori, T., and Watanabe, M. 2002. A blue-light-activated adenylyl cyclase mediates photoavoidance in Euglena gracilis. Nature 415, 6875, 1047–1051.

[103] Schroder-Lang, S., Schwarzel, M., Seifert, R., Strunker, T., Kateriya, S., Looser, J., Watanabe, M., Kaupp, U. B., Hegemann, P., and Nagel, G. 2007. Fast manipulation of cellular cAMP level by light in vivo. Nat Methods 4, 1, 39–42.

[104] Ryu, M.-H., Moskvin, O. V., Siltberg-Liberles, J., and Gomelsky, M. 2010. Natural and engineered photoactivated nucleotidyl cyclases for optogenetic applications. The Journal of biological chemistry 285, 53, 41501–41508.

[105] Stierl, M., Stumpf, P., Udwari, D., Gueta, R., Hagedorn, R., Losi, A., Gartner, W., Petereit, L., Efetova, M., Schwarzel, M., Oertner, T. G., Nagel, G., and Hegemann, P. 2011. Light modulation of cellular cAMP by a small bacterial photoactivated adenylyl cyclase, bPAC, of the soil bacterium Beggiatoa. The Journal of biological chemistry 286, 2, 1181–1188.

[106] Gomelsky, M. and Klug, G. 2002. BLUF: a novel FAD-binding domain involved in sensory transduction in microorganisms. Trends in biochemical sciences 27, 10, 497–500.

[107] Linder, J. U. and Schultz, J. E. 2003. The class III adenylyl cyclases: multi-purpose signalling modules. Cellular signalling 15, 12, 1081–1089.

[108] Kim, T., Folcher, M., Doaud-El Baba, M., and Fussenegger, M. 2015. A synthetic erectile optogenetic stimulator enabling blue-light-inducible penile erection. Angewandte Chemie (International ed. in English) 54, 20, 5933–5938.

[109] Avelar, G. M., Schumacher, R. I., Zaini, P. A., Leonard, G., Richards, T. A., and Gomes, S. L. 2014. A rhodopsin-guanylyl cyclase gene fusion functions in visual perception in a fungus. Curr Biol 24, 11, 1234–1240.

[110] Scheib, U., Stehfest, K., Gee, C. E., Korschen, H. G., Fudim, R., Oertner, T. G., and Hegemann, P. 2015. The rhodopsin-guanylyl cyclase of the aquatic fungus Blastocladiella emersonii enables fast optical control of cGMP signaling. Science signaling 8, 389, rs8.

[111] Gao, S., Nagpal, J., Schneider, M. W., Kozjak-Pavlovic, V., Nagel, G., and Gottschalk, A. 2015. Optogenetic manipulation of cGMP in cells and animals by the tightly light-regulated guanylyl-cyclase opsin CyclOp. Nature communications 6, 8046.

[112] Mizrak, D., Ruben, M., Myers, G. N., Rhrissorrakrai, K., Gunsalus, K. C., and Blau, J. 2012. Electrical activity can impose time of day on the circadian transcriptome of pacemaker neurons. Curr Biol 22, 20, 1871–1880.

[113] Nitabach, M. N., Wu, Y., Sheeba, V., Lemon, W. C., Strumbos, J., Zelensky, P. K., White, B. H., and Holmes, T. C. 2006. Electrical hyperexcitation of lateral ventral pacemaker neurons desynchronizes downstream circadian oscillators in the fly circadian circuit and induces multiple behavioral periods. The Journal of neuroscience : the official journal of the Society for Neuroscience 26, 2, 479–489.

[114] Wu, Y., Cao, G., and Nitabach, M. N. 2008. Electrical silencing of PDF neurons advances the phase of non-PDF clock neurons in Drosophila. Journal of biological rhythms 23, 2, 117–128.

[115] Depetris-Chauvin, A., Berni, J., Aranovich, E. J., Muraro, N. I., Beckwith, E. J., and Ceriani, M. F. 2011. Adult-specific electrical silencing of pacemaker neurons uncouples molecular clock from circadian outputs. Curr Biol 21, 21, 1783–1793.

[116] Guo, F., Yu, J., Jung, H. J., Abruzzi, K. C., Luo, W., Griffith, L. C., and Rosbash, M. 2016. Circadian neuron feedback controls the Drosophila sleep--activity profile. Nature 536, 7616, 292–297.

[117] Eck, S., Helfrich-Förster, C., and Rieger, D. 2016. The Timed Depolarization of Morning and Evening Oscillators Phase Shifts the Circadian Clock of Drosophila. Journal of biological rhythms 31, 5, 428–442.

[118] Hamada, F. N., Rosenzweig, M., Kang, K., Pulver, S. R., Ghezzi, A., Jegla, T. J., and Garrity, P. A. 2008. An internal thermal sensor controlling temperature preference in Drosophila. Nature 454, 7201, 217–220.

[119] Sabado, V., Vienne, L., Nunes, J. M., Rosbash, M., and Nagoshi, E. 2017. Fluorescence circadian imaging reveals a PDF-dependent transcriptional regulation of the Drosophila molecular clock. Scientific reports 7, 41560.

[120] Sabado, V. and Nagoshi, E. 2018. Single-cell Resolution Fluorescence Live Imaging of Drosophila Circadian Clocks in Larval Brain Culture. Journal of visualized experiments : JoVE, 131.

[121] Dennis Segebarth. 2014. Manipulation der Inneren Uhr von Drosophila melanogaster durch Aktivierung von ChR-XXL in Untergruppen des circadianen Netzwerks. Bachelor's Thesis, Julius-Maximilans-Universität Würzburg.

[122] McGuire, S. E., Roman, G., and Davis, R. L. 2004. Gene expression systems in Drosophila: a synthesis of time and space. Trends in genetics : TIG 20, 8, 384–391.

[123] Brand, A. H. and Perrimon, N. 1993. Targeted gene expression as a means of altering cell fates and generating dominant phenotypes. Development (Cambridge, England) 118, 2, 401–415.

[124] Keller, A., Sweeney, S. T., Zars, T., O'Kane, C. J., and Heisenberg, M. 2002. Targeted expression of tetanus neurotoxin interferes with behavioral responses to sensory input in Drosophila. Journal of neurobiology 50, 3, 221–233.

[125] Lee, T. and Luo, L. 1999. Mosaic analysis with a repressible cell marker for studies of gene function in neuronal morphogenesis. Neuron 22, 3, 451–461.

[126] Zeidler, M. P., Tan, C., Bellaiche, Y., Cherry, S., Hader, S., Gayko, U., and Perrimon, N. 2004. Temperature-sensitive control of protein activity by conditionally splicing inteins. Nature biotechnology 22, 7, 871–876.

[127] Gummadova, J. O., Coutts, G. A., and Glossop, N. R. J. 2009. Analysis of the Drosophila Clock promoter reveals heterogeneity in expression between subgroups of central oscillator cells and identifies a novel enhancer region. Journal of biological rhythms 24, 5, 353–367.

[128] Dolezelova, E., Dolezel, D., and Hall, J. C. 2007. Rhythm defects caused by newly engineered null mutations in Drosophila's cryptochrome gene. Genetics 177, 1, 329–345.

[129] Sanyal, S. 2009. Genomic mapping and expression patterns of C380, OK6 and D42 enhancer trap lines in the larval nervous system of Drosophila. Gene expression patterns : GEP 9, 5, 371–380.

[130] Venken, K. J. T., He, Y., Hoskins, R. A., and Bellen, H. J. 2006. P[acman]: A BAC Transgenic Platform for Targeted Insertion of Large DNA Fragments in <em>D. melanogaster</em&gt. Science 314, 5806, 1747.

[131] Ryan, M. D., Donnelly, M., Lewis, A., Mehrotra, A. P., Wilkie, J., and Gani, D. 1999. A Model for Nonstoichiometric, Cotranslational Protein Scission in Eukaryotic Ribosomes. Bioorganic Chemistry 27, 1, 55–79.

[132] Luke, G. A., Felipe, P. de, Lukashev, A., Kallioinen, S. E., Bruno, E. A., and Ryan, M. D. 2008. Occurrence, function and evolutionary origins of '2A-like' sequences in virus genomes. The Journal of general virology 89, Pt 4, 1036–1042.

[133] Furthmayr, H. 1977. Structural analysis of a membrane glycoprotein: Glycophorin A. J. Supramol. Struct. 7, 1, 121–134.

[134] Grant, C. W. and McConnell, H. M. 1974. Glycophorin in lipid bilayers. Proc Natl Acad Sci U S A 71, 12, 4653–4657.

[135] Liaw, C. W., Zamoyska, R., and Parnes, J. R. 1986. Structure, sequence, and polymorphism of the Lyt-2 T cell differentiation antigen gene. Journal of immunology (Baltimore, Md. : 1950) 137, 3, 1037–1043.

[136] Florijn, R. J., Slats, J., Tanke, H. J., and Raap, A. K. 1995. Analysis of antifading reagents for fluorescence microscopy. Cytometry 19, 2, 177–182.

[137] Cyran, S. A., Yiannoulos, G., Buchsbaum, A. M., Saez, L., Young, M. W., and Blau, J. 2005. The double-time protein kinase regulates the subcellular localization of the Drosophila clock protein period. The Journal of neuroscience : the official journal of the Society for Neuroscience 25, 22, 5430–5437.

[138] Pfeiffenberger, C., Lear, B. C., Keegan, K. P., and Allada, R. 2010. Locomotor activity level monitoring using the Drosophila Activity Monitoring (DAM) System. Cold Spring Harbor protocols 2010, 11, pdb.prot5518.

[139] Mrosovsky, N. 1996. Methods of measuring phase shifts: why I continue to use an Aschoff type II procedure despite the skepticism of referees. Chronobiology international 13, 5, 387–392.

[140] Schmid, B., Helfrich-Forster, C., and Yoshii, T. 2011. A new ImageJ plug-in "ActogramJ" for chronobiological analyses. Journal of biological rhythms 26, 5, 464–467.

[141] Risse, B., Thomas, S., Otto, N., Lopmeier, T., Valkov, D., Jiang, X., and Klambt, C. 2013. FIM, a novel FTIR-based imaging method for high throughput locomotion analysis. PloS one 8, 1, e53963.

[142] Risse, B., Otto, N., Berh, D., Jiang, X., and Klambt, C. 2014. FIM imaging and FIMtrack: two new tools allowing high-throughput and cost effective locomotion analysis. Journal of visualized experiments : JoVE, 94.

[143] Risse, B., Berh, D., Otto, N., Klambt, C., and Jiang, X. 2017. FIMTrack: An open source tracking and locomotion analysis software for small animals. PLoS computational biology 13, 5, e1005530.

[144] Dolezelova, E., Dolezel, D., and Hall, J. C. 2007. Rhythm defects caused by newly engineered null mutations in Drosophila's cryptochrome gene. Genetics 177, 1, 329–345.

[145] Kistenpfennig, C., Grebler, R., Ogueta, M., Hermann-Luibl, C., Schlichting, M., Stanewsky, R., Senthilan, P. R., and Helfrich-Forster, C. 2017. A New Rhodopsin Influences Light-dependent Daily Activity Patterns of Fruit Flies. Journal of biological rhythms 32, 5, 406–422.

[146] Jenett, A., Rubin, G. M., Ngo, T.-T. B., Shepherd, D., Murphy, C., Dionne, H., Pfeiffer, B. D., Cavallaro, A., Hall, D., Jeter, J., Iyer, N., Fetter, D., Hausenfluck, J. H., Peng, H., Trautman, E. T., Svirskas, R. R., Myers, E. W., Iwinski, Z. R., Aso, Y., DePasquale, G. M., Enos, A., Hulamm, P., Lam, S. C. B., Li, H.-H., Laverty, T. R., Long, F., Qu, L., Murphy, S. D., Rokicki, K., Safford, T., Shaw, K., Simpson, J. H., Sowell, A., Tae, S., Yu, Y., and Zugates, C. T. 2012. A GAL4-driver line resource for Drosophila neurobiology. Cell reports 2, 4, 991–1001.

[147] Guo, F., Chen, X., and Rosbash, M. 2017. Temporal calcium profiling of specific circadian neurons in freely moving flies. Proc Natl Acad Sci U S A 114, 41, E8780-E8787.

[148] Ozturk, N., Selby, C. P., Zhong, D., and Sancar, A. 2014. Mechanism of photosignaling by Drosophila cryptochrome: role of the redox status of the flavin chromophore. The Journal of biological chemistry 289, 8, 4634–4642.

[149] Fernandes, E. S., Fernandes, M. A., and Keeble, J. E. 2012. The functions of TRPA1 and TRPV1: moving away from sensory nerves. British journal of pharmacology 166, 2, 510–521.

[150] Harrisingh, M. C., Wu, Y., Lnenicka, G. A., and Nitabach, M. N. 2007. Intracellular Ca2+ regulates free-running circadian clock oscillation in vivo. The Journal of neuroscience : the official journal of the Society for Neuroscience 27, 46, 12489–12499.

[151] Ng, F. S., Tangredi, M. M., and Jackson, F. R. 2011. Glial cells physiologically modulate clock neurons and circadian behavior in a calcium-dependent manner. Curr Biol 21, 8, 625–634.

[152] Liang, X., Holy, T. E., and Taghert, P. H. 2016. Synchronous Drosophila circadian pacemakers display nonsynchronous Ca(2)(+) rhythms in vivo. Science 351, 6276, 976–981.

[153] Palacios-Munoz, A. and Ewer, J. 2018. Calcium and cAMP directly modulate the speed of the Drosophila circadian clock. PLoS genetics 14, 6, e1007433.

[154] Stueber, T., Eberhardt, M. J., Caspi, Y., Lev, S., Binshtok, A., and Leffler, A. 2017. Differential cytotoxicity and intracellular calcium-signalling following activation of the calcium-permeable ion channels TRPV1 and TRPA1. Cell calcium 68, 34–44.

[155] Collins, C. A. and DiAntonio, A. 2007. Synaptic development: insights from Drosophila. Current Opinion in Neurobiology 17, 1, 35–42.

[156] Koon, A. C., Ashley, J., Barria, R., DasGupta, S., Brain, R., Waddell, S., Alkema, M. J., and Budnik, V. 2010. Autoregulatory and paracrine control of synaptic and behavioral plasticity by octopaminergic signaling. Nat Neurosci 14, 190 EP -.

[157] Maiellaro, I., Lohse, M. J., Kittel, R. J., and Calebiro, D. 2016. cAMP Signals in Drosophila Motor Neurons Are Confined to Single Synaptic Boutons. Cell reports 17, 5, 1238–1246.

[158] Kahsai, L. and Zars, T. 2011. Learning and Memory in Drosophila: Behavior, Genetics, and Neural Systems. In International Review of Neurobiology : Recent advances in the use of Drosophila in neurobiology and neurodegeneration, N. Atkinson, Ed. Academic Press, 139–167.

[159] Kandel, E. R., Dudai, Y., and Mayford, M. R. 2014. The Molecular and Systems Biology of Memory. Cell 157, 1, 163–186.

[160] Li, Y., Guo, F., Shen, J., and Rosbash, M. 2014. PDF and cAMP enhance PER stability in Drosophila clock neurons. Proc Natl Acad Sci U S A 111, 13, E1284-90.

[161] Belvin, M. P., Zhou, H., and Yin, J. C. 1999. The Drosophila dCREB2 gene affects the circadian clock. Neuron 22, 4, 777–787.

[162] Katz, L. C. and Shatz, C. J. 1996. Synaptic activity and the construction of cortical circuits. Science 274, 5290, 1133–1138.

[163] Neely, M. D. and Nicholls, J. G. 1995. Electrical activity, growth cone motility and the cytoskeleton. The Journal of experimental biology 198, Pt 7, 1433–1446.

[164] Raab-Graham, K. F., Radeke, C. M., and Vandenberg, C. A. 1994. Molecular cloning and expression of a human heart inward rectifier potassium channel. Neuroreport 5, 18, 2501–2505.

[165] Hua, J. Y., Smear, M. C., Baier, H., and Smith, S. J. 2005. Regulation of axon growth in vivo by activity-based competition. Nature 434, 1022 EP -.

[166] Schmidpeter, P. A. M., Gao, X., Uphadyay, V., Rheinberger, J., and Nimigean, C. M. 2018. Ligand binding and activation properties of the purified bacterial cyclic nucleotide-gated channel SthK. The Journal of general physiology 150, 6, 821–834.

[167] Matsumoto, A., Matsumoto, N., Harui, Y., Sakamoto, M., and Tomioka, K. 1998. Light and temperature cooperate to regulate the circadian locomotor rhythm of wild type and period mutants of Drosophila melanogaster. Journal of insect physiology 44, 7-8, 587–596.

[168] Majercak, J., Sidote, D., Hardin, P. E., and Edery, I. 1999. How a circadian clock adapts to seasonal decreases in temperature and day length. Neuron 24, 1, 219–230.

[169] Low, K. H., Lim, C., Ko, H. W., and Edery, I. 2008. Natural variation in the splice site strength of a clock gene and species-specific thermal adaptation. Neuron 60, 6, 1054–1067.

[170] Low, K. H., Chen, W.-F., Yildirim, E., and Edery, I. 2012. Natural variation in the Drosophila melanogaster clock gene period modulates splicing of its 3'-terminal intron and mid-day siesta. PloS one 7, 11, e49536.

[171] Govorunova, E. G., Sineshchekov, O. A., Janz, R., Liu, X., and Spudich, J. L. 2015. NEUROSCIENCE. Natural light-gated anion channels: A family of microbial rhodopsins for advanced optogenetics. Science 349, 6248, 647–650.

[172] Zordan, M., Osterwalder, N., Rosato, E., and Costa, R. 2001. Extra ocular photic entrainment in Drosophila melanogaster. Journal of neurogenetics 15, 2, 97–116.

[173] Hanai, S., Hamasaka, Y., and Ishida, N. 2008. Circadian entrainment to red light in Drosophila: requirement of Rhodopsin 1 and Rhodopsin 6. Neuroreport 19, 14, 1441–1444.

[174] Zimmerman, J. E., Chan, M. T., Jackson, N., Maislin, G., and Pack, A. I. 2012. Genetic background has a major impact on differences in sleep resulting from environmental influences in Drosophila. Sleep 35, 4, 545–557.

[175] Freeman, M. 1996. Reiterative use of the EGF receptor triggers differentiation of all cell types in the Drosophila eye. Cell 87, 4, 651–660.

[176] Kramer, J. M. and Staveley, B. E. 2003. GAL4 causes developmental defects and apoptosis when expressed in the developing eye of Drosophila melanogaster. Genetics and molecular research : GMR 2, 1, 43–47.

[177] Liu, Y. and Lehmann, M. 2008. A genomic response to the yeast transcription factor GAL4 in Drosophila. Fly 2, 2, 92–98.

[178] Rezaval, C., Werbajh, S., and Ceriani, M. F. 2007. Neuronal death in Drosophila triggered by GAL4 accumulation. The European journal of neuroscience 25, 3, 683–694.

The following publications came as a result of the work on this thesis:

[95] Beck, S., Yu-Strzelczyk, J., Pauls, D., Constantin, O. M., Gee, C. E., Ehmann, N., Kittel, R. J., Nagel, G., and Gao, S. 2018. Synthetic Light-Activated Ion Channels for Optogenetic Activation and Inhibition. Frontiers in neuroscience 12, 643

6. Appendix

6.1. Abbreviations

ACRs	-	anion channelrhodopsins
aMe	-	the accessory medulla
ATP	-	Adenosine triphosphate
ATR	-	All-trans-retinal
BIFC	-	bimolecular fluorescence complementation
BLUF	-	blue-light sensing using FAD
bPAC	-	bacterial Photoactivated Adenylyl-cyclase
bPGC	-	bacterial Photoactivated Guanylyl-cyclase
cAMP	-	cyclic adenosine monophosphate
CD8	-	Cluster of differentiation #8
cGMP	-	cyclic guanosine monophosphate
ChR1	-	Channelrhodopsin 1
ChR2	-	Channelrhodopsin 2
clk	-	the clock gene *clock*
CLK	-	the clock protein Clock
CLSM	-	confocal laser scanning microscope
CNGC	-	cyclic nucleotide-gated channel
cNMP	-	cyclic nucleotide monophosphate
CRAC	-	Ca^{2+} release-activated Ca^{2+}-channel
CRY	-	the photoreceptor protein Cryptochrome
CT	-	circadian time
CYC	-	the clock protein Cycle
CyclOp	-	Cyclase Opsin
CyO	-	Curly of Oster balancer
DAMS	-	Drosophila activity monitoring system
DBT	-	the protein kinase Doubletime
DD	-	constant darkness
DEVC	-	Double Electrode Voltage Clamp
$DN1_a$	-	anterior dorsal clock neuron
$DN1_p$	-	posterior dorsal clock neuron
DNs	-	the dorsal clock neurons

DSHB	-	Developmental Studies Hybridoma Bank
dTRPA1	-	*Drosophila* Transient receptor potential cation channel, subfamily A, member 1
E	-	evening
E-box	-	enhancer box
ECL	-	extracellular loop
FAD	-	Flavin-Adenine-Dinucleotide
FIM	-	FTIR-based Imaging Method
FMDV	-	foot-and-mouth disease virus
FTIR	-	frustrated total internal reflection
GAL4	-	Regulatory protein GAL4
GFP	-	Green fluorescent protein
Glyco	-	Glycophorin
GSK-3	-	Glycogen Synthase Kinase 3
H-B	-	Hofbauer-Buchner
HEK	-	Human Embryonic Kidney
ICL	-	intracellular loop
IT	-	Information Technology
ITP	-	the ion transport peptide
JET	-	the clock protein Jetlag
LD	-	Light/Darkness
LED	-	Light emitting diode
l-LN$_v$s	-	the large ventral lateral clock neurons
LN$_d$s	-	the dorsal lateral clock neurons
LNs	-	the lateral clock neurons
LN$_v$s	-	the ventral lateral clock neurons
LOV	-	the Light-oxygen-voltage domain
LPNs	-	the lateral posterior clock neurons
M	-	morning
MKRS	-	M(3)76A^1 kar^1 ry^2 Sb^1 (allele names) balancer
NaN3	-	Sodium azide
NGS	-	Normal Goat Serum
NPF	-	the neuropeptide F
PACs	-	Photoactivated adenylyl-cyclases

PBS	-	Phosphate buffered saline
PDF	-	the neuroregulator protein Pigment Dispersing Factor
PDFR	-	the receptor protein Pigment Dispersing Factor Receptor
pdp1ε	-	the clock gene *PAR-domain protein 1ε*
PDP1Ɛ	-	the clock protein Par-Domain Protein 1Ɛ
per	-	the clock gene *period*
PER	-	the clock protein Period
PFA	-	Paraformaldehyde
PHR	-	Photolyase-Homologous Region
POC	-	posterior optic commissure
POT	-	posterior optic tract
PRC	-	Phase Response Curve
RD	-	Red light/Darkness
RH	-	Relative Humidity
Sco	-	the Scutoid balancer
SEM	-	Standard Error of the Mean
SGG	-	the clock protein SHAGGY
s-LN$_v$s	-	the small ventral lateral clock neurons
sNPF	-	the shortened neuropeptide F
SRI	-	Sensory Rhodospin I
SRII	-	Sensory Rhodopsin II
tim	-	the clock gene *timeless*
TIM	-	the clock protein Timeless
TM	-	transmembrane helix
TM6B	-	the “Tubby” balancer
TRP	-	Transient receptor potential
TTFL	-	transcriptional and translational feedback loop
UAS	-	Upstream activating sequence
V/P-box	-	VRI/PDP1ϵ binding sites
vri	-	the clock gene *vrille*
VRI	-	the clock protein Vrille
wt	-	wild type
YFP	-	Yellow Fluorescent Protein
ZT	-	Zeitgeber time

6.2. List of Figures

6.3. List of Tables

Acknowledgements

First of all I would like to thank my doctorate supervisor Prof. Dr. Georg Nagel and Prof. Dr. Charlotte Förster who gave me the opportunity to work on this PhD project under their supervision and in their respective laboratory groups. Their combined efforts, help and suggestions significantly shaped this project.
I would also like to extend my thanks to my co-supervisors Prof. Dr. Robert Kittel and Prof. Dr. Tobias Langenhan for their helpful discussions on my project.

I would also like to thank Dr. Shiqiang Gao for his substantial help and work regarding the design of all the optogenetic tools that have been used by me over the course of this project and for being a tremendously competent corresponding author on our scientific publication.
Furthermore, I would like to thank Dr. Dirk Rieger for all the time and effort spent on training, teaching and supervising me in all things related to *Drosophila* and the circadian clock.
I would also like to extend my thanks to Dr. Dennis Pauls who supervised and taught me in using the FIM setup and the FIMtrack software, which was essential for our scientific publication.

Additionally, I would like to thank Dr. Frank Schubert for all the help he provided me with while we were sharing a lab and workspace.
I also want to thank Dr. Enrico Bertollini for helping me out in matters big or small, whenever he could.

My thanks also goes out to Konrad Öchsner and Christian Smietana for designing, building and programming all the electrical appliances and software programs that I was using over the course of this project.

Lastly, I want to thank all the members of the Neurophysiology Department and Biophysics Department for their help, support and the friendly and enjoyable working atmosphere.

Curriculum Vitae

- removed for library printing -

Affidavit

I hereby declare that my thesis entitled: *„Using optogenetics to influence the circadian clock of Drosophila melanogaster*"" is the result of my own work. I did not receive any help or support from commercial consultants. All sources and / or materials applied are listed and specified in the thesis. Furthermore I verify that the thesis has not been submitted as part of another examination process neither in identical nor in similar form. Besides I declare that if I do not hold the copyright for figures and paragraphs, I obtained it from the rights holder and that paragraphs and figures have been marked according to law or for figures taken from the internet, the hyperlink has been added accordingly.

Konstanz, 03.02.2019 Signature

_____

Eidesstattliche Erklärung

Hiermit erkläre ich an Eides statt, die Dissertation: „Die Verwendung der Optogenetik zur Beeinflussung der circadianen Uhr von *Drosophila melanogaster*“, eigenständig, d. h. insbesondere selbständig und ohne Hilfe eines kommerziellen Promotionsberaters, angefertigt und keine anderen, als die von mir angegebenen Quellen und Hilfsmittel verwendet zu haben. Ich erkläre außerdem, dass die Dissertation weder in gleicher noch in ähnlicher Form bereits in einem anderen Prüfungsverfahren vorgelegen hat. Weiterhin erkläre ich, dass bei allen Abbildungen und Texten bei denen die Verwertungsrechte (Copyright) nicht bei mir liegen, diese von den Rechtsinhabern eingeholt wurden und die Textstellen bzw. Abbildungen entsprechend den rechtlichen Vorgaben gekennzeichnet sind sowie bei Abbildungen, die dem Internet entnommen wurden, der entsprechende Hypertextlink angegeben wurde.

Konstanz, 03.02.2019 Unterschrift

_____